United States
Environmental
Protection
Agency

Office of Air Quality
Planning and Standards
Research Triangle Park, NC 27711

EPA-450/4-90-006D
APRIL 1990

AIR

EPA

URBAN AIRSHED MODEL STUDY OF FIVE CITIES

Low-Cost Application of the Model to Atlanta and Evaluation of the Effects of Biogenic Emissions on Emission Control Strategies

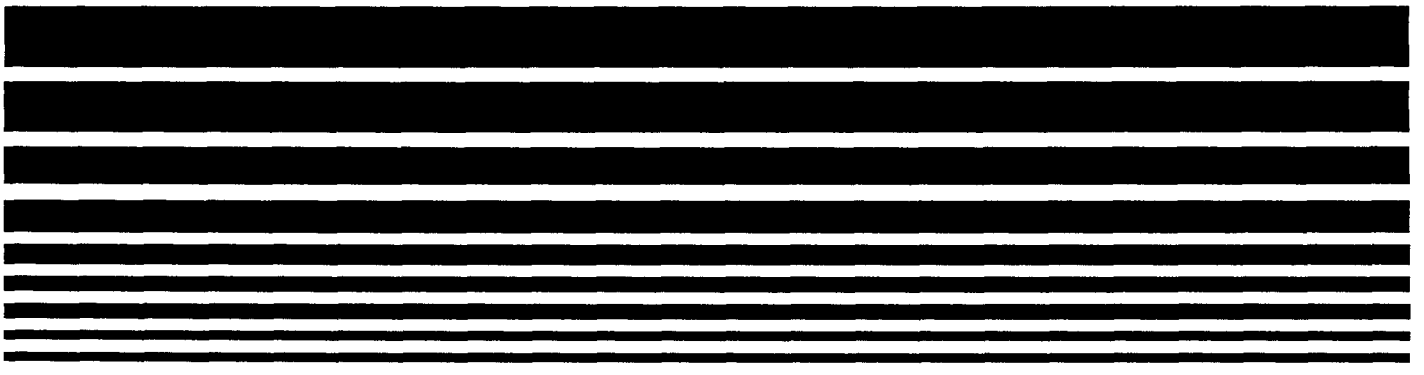

EPA-450/4-90-006D

URBAN AIRSHED MODEL STUDY OF FIVE CITIES

Low-Cost Application of the Model to Atlanta and Evaluation of the Effects of Biogenic Emissions on Emission Control Strategies

By

Ralph E. Morris
Thomas C. Myers
Marianne C. Causley
LuAnn Gardner
Edward L. Carr

Systems Applications, Inc.
101 Lucas Valley Road
San Rafael, CA 94903

EPA Project Officers:

Gerald L. Gipson, Atmospheric Research and Exposure Assessment Laboratory
Richard D. Scheffe, Office of Air Quality Planning and Standards
John C. Chamberlin, Office of Policy Planning and Evaluation

OFFICE OF AIR QUALITY PLANNING AND STANDARDS

U. S. ENVIRONMENTAL PROTECTION AGENCY

RESEARCH TRIANGLE PARK, NC 27711

APRIL 1990

Disclaimer

This material has been funded wholly or in part by the United States Environmental Protection Agency. It has been subject to the agency's review, and it has been approved for publication as an EPA document. Mention of trade names or commercial products does not constitute endorsement or recommendation for use.

Contents

Appendix A: Emissions Data Used in the Application of the UAM to Atlanta

Appendix B: Hourly Wind Fields for UAM Layer 1 Used in Diagnostic Run 1

Appendix C: Hourly Predicted Ozone Concentrations (pphm) for Diagnostic Run 1

Appendix D: Hourly Wind Fields for UAM Layer Used in Diagnostic Run 2 (Base Case Simulation with Biogenics)

Appendix E: Hourly Predicted Ozone Concentrations (pphm) for Diagnostic Run 2

Appendix F: Percent Contribution of Initial Concentrations, Boundary Conditions (four lateral faces plus top boundary), Anthropogenic Area Source Emissions, Point Source Emissions, and Biogenic Emissions to Hourly Tracer, NO_x, and VOC Concentrations on 4 June 1984

Appendix G: Sensitivity Analysis of the Calculations of Ozone Concentrations and Effects of Emission Controls on Ozone Concentrations to Wind Speed Specification

1 INTRODUCTION

The job of reducing ozone concentrations to levels below the National Ambient Air Quality Standard (NAAQS) has proven to be far more difficult than was thought when the Clean Air Act was passed and amended. The level of ozone precursor emissions remains too high; either emission reductions have been too small or have been required of the wrong sources, or both.

A plethora of technical explanations has been offered for failure to attain the ozone standard. These include perceived weaknesses in the attainment planning process (Federal Registrar, Vol. 52, No. 226, November 24, 1987; OTA 1988a,b,c), incomplete understanding or recognition of the anthropogenic and natural factors that cause elevated tropospheric ozone levels (Science, 1988), the failure to consider the effects of natural emissions (Chameides et al., 1988; Morris et al., 1989), use of a simplistic modeling approach (OTA, 1988a; Seinfeld, 1988a; Burton, 1988), and failure to reduce the amount of emissions intended, either through overestimates of the effectiveness of control technology or failure to account for certain categories of emission sources. The EPA, after lengthy consideration, has proposed a comprehensive policy that includes major changes in the planning process for reducing ozone concentrations (Federal Registrar, Vol. 52, No. 226, November 24, 1987). These changes include improvements in modeling practices and requirements for improving the data to support improved modeling practices. The EPA is now evaluating public comments on the proposed policy.

USE OF THE URBAN AIRSHED MODEL

The EPA recommends that states use the Urban Airshed Model (UAM) for the modeling of ozone and photochemical reactive pollutants in urban areas (EPA, 1986). An alternative approach, the Empirical Kinectics Modeling Approach (EKMA), has been accepted for demonstrating attainment of the ozone standard in most State Implementation Plans (Federal Registrar, Vol. 52, No. 226, 1987). The UAM and EKMA are quite different types of models; the UAM is a three-dimensional grid model while the EKMA is a trajectory box model.

A reluctance to use the UAM in the past is based on the perception that it requires using data from costly intensive measurement studies and requires extensive computational resources. Most of the cost of applying the UAM is attributed to the practice of conducting an extensive evaluation of UAM performance, which usually

entails many diagnostic simulations. This evaluation enables us to understand why the UAM performs as it does for a particular application and, if deemed necessary, to take actions to improve model performance. Historically, it has been expected that the UAM will calculate hourly ozone concentrations to within approximately 15 to 20 percent of the observed peak value (Seinfeld, 1988a; Burton, 1988). More recent applications of the UAM to the Los Angeles basin have used routinely available meteorological data and predicted observed ozone levels with a high degree of skill (Seinfeld, 1988a; Burton, 1988; Hogo, Mahoney, and Yocke 1988). A recent application of the UAM to the New York metropolitan area used simple inputs, i.e., constant wind fields and mixing depths (Rao 1987).

This simplified use of the UAM, relying on routinely available data and reducing the requirement for strict evaluations of model performance, offers air quality managers a practical air quality assessment tool for identifying emission control strategies that demonstrate attainment of the ozone NAAQS. This simplified approach is called Practice-for-Low-Cost-Airshed-Application-for-Nonattainment-Regions (PLANR). The PLANR use of the UAM requires almost the same quantity and quality of inputs as EKMA, and the overall application cost is substantially reduced. The possible exception is the emissions inventory, which in PLANR applications should contain the same spatially (horizontally and vertically) and temporally varying emissions used in standard UAM applications (such detail is necessary to account for the differing reactivities of VOC emissions). However, local agencies generally have emissions inventories at hand; in addition, UAM input inventories can be readily estimated from existing national emissions inventories (e.g., the National Acid Precipitation Program 1980 and 1985 inventories). Knowledge of current emission rates is needed to estimate the emission controls required to achieve attainment of the ozone NAAQS.

The PLANR use of the UAM may not be appropriate for all nonattainment regions. When attainment is expected to be imminent, improved methods for using EKMA may be adequate. In other, more complex situations, such as the Los Angeles basin, the Houston region, and the New York Metropolitan area among others, the complexity of meteorological conditions and the emissions distribution and the severity of the ozone attainment problem probably require a more detailed application of the UAM. The application of UAM to these more complex situations, called Practice-of-Airshed-Application-in-Complex-Regions (PACR), would involve more extensive model performance requirements and hence more diagnostic simulations, and a resultant increase in costs. However, even for a complex nonattainment region, the PLANR approach would probably be more comprehensive and reliable than EKMA for estimating the controls needed to achieve ozone attainment.

THE "FIVE CITIES" UAM STUDY

The EPA has funded a study of the PLANR approach in five urban areas in the U.S. (New York, St. Louis, Atlanta, Philadelphia, and Dallas-Ft. Worth). The main objectives of this "Five Cities" study are to:

(1) Demonstrate the usefulness of PLANR for air quality planning;

(2) Determine the effects of alternative fuels and alternative Reid vapor pressure values for fuels on urban ozone concentrations;

(3) Demonstrate the use of PLANR to evaluate SIP control strategies and compare results with those obtained with EKMA; and

(4) Transfer the UAM model, modeling data bases, and applications technology to the states for use in future SIPs.

In addition, the study includes two city-specific analyses:

(1) For the St. Louis and Philadelphia areas, comparison of the PLANR use of the UAM (i.e., using only routinely available data) with applications of the UAM that use an extensive data base; and

(2) The effects of biogenic emissions on anthropogenic emission reductions in the Atlanta area.

Previous reports on the "Five Cities" study have documented the PLANR use of UAM and the evaluation of alternative fuel emission scenarios for the New York metropolitan area and the city of St. Louis (Morris et al., 1989a). This report presents the PLANR use of the UAM for Atlanta and analyzes the effects of biogenic emissions on the anthropogenic VOC emission reductions required to meet attainment of the ozone NAAQS. Recently, the EKMA model was applied to Atlanta for 4 June 1984 to estimate the effects of biogenic emissions on VOC emission controls needed to bring Atlanta into attainment of the ozone NAAQS (Chameides et al., 1988). One of the purposes of this study is to repeat this analysis using a more comprehensive model, the UAM(CB-IV).

2 DESCRIPTION OF THE CB-IV VERSION OF THE URBAN AIRSHED MODEL

The Urban Airshed Model (UAM) is a three-dimensional grid model designed to calculate the concentrations of both inert and chemically reactive pollutants by simulating the various physical and chemical processes that take place in the atmosphere. The basis of the UAM is the atmospheric diffusion or species continuity equation. This equation represents a mass balance in which all of the relevant emissions, transport, diffusion, chemical reaction, and removal processes are expressed in mathematical terms. Based on the grid concept, the model is generally employed to simulate an 8- to 72-hour period during which episodic meteorological conditions persist.

Because the model can resolve both spatial and temporal features of the concentration field, it is well suited to the analysis of future control strategies and their effects on air quality in various parts of the modeling region. Before the model is used for such an analysis, its ability to replicate measurements from an historical ozone episode is tested. Model inputs are prepared from observed meteorological, emission, and air quality data for a particular day or days. Once the model inputs have been adjusted within the range of their uncertainty so that the model performs within prescribed levels, the emission inventory can be changed to represent assumptions about future emission scenarios. The model is then re-run with the forecasted emissions, and the resulting hourly ozone patterns are what the model predicts is likely to occur under meteorological conditions similar to the historical episode.

The UAM is the only air quality model recommended by the EPA for photochemical or reactive pollutant modeling applications involving entire urban areas (EPA, 1986). The EPA guidelines refer to the 1978-1980 version of the UAM; the formulation of that version is discussed by Ames and others (1985a,b). Many improvements to the UAM have been made over the last 10 years. The two most significant are:

Incorporation of the latest version of the Carbon-Bond Mechanism, the CB-IV (Gery, Whitten, and Killus, 1988)

Use of the Smolarkiewicz algorithm for advection (Smolarkiewicz, 1983)

USE OF THE SMOLARKIEWICZ ALGORITHM TO SOLVE THE ADVECTION EQUATION

Grid-based air quality simulation models require a numerical approximation of the horizontal advection terms in the species conservation equations. The 1978-1980 version of the Urban Airshed Model (UAM) used a variant of the Sharp and Smooth Transport Algorithm (SHASTA) originally formulated by Boris and Book (1973). Since 1977 there have been many comparative studies of advection schemes. Examples of such studies relevant to the UAM are those of Zalesak (1970), Schere (1983), Chock and Dunker (1983), Chock (1985), Smolarkiewicz (1983), and Yamertino and Scire (1985). In each of these studies an idealized scalar function (a cone, block, ellipse, or cosine wave) representative of a concentration distribution is advected by a rotating wind field (constant angular velocity). The rotating wind field provides a range of Courant numbers, depending on the radial distance from the center of the domain. The degree to which the attributes of the idealized function (total mass, peak value, mean value, and gradients) are preserved indicates the accuracy of the scheme.

The above studies showed that a number of advection schemes were more accurate than SHASTA, as measured by the idealized tests. For the UAM, a number of specific requirements constrained the selection of alternative to SHASTA. First, it is important that the scheme be positive definite, i.e., that it not result in negative concentrations. Second, the scheme should use forward time differencing to minimize storage requirements and to insure compatibility with the chemical mechanism numerical solution scheme. Third, the ability of an advection scheme to represent the magnitudes and locations of peak concentrations is of major importance in regulatory applications. Fourth, to handle complex airflows, the scheme should display relatively uniform accuracy over a wide range of Courant numbers (i.e., wind speeds).

Further review indicated that the advection scheme developed by Smolarkiewicz (1983) represented the best combination of accuracy and economy. The Smolarkiewicz scheme is conceptually similar to SHASTA in that a highly diffusive transport step is followed by an anti-diffusive correction step. The transport step is essentially the well-known "upstream" finite-difference scheme. The correction step involves a second exercise of the upstream finite difference scheme, substituting the anti-diffusive velocity for the actual velocity. The Smolarkiewicz scheme is positive definite and forward in time, and can be used in either a time-split or multidimensional mode. Smolarkiewicz demonstrated that the scheme was superior in both accuracy and economy to the multidimensional generalization of SHASTA formulated by Zalesak (1979). In applications to the Los Angeles area and Kern County, California, the UAM with the Smolarkiewicz algorithm produced results that were more accurate than those produced in earlier applications using SHASTA (Hogo, Mahoney, and Yocke, 1988; Whitten et al., 1985).

USE OF THE CB-IV TO SOLVE PHOTOCHEMISTRY

The latest version of the Carbon-Bond Mechanism (CBM-IV) was recently implemented in the UAM (Gery, Whitten, and Killus, 1988). Whenever a new chemical kinetics mechanisms is merged into a complex air quality simulation model, the predictive capabilities and solution speed of the new computer code require optimization and evaluation. This process is even more important now because the recent gas-phase chemical kinetics mechanisms (CAL, RADM, and the CBM-IV) are larger than previous mechanisms, and therefore require significantly more computing time. The CBM-IV reactions are shown in Table 1. There are some minor differences between the original CB-IV and the version implemented in the UAM. For the examination of ethanol (ETOH) blended fuels, ETOH was added as a species. The ethanol reaction is ETOH + OH → ALD2 + HO_2 with a rate constant of 4,300 1/ppm-min. Both numerical and chemical improvements were made to the CB-IV implementation in the UAM so that computational speed could be increased and solution uncertainty diminished.

The implementation of the CB-IV in the UAM used a modified Crank-Nicholson algorithm for the simultaneous solution of the differential equations that represent the chemical changes for each species. This numerical integration scheme produced results that were within a few percent of those obtained with the previous (Gear) algorithm over a wide range of atmospheric conditions (Morris et al., 1989a,c).

TABLE 1. The Carbon Bond Mechanism-IV.*

Number	Reaction[1]	Reaction Rate Data: Pre-factor ($ppm^{-n}min^{-1}$)	Temp. Factor exp((-E/R)/T)	Rate Constant @ 298K k_{298} ($ppm^{-n}min^{-1}$)
1)	NO2 -hν1-> NO + O			see notes
2)	O -----> O3	8.383 E+04	*EXP(1175/T)	4.323 E+06
3)	O3 + NO -----> NO2	2.643 E+03	*EXP(- 1370/T)	2.664 E+01
4)	O + NO2 -----> NO	1.375 E+04		1.375 E+04
5)	O + NO2 -----> NO3	2.303 E+02	*EXP(687/T)	2.309 E+03
6)	O + NO -----> NO2	3.233 E+02	*EXP(602/T)	2.438 E+03
7)	O3 + NO2 -----> NO3	1.760 E+02	*EXP(- 2450/T)	4.731 E-02
8)	O3 -hν1-> O	5.300 E-02		5.300 E-02×k_1
9)	O3 -hν4-> O1D			see notes
10)	O1D -----> O	1.147 E+05	*EXP(390/T)	4.246 E+05
11)	O1D + H2O -----> 2.00H	3.260		3.260
12)	O3 + OH -----> HO2	2.344 E+03	*EXP(- 940/T)	1.000 E+02
13)	O3 + HO2 -----> OH	2.100 E+01	*EXP(- 580/T)	2.999
14)	NO3 -hν1-> 0.89NO2 + 0.89O + 0.11NO	3.390 E+01		3.390 E+01×k_1
15)	NO3 + NO -----> 2.00NO2	1.909 E+04	*EXP(250/T)	4.416 E+04
16)	NO3 + NO2 -----> NO + NO2	3.660 E+01	*EXP(- 1230/T)	5.901 E-01
17)	NO3 + NO2 -----> N2O5	7.849 E+02	*EXP(256/T)	1.853 E+03
18)	N2O5 + H2O -----> 2.00HNO3	1.900 E-06		1.900 E-06
19)	N2O5 -----> NO3 + NO2	2.110 E+16	*EXP(-10897/T)	2.776
20)	NO + NO -----> 2.00NO2	2.600 E-05	*EXP(530/T)	1.539 E-04
21)	NO + NO2 + H2O -----> 2.00HONO	1.600 E-11		1.600 E-11
22)	OH + NO -----> HONO	6.554 E+02	*EXP(806/T)	9.799 E+03
23)	HONO -hν1-> OH + NO	1.975 E-01		1.975 E-01×k_1
24)	OH + HONO -----> NO2	9.770 E+03		9.770 E+03
25)	HONO + HONO -----> NO + NO2	1.500 E-05		1.500 E-05
26)	OH + NO2 -----> HNO3	1.537 E+03	*EXP(713/T)	1.682 E+04
27)	OH + HNO3 -----> NO3	7.600	*EXP(1000/T)	2.179 E+02
28)	HO2 + NO -----> OH + NO2	5.482 E+03	*EXP(240/T)	1.227 E+04
29)	HO2 + NO2 -----> PNA	1.640 E+02	*EXP(749/T)	2.025 E+03
30)	PNA -----> HO2 + NO2	2.876 E+15	*EXP(-10121/T)	5.115
31)	OH + PNA -----> NO2	1.909 E+03	*EXP(380/T)	6.833 E+03
32)	HO2 + HO2 -----> H2O2	8.739 E+01	*EXP(1150/T)	4.144 E+03
33)	HO2 + HO2 + H2O -----> H2O2	7.690 E-10	*EXP(5800/T)	2.181 E-01
34)	H2O2 -hν3-> 2.00H	2.550 E-01		2.550 E-01×k_{39}
35)	OH + H2O2 -----> HO2	4.720 E+03	*EXP(- 187/T)	2.520 E+03
36)	OH + CO -----> HO2	3.220 E+02		3.220 E+02
37)	FORM + OH -----> HO2 + CO	1.500 E+04		1.500 E+04
38)	FORM -hν2-> CO + 2.00HO2			see notes
39)	FORM -hν3-> CO			see notes
40)	FORM + O -----> OH + HO2 + CO	4.302 E+04	*EXP(- 1550/T)	2.370 E+02
41)	FORM + NO3 -----> HNO3 + HO2 + CO	9.300 E-01		9.300 E-01
42)	ALD2 + O -----> C2O3 + OH	1.739 E+04	*EXP(- 986/T)	6.360 E+02
43)	ALD2 + OH -----> C2O3	1.037 E+04	*EXP(250/T)	2.400 E+04
44)	ALD2 + NO3 -----> C2O3 + HNO3	3.700		3.700
45)	ALD2 -hν6-> FORM + XO2 + CO + 2.00HO2			see notes
46)	C2O3 + NO -----> NO2 + XO2 + FORM + HO2	7.915 E+03	*EXP(250/T)	1.831 E+04
47)	C2O3 + NO2 -----> PAN	1.180 E-04	*EXP(5500/T)	1.223 E+04
48)	PAN -----> C2O3 + NO2	5.616 E+18	*EXP(-14000/T)	2.220 E-02
49)	C2O3 + C2O3 -----> 2.00FORM + 2.00XO2 + 2.00HO2	3.700 E+03		3.700 E+03
50)	C2O3 + HO2 -----> 0.79FORM + 0.79XO2 + 0.79HO2 + 0.79OH	9.600 E+03		9.600 E+03
51)	OH -----> XO2 + FORM + HO2	6.521 E+03	*EXP(- 1710/T)	2.100 E+01

(Continued)

* As currently implemented in the UAM (CB-IV), ethanol and methanol have been added to the CB-IV and can be treated as explicit species.

87048

88097
88151
89053

TABLE 1. Concluded.

Number	Reaction[1]	Reaction Rate Data: Pre-factor ($ppm^{-n}min^{-1}$)	Temp. Factor exp((-E/R)/T)	Rate Constant @ 298K k_{298} ($ppm^{-n}min^{-1}$)
52)	PAR + OH -----> 0.87XO2 + 0.13XO2N + 0.11HO2 + 0.11ALD2 + 0.76ROR - 0.11PAR	1.203 E+03		1.203 E+03
53)	ROR -----> 1.10ALD2 + 0.96XO2 + 0.94HO2 + 0.04XO2N + 0.02ROR - 2.10PAR	6.250 E+16	*EXP(- 8000/T)	1.371 E+05
54)	ROR -----> HO2	9.545 E+04		9.545 E+04
55)	ROR + NO2 ----->	2.200 E+04		2.200 E+04
56)	O + OLE -----> 0.63ALD2 + 0.38HO2 + 0.28XO2 + 0.30CO + 0.20FORM + 0.02XO2N + 0.22PAR + 0.20OH	1.756 E+04	*EXP(- 324/T)	5.920 E+03
57)	OH + OLE -----> FORM + ALD2 + XO2 + HO2 - PAR	7.740 E+03	*EXP(504/T)	4.200 E+04
58)	O3 + OLE -----> 0.50ALD2 + 0.74FORM + 0.33CO + 0.44HO2 + 0.22XO2 + 0.10OH - PAR	2.104 E+01	*EXP(- 2105/T)	1.800 E-02
59)	NO3 + OLE -----> 0.91XO2 + FORM + ALD2 + 0.09XO2N + NO2 - PAR	1.135 E+01		1.135 E+01
60)	O + ETH -----> FORM + 0.70XO2 + CO + 1.70HO2 + 0.30OH	1.540 E+04	*EXP(- 792/T)	1.080 E+03
61)	OH + ETH -----> XO2 + 1.56FORM + HO2 + 0.22ALD2	3.000 E+03	*EXP(411/T)	1.192 E+04
62)	O3 + ETH -----> FORM + 0.42CO + 0.12HO2	1.856 E+01	*EXP(- 2633/T)	2.700 E-03
63)	OH + TOL -----> 0.08XO2 + 0.36CRES + 0.44HO2 + 0.56TO2	3.106 E+03	*EXP(322/T)	9.150 E+03
64)	TO2 + NO -----> 0.90NO2 + 0.90HO2 + 0.90OPEN	1.200 E+04		1.200 E+04
65)	TO2 -----> CRES + HO2	2.500 E+02		2.500 E+02
66)	OH + CRES -----> 0.40CRO + 0.60XO2 + 0.60HO2 + 0.30OPEN	6.100 E+04		6.100 E+04
67)	CRES + NO3 -----> CRO + HNO3	3.250 E+04		3.250 E+04
68)	CRO + NO2 ----->	2.000 E+04		2.000 E+04
69)	OPEN -h ν2-> C2O3 + HO2 + CO	9.040		9.040 $\times k_{38}$
70)	OPEN + OH -----> XO2 + 2.00CO + 2.00HO2 + C2O3 + FORM	4.400 E+04		4.400 E+04
71)	OPEN + O3 -----> 0.03ALD2 + 0.62C2O3 + 0.70FORM + 0.03XO2 + 0.69CO + 0.08OH + 0.76HO2 + 0.20MGLY	8.030 E-02	*EXP(- 500/T)	1.500 E-02
72)	OH + XYL -----> 0.70HO2 + 0.50XO2 + 0.20CRES + 0.80MGLY + 1.10PAR + 0.30TO2	2.453 E+04	*EXP(116/T)	3.620 E+04
73)	OH + MGLY -----> XO2 + C2O3	2.600 E+04		2.600 E+04
74)	MGLY -h ν2-> C2O3 + HO2 + CO	9.640		9.640 $\times k_{38}$
75)	O + ISOP -----> 0.60HO2 + 0.80ALD2 + 0.55OLE + 0.50XO2 + 0.50CO + 0.45ETH + 0.90PAR	2.700 E+04		2.700 E+04
76)	OH + ISOP -----> XO2 + FORM + 0.67HO2 + 0.40MGLY + 0.20C2O3 + 1.00ETH + 0.20ALD2 + 0.13XO2N	1.420 E+05		1.420 E+05
77)	O3 + ISOP -----> FORM + 0.40ALD2 + 0.55ETH + 0.20MGLY + 0.10PAR + 0.06CO + 0.44HO2 + 0.10OH	1.800 E-02		1.800 E-02
78)	NO3 + ISOP -----> XO2N	4.700 E+02		4.700 E+02
79)	XO2 + NO -----> NO2	1.200 E+04		1.200 E+04
80)	XO2 + XO2 ----->	2.550 E+01	*EXP(1300/T)	2.000 E+03
81)	XO2N + NO ----->	1.000 E+03		1.000 E+03

3 MODELING EPISODE AND DOMAIN SELECTION

EPISODE SELECTION

Table 2 lists all days from the years 1984 to 1987 in Georgia (either Atlanta or Columbus) in which the maximum daily ozone concentration at any monitor in the AIRS data base exceeds the National Ambient Air Quality Standard of 120 ppb. Of the 62 days where ozone concentrations in Georgia are greater than or equal to 120 ppb, 61 pertain to Atlanta and one (3/18/84) to Columbus (note that on other days Columbus may have an exceedence of the ozone standard but the ozone concentrations are less than recorded in Atlanta). The most striking feature of the occurrence of elevated ozone concentrations in Atlanta are the months of July and August, 1987, where in a 21 day period (19 July to 7 August 1987) there were 15 exceedences of ozone NAAQS. This period also included the very highest observed ozone concentration in Atlanta (201 ppb on 31 July 1987). On most days during this period, most ozone monitors in Georgia, including Columbus, are recording high ozone concentrations. This seems to indicate a region wide buildup of ozone concentrations over an extended length of time and area. Thus, the elevated ozone concentrations in Atlanta during July and August, 1987, may be attributable to regional-scale in addition to urban-scale ozone formation.

For Atlanta, the city specific analysis will analyze the effects of biogenic emissions on urban ozone formation and on the effects of anthropogenic VOC emissions strategies designed to reduce ozone. A previous study on the effects of biogenic emissions for Atlanta used the EKMA model to analyze ozone formation on 4 June 1984. It is highly desirable that this day also be chosen for the city-specific UAM analysis as long as there are no other specific reasons, such as excessive wind shear or other unusual meteorological phenomena, that would preclude its selection. On 4 June 1984, the maximum daily ozone concentration was 147 at Conyers, Georgia. For the two day period of 3 to 4 June 1984, winds are predominantly from the northwest sector with some southwesterlies late on 4 June. Maximum daily ozone concentrations on 4 June are 78 ppb (DLLS) upwind of Atlanta and 130 (DKLB) and 147 (CNYR) ppb at distances of, respectively, 15 and 40 km downwind of Atlanta (see Figure 1). Thus, it appears that there is not a large amount of transported ozone into the Atlanta region on 4 June 1984 and the ozone exceedence is predominantly due to emissions from the Atlanta area.

Since the 4 June 1984 ozone event is not overly influenced by transported ozone and, as will be shown in the next section, does not contain any unusual meteorological

TABLE 2. Highest ozone days in Atlanta, 1984 - 1987.

Rank	Peak O3	Monitor	Date	Maximum Daily Ozone 130890002 Panthers. DKLB	130970002 Sweetwat. SWTR	131210053 MLK MLKM	132150008 Columbus COLO	132470001 Conyers CNYR
1	201.	130890002	7/31/87	201.	98.	141.	118.	163
2	169.	130890002	8/ 1/87	169.	130.	138.	80.	158.
3	168.	130970002	7/24/87	140.	168.	155.	113.	90.
4	165.	132470001	6/26/86	163.	-99.	-99.	95.	165.
5	164.	130890002	7/18/86	164.	-99.	-99.	90.	142.
6	164.	130890002	7/23/86	164.	-99.	-99.	92.	111.
7	160.	130890002	6/27/86	160.	-99.	-99.	67.	131.
8	157.	132470001	8/ 2/87	138.	88.	128.	70.	157.
9	155.	132470001	7/10/84	115.	-99.	-99.	53.	155.
10	155.	130970002	7/23/87	154.	155.	153.	100.	85.
11	155.	130970002	7/25/87	113.	155.	118.	90.	94.
12	152.	132150008	3/18/84	60.	-99.	-99.	152.	-99.
13	151.	130890002	7/31/86	151.	-99.	-99.	108.	114.
14	150.	132470001	6/ 9/87	129.	73.	103.	75.	150.
15	150.	130970002	7/30/87	112.	150.	113.	93.	93.
16	149.	131210053	7/26/87	129.	100.	149.	98.	88.
17	147.	132470001	6/ 4/84	130.	-99.	-99.	83.	147.
18	147.	132470001	8/22/84	118.	-99.	-99.	78.	147.
19	146.	130890002	8/ 3/87	146.	118.	128.	80.	129.
20	145.	132470001	6/26/85	115.	-99.	-99.	72.	145.
21	145.	132470001	7/12/85	118.	-99.	-99.	65.	145.
22	144.	132470001	6/10/87	137.	95.	115.	85.	144.
23	142.	130890002	4/26/86	142.	-99.	-99.	100.	105.
24	140.	130970002	8/21/87	99.	140.	104.	68.	98.
25	140.	132470001	6/16/86	118.	-99.	-99.	108.	140.
26	137.	130890002	7/22/86	137.	-99.	-99.	80.	84.
27	137.	132470001	8/ 2/86	112.	-99.	-99.	103.	137.
28	136.	130890002	8/ 4/87	136.	100.	113.	75.	116.
29	136.	130890002	8/ 5/87	136.	95.	103.	100.	120.
30	136.	130890002	6/28/84	136.	-99.	-99.	55.	122.
31	135.	130890002	6/ 6/85	135.	-99.	-99.	67.	122.
32	135.	130890002	7/29/87	135.	128.	118.	88.	133.
33	133.	130970002	6/11/87	103.	133.	103.	120.	86.
34	133.	130970002	9/ 3/87	91.	133.	95.	78.	80.
35	133.	132470001	9/14/84	105.	-99.	-99.	103.	133.
36	132.	132470001	6/ 2/87	109.	68.	86.	63.	132
37	132.	132470001	9/ 2/87	108.	88.	89.	90.	132.
38	131.	132470001	8/ 1/86	114.	-99.	-99.	85.	131.
39	131.	130890002	5/13/85	131.	-99.	-99.	83.	72.
40	130.	132470001	6/ 4/85	120.	-99.	-99.	-99.	130.
41	130.	130890002	6/24/87	130.	75.	104.	53.	118.
42	130.	132150008	7/27/87	108.	108.	94.	130.	120.
43	130.	132470001	8/ 7/87	129.	78.	107.	63.	130.
44	129.	132470001	8/ 4/86	114.	-99.	-99.	103.	129
45	129.	130890002	7/19/86	129.	-99.	-99.	90.	112.
46	128.	132470001	6/ 3/87	103.	65.	72.	75.	128.
47	127.	130890002	8/18/84	127.	-99.	-99.	83.	100.
48	127.	132470001	6/ 5/85	92.	-99.	-99.	67.	127.
49	126.	130890002	7/19/87	126.	115.	109.	73.	75.
50	125.	132470001	8/23/87	115.	78.	96.	83.	125.
51	125.	132470001	6/ 1/84	97.	-99.	-99.	75.	125.
52	125.	132470001	6/ 3/84	105.	-99.	-99.	70.	125.
53	125.	132470001	7/11/85	118.	-99.	-99.	63.	125.
54	125.	130890002	7/ 8/86	125.	-99.	-99.	60.	123.
55	123.	130890002	8/16/86	123.	-99.	-99.	78.	93.
56	123.	130890002	7/21/86	123.	-99.	-99.	90.	110.
57	122.	132470001	7/20/85	115.	-99.	-99.	83.	122.
58	122.	132470001	8/ 1/85	95.	-99.	-99.	85.	122.
59	122.	130890002	7/26/86	122.	-99.	-99.	78.	74.
60	121.	130890002	6/22/86	121.	-99.	-99.	78.	85.
61	120.	130890002	7/22/87	120.	98.	116.	68.	82.
62	120.	130970002	8/20/87	100.	120.	108.	75.	96.

89059

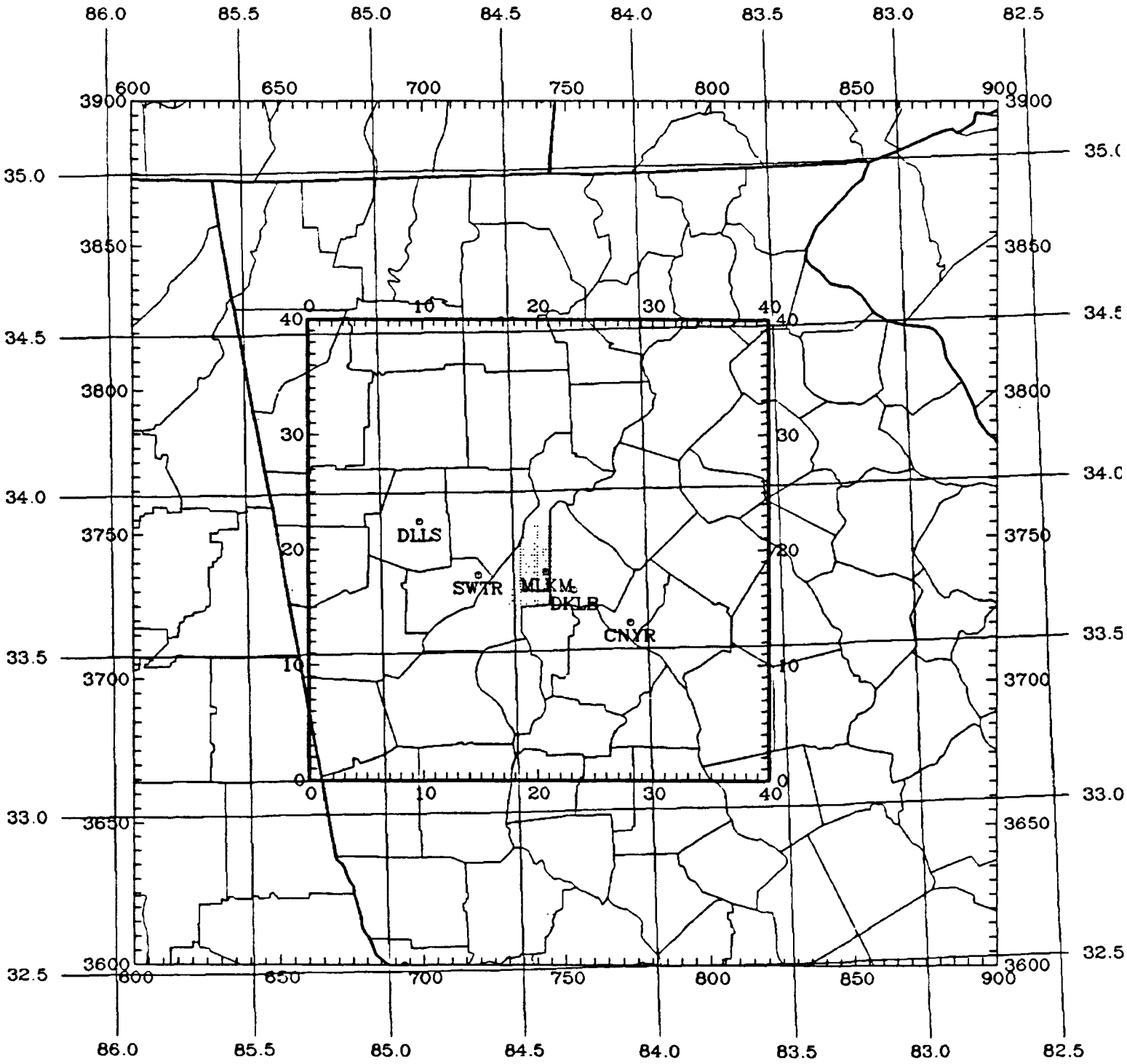

Figure 1. UAM modeling domain for Atlanta. Modeling domain consists of 40 by 40 array of 4 km grid cells with an origin at UTM coordinates 660 km easting, 3665 km northing, zone 16.

conditions it appears to be an appropriate day for the city-specific biogenic analysis for Atlanta and a demonstration of the PLANR use of the UAM. Since it is desirable to minimize the effects of initial conditions in any UAM simulation, the UAM modeling episode will be initialized on 3 June 1984 and terminated the evening of 4 June 1984. Thus, UAM modeling inputs will be prepared for 3 and 4 June 1984 with the actual starting time on 3 June to be determined from an inert tracer simulation.

It should be noted that other days listed in Table 2 may be more appropriate for demonstrating ozone attainment in a State Implementation Plan (SIP). Generally, it would be desirable for a SIP to pick a day with a higher ozone concentration, a day closer in time to current, a day in which the elevated ozone concentrations can be attributed to Atlanta, and a day that represents typical meteorological conditions that produces ozone exceedences in Atlanta. The very highest ozone concentration in Table 1 (201 ppb observed on 31 July 1987) appears not to be a prototypical event since it is almost 20 percent higher than any of the other high ozone events over the four year period.

MODELING DOMAIN SELECTION

The modeling domain for the 3 - 4 June 1984 UAM modeling episode should include a fairly large fetch upwind of the city of Atlanta in order to account for sufficient amounts of biogenic emissions upwind of the urban core of Atlanta. The modeling domain should also include enough area downwind of Atlanta in order to capture the maximum ozone concentrations that will be formed. Grid spacing should be sufficiently small in order to resolve the anthropogenic emission distribution in Atlanta. To determine the UAM modeling domain synoptic weather maps along with upper-air data from Athens and Waycross, Georgia; Nashville, Tennessee; and Centreville-Brent, Alabama, and surface data from South Dekalb were analyzed to determine the mean flow conditions that existed on 3-4 June 1984.

Meteorological Conditions on 3-4 June 1984

The days of 3 and 4 June 1984 saw the passage of a high pressure system. The 500 mb height contours at 0700 EST on 4 June 1984 shows the approaching high pressure ridge towards Atlanta. The 500 mb high pressure ridge passed through the region during the evening of the 4th of June. The axis of the surface high pressure system passed through the modeling region during the afternoon of the 4th. On the 3rd of June, daytime low level winds (<600m) were from the west at 3-6 ms^{-1} throughout the modeling region while aloft the winds were in the same direction, but stronger. As the axis of the high pressure system moved near the modeling region, a slight easterly component to the wind field developed (a result of the circulation about the high pressure system). This flow was first seen in the upper levels (> 600m) on the morning of the 4th, but by mid morning was seen in the surface layer. After the passage of the high pressure system, the winds became southwesterly. The weather

conditions during the modeling period were clear, hot and humid. Maximum temperatures were in the upper 80's and dew point temperatures in the low 60's.

Modeling Domain Definition

Figure 1 gives a region-wide perspective of the modeling domain for Atlanta. As pictured in Figure 1, this modeling domain consists of a 40 by 40 array of 4 km square grid cells. The proposed modeling domain origin is located at UTM coordinates 660 km easting, 3665 km northing in zone 16 and extends 160 km in the east and north direction. As stated in the Atlanta UAM modeling protocol (SAI, 1988) 5 vertical layer structure is to be used in the UAM: two below the mixing height and three above. The region top will be based on the maximum mixing height occurring during the modeling episode.

In order to accommodate the city-specific analysis of the effects of biogenic emissions on urban ozone formation in Atlanta, there is a region 75 to 100 km wide upwind of Atlanta. This will allow for a 4 to 12 hour loading of biogenic emissions into the atmosphere upwind from the outskirts of Atlanta.

4 PREPARATION OF MODEL INPUTS

An important requirement of the PLANR use of the UAM is that the procedures used to prepare model inputs should be consistent with traditional applications of the model. Procedures to be followed in preparing UAM inputs with limited data availability must be flexible and clearly stated. When there is a lack of data, there must be recommended procedures to be used. However, flexibility is an important component of the construction of UAM inputs when limited data are available. These procedures are currently being refined and evaluated to determine the optimum methodologies for generating UAM inputs with limited data availability.

The preprocessor programs supplied with the 1978-1980 version of the UAM generally rely on an intensive measurement program; data are interpolated from these measurements to obtain gridded fields of input parameters required by the UAM. Over the last 10 years, many of these programs have become outdated. More recent applications of the UAM have prepared input files using only routinely available (although fairly dense) meteorological and air quality data (Hogo, Mahoney, and Yocke, 1988). However, the procedures used for input preparation have been developed on a case-by-case basis and are tailored to data availability. In this section we discuss the initial application of the PLANR procedures for preparing meteorological, air quality, and terrain inputs for the UAM in which UAM modeling inputs are prepared using only routinely available data.

ROUTINE DATA AVAILABLE FOR ATLANTA

On June 3 and 4, 1984 there were six surface meteorological observation sites operating in and around the city of Atlanta. Table 3 lists the six surface sites along with the locations and meteorological variables available at each site. There were no upper-air observation sites located within the UAM modeling domain. Thus, we made use of upper-air observations from five sites that surround the UAM modeling domain for generating wind and mixing height inputs. These five upper-air sites, their locations, and the distance to the city of Atlanta are given in Table 4. The closest upper-air site to Atlanta is Athens Georgia, approximately 100 km to the east-northeast. Air quality data in and around Atlanta during June, 1984 consisted of three monitoring sites as listed in Table 5. There were no air quality data available near the boundaries of the modeling domain for use in prescribing boundary conditions.

TABLE 3. Surface meteorological observation sites, locations, and variables in the Atlanta region.

Site Name	Location UTM (Zone 16) UTMX	UTMY	Variables Measured
Atlanta Hartsfield International Airport	739.580	3726.148	WS, WD, T, T_D, P
Dobbins Naval Air Station	729.590	3755.498	WS, WD, T, T_D, P
Fulton County (Charlie Brown) Airport	729.947	3740.709	WS, WD, T, T_D
Dekalb Peachtree Airport	749.724	3752.306	WS, WD, T, T_D
Conyers Monastery Monitor	772.248	3719.869	WS, WD
South Dekalb Panthersville Monitor	752.780	3730.991	WS, WD, T, T_D

89053 3

TABLE 4. Upper-air observation sites, locations, and distance from Atlanta used in this study.

Site Name	Location Lat	Location Long	UTM Coordinates (Zone 16) UTMX	UTM Coordinates (Zone 16) UTMY	Distance from Atlanta (km)
Athens, GA	35° 57'	83° 19'	839.644	3763.429	109
Nashville, TN	36° 15'	86° 34'	538.182	4012.482	199
Greensboro, NC	36° 5'	79° 57'	1134.426	4016.946	491
Waycross, GA	31° 15'	82° 24'	937.394	3467.152	328
Centerville-Brent, AL	32° 54'	87° 15'	475.841	3640.638	275

TABLE 5. Ozone monitor names and locations.

Monitor JD	Monitor Name	UTM Location (Zone 16) UTMX	UTM Location (Zone 16) UTMY	Years Available (1984 - 1987)
130890002	DeKalb Jr. College (DKLB)	752.78	3730.99	1984 - 1987
130970002	Sweetwater Creek State Park (SWTR)	719.28	3736.10	1987
131210053	MLK Marta Station (MLKM)	743.10	3737.15	1987
132150008	Columbus Airport (COLO)	693.15	3799.91	1984 - 1987
132470001	Conyers Monastery (CNYR)	772.25	3719.87	1984 - 1987

89053 3

PREPARATION OF UAM INPUT FILES

The following paragraphs describe how the UAM input files were prepared for the PLANR application of the UAM to Atlanta.

DIFFBREAK

This file contains the daytime mixing height or nighttime inversion height for each column of cells at the beginning and end of each hour of the simulation. Hourly mixing heights were estimated at several surface meteorological sites through use of the hourly surface measurements of temperature and the twice daily upper-air observations from a representative upper-air site. The Athens Georgia upper-air site was felt to be most representative of upper-air conditions in Atlanta because its proximity to Atlanta. For three of the surface meteorological observation sites that recorded temperature (Fulton County Airport, Dobbins Air Force Base, and South Dekalb monitor) the diurnal variations in mixing heights were calculated using the RAMMET meteorological processor. These hourly values were then input into the standard UAM mixing height interpolation program, DFSNBK (Ames et al., 1985b) using the 1/r interpolation option to produce the hourly spatially varying fields of mixing heights. The maximum daily mixing height varied from approximately 1200 to 1350 meters above ground across the region. Two of the surface observations sites that recorded temperature were not used in the generation of the DIFFBREAK file; one (Dekalb Peachtree Airport) had missing temperature data for 4 June 1984 and data from the other site (Atlanta Hartsfield International Airport) were not available in time to perform the mixing height analysis.

REGIONTOP

This file contains the height of each column of cells at the beginning and end of each hour of the simulation. If this height is greater than the mixing height, the cell or cells above the mixing height are assumed to be within an inversion. For the application of the UAM(CB-IV) to Atlanta a constant 1,400 m AGL region top was used. This value was picked because it is 50 m above the maximum mixing height; thus all five vertical layers of the UAM are contained within the well mixed layer, offering the maximum vertical resolution possible with the five-layer UAM configuration.

WIND

This file contains the x and y components of the wind velocity for every grid cell for each hour of the simulation. There are two steps in creating the wind fields for Atlanta: (1) application of the Diagnostic Wind Model (DWM) (Morris et al., 1988, 1989a; Douglas and Kessler, 1988) using 15 vertical levels and data from the six surface and five upper-air meteorological observation sites; and (2) vertical interpola-

tion of the 15-layer hourly wind fields into the five-layer UAM configuration used for the Atlanta application (see Morris et al., 1989a).

The DWM creates an hourly 15-layer wind field by first creating a wind field by adjusting a domain-mean wind (based on upper-air observations) for terrain effects (kinematic effects, thermodynamically generated slope flows, blocking, and deflection). Then the observational information is added to the wind field by weighting the initial wind field heavily away from the observations and the observed winds heavily in the vicinity of the observations.

The 15-layer wind fields created by the DWM are then vertically averaged into the UAM five layer configuration. Since the surface observations provide a more detailed representation of the air flows in the vicinity of Atlanta and their presence is only felt within the lowest layer of the DWM, the first UAM vertical layer was assumed to have the same wind field as the first DWM layer. The DWM first layer is also weighted 50 percent in the second UAM vertical layer. The wind fields for the remainder of the UAM vertical layers were obtained from the DWM wind fields using weighted averaging. The resultant five-layer wind field was then modified using the procedure suggested by O'Brien (1970), which minimizes the vertical velocity out of the top of the region. In this manner, the boundary concentration assumed to exist above the region top (TOPCONC) does not greatly influence concentrations within the modeling domain.

For the application of the UAM to Atlanta, three separate wind fields were created corresponding to evaluation runs number 1 and 2 and a sensitivity test reported in Appendix G. As will be discussed later in the section on the evaluation of the UAM, these wind fields were created using the procedures described above but differed in definition of the domain-mean wind and the surface observation sites used.

METSCALARS

This file contains the hourly values of the meteorological parameters that do not vary spatially. These scalars are the NO_2 photolysis rate constant, the concentration of water vapor, the temperature gradient above and below the inversion base, the atmospheric pressure, and the exposure class. The NO_2 photolysis rates were calculated for the CB-IV mechanism using procedures described by Schere and Demerjian (1977) and actinic flux data collected by Bass and co-workers (1980) (see Gery, Whitten, and Killus, 1988). The concentration of water was based on measurements of temperature and dewpoint at three of the surface meteorological observation sites. These three values were averaged to obtain the hourly input for the UAM. Water concentrations ranged from approximately 14,000 to 18,000 ppm. An atmospheric pressure value of 1 atmosphere was used.

Exposure class is a measure of near surface stability: +3 during high solar intensity to -2 at night with no clouds. Exposure class was assigned based on the solar inten-

sity: a value of 2 at night and daytime values of either 0 (one hour day/night transition period) to 3. The temperature gradients below (TGRADBELOW) and above (TGRADABOVE) the inversion were based on the twice-daily upper-air soundings taken at Athens, Georgia, and hourly surface temperatures observed at Charlie Brown Airport. Values for TGRADBELOW from the surface to the mixing height (approximately 1300 m AGL) from the Athens evening sounding (1900 LST) are -0.0096, -0.0103, and -0.0107 K/m for June 2 through 4, respectively. Based on these measurements, values for TGRADBELOW were -0.0105 K/m for exposure classes 2 and 3, -0.01 K/m for exposure class 1, and -0.098 for exposure class 0.

The Athens morning sounding (0700 LST) measured values for TGRADBELOW of 0.018 and 0.030 K/m on June 3 and 4 respectively, assuming a mechanical mixing height of 250 m AGL. Observed temperatures at 250 m on 3 and 4 June were, respectively, 295.6 and 297.8 K. Nighttime hourly values for TGRADBELOW were then calculated for June 3 and 4 based on the surface temperature at the Charlie Brown Airport and the measured value at 250 m from the 0700 LST sounding.

For predawn hours, the temperature gradient from 250 m to the region top (1,400 m) from the 0700 sounding at Athens was used, resulting in values for TGRADABOVE of -0.0025 and -0.0075 °K/m for June 3 and 4, respectively. For daytime hours a temperature at the mixing height was calculated for each hour of the day using the surface measurement at the Charlie Brown Airport and the value for TGRADBELOW. Then the hourly temperature gradient between the mixing height and the region top was estimated using the calculated value at the mixing height and the measured temperature from the 0700 sounding at Athens at 1,400 m AGL (290.8 and 290.7 K on June 3 and 4, respectively)

AIRQUALITY

This file contains the initial concentrations of each species for each grid cell at the start of the simulation. Since the UAM was initiated at 12 noon on June 3, 1984, most of the material from the initial conditions were advected out of the region by the morning of 4 June; thus, initial concentrations do not influence ozone formation on 4 June. Accordingly, initial concentrations were assigned to "clean values" as follows:

VOC	25 ppbc (using EKMA default speciation)
ISOP	0.001 ppb
NO_x	1 ppb (split 3/4 NO_2, 1/4 NO)
O_3	40 ppb
CO	200 ppb

89059r2 2

BOUNDARY

This file contains the location of the modeling region boundaries. It also contains the concentration of each species that is used as the boundary condition along each boundary segment at each vertical level. For the application of the UAM to Atlanta, the minimum of a one-cell buffer of unsimulated cells was used (i.e. the boundary conditions), resulting in a simulation region of 152 km by 152 km. As will be discussed in the section on the evaluation of the UAM, two sets of boundary conditions were derived for evaluation runs number 1 and 2. For evaluation run number 1, "clean" values (listed previously) were specified for boundary conditions. However, these clean values may underestimate background concentrations because of the biogenic emissions which increase background VOC and ISOP (isoprene) concentrations above the clean background level. Thus in order to determine a better estimate of background conditions, a UAM simulation was carried out with no anthropogenic emissions (i.e., biogenic emissions and clean boundary concentrations only). During the day, isoprene and VOC concentrations ranged from approximately 0.5 to 2.0 ppb and 35 to 75 ppbC, respectively. Thus for the second evaluation simulation, a 1 ppb ISOP boundary condition was prescribed and VOC boundary conditions were set at 40 ppbC, where the increase from the clean value of 25 ppb was mainly (92%) due to the lower reactive PAR species and the remainder of the increase was due to increases in OLE. Boundary conditions for ozone (40 ppb) and NO_x (1 ppb) were the same as used in evaluation run 1.

TOPCONC

This file contains the concentration of each species for the area above the modeling region. Since the wind fields are processed to eliminate the vertical velocity through the region top, the model results are not sensitive to TOPCONC. Accordingly, the clean concentration values listed previously were used.

TEMPERATUR

This file contains the hourly temperature for each surface layer grid cell. Hourly spatial varying temperatures were obtained by using 1/r interpolation from the surface meteorological observations.

EMISSIONS

This file contains the ground-level emissions of NO, NO_2, CB-IV VOC species categories, and CO for each grid square for each hour of the simulation. Anthropogenic emission estimates were obtained from the 1985 NAPAP county-wide emissions inventory through a several step process which includes updating mobile source emissions from MOBILE-3 to MOBILE-4 based emission factors, applying summer week-

day and episodic temperature adjustments, gridding of data using a known surrogate distribution, and speciation of the VOC and NO_x emissions into the CB-IV mechanism species.

The NAPAP motor vehicle emission categories were split into exhaust and evaporative emissions based on splitting factors using the MOBILE-3 emissions program and the same average temperature as was used in generating the NAPAP inventory. The MOBILE-4 emissions program was then exercised for the episodic temperature conditions on 4 June 1984 to obtain episodic evaporative and exhaust emissions. Estimate of running loss emissions (which are not included in the NAPAP inventory) were then obtained by applying the ratio of the running loss to the exhaust emission factors from the MOBILE-4 to the mobile exhaust VOC emission rate.

The county-wide area source emissions were then mapped to the 40 by 40 4 km^2 modeling domain by assigning each area source Source Classification Code (SCC) category to a known surrogate distribution. Known surrogate distributions include: agriculture, urban, rural, and water from the national Geographical Information Services land-use data base; population from the 1980 census; airports and limited access roadways based on digitizing the locations of airports and freeways from standard USGS maps; and spatial coverage based on the fractional coverage of each grid cell in each county. The gridded area source emissions were then adjusted to hourly emissions for a summer weekday and speciated into CB-IV species based on their SCC codes.

Estimates of biogenic VOC emissions were obtained from EPA's Atmospheric Research and Exposure Assessment Laboratory (EPA/AREAL) on a 1/4° longitude by 1/6° latitude grid for the entire Southeast. The EPA/AREAL had biogenic emission estimates for the entire Southeast for a two-week period during 1980. These emission estimates consider the effects of episodic temperature and solar intensity on the biogenic emission estimates. Based on analysis of surface temperatures, it was determined that 26 August 1980 provided the best match with episodic temperature and light intensity conditions of 4 June 1984. The biogenic emissions from the 1/4° by 1/6° grid were gridded onto the 4 km square grid cells used in the UAM modeling based on spatial covering of grid cells. The biogenic emissions from EPA/AREAL were already speciated into CB-IV species.

The final EMISSIONS file was obtained by merging the gridded NAPAP area source emissions with the low-level point sources and the biogenic emissions. The resultant anthropogenic and biogenic emission rates and their spatial distribution are given in Appendix A. Of particular note is that biogenic VOC emissions account for approximately 55 percent of the VOC emissions within the modeling domain.

PTSOURCE

This file contains the point source information, including the stack height, temperature and flow rate, the plume rise, the grid cell into which the emissions are emitted, and the emissions rates for NO, NO_2, CB-IV VOC categories, and CO for each point source for each hour. The 1985 NAPAP point source emissions file was separated into low-level and elevated points based on plume rise estimates. Those point sources whose plume rise was less than 25 m for typical atmospheric conditions were considered low-level sources and were merged with the EMISSIONS file after applying the summer weekday and diurnal emission profiles supplied as part of the NAPAP point source inventory.

Elevated point sources from the 1985 NAPAP point source file were adjusted to summer episodic conditions with diurnal variation using the adjustments given in the point source file. The emissions were then speciated into CB-IV species based on their SCC and SIC codes. The resultant data was run through the UAM point source preprocessor for input to the UAM. As shown in Appendix A, point source NO_x (including electrical utilities) emissions account for approximately 50 percent of the total NO_x emissions within the modeling domain.

TERRAIN

This file contains the value of the surface roughness and deposition factor for each grid square. Each 4 km^2 grid cell was assigned to a land-use category based on the digitization of a standard USGS map of the modeling region. The land-use categories were then converted to roughness lengths and vegetation factors according to data published by Argonne National Laboratory (see Morris et al., 1989a).

CHEMPARAM

This file contains information regarding the chemical species to be simulated, including reaction rate constants, upper and lower bounds, activation energy, and reference temperature. Reaction rate constants correspond to those given in the report documenting the CB-IV mechanism (Gery, Whitten, and Killus, 1988), except that reactions for methanol (MEOH) and ethanol (ETOH) have also been added to the mechanism (see Morris et al., 1989a).

SIMCONTROL

This file contains the simulation control information, such as the time of the simulation, file option information, default information, and information on integration and chemistry time steps.

5 DEVELOPMENT OF A PLANR BASE CASE FOR ATLANTA

One of the key components of the PLANR use of the UAM is a limitation on the number of diagnostic simulations used to arrive at a base case. This is achieved by relaxing the strict model performance standards expected of the UAM in the past. Although the goal is to achieve a statisfactory level of performance with as few diagnostic simulations as possible, the model must show some skill in predicting ozone observations in order to have confidence that the model will respond properly to changes in emissions.

The minimal performance goal in the past was to have the predicted regional maximum ozone concentration be within 30 percent and in the general location of the peak observed value. Model performance has been considered good if the predicted peak ozone is within 15 percent. Clearly, when model inputs are based only on sparse routine data, rather than intensively measured data as in the past, model performance cannot be expected to always be as good in the past. However, there should be some minimal expectations of model performance since incorrect characterization of base case ozone concentrations may lead to incorrect calculations of ozone reductions due to alternative emission inputs.

The protocols for several recent UAM studies of the impacts of California offshore drilling emissions (Haney et al., 1986; Yocke et al., 1985) defined a minimal model performance standard as follows: (1) the UAM-predicted regional maximum ozone concentration should be within 20 percent and in the general location of the observed maximum, and (2) the UAM predicted maximum at the location of the observed maximum should be within 30 percent of the observed value.

We adopted this model performance standard as a performance goal for the PLANR application of the UAM for Atlanta. However, model evaluation should always include discussions on whether the right answer is being obtained for the right reason. In addition, it may be useful to discuss approaches that may improve UAM performance but which also may deviate slightly from the demonstration of the PLANR use of the UAM. The PLANR use of the UAM for Atlanta discussed here involved three diagnostic simulations before an adequate base case was obtained that satisfied the minimal performance goal.

DIAGNOSTIC RUN 1

In the first diagnostic simulation, the UAM was exercised with clean boundary conditions (i.e., 40 ppb ozone, 25 ppbc VOC, 0.001 ppb ISOP, and 1 ppb NO_x), anthropogenic and biogenic emissions, and a first estimate of the wind field. The wind field was created using the DWM: the vertically varying domain-mean wind was defined as the vector average from the five upper-air soundings surrounding the modeling domain. The upper-air data obtained from the National Climatic Data Center (NCDC) on the TD9743 format was missing data from the lowest 1,500 m AGL of the 0700 June 4 upper-air sounding at Athens, Georgia. In addition, surface wind data was used from all of the surface sites, except Atlanta Hartsfield Airport, which was inadvertently left out of the initial analysis. Appendix B contains the wind fields generated by the DWM using the routine data from Atlanta and the procedures discussed above.

Hourly average predicted ozone concentrations for evaluation run 1 are contained in Appendix C. A comparison of predicted versus observed hourly ozone concentrations for the three monitors within the UAM modeling domain is given in Figure 2. As seen in Appendix C and Figure 2, the regional maximum predicted ozone concentration is 13.54 pphm, within 8 percent of the observed maximum of 14.7 at the Conyers Monastery (CNYR) ozone monitor. However, the predicted regional maximum is approximately 28 km (7 grid cells) to the north-north-west of the observed value. The maximum predicted ozone at the CNYR site for evaluation run 1 is 8.79 pphm, an approximate 40 percent underprediction of the observed maximum at that site. Model performance is better at the South Dekalb ozone monitor, where the maximum daily observed value of 13.0 pphm is reproduced to within 15 percent (11.1 pphm). However, concentrations are underpredicted at the Dallas (DLLS) ozone monitor, which lies upwind of the city of Atlanta. The maximum daily observed ozone concentration at DLLS of 7.8 pphm is underpredicted by about 60 percent (4.6 pphm).

DIAGNOSTIC RUN 2

Improvements Over Diagnostic Run 1

An analysis of the observed ozone features for 4 June 1984 indicates two major deviations of the predictions from the observations for diagnostic run 1: (1) the gross underprediction of the upwind monitor indicates that the ozone and ozone precursor loadings upwind of Atlanta are too low; and (2) the predicted cloud of elevated ozone concentrations appears to be too far north during the afternoon of 4 June 1984.

The fact that diagnostic run 1 is underpredicting the ozone at the upwind (DLLS) monitor is not surprising since clean background concentrations were used for the upwind boundary conditions. In particular, given the presence of biogenic VOC emissions in the area, the boundary VOC concentrations used in diagnostic run 1 (25 ppbc

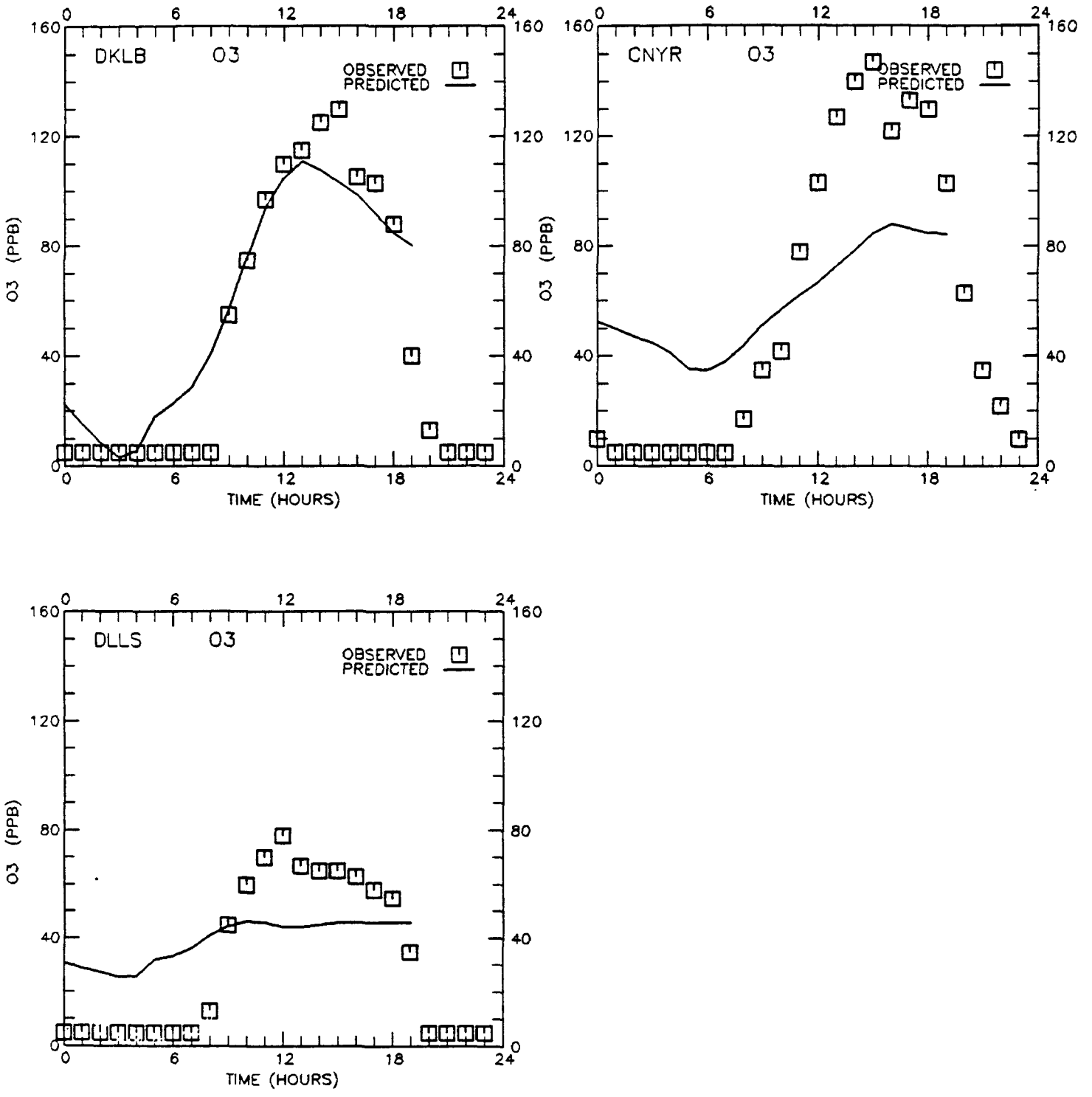

FIGURE 2. Observed and predicted ozone concentrations (ppb) for the Atlanta evaluation run 1.

VOC; 0.001 ppb ISOP) are probably too low. In order to determine the magnitudes of VOC concentrations to use as boundary conditions, a UAM simulation without the anthropogenic emissions (i.e., biogenic emissions and clean boundary conditions only) was performed. This simulation of biogenic emissions only produced a maximum buildup of ISOP and VOC concentrations that ranged across the modeling domain from, respectively, 0.5 to 2.0 ppb and 35 to 75 ppbC. Thus we chose values a little lower than the midpoint of the maximum buildup, 1 ppb for ISOP and 40 ppbC for VOC, as boundary conditions in diagnostic run 2.

An examination of the observed ozone concentrations at the DLLS monitor on 4 June 1984 (see Figure 2) reveals that the observed maximum daily ozone concentration of 7.8 pphm occurs fairly early in the day (12 noon). This suggests that the peak observed ozone concentration at DLLS is mainly due to entrainment of ozone concentrations aloft as the mixing height rises rather than to local production of ozone due to local sources. Thus the boundary concentrations for ozone, and possibly NO_x, could justifiably be increased. However, we elected to keep the fairly low values for ozone and NO_x boundary conditions (40 and 1 ppb, respectively) for diagnostic run 2.

An examination of the observed winds, the predicted wind fields in diagnostic run 1 (Appendix B), and patterns of predicted hourly ozone concentrations (Appendix C) indicates that a southerly component in the wind field may occur too early in the afternoon. The persistence of a more northerly component in the winds in the late morning and early afternoon would result in the predicted cloud of elevated ozone concentrations impacting the CNYR monitor, producing a higher peak at that site. However, the wind measurements at the CNYR site observed southerly winds from about noon on. To determine whether this southerly wind was due to local effects or larger-scale flow features, the Georgia State meteorologist was consulted. The CNYR wind observation site is located near a grove of trees and may not be representative of mesoscale wind flows, and the Atlanta Hartsfield Airport wind observation site (which was inadvertently left out of the original analysis) was better sited (D. Kemmerick, personal communication, 1989). Thus, the CNYR wind measurement was eliminated and the Atlanta Hartsfield Airport winds added for the next evaluation run.

A new definition of the domain-mean wind was also used for the diagnostic run 2. Instead of a linear interpolation to the hour in question of a vector average of the five twice-daily upper-air soundings that surround Atlanta, most of which are over 200 km away, the Athens Georgia upper-air sounding alone was used to define the domain mean wind. Wind data for the lowest 1,500 m of the 4 June sounding at 1900 LST was supplied by the state of Georgia.

A further modification was made on the boundary definition of the diagnostic run 2. An examination of the spatial distribution of emissions (Appendix A) and the predicted hourly ozone concentrations from diagnostic run 1 (Appendix C) indicated that portions of the northern, southern, and western portions of the modeling domain could be eliminated without affecting the results. The boundary was thus modified

and diagnostic run 1 was rerun to verify that the new boundary did not affect the computations.

Results of the Simulation

Diagnostic run 2 differed from run 1 in that (1) a higher VOC value was used (40 compared to 25 ppbC) and higher ISOP boundary conditions were used (1 compared to 0.001 ppb); (2) the domain-mean wind for the DWM came from the Athens upper-air sounding rather than a vector average from the five upper-air soundings; (3) the CNYR surface wind measurement was eliminated and the Atlanta Hartsfield wind measurement added to the analysis; (4) a minor mistake in the emissions inventory was corrected; and (5) the boundary was modified. The new UAM layer 1 wind fields generated for diagnostic run 2 are shown in Appendix D. The resulting predicted hourly ozone concentrations for evaluation run 2 are given in Appendix E. The predicted regional maximum ozone concentration is 13.2 pphm, within approximately 10 percent of the observed maximum. The predicted maximum ozone is approximately 22 km to the north of the observed maximum ozone. However, as shown in Figure 3, at the location of the peak observed ozone, the maximum observation is replicated to within less than 30 percent. In addition, the daily maximum observed ozone concentrations at the DKLB and DLLS monitor are reproduced to within, respectively, 18 and 36 percent.

Comparison of UAM grid cell-average concentrations with the point observations at the site of the observed ozone is a particularly stringent test. A slight incorrect characterization of the wind field, as is very likely when sparse data sets are used, will result in the placement of the elevated ozone plume away from the ozone monitor resulting in poor model performance statistics. However, this displacement of the ozone plume may not affect the model's response to emission control requirements. Thus it has been suggested that concentrations in adjacent grid cells (i.e., nearest neighbor) also be compared with the observed value in order to determine whether the ozone cloud is just slightly displaced (Seinfeld, 1988a; Burton, 1988). Figures 4 and 5 compare the observed and predicted hourly ozone concentrations resulting from a one-cell and two-cell search of the predicted concentrations closest to the observed values. At the CNYR monitor the predicted maximum daily ozone concentration for the point, a one-cell search, and a two-cell search matches the observed value of 14.7 pphm to within, respectively, 29, 25, and 22 percent. However, at the other two monitors (DKLB and DLLS), the nearest-neighbor analysis also produced improvements in model performance; the point, one-cell search, and two-cell search matches the peak observed observation to within 18, 8, and 5 percent for the DKLB monitor, and 36, 32, and 23 prcent for the DLLS monitors. For the CNYR monitor, it appears the elevated cloud of ozone concentrations is too far north. At the DKLB monitor the predicted ozone concentrations in the general vicinity (i.e., within two grid cells) are in very good agreement with the observed maximum values.

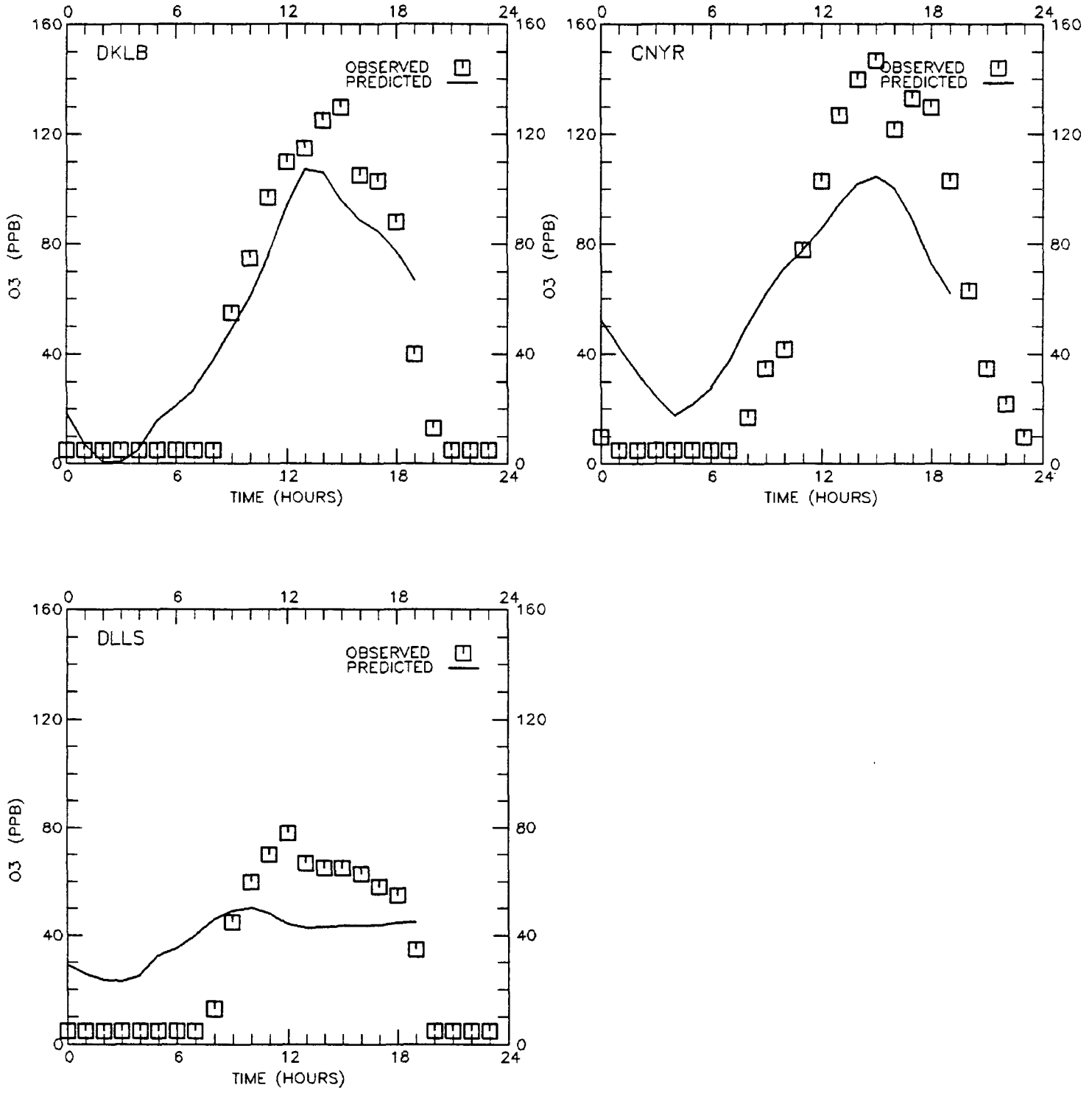

FIGURE 3. Observed and predicted ozone concentrations (ppb) for the Atlanta evaluation run 2.

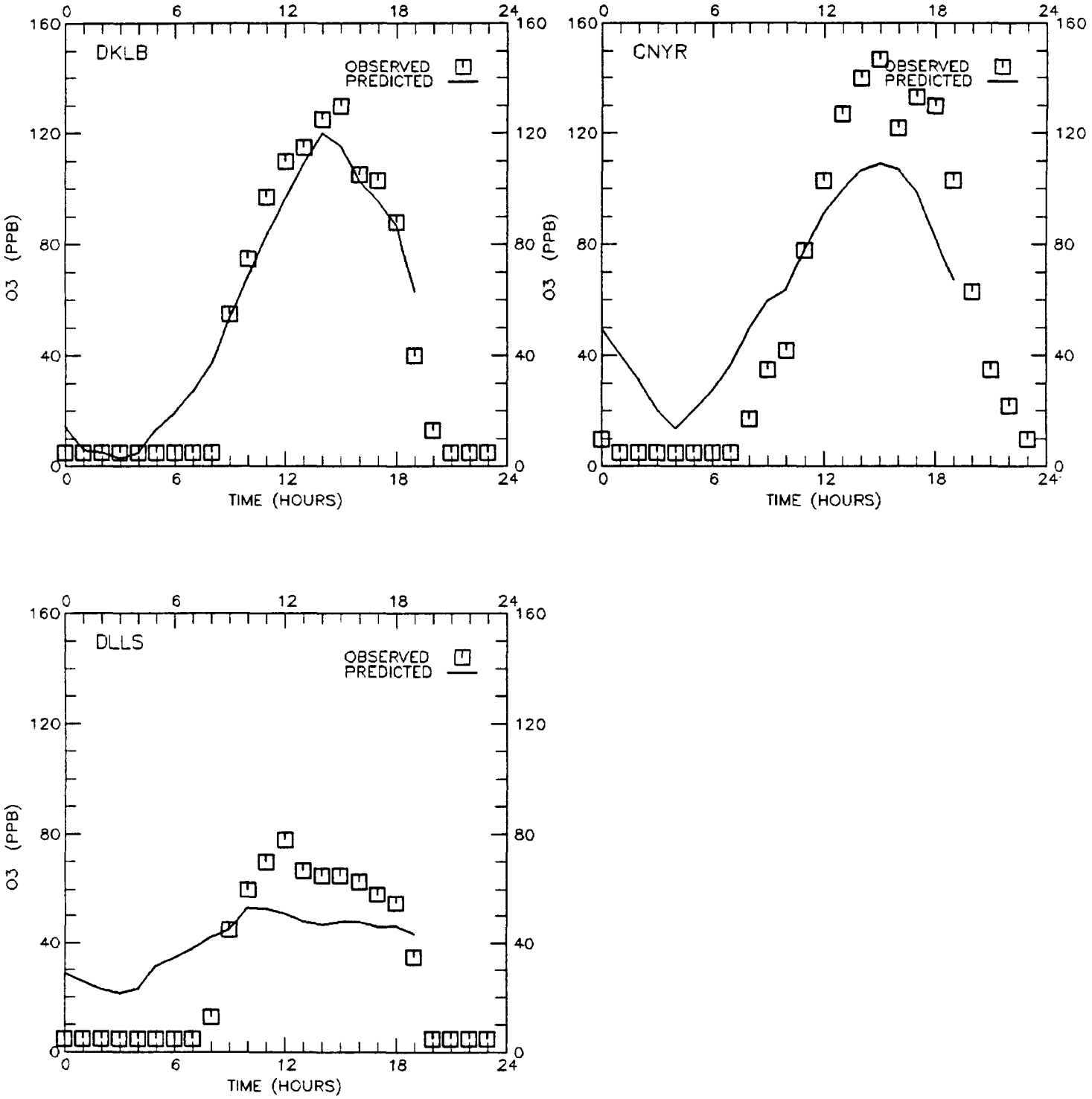

FIGURE 4. Observed and nearest-neighbor predicted (one-cell search) ozone concentrations (ppb) for the Atlanta evaluation run 2.

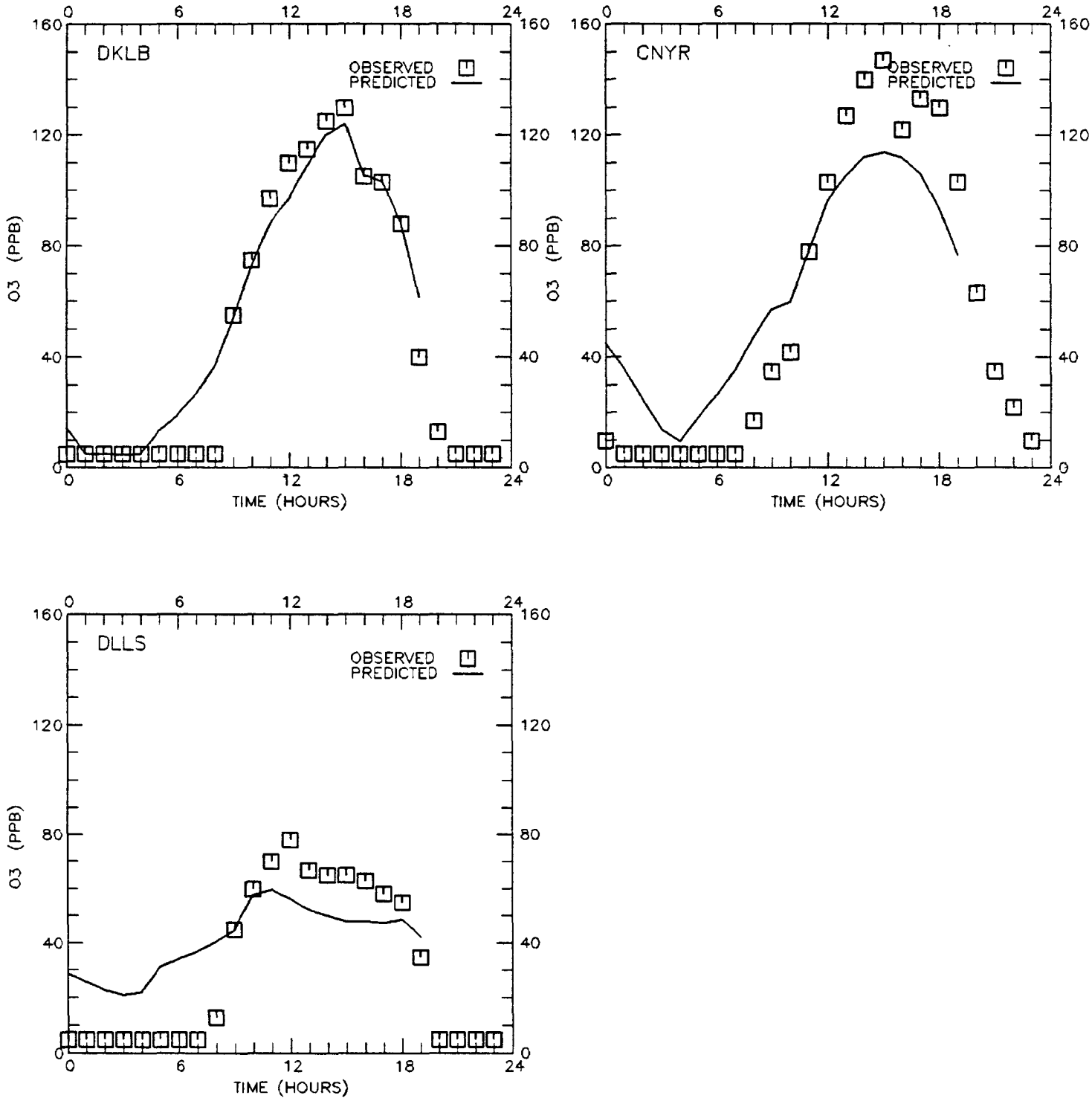

FIGURE 5. Observed and nearest-neighbor predicted (two-cell search) ozone concentrations (ppb) for the Atlanta evaluation run 2.

Figure 6 shows a scatter plot and model performance statistics between predicted and observed hourly ozone concentrations for evaluation Run 2. Also contained in Figure 6 are analyses of the residuals of the predicted and observed ozone concentrations. As indicated in Figure 6 and the time series plots in Figure 3, diagnostic run 2 tends to overpredict the nighttime ozone concentrations and underpredict the peak daytime values. As a result, the bias between predicted and observed hourly ozone concentrations is very low (less than 1 percent). However, the gross error (average absolute error) is fairly high (43 percent). The predicted hourly ozone concentrations for diagnostic run 2 follow the diurnal and spatial variations of the observations well, as indicated by the high correlation coefficient of 0.9. Nevertheless, even when all time and space constraints are removed, the simulated peak ozone value 13.2 pphm is 10% less than the observed peak (14.7 pphm).

Possible Improvements to Diagnostic Run 2

Improvements in model performance from diagnostic run 2 could be obtained by raising the VOC, NO_x, and ozone boundary conditions, which may be justified based on the underprediction of the ozone at the upwind monitor (DLLS) and the low values current being used. The peak observed ozone concentration at the upwind monitor occurs fairly early in the day (12 noon), which indicates it is probably due to entrainment of an elevated ozone concentration aloft rather than local chemistry.

Improvements can also be made in the wind field. The wind field still has a significant southerly component in the late morning and afternoon, which appears to advect the elevated ozone cloud away from the CNYR monitor. Some wind shear is also present between UAM layers 1 and 2, which broadens the ozone peak from the urban emissions, resulting in a lower predicted regional maximum ozone concentration. Since in the afternoon UAM layers 1 and 2 are both contained within the well-mixed layer, one would not expect there to be significant amounts of wind shear between these layers. As noted earlier, during 4 June 1984 a high-pressure ridge passed across Atlanta, which resulted in a turning of the winds from the NNE to the SSW. This turning is present in the 0700 and 1900 LST upper-air soundings at Athens, but the exact hours of the turning of the upper-level winds cannot be determined from the hourly surface wind measurements, which are subjected to local influences. The use of linear interpolation of the 0700 and 1900 LST soundings at Athens results in a continuous turning of the wind throughout the day, when in actuality it probably occurs within a few hours as the high-pressure ridge passes through. If the upper-level winds persist with a more northerly component during the morning hours, as is present in the 0700. Athens sounding, and then turns to the SSW in the afternoon, the elevated ozone cloud could then possibly impact the CNYR monitor at the proper time. In addition, use of identical wind fields in layers 1 and 2 during periods of rapid vertical mixing to eliminate the wind shear below the mixing height may result in a sharper predicted peak concentration; the Athens upper-air sounding does support the presence of some wind shear in the mixed-layer.

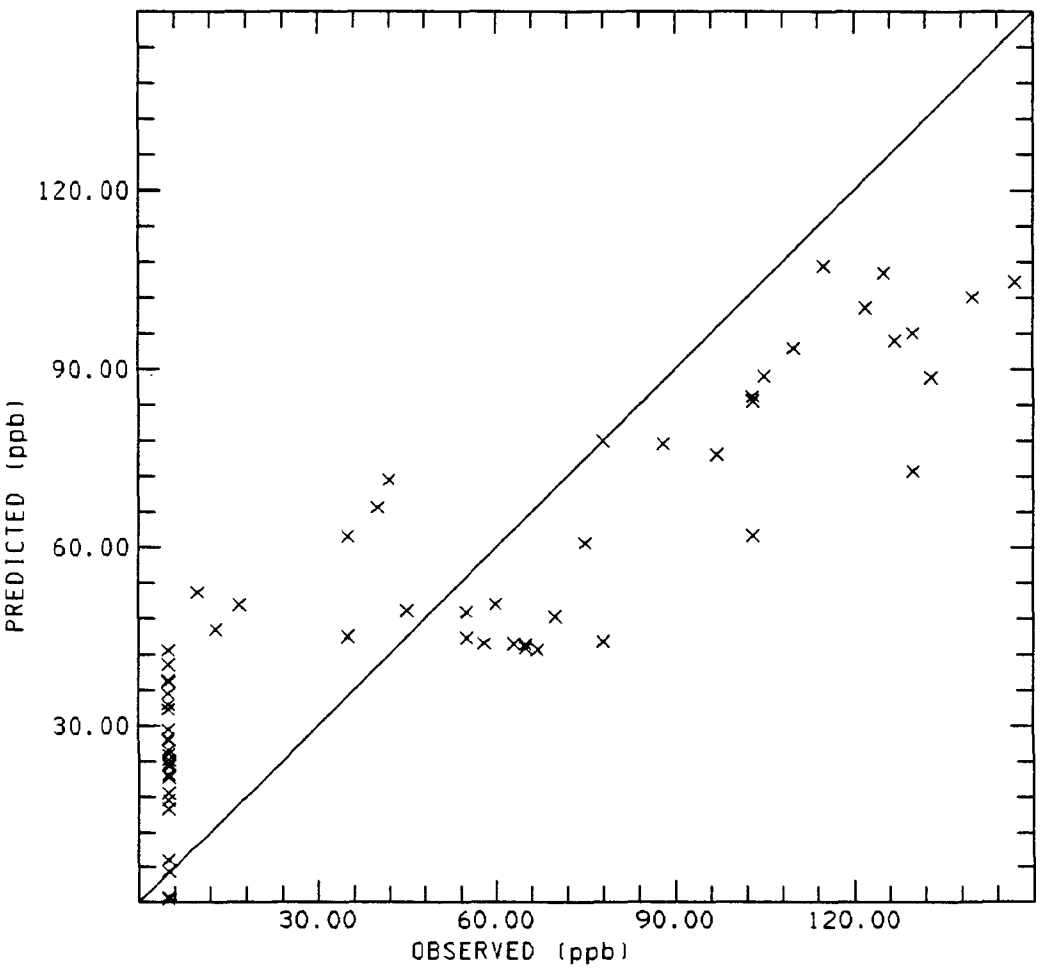

MOMENTS OF THE PROBABILITY DENSITY FUNCTION

	OBSERVED	PREDICTED
AVERAGE	50.39999	50.88372
STANDARD DEVIATION	47.63355	29.03820
SKEWNESS	0.51320	0.36600
KURTOSIS	-1.22432	-0.88317
OTHER MEASURES		
MEDIAN	40.00000	44.24000
UPPER QUARTILE	88.00000	72.92999
LOWER QUARTILE	5.00000	27.54000
MINIMUM VALUE	5.00000	0.53000
MAXIMUM VALUE	147.00000	107.30000

SKILL OF PREDICTION PARAMETERS

CORRELATION COEFFICIENT OF PREDICTED VERSUS OBSERVED 0.896
THE BOUNDS OF THE CORRELATION AT THE CONFIDENCE LEVEL OF 0.050 ARE
LOW BOUND 0.831 HIGH BOUND 0.937
RATIO OF OVER TO UNDER PREDICTIONS 1.069
PERCENT OF OVER PREDICTIONS GREATER THAN 200 PERCENT OF THE OBSERVED 38.333
PERCENT OF UNDER PREDICTIONS LESS THAN 50 PERCENT OF THE OBSERVED 3.333

FIGURE 6a. Scatterplot and model performance statistics for hourly ozone concentrations and evaluation run 2 (N = 60).

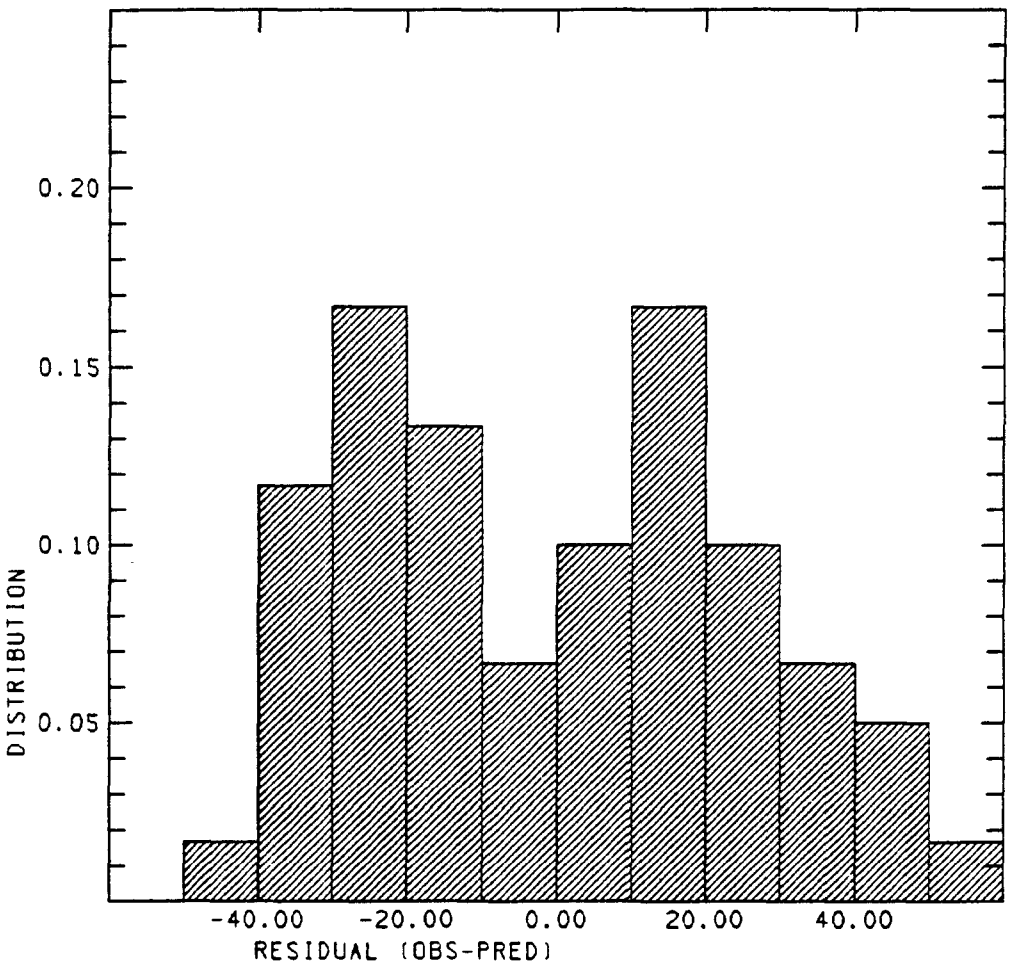

THE BINSIZE EQUALS 10.000

RESIDUAL ANALYSIS

AVERAGE	-0.48384
STANDARD DEVIATION	25.16143
SKEWNESS	0.20968
KURTOSIS	-1.08769
OTHER MEASURES	
MEDIAN	-0.21000
UPPER QUARTILE	18.80000
LOWER QUARTILE	-22.82000
MINIMUM VALUE	-42.45000
MAXIMUM VALUE	57.07001

BIAS CONFIDENCE INTERVAL
AT THE 0.0500 LEVEL
LOWER BOUND -12.5186
UPPER BOUND 11.5509

STD RESIDUAL CONFIDENCE INTERVAL
AT THE 0.0500 LEVEL
LOWER BOUND 480.3294
UPPER BOUND 879.6230

THE MEASURES OF GROSS ERROR
THE ROOT MEAN SQUARE ERROR IS 24.96
THE AVERAGE ABSOLUTE ERROR IS 21.88

VARIOUS MEASURES OF RELATIVE VARIABILITY
OBSERVATION COEFFICIENT OF VARIATION
0.9451
RESIDUAL COEFFICIENT OF VARIATION
0.4992
RATIO OF RESIDUAL TO OBSERVED ST. DEV.
- 0.5282

FIGURE 6b. Residual analysis of observed minus predicted hourly ozone concentrations for evaluation run 2 (N = 60).

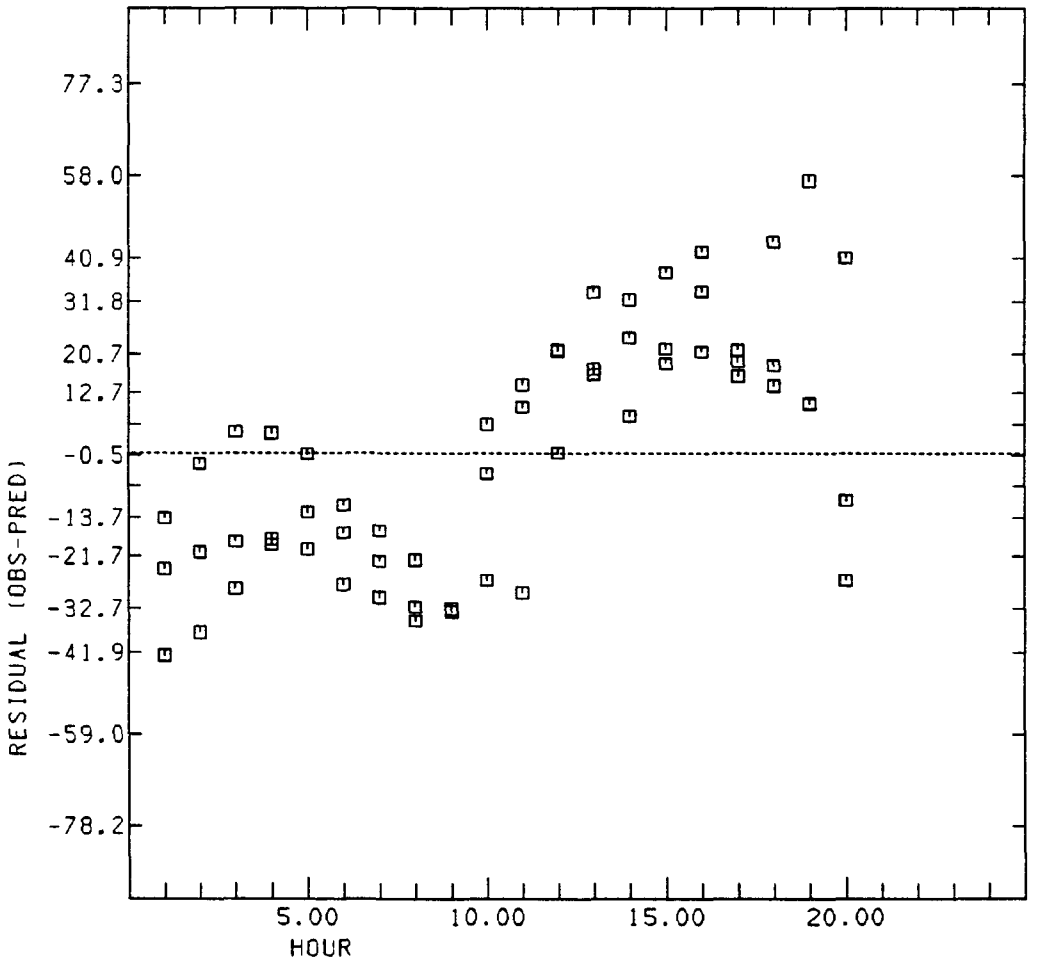

THE LINEAR MODEL PARAMETERS
THE CORRELATION IS 0.6804
THE LOWER BOUND IS 0.5155
THE UPPER BOUND IS 0.7967
AT THE 0.0500 PERCENT LEVEL
THE Y-X LINEAR MODEL INTERCEPT IS 10.576
THE Y-X LINEAR MODEL SLOPE IS 0.157
THE X-Y LINEAR MODEL INTERCEPT IS -31.398
THE X-Y LINEAR MODEL SLOPE IS 2.944

FIGURE 6c. Plot of residuals versus time of day for evaluation run 2 (N = 60).

In addition, there is a very large uncertainty in the biogenic emission rates and speciation as well as uncertainties in the chemistry of biogenic species. Another possible explanation for the underprediction of the observed ozone peak at Conyers is that the 1985 NAPAP inventory underestimates the amount of VOC emissions. There are still many uninventoried sources whose individual emissions may be small, but when combined together may produce a significant impact. A further possible reason for the underprediction is that the wind speeds are too high. There has been some discussion that wind speeds reported at FAA sites (instantaneous 1-minute averages) tend to be higher than the hourly integrated values. Thus, as a sensitivity simulation, all observed wind speeds at FAA sites were reduced 50 percent and new UAM wind fields were created. The results of this sensitivity test are discussed in Appendix G.

Although implementation of some of the above changes to the boundary conditions and wind fields would probably improve model performance, the use of those procedures may not be consistent with some of the objectives of this study, namely the demonstration of the PLANR use of the UAM. Thus, since model performance from diagnostic run 2 satisfies the model performance goal, it was deemed a suitable base case. Nevertheless we recommend that when the UAM(CB-IV) and associated preprocessor programs are delivered to the state of Georgia, they should carry out sensitivity studies like those discussed above (and presented in Appendix G), which may improve the UAM inputs data bases and model performance. This exercise will also help them gain experience with the causes and effects of UAM inputs on predicted ozone concentrations.

6 APPLICATION OF THE UAM TO ATLANTA FOR EMISSION REDUCTION SCENARIOS

The UAM was exercised for several different emission scenarios using the UAM modeling inputs corresponding to evaluation run 2. Two base case emission scenarios are used: with biogenic emissions and without biogenic emissions. Different across the board anthropogenic VOC emission reduction scenarios are examined in order to determine what level of anthropogenic VOC emission reductions are required in order to reduce the peak observed ozone concentration of 14.7 pphm to below the NAAQS ozone standard of 12 pphm. The following emission scenarios were used:

Base case (all anthropogenic emissions) with biogenic emissions
- 30% reduction in anthropogenic VOC emissions
- 60% reduction in anthropogenic VOC emissions
- 90% reduction in anthropogenic VOC emissions

Base Case (all anthropogenic emissions) without biogenic emissions
- 30% reduction in anthropogenic emissions
- 60% reduction in anthropogenic emissions
- 90% reduction in anthropogenic emissions

TRACER SIMULATION

Before conducting a UAM modeling analysis, it is useful to perform a weighted tracer simulation for the two principle ozone precursors, VOC and NO_x, in order to obtain a rough estimate of contributions of initial concentrations, boundary conditions, and emissions to predicted concentration levels. In a weighted tracer simulation, the UAM is run in an inert mode (i.e., no chemistry or deposition) with several different "colored" tracers (species) that represent the major contributers to VOC and NO_x concentrations within the modeling domain. In the weighted tracer simulation for Atlanta different colored tracers were used for initial concentrations, lateral boundary conditions (four colors, one for each face), top boundary conditions, anthropogenic area source emissions, biogenic area source emissions, and point source emissions.

Appendix F displays the results of this tracer simulation at 0800, 1200, and 1600 LST on 4 June 1984. By 0800 initial concentrations of NO_x (Appendix F-1a) and VOC (Appendix F-2a) are almost completely advected out of the region and only affect

the extreme southeastern portion of the modeling domain. By noon (Appendixes F-3 and F-4), initial concentrations have no influence in the modeling domain. At noon, NO_x concentrations are dominated by emissions, where, downwind of Atlanta (i.e., the location of the maximum predicted ozone concentration) area source NO_x contributes over 70 percent, point sources contribute about 20 percent, and boundary NO_x contributes approximately 10 percent. Boundary VOC contributes a higher percentage to the total tracer VOC downwind of Atlanta than seen for NO_x where the percentage contribution of boundary, anthropogenic emissions, and biogenic emissions at 12 noon are approximately 30, 50, and 20 percent. The relative contributions to total NO_x and VOC tracer at 1600 LST is approximately the same as for 12 noon (Appendixes F-5 and F-6).

In regions of the UAM modeling domain away from the influences of emissions from the city of Atlanta, biogenic and boundary VOC dominate the total VOC tracer concentration. Because of the presence of several large power plants within the UAM modeling domain (see Appendixes F-3d and F-5d) the point source NO_x dominates the NO_x tracer concentrations downwind of the power plants and the boundary NO_x concentration does not contribute significantly to NO_x tracer concentrations in the interior of the UAM modeling domain.

UAM MODELING RESULTS

The predicted regional maximum ozone concentration for the base case with and without biogenic emissions are, respectively, 13.22 and 12.28 pphm. The modeling objective is to compare the levels of anthropogenic VOC control (with and without biogenics) required to effect similar percentage reductions in the regional peak ozone changes. Since the base case peaks are dissimilar, the simulations will address the level of reductions required to reduce regional peak ozone by 18.4 percent (equivalent to reducing the observed peak from 14.7 to 12.0 pphm).

Table 6 lists the predicted regional maximum ozone concentrations, percent reduction of the maximum ozone concentration, and the maximum predicted ozone concentration normalized to the observed peak value for each of the emission scenarios. The results from Table 6 are graphically shown in Figure 7. According to Figure 7, to reduce the regional maximum ozone concentration 18.4 percent (i.e., reduce the maximum observation from 14.7 to 12.0 pphm), a 100 and 62 percent control of anthropogenic VOC emissions is required for the cases with and without biogenic emissions, respectively. (Since the UAM underpredicts peak ozone (13.2 pphm) relative to the observed peak (14.7 pphm), model calculations for attainment were adjusted by normalizing the predicted peak ozone to the observed peak.) If one considers the ozone NAAQS as 12.4 pphm, then an 87 and 52 percent control of anthropogenic VOC emissions are required to reduce the predicted regional maximum ozone concentration by 15.6 percent for the, respectively, scenarios with and without biogenic emissions. In either case, the model calculations indicate that the inclusion of biogenic emissions in VOC control strategies for Atlanta on this day results in an

TABLE 6. Regional maximum ozone concentrations (pphm) predicted by the UAM for the different emission scenarios.

	Maximum Ozone Concentration pphm	Percent Reductions from Base Case	Maximum Ozone Normalized to Peak Observation (pphm)
Peak Observed	14.7	0.0	14.7
Ozone NAAQS*	12.0	18.4	12.0
<u>With Biogenics</u>			
0% VOC Reduction	13.22	0.0	14.7
30% VOC Reduction	12.68	4.1	14.1
60% VOC Reduction	11.91	9.9	13.2
90% VOC Reduction	11.08	16.2	12.3
<u>Without Biogenics</u>			
0% VOC Reduction	12.28	0.0	14.7
30% VOC Reduction	11.16	9.1	13.4
60% VOC Reduction	10.09	17.8	12.1
90% VOC Reduction	8.98	26.9	10.7

* Technically, the ozone NAAQS is 0.12 ppm rounded. Thus, an ozone concentration of 12.4 pphm (15.6% reduction from observed peak) is considered attainment.

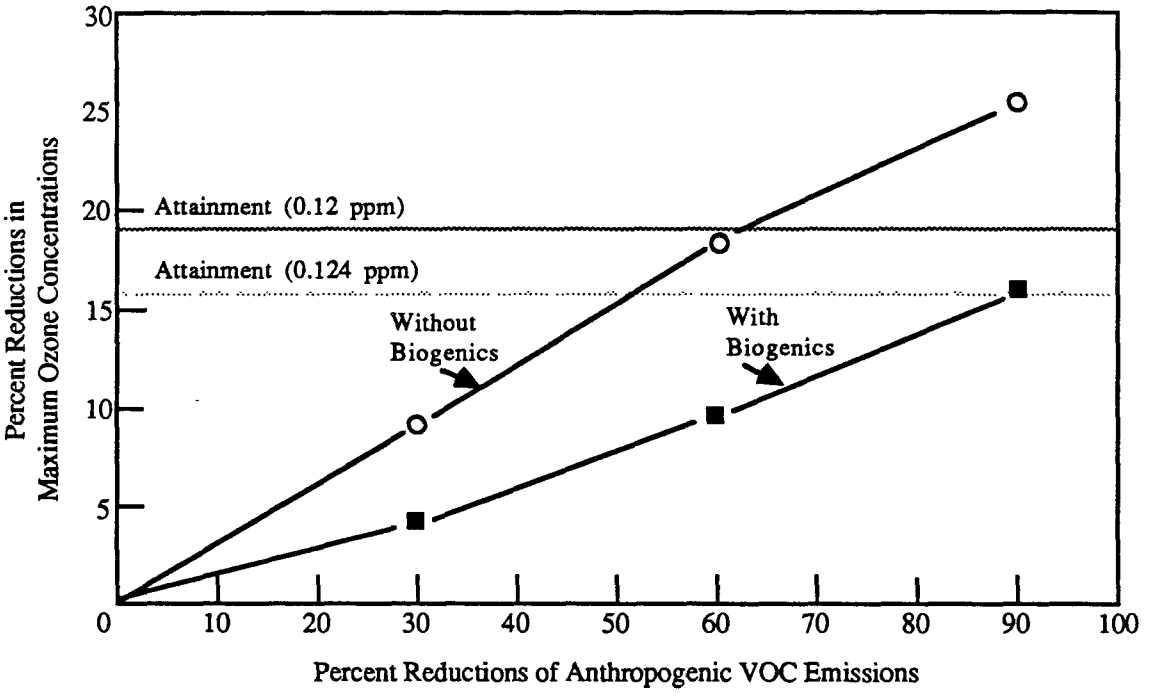

FIGURE 7. Relationship between percent reduction of anthropogenic VOC emissions to percent reduction of the regional maximum ozone concentration with and without biogenic emissions.

additional 35 to 40 percent control on anthropogenic VOC emissions over the case when biogenic emissions are not included.

COMPARISON WITH A PREVIOUS STUDY

As noted previously, a similar analysis of effects of biogenic emissions on VOC control strategies for Atlanta on this day was carried out by Chameides and co-workers using the EKMA model (Chameides et al., 1988). Over the 15-hour EKMA modeling period they estimated biogenic emissions to be 30 kg/km^2 for isoprene, and a total biogenic VOC emission rate of 50 kg/km^2. They also estimated daily total biogenic emission rate of 65 kg/km^2. In their EKMA analysis, biogenic emission rates were varied from zero to 50 kg/km^2 and were assumed to be isoprene. The EPA has summarized biogenic VOC flux rates for 12 other biogenic VOC inventories (EPA, 1984). These values for the other biogenic inventories generally range from 780 to 2,540 µg/m^2-h, with one extreme value at 8,890 µg/m^2-h. The biogenic emission rates of 30, 50, and 65 kg/km^2 reported by Chameides and co-workers translate into biogenic flux rates of 2,000, 3,333, and 2,708 µg/m^2-h. (Note that the 65 kg/km^2 is a daily total.) In our study we used a 24-hour average biogenic emission flux for the UAM modeling domain of 2,197 µg/m^2-h. Thus our study and the work of Chameides and co-workers used similar estimates of biogenic emission flux rates that are on the high end, but well within the range of biogenic fluxes of other studies (EPA, 1984). Due to the large amount of foliage in the Southeast, it is expected that biogenic emission fluxes for the Atlanta region are on the high end of continental flux estimates.

However, there are some differences in the emissions used in this study and those used in the work of Chameidies and co-workers. These differences include the speciation of the biogenic emissions into CB-IV species and the total anthropogenic VOC and NO_x emissions used. Chameides and co-workers assumed that all of the biogenic emissions were isoprene in their EKMA analysis, whereas our study assumed that isoprene made up only 19 percent by weight of the 24-hour total biogenic emissions. (Note that isoprene contributed about 25 percent of the total biogenics for the 15 daylight hours.) The less reactive CB-IV species PAR made up the largest portion of the biogenic emissions in this study (65 percent by weight), with the remainder of the biogenic emissions assumed to be the CB-IV species OLE. Since isoprene is much more reactive than PAR, Chameides and co-workers used a more reactive biogenic emissions inventory than was used in our study.

Chameides and co-workers estimated that without biogenic emissions, a 30 percent reduction of anthropogenic emissions is required in order to reduce the maximum observed ozone concentration of 14.7 to 12.0 pphm. In contrast, we estimated that a 62 percent control of anthropogenic VOC emissions is required to reduce the maximum observed value from 14.7 to 12.0 pphm without biogenics. There may be several reasons for the differences in VOC emission control requirements predicted by the UAM and EKMA.

(1) A lower base case maximum daily ozone concentration (12.28 pphm) was used in UAM than was used in the EKMA (14.7 pphm). Thus, a larger percentage of the UAM-predicted maximum daily ozone concentration is due to background concentrations, which will not be affected by emission control strategies.

(2) The UAM was exercised with boundary conditions that reflected the presence of upwind emission sources (anthropogenic and biogenic). Thus, again, a larger fraction of the UAM-predicted maximum daily ozone concentration is due to background, which will not be affected by anthropogenic VOC reductions.

(3) Due to changes in the reactivity and chemistry of the atmosphere in the different emission reduction scenarios, the regional maximum ozone concentration predicted by the UAM does not occur at the same location in each scenario. If changes in emissions causes the maximum ozone concentration to lie outside of the EKMA trajectory, then the maximum observed ozone cannot be simulated by EKMA, and EKMA will overstate the ozone reductions due to the emission reductions.

(4) The observed vertical wind profile at Athens, Georgia and the UAM layer 1 and 2 wind fields both exhibit some wind shear in the mixed-layer. This wind shear, which cannot be simulated by EKMA, results in a larger portion of the predicted maximum ozone concentration being attributable to background conditions rather than to urban emissions from Atlanta.

(5) The UAM modeling analysis included the emissions from several large power plants in the region (50 percent of the NO_x inventory) that were not accounted for in the EKMA analysis. These NO_x emissions combined with the background VOC concentrations may produce ozone concentrations that will not be affected by the anthropogenic VOC emission reductions.

(6) The anthropogenic emission inventory used in this study most probably underestimates actual anthropogenic VOC emissions. The annual NAPAP inventory, which is probably an underestimate to begin with, is adjusted to a typical summer weekday based on average summer conditions. Ozone episodes tend to be highly correlated with hotter than normal temperatures, although 4 June 1984 was not an excessively hot day. Except for mobile sources, which were adjusted to episodic temperature conditions based on MOBILE-4, VOC emissions (e.g., solvent use and other evaporative emissions) were not adjusted to the higher emission rates expected on a hotter than normal day.

(7) The wind speeds may be too high in the UAM simulation, causing excessive dilution of the urban plume.

Of particular note in these differences is the underprediction of the observed peak ozone concentration (14.7 pphm) by the UAM in evaluation run 2 (13.2 pphm). To investigate this effect, a sensitivity test reduced the observed wind speeds at some of the surface sites. The results of this sensitivity test are discussed in Appendix G.

Despite the differences between our study and the study reported by Chameides and co-workers (1988), both studies conclude that by including biogenic emissions in an attainment demonstration for Atlanta for June 4 1984, an additional 35 to 40 percent anthropogenic emission reduction over the case without biogenics is required to meet attainment of the ozone NAAQS. Chameides and co-workers report that the anthropogenic VOC emission control requirements increase from 30 to 70 percent, whereas we report that an increase from 62 to 100 percent is needed. However, because the UAM underpredicts the peak observed ozone concentration, and for the reasons cited above, it is probable that the UAM is overstating the VOC emission control requirements.

DISCUSSION

There were two main objectives of this study: (1) the demonstration of the PLANR use of the UAM for the city of Atlanta, and (2) the analysis of the effects of biogenic emissions on VOC control strategies. Using only routinely available data, it has be shown that adequate UAM modeling inputs can be created using objective techniques and a minimal amount of diagnostic simulations. It has also been demonstrated that biogenic emissions do affect VOC control strategies for ozone attainment. However, in a sense these two objectives are not entirely consistent with each other, since more accurate results of the effects of biogenic emissions on ozone attainment demonstration would most likely be obtained if the UAM base case simulation exhibited better model performance. Improved UAM modeling inputs could be generated either by using data from an intensive measurement network or through modifying the existing inputs by an experienced UAM model user. However, neither of these approaches is consistent with the demonstration of the PLANR use of the UAM. Because of this conflict of objectives, additional uncertainties are introduced into the analysis of the effects of biogenic. These uncertainties are addressed somewhat in the sensitivity analysis discussed in Appendix G.

As noted previously, several other sources of uncertainity in the analysis need to be recognized when interpreting the results. Foremost among these are the uncertainties in the biogenic and anthropogenic emission inventories. These uncertainties may be biased in such a fashion that the calculated effects of biogenic emissions presented here possibly are overestimates of the actual effects. This is because the biogenic VOC emissions may be overestimates of actual emissions, and the anthropogenic VOC emissions are most likely underestimates of actual emissions. Recent analysis of biogenic emissions have indicated that 15 to 35 percent of the biogenic emissions are reacted away before leaving the forest canopy, thus those emissions

cannot contribute to the formation of ozone. The 1985 NAPAP inventory only included major VOC emission sources; smaller sources, such as small evaporative sources whose annual emission rate was lower than the cutoff, were not included in the analysis. Many of these smaller sources have peak emission rate during the summer. The uncertainties in the emission inventories contribute substantially to the uncertainties in this analysis. It is expected that use of a better quality anthropogenic emission inventory, representative of actual emission rates, will not only lessen the uncertainties in the analysis of the effects of biogenic emissions, but will also improve model performance of the base case.

Even with the uncertainties in the modeling analysis presented here, two important conclusions can be drawn concerning attainment of the ozone standard for the city of Atlanta. First, biogenic emissions do contribute to some extent to VOC concentrations in the Atlanta region and therefore may lessen the effects of ozone attainment strategies aimed solely at reducing VOC emissions. Although it is suspected that the results presented here are overestimates (i.e., the actual effects of biogenic emissions may be less than presented here), biogenic emissions should be recognized in future modeling studies. The second major conclusion is that a high-quality emission inventory that represents actual emission rates is needed to properly calculate the effects of emission reduction strategies.

References

Ames, J., T. C. Myers, L. E. Reid, D. C. Whitney, S. H. Golding, S. R. Hayes, and S. D. Reynolds. 1985a. SAI Airshed Model Operations Manuals. Volume I--User's Manual. U.S. Environmental Protection Agency (EPA-600/8-85-007a).

Ames, J., S. R. Hayes, T. C. Myers, and D. C. Whitney. 1985b. SAI Airshed Model Operations Manuals. Volume II--System's Manual. U.S. Environmental Protection Agency (EPA-600/8-85-007b).

Bass, A. M., L. C. Glasgow, C. Miller, J. P. Jesson, and D. L. Filken. 1980. Planet Space Sci., 28:675.

Boris, J. P., and D. L. Book. 1973. Flux-corrected transport: I. SHASTA, a fluid transport algorithm that works. J. Comp. Phys., 11:38-69.

Burton, C. S. 1988. Comments on "Ozone Air Quality Models." J. Air Pollut. Control Assoc., 38(9):1119-1128.

Chameides, W. L., R. W. Lindsay, J. Richardson, and C. S. Kiang. 1988. The role of biogenic hydrocarbons in urban photochemical smog: Atlanta as a case study. Science, 241:1473-1475.

Chock, D. P., and A. M. Dunker. 1983. A comparison of numerical methods for solving the advection equation. Atmos. Environ., 17:11-24.

Chock, D. P. 1985. A comparison of numerical methods for solving the advection equation--II. Atmos. Environ., 19:571-586.

Douglas, S., and R. Kessler. 1988. "User's Guide to the Diagnostic Wind Model. Version 1.0." Systems Applications, Inc., San Rafael, California.

EPA. 1984. Air Quality Criteria for Ozone and Other Photochemical Oxidants--Draft. Volume II. U.S. Environmental Protection Agency (EPA-600/8-84-020A).

EPA. 1986. Guideline on Air Quality Models (Revised). U.S. Environmental Protection Agency (EPA-450/2-78-027R).

Federal Register. 1987. "State Implementation Plans; Approval of Post-1987 Ozone and Carbon Monoxide Plan Revisions for Areas Not Attaining the National Ambient Air Quality Standards; Notice." Federal Register, Vol. 52, No. 226 (November 24, 1987).

Gery, M. W., G. Z. Whitten, and J. P. Killus. 1988. "Development and Testing of the CBM-IV for Urban and Regional Modeling." Systems Applications, Inc., San Rafael, California (SYSAPP-88/002).

Haney, J. L., D. R. Souten, T. W. Tesche, L. R. Chinkin, H. Hogo, and M. C. Dudik. 1986. "Evaluation and Applications of the PARIS Photochemical Model in the South Central Coast Air Basin." Volume I. Systems Applications, Inc., San Rafael, California (SYSAPP-86/065).

Hogo, H., L. A. Mahoney, and M. A. Yocke. 1988. "Draft Air Quality Management Plan 1988 Revision. Draft Appendix V-R. Urban Airshed Model Performance Evaluation for 5-7 June 1985." Systems Applications, Inc., San Rafael, California (SYSAPP-88/138).

Morris, R. E., M. W. Gery, M. K. Liu, G. E. Moore, C. Daly, and S. M. Greenfield. 1989b. "Sensitivity of a Regional Oxidant Model to Variations in Climate Parameters. Volume I: Results." Systems Applications, Inc., San Rafael, California (SYSAPP-89/014a).

Morris, R. E., R. C. Kessler, S. G. Douglas, K. R. Styles, and G. E. Moore. 1988. "Rocky Mountain Acid Deposition Model Assessment Acid Rain Mountain Mesoscale Model (ARM3)." Systems Applications, Inc., San Rafael, California (SYSAPP-88/152).

Morris, R. E., T. C. Myers, H. Hogo, L. R. Chinkin, L. A. Gardner, and R. G. Johnson. 1989a. "A Low-Cost Application of the Urban Airshed Model to the New York Metropolitan Area and the City of St. Louis." Systems Applications, Inc., San Rafael, California (SYSAPP-89/038).

O'Brien, J. J. 1970. A note on the vertical structure of the eddy exchange coefficient in the planetary boundary layer. J. Atmos. Sci., 27:1213-1215.

OTA. 1988a. "Urban Ozone and the Clean Air Act: Problems and Proposals for Change." Office of Technology Assessment, Washington, D.C.

OTA. 1988b. "Ozone and the Clean Air Act: Summary of OTA Workshop with State and Local Air Pollution Control Agency Officials." Office of Technology Assessment, Washington, D.C.

OTA. 1988c. "Ozone and the Clean Air Act: A Summary of OTA Workshops on Congressional Options to Address Nonattainment of the Ozone Standard." Office of Technology Assessment, Washington, D.C.

89059 5

Rao, S. T. 1987. "Application of the Urban Airshed Model to the New York Metropolitan Area." U.S. Environmental Protection Agency, Research Triangle Park, North Carolina (EPA-450/4-87-011).

SAI. 1988. "Protocol Document for Urban Airshed and EKMA Modeling in the Atlanta Metropolitan Area." Systems Applications, Inc., San Rafael, California (SYSAPP-88/157).

Schere, K. L. 1983. An evaluation of several numerical advection schemes. Atmos. Environ., 17:1897-1907.

Schere, K. L., and K. L. Demerjian. 1977. "Calculation of Selected Photolytic Rate Constants over a Diurnal Range. A Computer Algorithm." U.S. Environmental Protection Agency, Research Triangle Park, North Carolina (EPA-600/4-77-015).

Science. 1988. Rural and urban ozone. Editorial in Science, 241(4873):1569.

Seinfeld, J. H. 1988a. Ozone air quality models. A critical review. J. Air Pollut. Control Assoc., 38(5):616.

Seinfeld, J. H. 1988b. Closing remarks. J. Air Pollut. Control Assoc., 38(8):1136-1137.

Smolarkiewicz, P. K. 1983. A simple positive definite advection scheme with small implicit diffusion. Monthly Weather Review, 111:479-486.

Whitten, G. Z., J. P. Killus, and H. Hogo. 1980. "Modeling of Simulated Photochemical Smog with Kinetic Mechanisms. Volume 1. Final Report." Systems Applications, Inc., San Rafael, California (EPA-600/3-80-028a).

Whitten, G. Z., T. C. Meyers, C. Daly, L. R. Chinkin, S. D. Reynolds, N. M. Yonkow, and B. Austin. 1985. "Application of the Urban Airshed Model to Kern County." Systems Applications, Inc., San Rafael, California (SYSAPP-85/200).

Yamartino, R. J., and J. S. Scire. 1984. "ADOM/TADAP Model Development Program. Volume 3. The Transport and Diffusion Modules." Environmental Research & Technology, Inc., Concord, Massachusetts (P-B980-210).

Yocke, M. A., R. E. Morris, H. Hogo, L. R. Chinkin, and L. A. Mahoney. 1985. "Analysis of the Air Quality Impacts of the San Miguel Project. Volume I." Systems Applications, Inc., San Rafael, California (SYSAPP-85/127).

Zalesak, S. T. 1979. Fully multi-dimensional flux-corrected transport algorithms for fluids. J. Comput. Phys., 31:335-362.

Appendix A

EMISSIONS DATA USED IN THE APPLICATION OF THE UAM TO ATLANTA

Emissions type: Total Merged by Source Category (tons/day) for day 84155

CODE	Source Name	THC	RHC	CO	NOx	SOx	TSP
100	FUEL COMBUSTION	0.00	0.00	0.00	0.00	0.00	0.00
110	AGRICULTURAL	0.00	0.00	0.00	0.00	0.00	0.00
120	OIL AND GAS PRODUCTION	0.00	0.00	0.00	0.00	0.00	0.00
130	PETROLEUM REFINING	0.00	0.00	0.01	0.08	0.08	0.01
140	OTHER MANUFACTURING/INDUSTRIAL	0.55	0.22	1.37	8.10	4.12	0.58
150	ELECTRIC UTILITIES	0.02	0.01	0.06	1.38	0.16	0.04
160	OTHER SERVICES AND COMMERCE	0.14	0.06	0.58	2.85	1.83	0.18
170	RESIDENTIAL	0.18	0.01	0.70	3.44	0.17	0.11
199	OTHER	0.00	0.00	0.00	0.00	0.00	0.00
200	WASTE BURNING	0.00	0.00	0.00	0.00	0.00	0.00
210	AGRICULTURAL DEBRIS	0.70	0.55	4.11	0.09	0.00	0.62
220	RANGE MANAGEMENT	0.00	0.00	0.00	0.00	0.00	0.00
230	FOREST MANAGEMENT	0.00	0.00	0.00	0.00	0.00	0.00
240	INCINERATION	2.73	0.36	7.93	0.05	0.03	0.98
299	OTHER	16.58	16.26	46.93	2.78	0.40	10.67
300	SOLVENT USE	0.00	0.00	0.00	0.00	0.00	0.00
310	DRY CLEANING	4.80	2.44	0.00	0.00	0.00	0.00
320	DEGREASING	7.14	6.03	0.00	0.00	0.00	0.00
330	ARCHITECTURAL COATING	19.57	18.60	0.00	0.00	0.00	0.00
340	OTHER SURFACE COATING	65.04	63.87	0.00	0.00	0.00	0.87
350	ASPHALT PAVING	0.00	0.00	0.00	0.00	0.00	0.00
360	PRINTING	13.92	11.21	0.00	0.00	0.00	0.00
370	DOMESTIC	0.00	0.00	0.00	0.00	0.00	0.00
380	INDUSTRIAL SOLVENT USE	0.00	0.00	0.00	0.00	0.00	0.00
399	OTHER	75.41	55.22	0.00	0.00	0.00	0.00
400	PETROLEUM PROCESS, STORAGE & TRANSFER	0.00	0.00	0.00	0.00	0.00	0.00
410	OIL AND GAS EXTRACTION	12.61	4.89	0.00	0.00	0.00	0.00
420	PETROLEUM REFINING	13.35	9.86	0.15	0.00	0.00	0.05
430	PETROLEUM MARKETING	33.98	32.85	0.00	0.00	0.00	0.00
499	OTHER	0.00	0.00	0.00	0.00	0.00	0.00
500	INDUSTRIAL PROCESSES	0.00	0.00	0.00	0.00	0.00	0.00
510	CHEMICAL	15.12	10.01	0.00	0.10	6.07	0.25
520	FOOD AND AGRICULTURAL	0.87	0.58	0.00	0.00	0.00	0.00
560	MINERAL PROCESSES	1.96	1.46	0.17	6.00	4.55	3.55
570	METAL PROCESSES	2.98	2.93	0.04	0.02	4.11	1.29
580	WOOD AND PAPER	18.83	18.52	0.00	0.02	0.01	0.97
599	OTHER	62.67	50.01	0.00	0.00	0.00	0.00
600	MISC PROCESSES	0.00	0.00	0.00	0.00	0.00	0.00
610	PESTICIDE APPLICATION	0.00	0.00	0.00	0.00	0.00	0.00
620	FARMING OPERATIONS	0.00	0.00	0.00	0.00	0.00	0.00
630	CONSTRUCTION AND DEMOLITION	0.00	0.00	0.00	0.00	0.00	0.00
640	ENTRAINED ROAD DUST - PAVED	0.00	0.00	0.00	0.00	0.00	0.00
650	ENTRAINED ROAD DUST - UNPAVED	0.00	0.00	0.00	0.00	0.00	0.00
660	UNPLANNED FIRES	1.69	1.33	7.70	0.18	0.00	1.77
680	WASTE DISPOSAL	0.78	0.31	0.00	0.00	0.00	0.00
685	NATURAL SOURCES	0.00	0.00	0.00	0.00	0.00	0.00
699	OTHER	0.32	0.24	0.02	0.02	0.01	0.47
700	ON ROAD VEHICLES	0.00	0.00	0.00	0.00	0.00	0.00
710	LIGHT DUTY PASSENGER	580.06	547.14	1454.22	156.13	9.42	133.86
720	LIGHT AND MEDIUM DUTY TRUCKS	113.24	106.19	311.91	38.63	2.87	29.76

Emissions type: Total Merged by Source Category (tons/day) for day 84155

CODE	Source Name	THC	RHC	CO	NOx	SOx	TSP
730	HEAVY DUTY GAS TRUCKS	32.33	30.53	163.35	12.75	0.63	4.87
740	HEAVY DUTY DIESEL TRUCKS	13.71	12.41	50.36	121.06	14.48	29.01
750	MOTORCYCLES	0.00	0.00	0.00	0.00	0.00	0.00
799	OTHER	0.00	0.00	0.00	0.00	0.00	0.00
800	OTHER MOBILE	0.00	0.00	0.00	0.00	0.00	0.00
810	OFF ROAD VEHICLES	0.00	0.00	0.00	0.00	0.00	0.00
820	TRAINS	4.29	3.89	6.71	19.11	2.94	1.29
830	SHIPS	5.82	5.49	17.95	0.23	0.04	0.00
850	AIRCRAFT - GOVERNMENT	1.17	0.97	2.19	0.47	0.06	0.93
860	AIRCRAFT - OTHER	7.90	6.51	42.84	9.39	1.01	0.48
870	MOBILE EQUIPMENT	0.00	0.00	0.00	0.00	0.00	0.00
880	UTILITY EQUIPMENT	0.00	0.00	0.00	0.00	0.00	0.00
891	SEEPS/BIOGENIC	0.00	0.00	0.00	0.00	0.00	0.00
892	CHANNEL SHIPPING	0.00	0.00	0.00	0.00	0.00	0.00
893	OCS AND RELATED SOURCES	0.00	0.00	0.00	0.00	0.00	0.00
894	TIDELAND PLATFORMS	0.00	0.00	0.00	0.00	0.00	0.00
900	UNSPECIFIED SOURCES	11.40	9.52	27.82	367.91	2065.01	50.77
TOTAL ANTHROPOGENIC EMISSIONS		1141.89	1030.45	2147.11	750.79	2118.01	273.41
TOTAL BIOGENIC EMISSIONS		1277.00	1277.00	0.00	0.00	0.00	0.00
TOTAL ANTHROPOGENIC + BIOGENIC		2418.89	2307.45	2147.11	750.79	2118.01	273.41

Emissions type: Total Merged by Source Category (tons/day) for day 84155

CODE	Source Name	OLE	PAR	TOL	XYL	FORM
100	FUEL COMBUSTION	0.00	0.00	0.00	0.00	0.00
110	AGRICULTURAL	0.00	0.00	0.00	0.00	0.00
120	OIL AND GAS PRODUCTION	0.00	0.00	0.00	0.00	0.00
130	PETROLEUM REFINING	0.00	0.00	0.00	0.00	0.00
140	OTHER MANUFACTURING/INDUSTRIAL	0.01	0.08	0.00	0.00	0.01
150	ELECTRIC UTILITIES	0.00	0.01	0.00	0.00	0.00
160	OTHER SERVICES AND COMMERCE	0.00	0.05	0.00	0.00	0.01
170	RESIDENTIAL	0.00	0.01	0.00	0.00	0.00
199	OTHER	0.00	0.00	0.00	0.00	0.00
200	WASTE BURNING	0.00	0.00	0.00	0.00	0.00
210	AGRICULTURAL DEBRIS	0.03	0.38	0.00	0.00	0.00
220	RANGE MANAGEMENT	0.00	0.00	0.00	0.00	0.00
230	FOREST MANAGEMENT	0.00	0.00	0.00	0.00	0.00
240	INCINERATION	0.01	0.08	0.00	0.00	0.00
299	OTHER	2.07	10.94	0.00	0.00	0.00
300	SOLVENT USE	0.00	0.00	0.00	0.00	0.00
310	DRY CLEANING	0.03	2.09	0.14	0.17	0.00
320	DEGREASING	0.04	3.45	1.29	0.59	0.00
330	ARCHITECTURAL COATING	0.76	13.52	3.58	0.60	0.00
340	OTHER SURFACE COATING	0.34	29.94	24.49	8.05	0.00
350	ASPHALT PAVING	0.00	0.00	0.00	0.00	0.00
360	PRINTING	0.02	11.05	0.12	0.00	0.00
370	DOMESTIC	0.00	0.00	0.00	0.00	0.00
380	INDUSTRIAL SOLVENT USE	0.00	0.00	0.00	0.00	0.00
399	OTHER	0.00	29.75	0.00	0.00	0.31
400	PETROLEUM PROCESS, STORAGE & TRANSFER	0.00	0.00	0.00	0.00	0.00
410	OIL AND GAS EXTRACTION	0.00	4.89	0.00	0.00	0.00
420	PETROLEUM REFINING	0.18	8.74	0.06	0.31	0.57
430	PETROLEUM MARKETING	0.72	16.05	6.59	9.00	0.02
499	OTHER	0.00	0.00	0.00	0.00	0.00
500	INDUSTRIAL PROCESSES	0.00	0.00	0.00	0.00	0.00
510	CHEMICAL	1.25	4.93	1.24	0.11	0.09
520	FOOD AND AGRICULTURAL	0.06	0.35	0.05	0.01	0.01
560	MINERAL PROCESSES	0.05	1.22	0.02	0.12	0.02
570	METAL PROCESSES	0.00	1.34	1.27	0.28	0.00
580	WOOD AND PAPER	0.01	8.44	8.01	1.75	0.00
599	OTHER	8.10	30.72	6.00	0.51	0.51
600	MISC PROCESSES	0.00	0.00	0.00	0.00	0.00
610	PESTICIDE APPLICATION	0.00	0.00	0.00	0.00	0.00
620	FARMING OPERATIONS	0.00	0.00	0.00	0.00	0.00
630	CONSTRUCTION AND DEMOLITION	0.00	0.00	0.00	0.00	0.00
640	ENTRAINED ROAD DUST - PAVED	0.00	0.00	0.00	0.00	0.00
650	ENTRAINED ROAD DUST - UNPAVED	0.00	0.00	0.00	0.00	0.00
660	UNPLANNED FIRES	0.07	0.92	0.00	0.00	0.00
680	WASTE DISPOSAL	0.04	0.20	0.00	0.00	0.00
685	NATURAL SOURCES	0.00	0.00	0.00	0.00	0.00
699	OTHER	0.02	0.15	0.02	0.01	0.00
700	ON ROAD VEHICLES	0.00	0.00	0.00	0.00	0.00
710	LIGHT DUTY PASSENGER	16.14	385.49	58.29	52.64	1.43
720	LIGHT AND MEDIUM DUTY TRUCKS	3.29	73.96	11.12	10.54	0.31

Emissions type: Total Merged by Source Category (tons/day) for day 84155

CODE	Source Name	OLE	PAR	TOL	XYL	FORM
730	HEAVY DUTY GAS TRUCKS	0.77	23.21	1.47	2.12	0.07
740	HEAVY DUTY DIESEL TRUCKS	0.76	6.66	2.95	0.27	0.71
750	MOTORCYCLES	0.00	0.00	0.00	0.00	0.00
799	OTHER	0.00	0.00	0.00	0.00	0.00
800	OTHER MOBILE	0.00	0.00	0.00	0.00	0.00
810	OFF ROAD VEHICLES	0.00	0.00	0.00	0.00	0.00
820	TRAINS	0.24	2.09	0.92	0.08	0.22
830	SHIPS	0.14	4.15	0.27	0.39	0.01
850	AIRCRAFT - GOVERNMENT	0.13	0.31	0.02	0.02	0.13
860	AIRCRAFT - OTHER	0.88	2.22	0.14	0.14	0.86
870	MOBILE EQUIPMENT	0.00	0.00	0.00	0.00	0.00
880	UTILITY EQUIPMENT	0.00	0.00	0.00	0.00	0.00
891	SEEPS/BIOGENIC	0.00	0.00	0.00	0.00	0.00
892	CHANNEL SHIPPING	0.00	0.00	0.00	0.00	0.00
893	OCS AND RELATED SOURCES	0.00	0.00	0.00	0.00	0.00
894	TIDELAND PLATFORMS	0.00	0.00	0.00	0.00	0.00
900	UNSPECIFIED SOURCES	0.52	5.97	0.70	1.12	0.14
TOTAL	ANTHROPOGENIC EMISSIONS	36.65	683.35	128.77	88.83	5.45
TOTAL	BIOGENIC EMISSIONS	242.34	969.40	0.00	0.00	0.00
TOTAL	ANTHROPOGENIC + BIOGENIC	278.99	1652.75	128.77	88.83	5.45

Emissions type: Total Merged by Source Category (tons/day) for day 84155

CODE	Source Name	ALD2	ETH	MEOH	ETOH	ISOP
100	FUEL COMBUSTION	0.00	0.00	0.00	0.00	0.00
110	AGRICULTURAL	0.00	0.00	0.00	0.00	0.00
120	OIL AND GAS PRODUCTION	0.00	0.00	0.00	0.00	0.00
130	PETROLEUM REFINING	0.00	0.00	0.00	0.00	0.00
140	OTHER MANUFACTURING/INDUSTRIAL	0.00	0.08	0.00	0.05	0.00
150	ELECTRIC UTILITIES	0.00	0.00	0.00	0.00	0.00
160	OTHER SERVICES AND COMMERCE	0.00	0.00	0.00	0.00	0.00
170	RESIDENTIAL	0.00	0.00	0.00	0.00	0.00
199	OTHER	0.00	0.00	0.00	0.00	0.00
200	WASTE BURNING	0.00	0.00	0.00	0.00	0.00
210	AGRICULTURAL DEBRIS	0.00	0.14	0.00	0.00	0.00
220	RANGE MANAGEMENT	0.00	0.00	0.00	0.00	0.00
230	FOREST MANAGEMENT	0.00	0.00	0.00	0.00	0.00
240	INCINERATION	0.00	0.26	0.00	0.00	0.00
299	OTHER	0.00	3.25	0.00	0.00	0.00
300	SOLVENT USE	0.00	0.00	0.00	0.00	0.00
310	DRY CLEANING	0.00	0.00	0.00	0.00	0.00
320	DEGREASING	0.04	0.61	0.00	0.00	0.00
330	ARCHITECTURAL COATING	0.14	0.00	0.00	0.00	0.00
340	OTHER SURFACE COATING	1.05	0.00	0.00	0.00	0.00
350	ASPHALT PAVING	0.00	0.00	0.00	0.00	0.00
360	PRINTING	0.03	0.00	0.00	0.00	0.00
370	DOMESTIC	0.00	0.00	0.00	0.00	0.00
380	INDUSTRIAL SOLVENT USE	0.00	0.00	0.00	0.00	0.00
399	OTHER	0.00	0.00	0.00	25.15	0.00
400	PETROLEUM PROCESS, STORAGE & TRANSFER	0.00	0.00	0.00	0.00	0.00
410	OIL AND GAS EXTRACTION	0.00	0.00	0.00	0.00	0.00
420	PETROLEUM REFINING	0.00	0.00	0.00	0.00	0.00
430	PETROLEUM MARKETING	0.46	0.00	0.00	0.00	0.00
499	OTHER	0.00	0.00	0.00	0.00	0.00
500	INDUSTRIAL PROCESSES	0.00	0.00	0.00	0.00	0.00
510	CHEMICAL	0.31	1.80	0.26	0.02	0.00
520	FOOD AND AGRICULTURAL	0.01	0.07	0.01	0.01	0.00
560	MINERAL PROCESSES	0.00	0.02	0.00	0.00	0.00
570	METAL PROCESSES	0.05	0.00	0.00	0.00	0.00
580	WOOD AND PAPER	0.30	0.00	0.00	0.00	0.00
599	OTHER	0.62	2.86	0.38	0.30	0.00
600	MISC PROCESSES	0.00	0.00	0.00	0.00	0.00
610	PESTICIDE APPLICATION	0.00	0.00	0.00	0.00	0.00
620	FARMING OPERATIONS	0.00	0.00	0.00	0.00	0.00
630	CONSTRUCTION AND DEMOLITION	0.00	0.00	0.00	0.00	0.00
640	ENTRAINED ROAD DUST - PAVED	0.00	0.00	0.00	0.00	0.00
650	ENTRAINED ROAD DUST - UNPAVED	0.00	0.00	0.00	0.00	0.00
660	UNPLANNED FIRES	0.00	0.33	0.00	0.00	0.00
680	WASTE DISPOSAL	0.00	0.08	0.00	0.00	0.00
685	NATURAL SOURCES	0.00	0.00	0.00	0.00	0.00
699	OTHER	0.01	0.01	0.00	0.00	0.00
700	ON ROAD VEHICLES	0.00	0.00	0.00	0.00	0.00
710	LIGHT DUTY PASSENGER	15.58	17.21	0.00	0.00	0.36
720	LIGHT AND MEDIUM DUTY TRUCKS	3.10	3.80	0.00	0.00	0.08

Emissions type: Total Merged by Source Category (tons/day) for day 84155

CODE	Source Name	ALD2	ETH	MEOH	ETOH	ISOP
730	HEAVY DUTY GAS TRUCKS	1.49	1.37	0.00	0.00	0.03
740	HEAVY DUTY DIESEL TRUCKS	0.66	0.40	0.00	0.00	0.00
750	MOTORCYCLES	0.00	0.00	0.00	0.00	0.00
799	OTHER	0.00	0.00	0.00	0.00	0.00
800	OTHER MOBILE	0.00	0.00	0.00	0.00	0.00
810	OFF ROAD VEHICLES	0.00	0.00	0.00	0.00	0.00
820	TRAINS	0.21	0.12	0.00	0.00	0.00
830	SHIPS	0.26	0.26	0.00	0.00	0.01
850	AIRCRAFT - GOVERNMENT	0.08	0.27	0.00	0.00	0.00
860	AIRCRAFT - OTHER	0.54	1.74	0.00	0.00	0.00
870	MOBILE EQUIPMENT	0.00	0.00	0.00	0.00	0.00
880	UTILITY EQUIPMENT	0.00	0.00	0.00	0.00	0.00
891	SEEPS/BIOGENIC	0.00	0.00	0.00	0.00	0.00
892	CHANNEL SHIPPING	0.00	0.00	0.00	0.00	0.00
893	OCS AND RELATED SOURCES	0.00	0.00	0.00	0.00	0.00
894	TIDELAND PLATFORMS	0.00	0.00	0.00	0.00	0.00
900	UNSPECIFIED SOURCES	1.02	0.03	0.04	0.00	0.00
TOTAL ANTHROPOGENIC		25.99	34.71	0.68	25.54	0.48
TOTAL BIOGENIC		0.00	0.00	0.00	0.00	276.09
TOTAL ANTHROPOGENIC + BIOGENIC		25.99	34.71	0.68	25.54	276.57

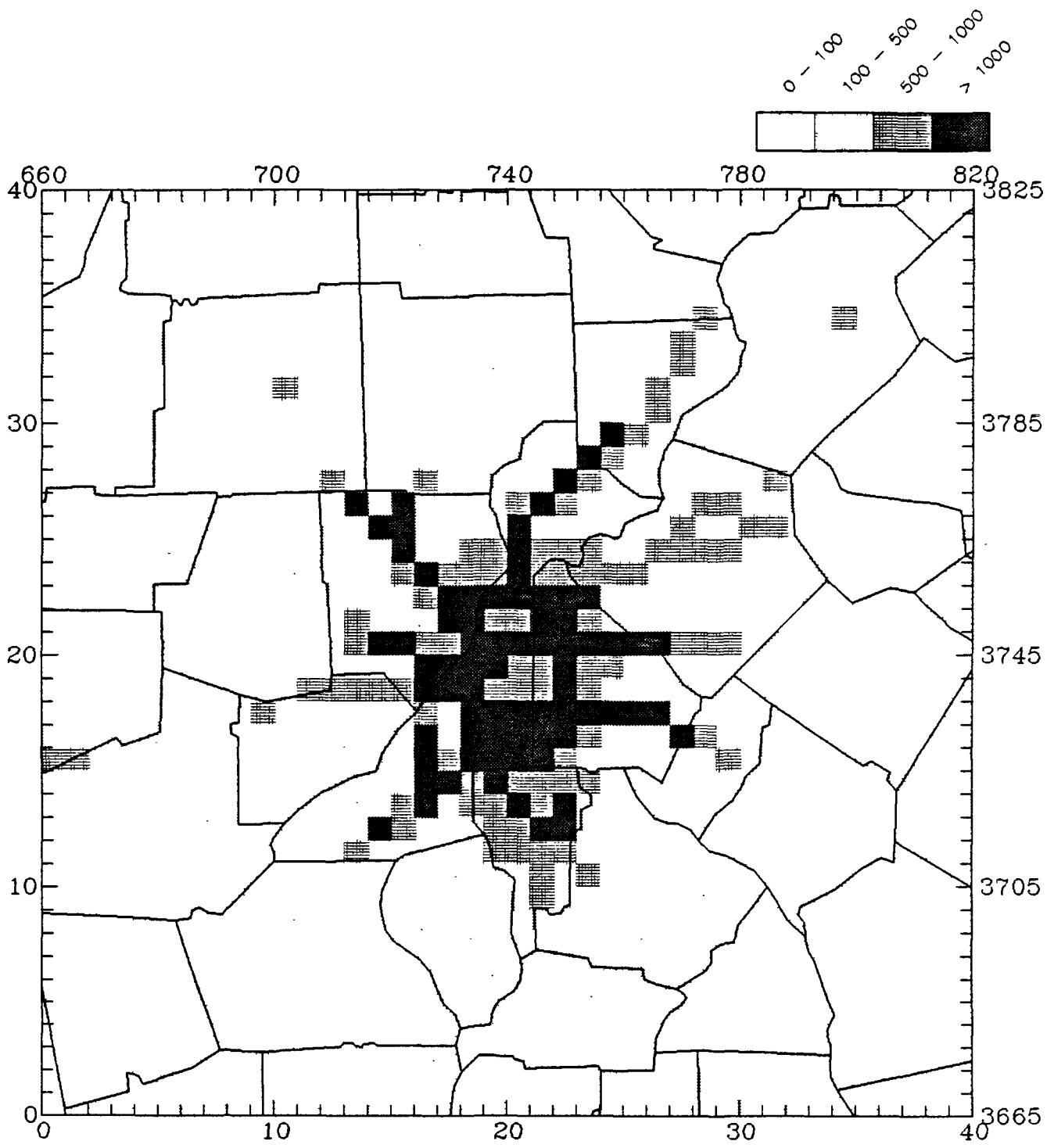

ATLANTA -- 1985 base
NOx

Area source and low-level point source NO_x emissions (kg/day)

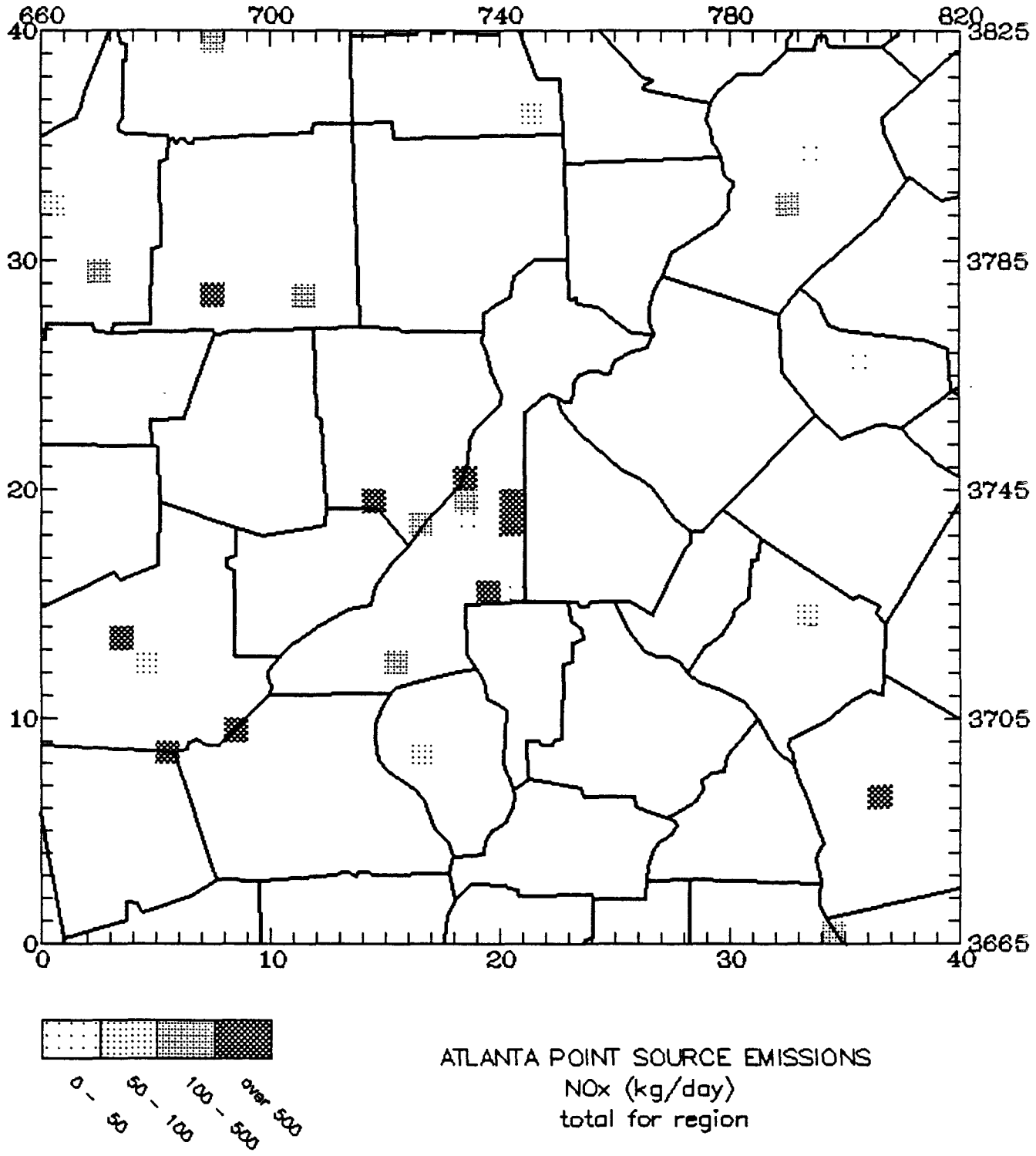
660
700
740
780
820
40
30
20
10
0
3825
3785
3745
3705
3665
0
10
20
30
40
0 - 50
50 - 100
100 - 500
over 500
ATLANTA POINT SOURCE EMISSIONS
NOx (kg/day)
total for region

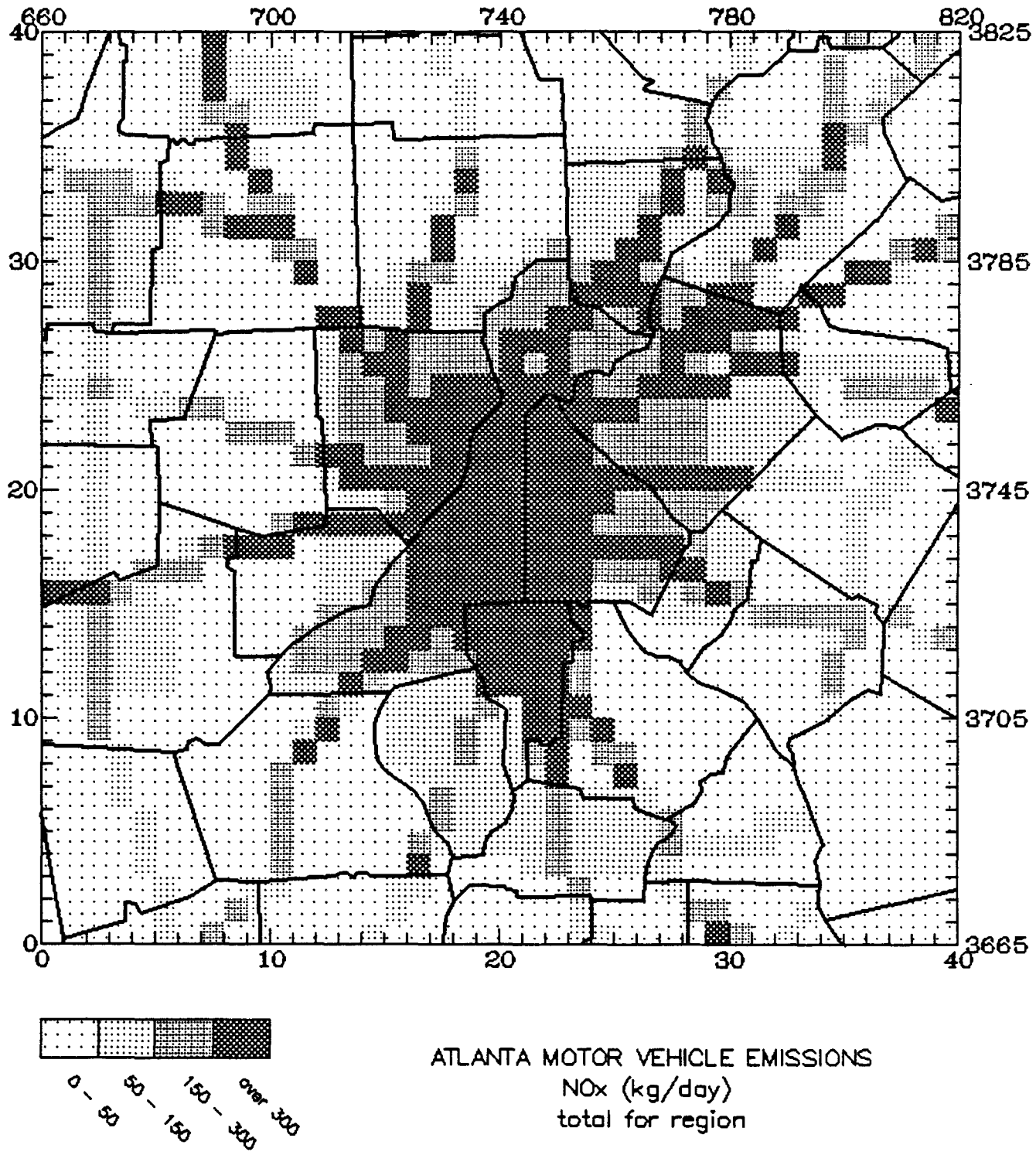
660
700
740
780
820
3825
3785
3745
3705
3665
40
30
20
10
0
0
10
20
30
40
0 - 50
50 - 150
150 - 300
over 300
ATLANTA MOTOR VEHICLE EMISSIONS
NOx (kg/day)
total for region

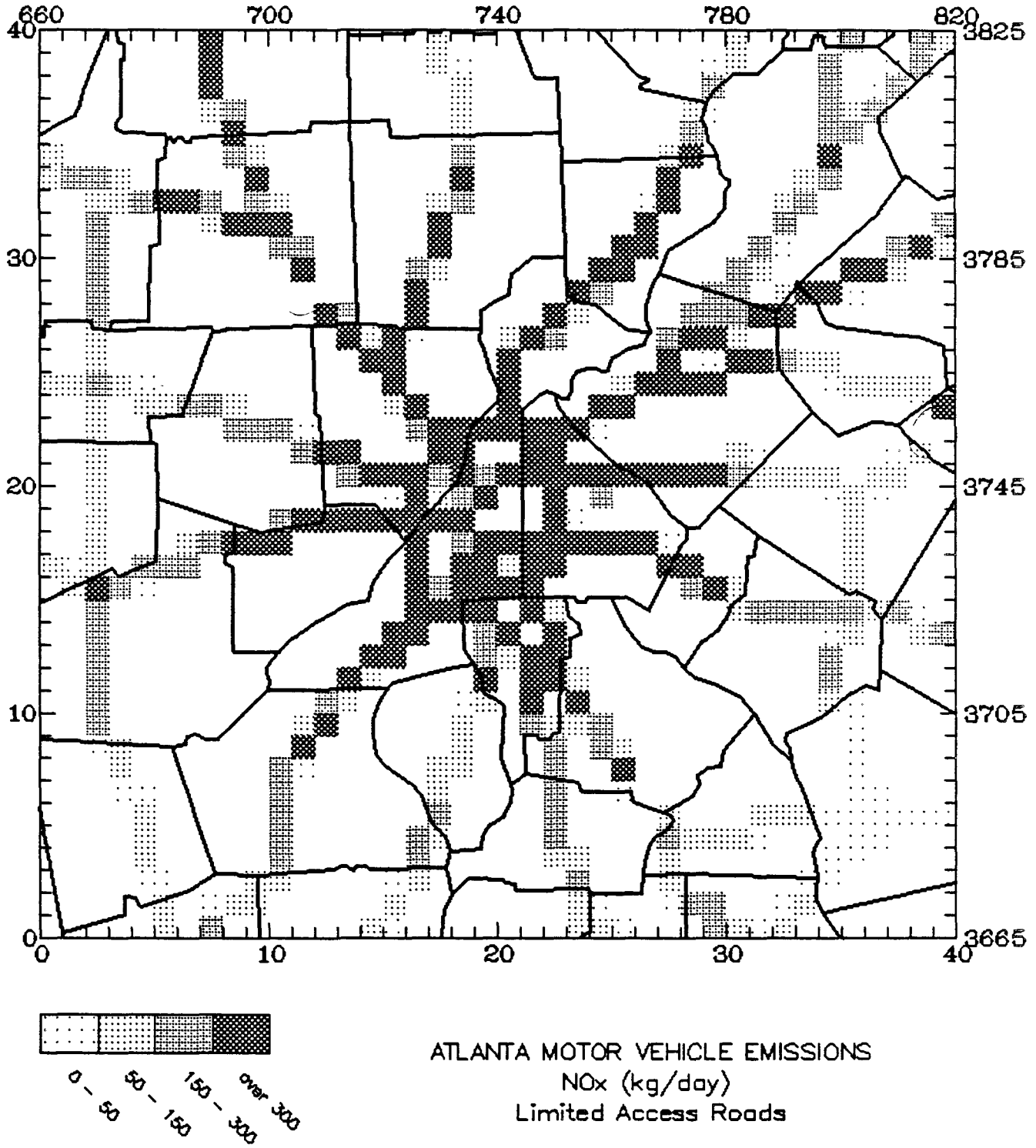
660
700
740
780
820
40
30
20
10
0
0
10
20
30
40
3825
3785
3745
3705
3665
0 - 50
50 - 150
150 - 300
over 300
ATLANTA MOTOR VEHICLE EMISSIONS
NOx (kg/day)
Limited Access Roads

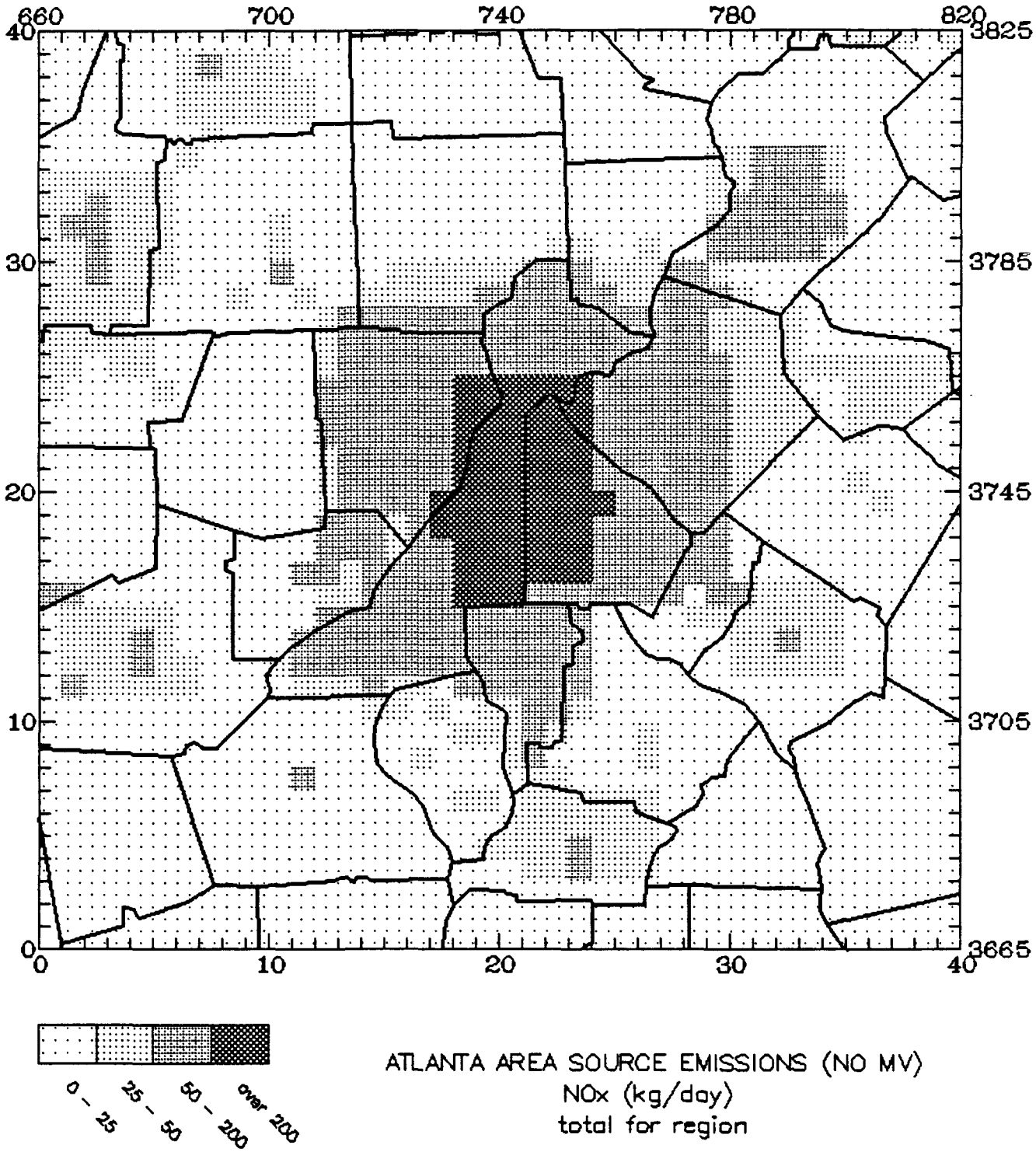
660
700
740
780
820
40
30
20
10
0
3825
3785
3745
3705
3665
0
10
20
30
40
0 - 25
25 - 50
50 - 200
over 200
ATLANTA AREA SOURCE EMISSIONS (NO MV)
NOx (kg/day)
total for region

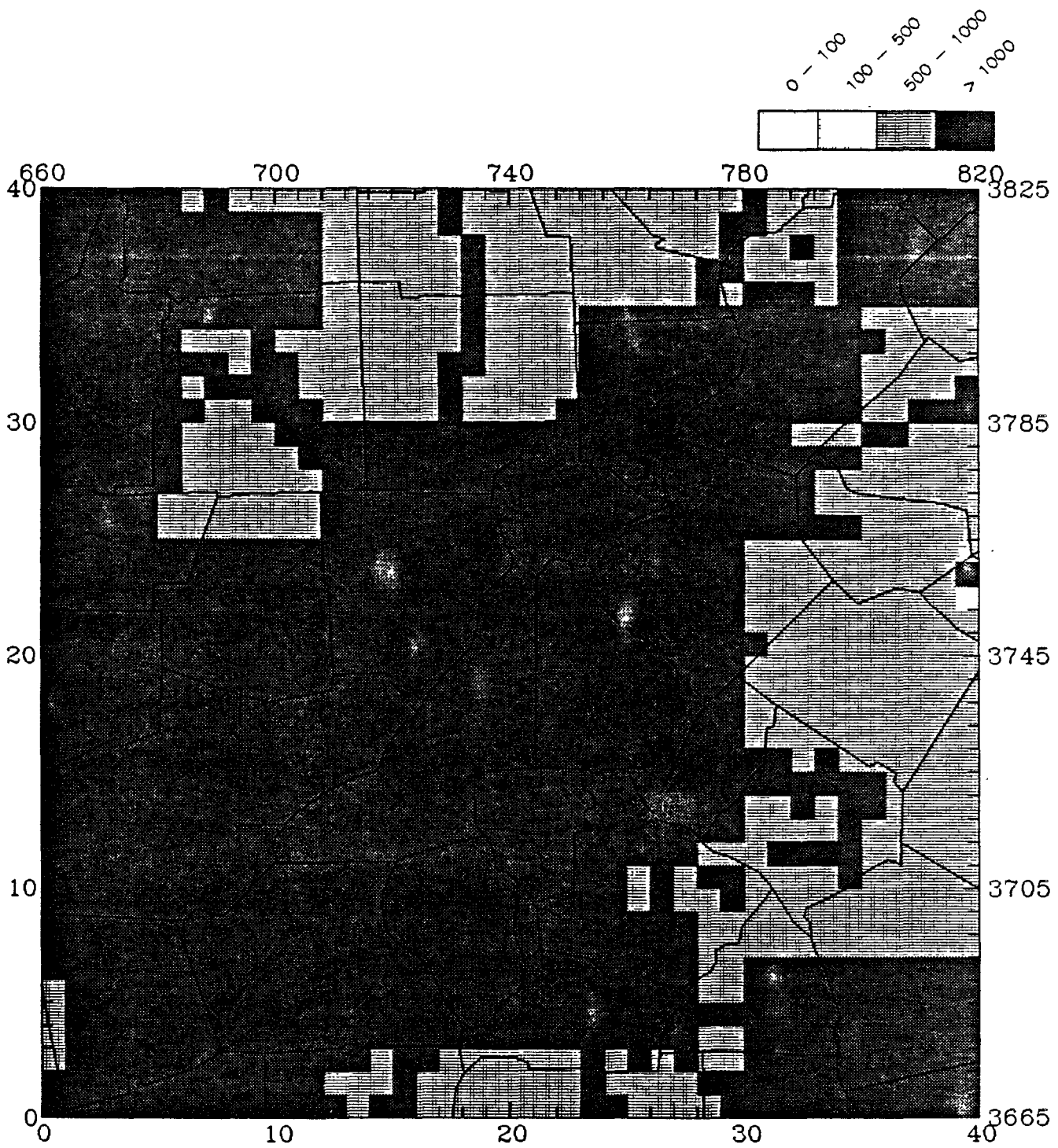

ATLANTA -- 1985 base
RHC

Anthropogenic area source and low-level point source plus biogenic VOC emissions (kg/day).

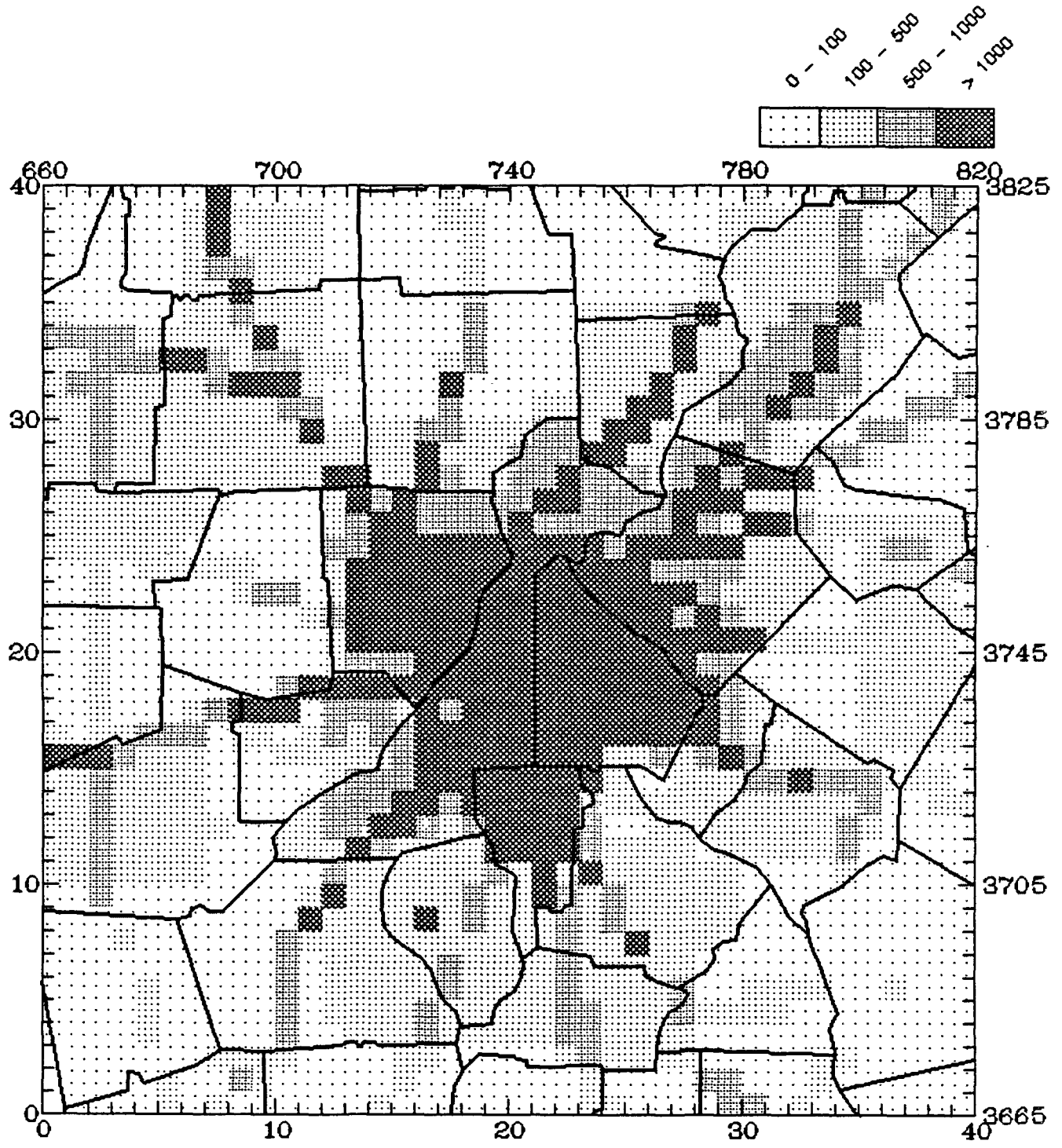

ATLANTA -- 1985 base -- anthropogenic only
RHC

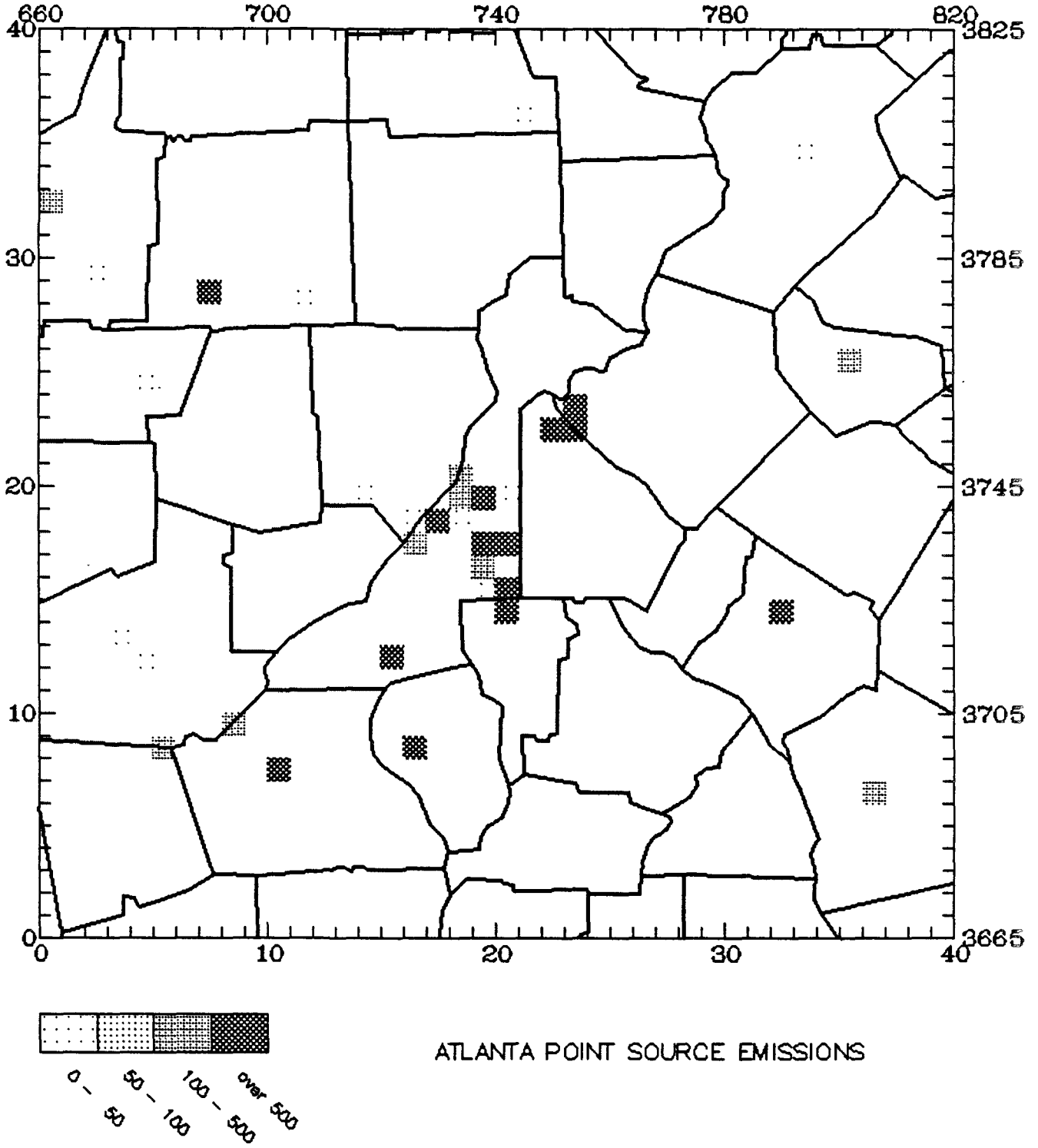

ATLANTA POINT SOURCE EMISSIONS

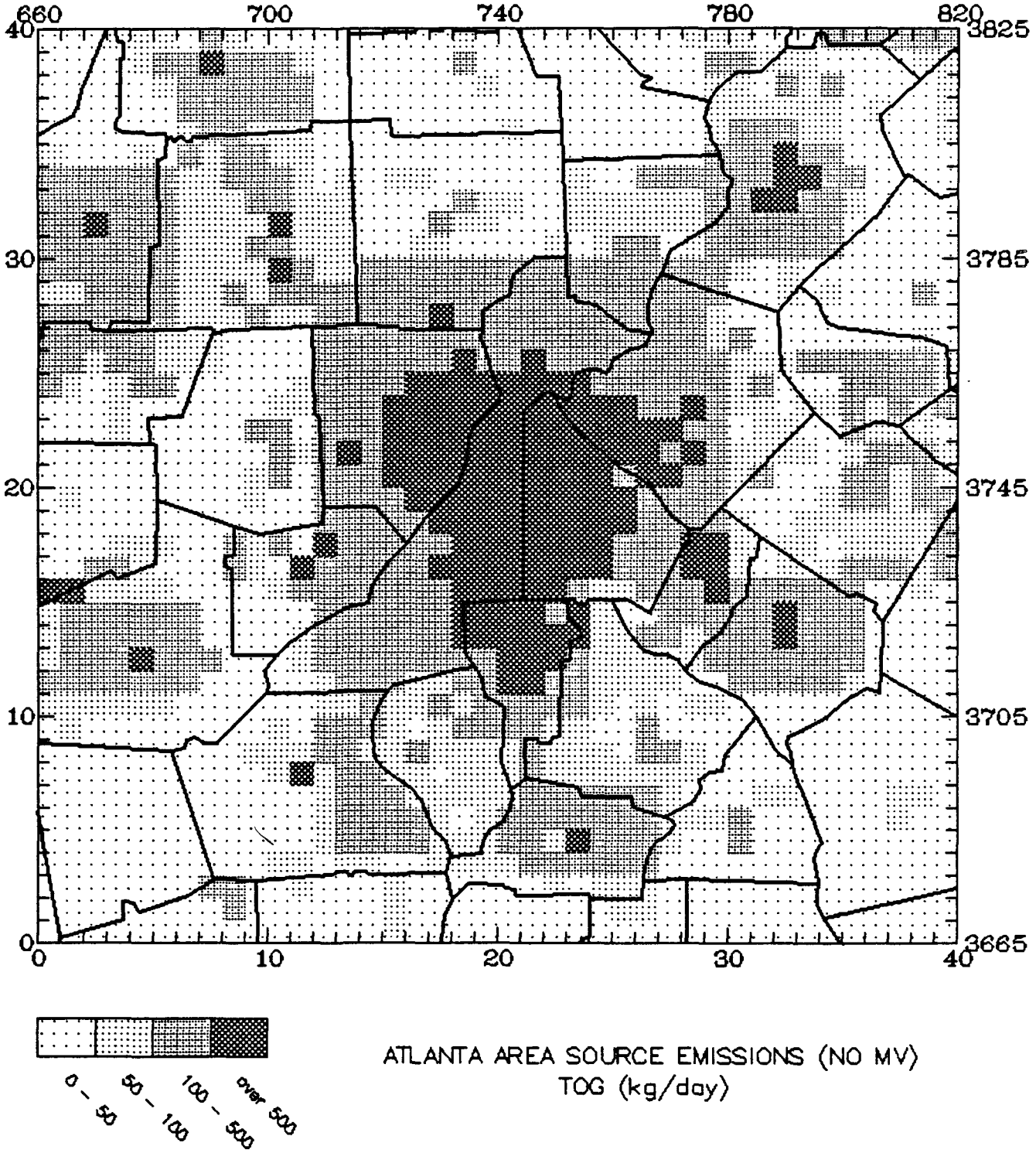
660
700
740
780
820
40
30
20
10
0
0
10
20
30
40
3825
3785
3745
3705
3665
0 - 50
50 - 100
100 - 500
over 500
ATLANTA AREA SOURCE EMISSIONS (NO MV)
TOG (kg/day)

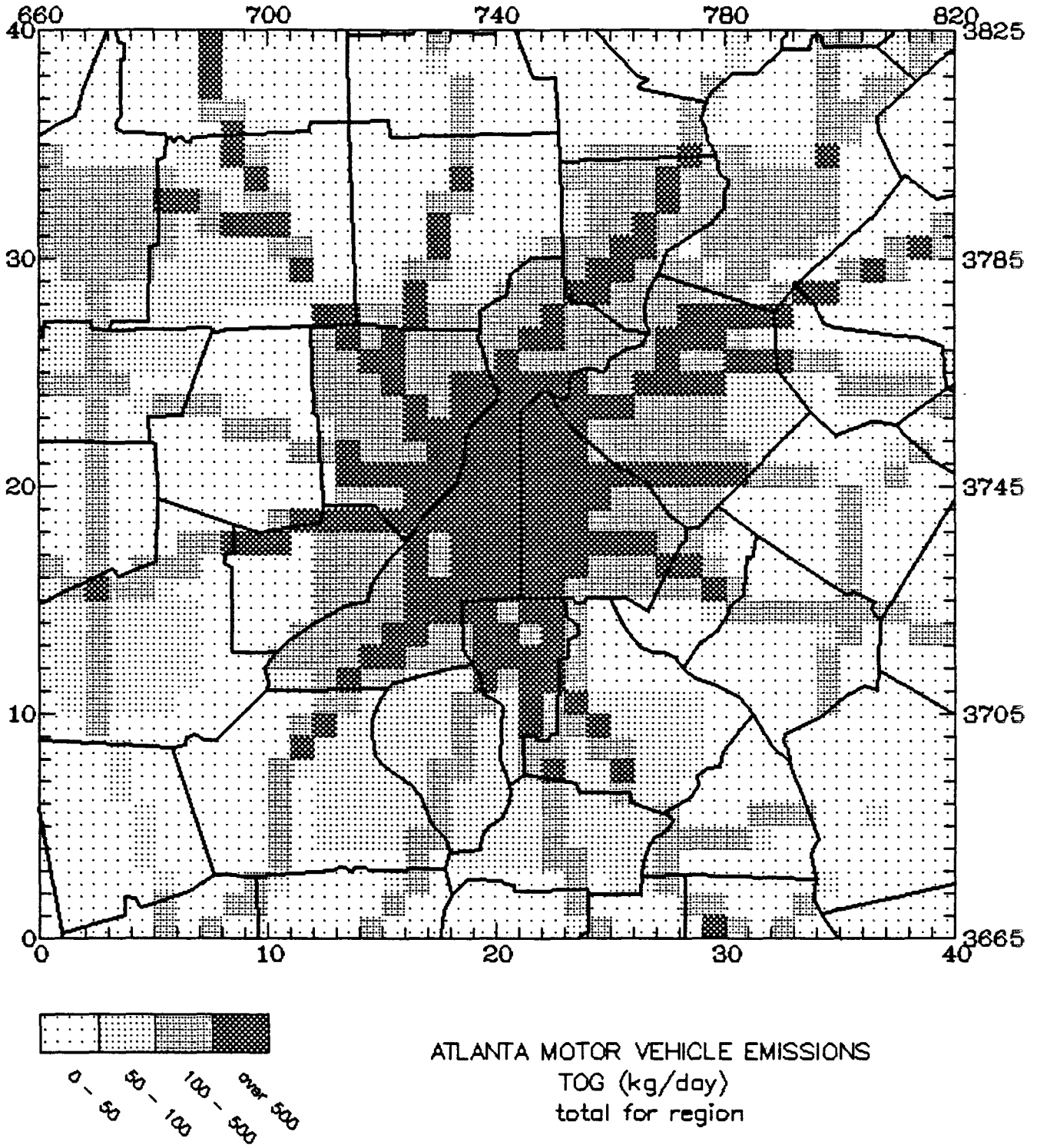

ATLANTA MOTOR VEHICLE EMISSIONS
TOG (kg/day)
total for region

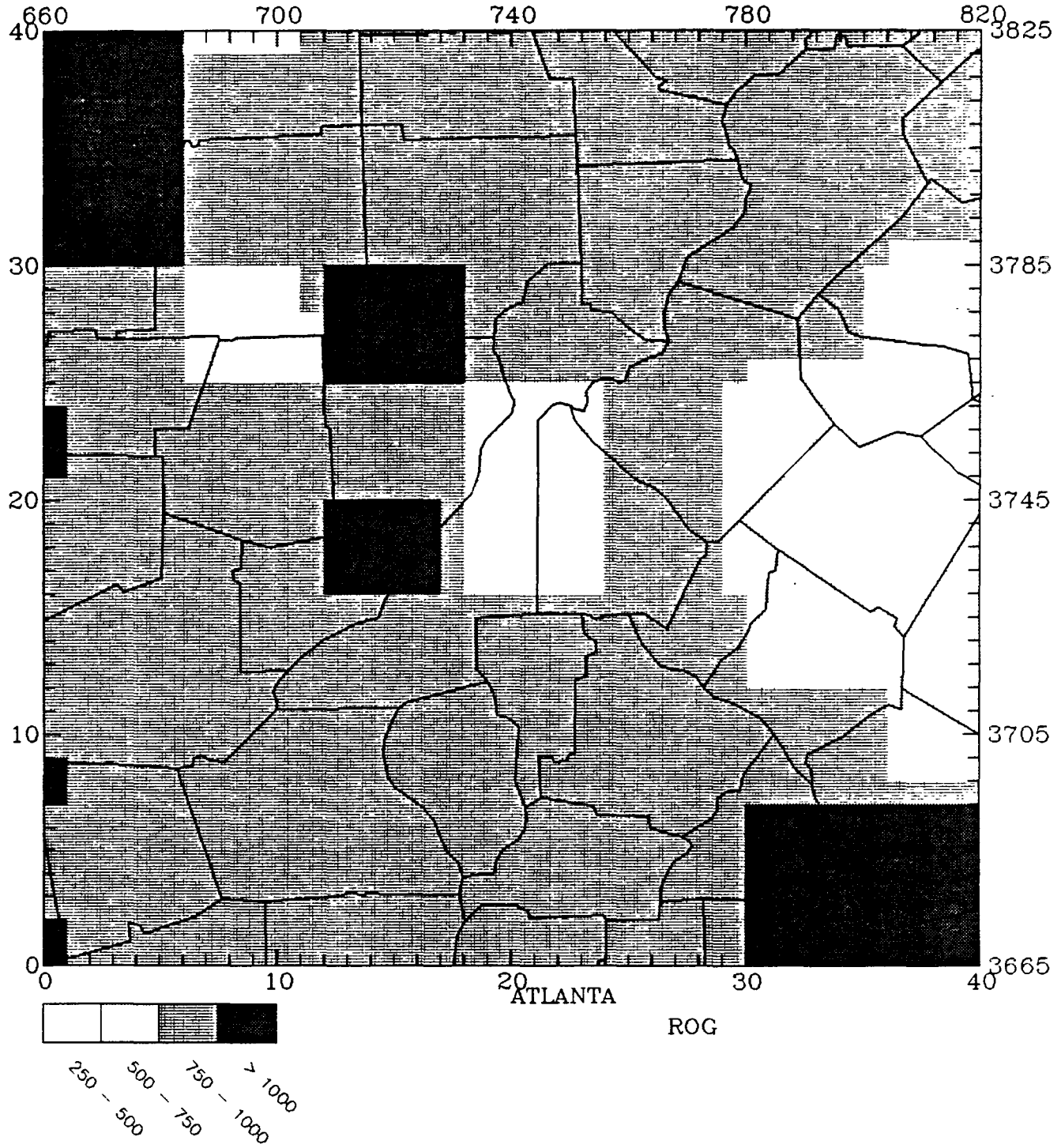

Total biogenic VOC emissions (kg/day) for the Atlanta UAM modeling domain

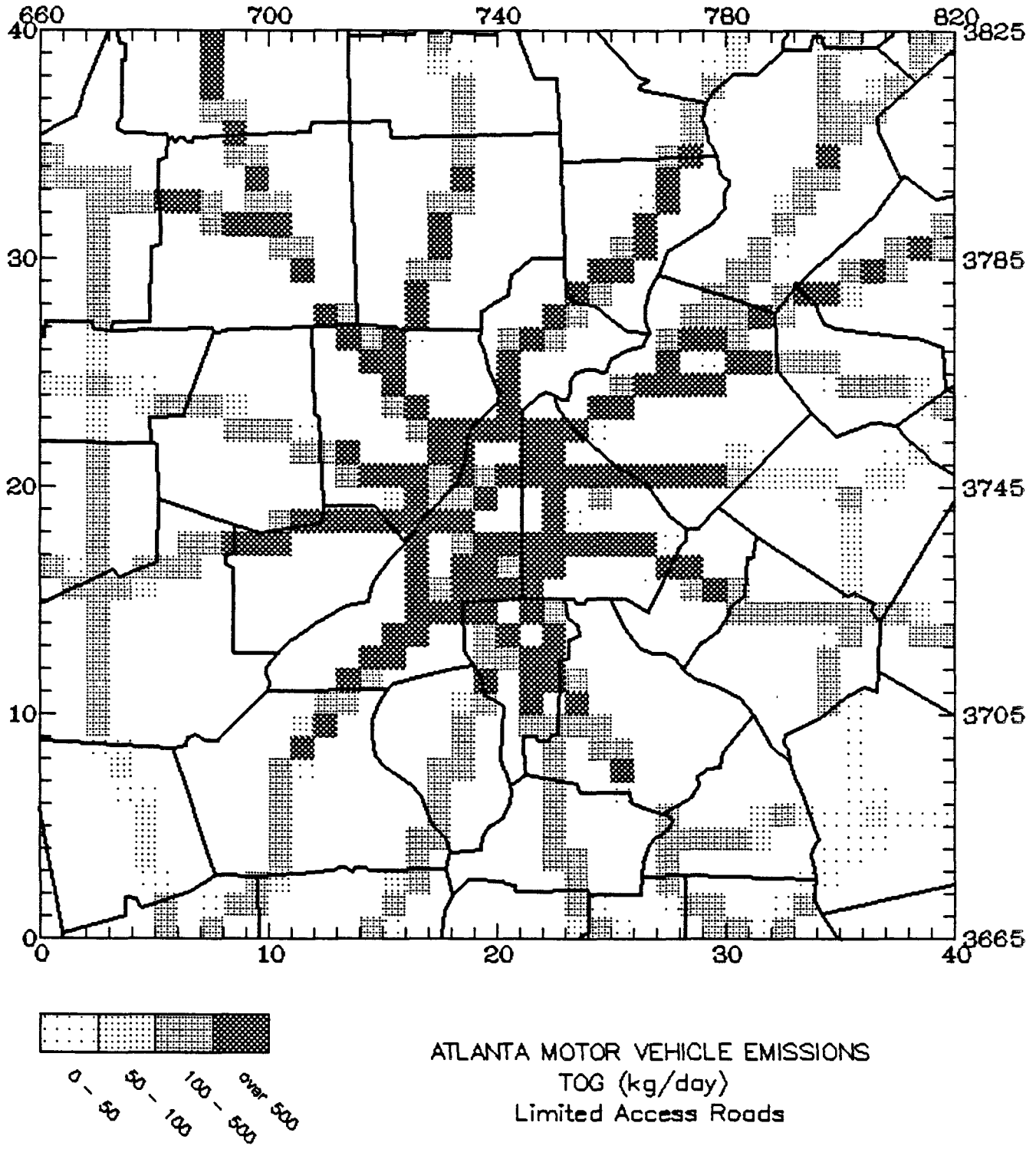

ATLANTA MOTOR VEHICLE EMISSIONS
TOG (kg/day)
Limited Access Roads

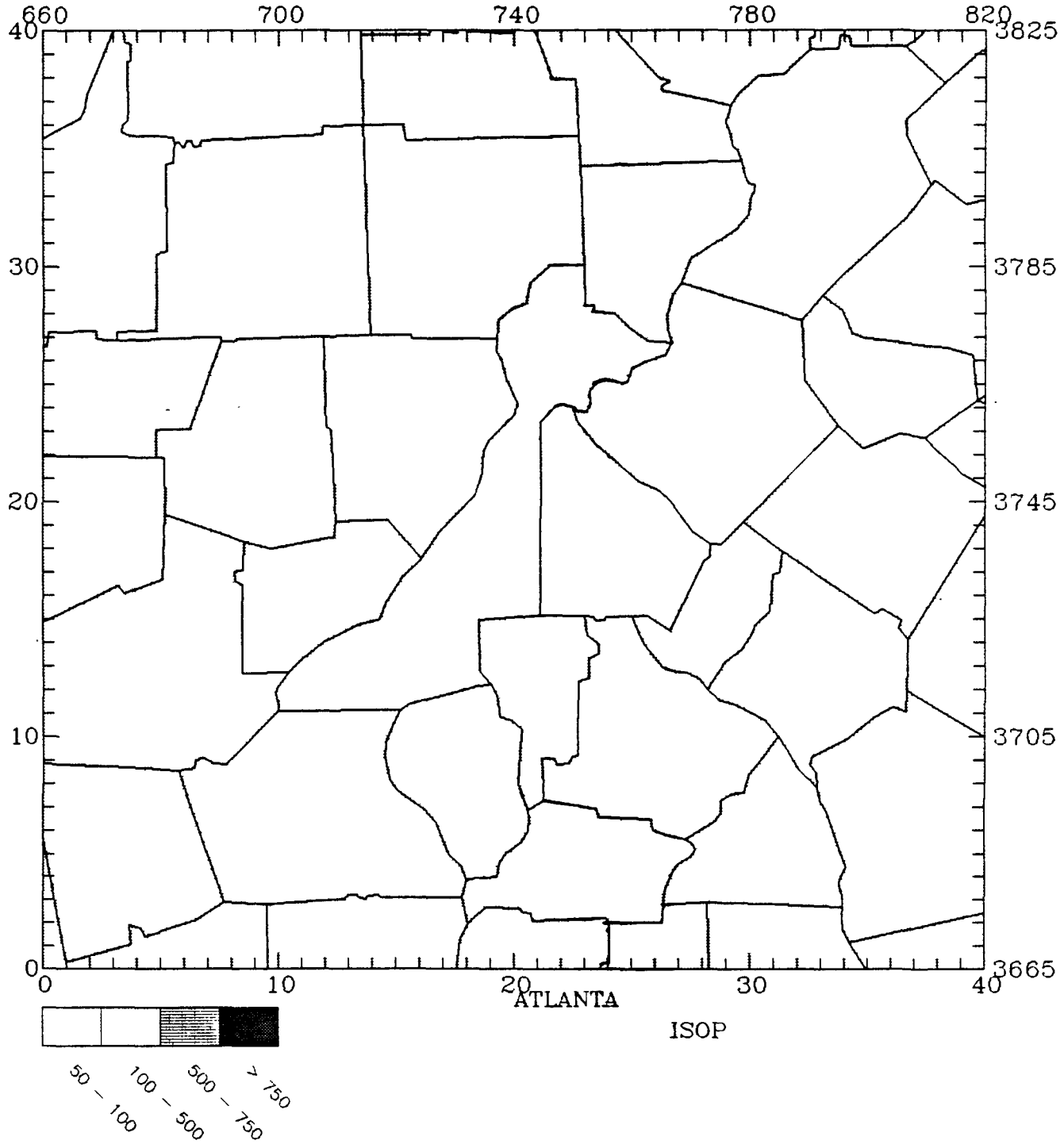

Total biogenic ISOP emissions (kg/day) for the Atlanta UAM modeling domain

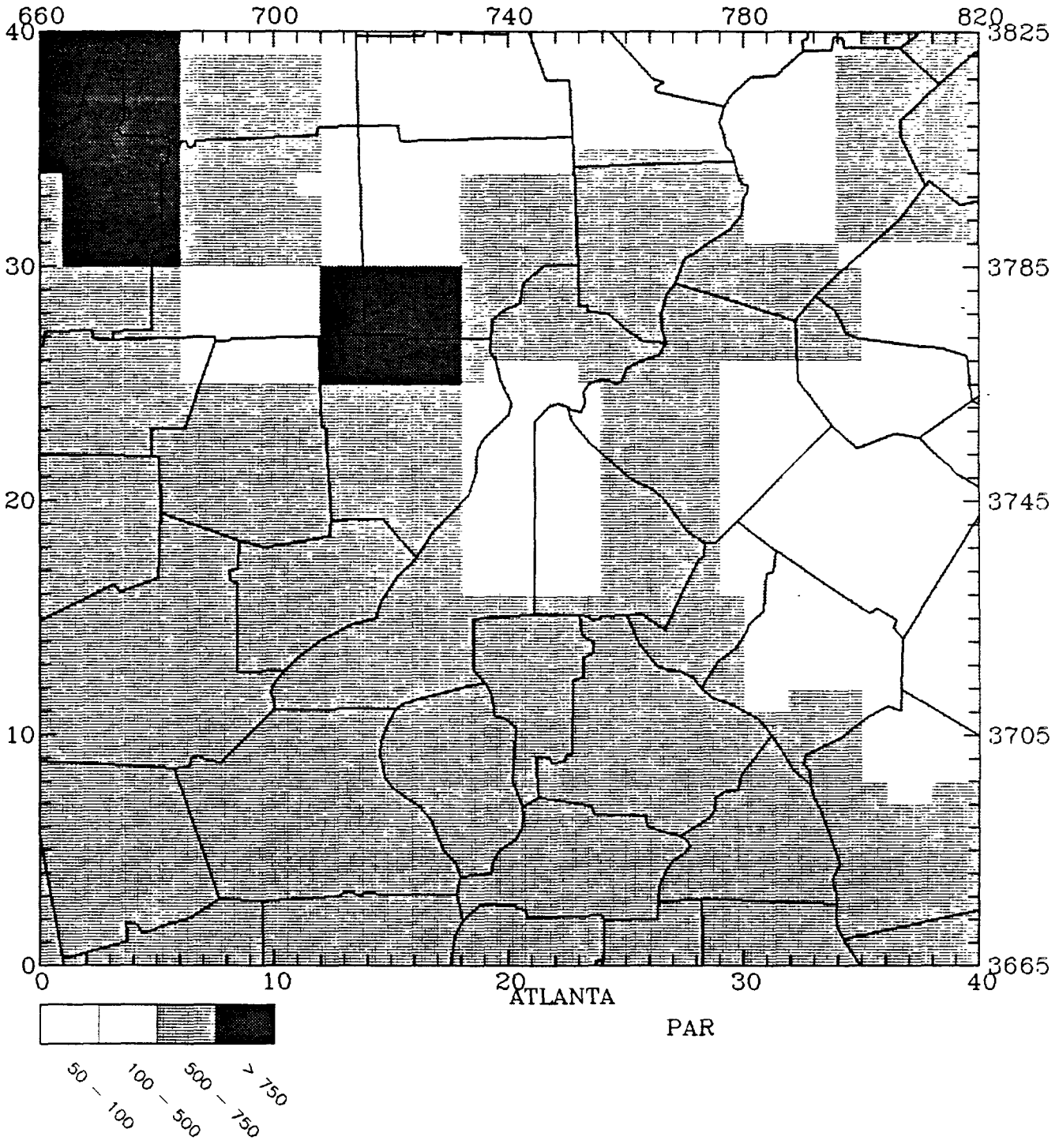

Total biogenic PAR emissions (kg/day) for the Atlanta UAM modeling domain

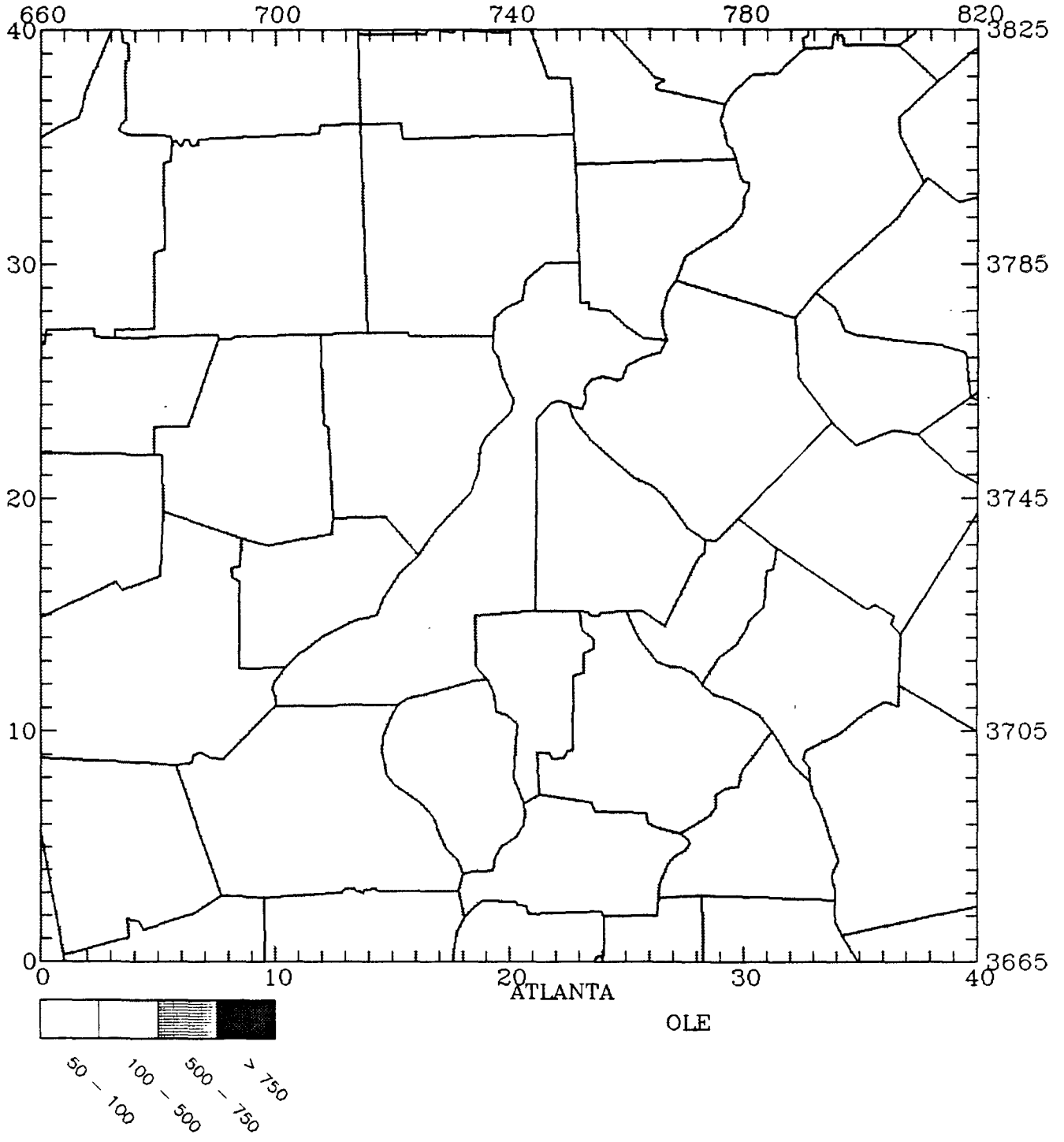

Total biogenic OLE emissions (kg/day) for the Atlanta UAM modeling domain

Appendix B

HOURLY WIND FIELDS FOR UAM LAYER 1 USED IN DIAGNOSTIC RUN 1

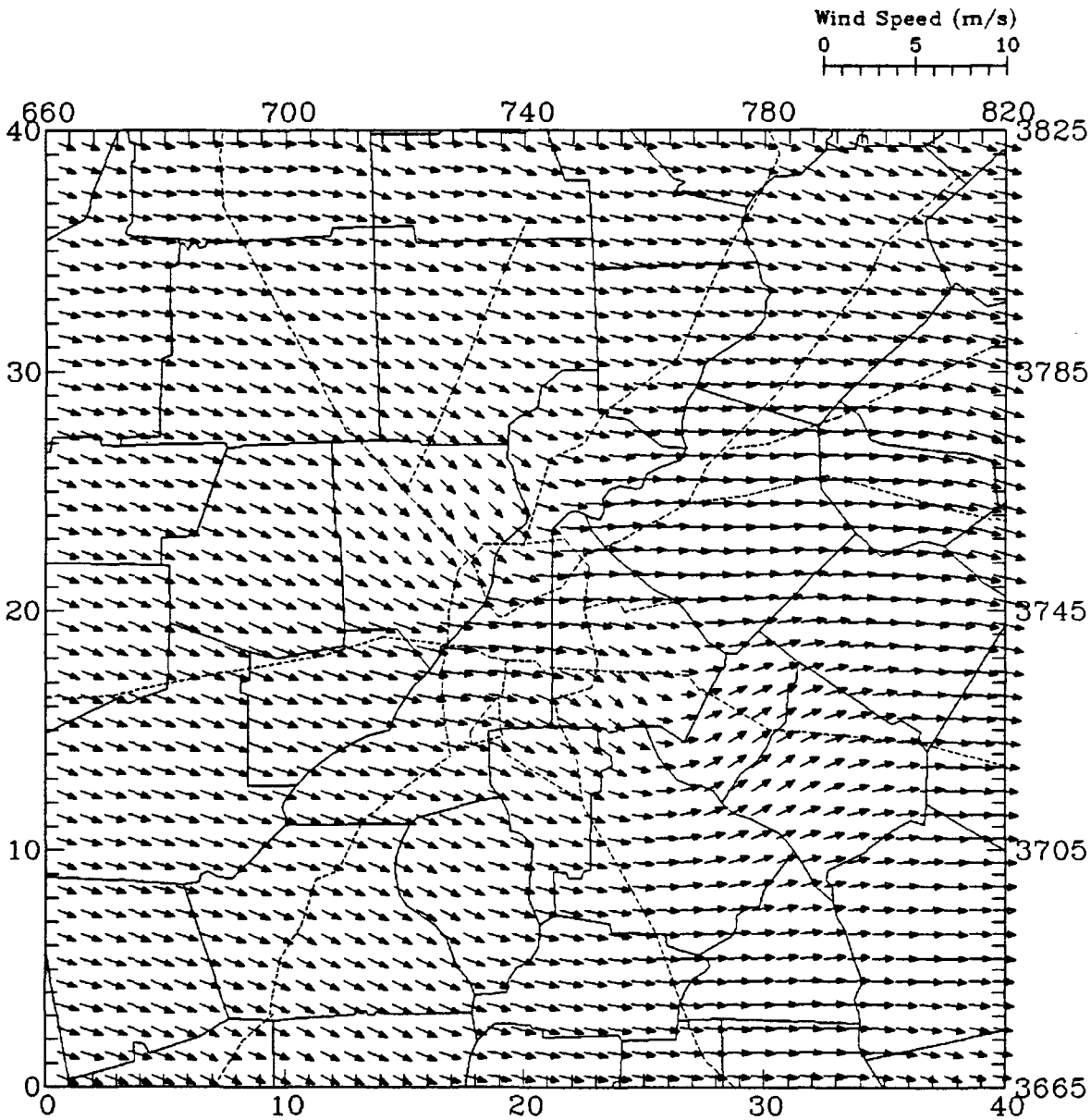

Atlanta PLANR Winds
Layer 1 at hour 10 on 84156

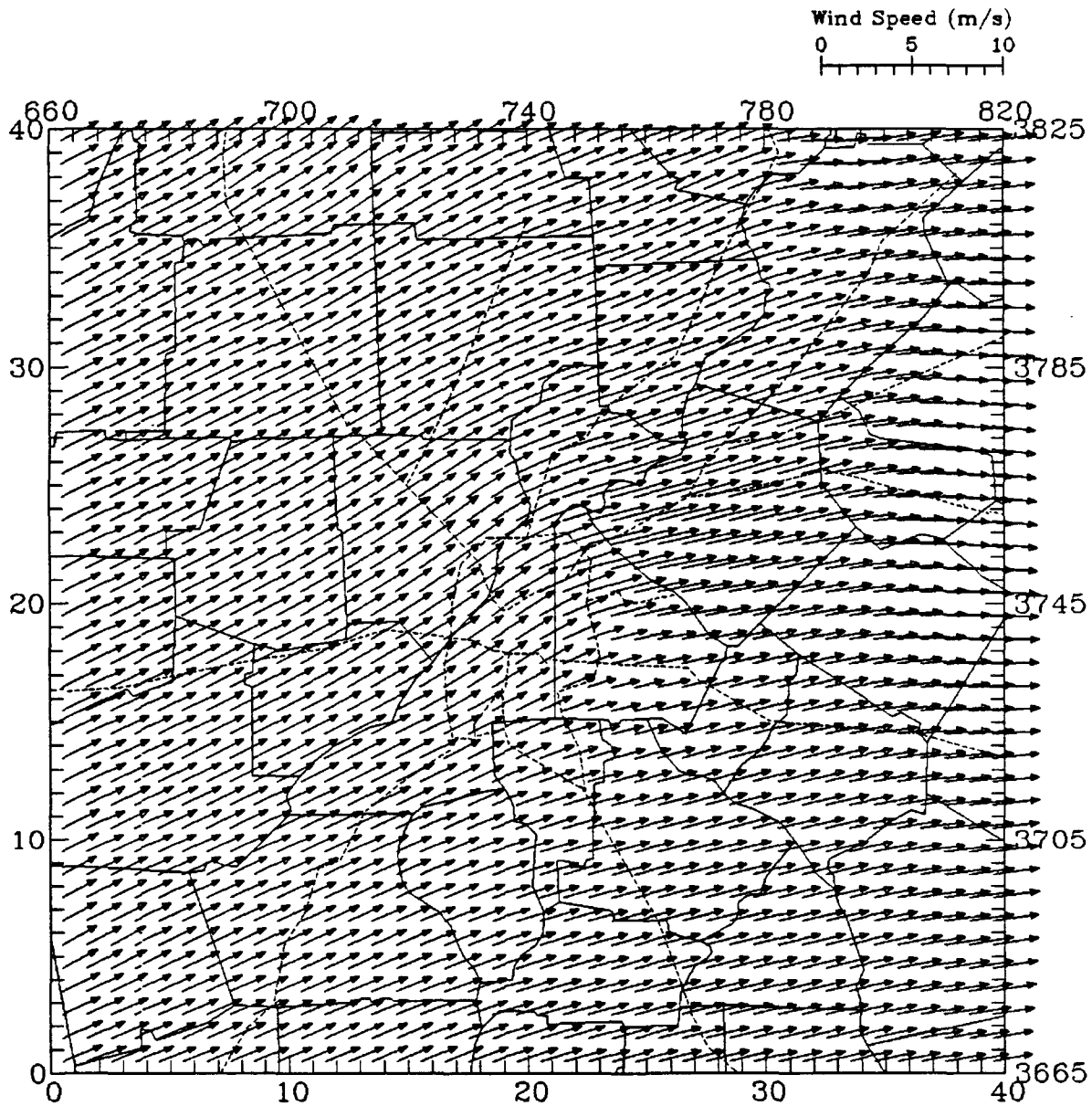

Atlanta PLANR Winds
Layer 1 at hour 11 on 84156

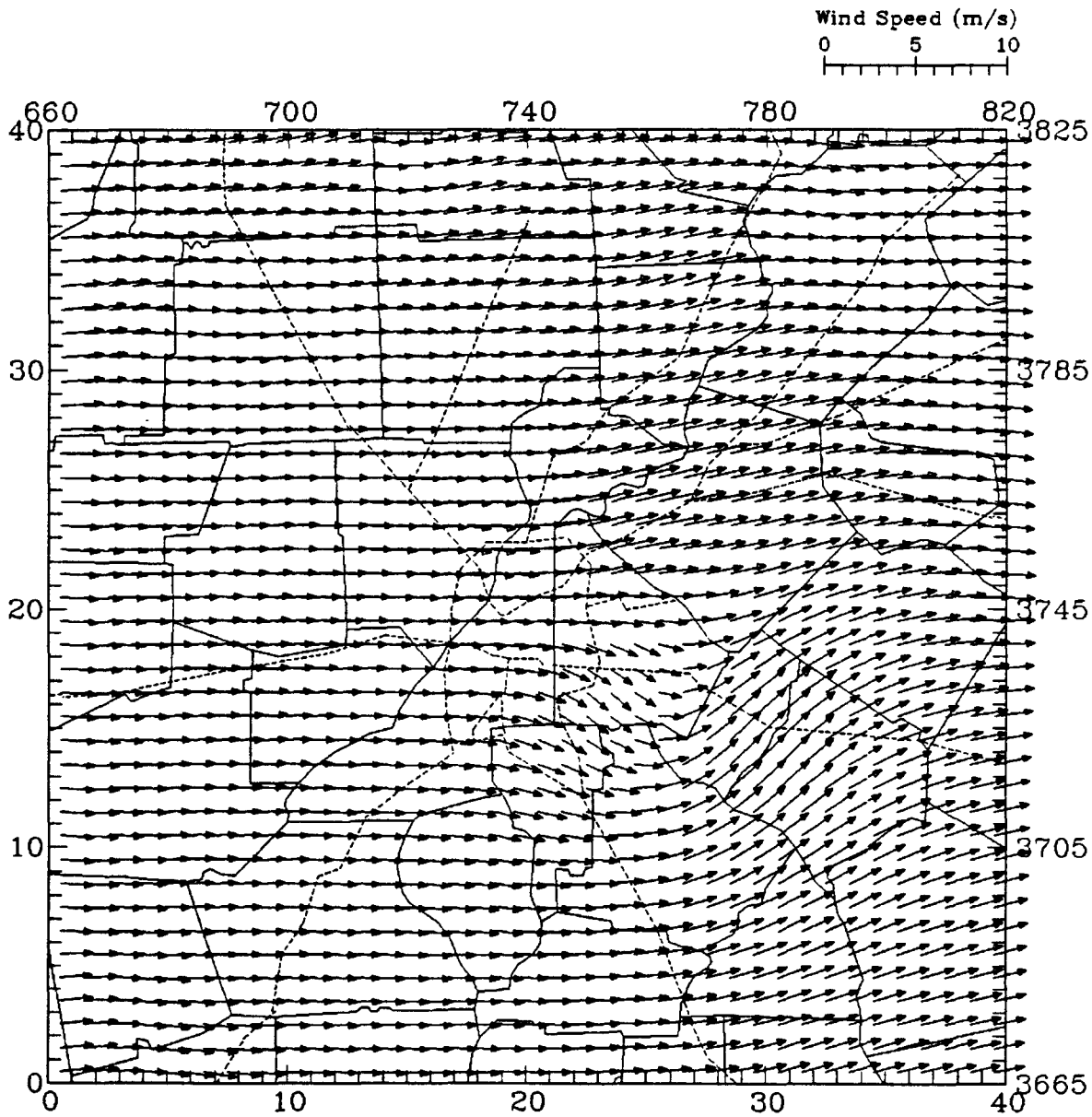

Atlanta PLANR Winds
Layer 1 at hour 12 on 84156

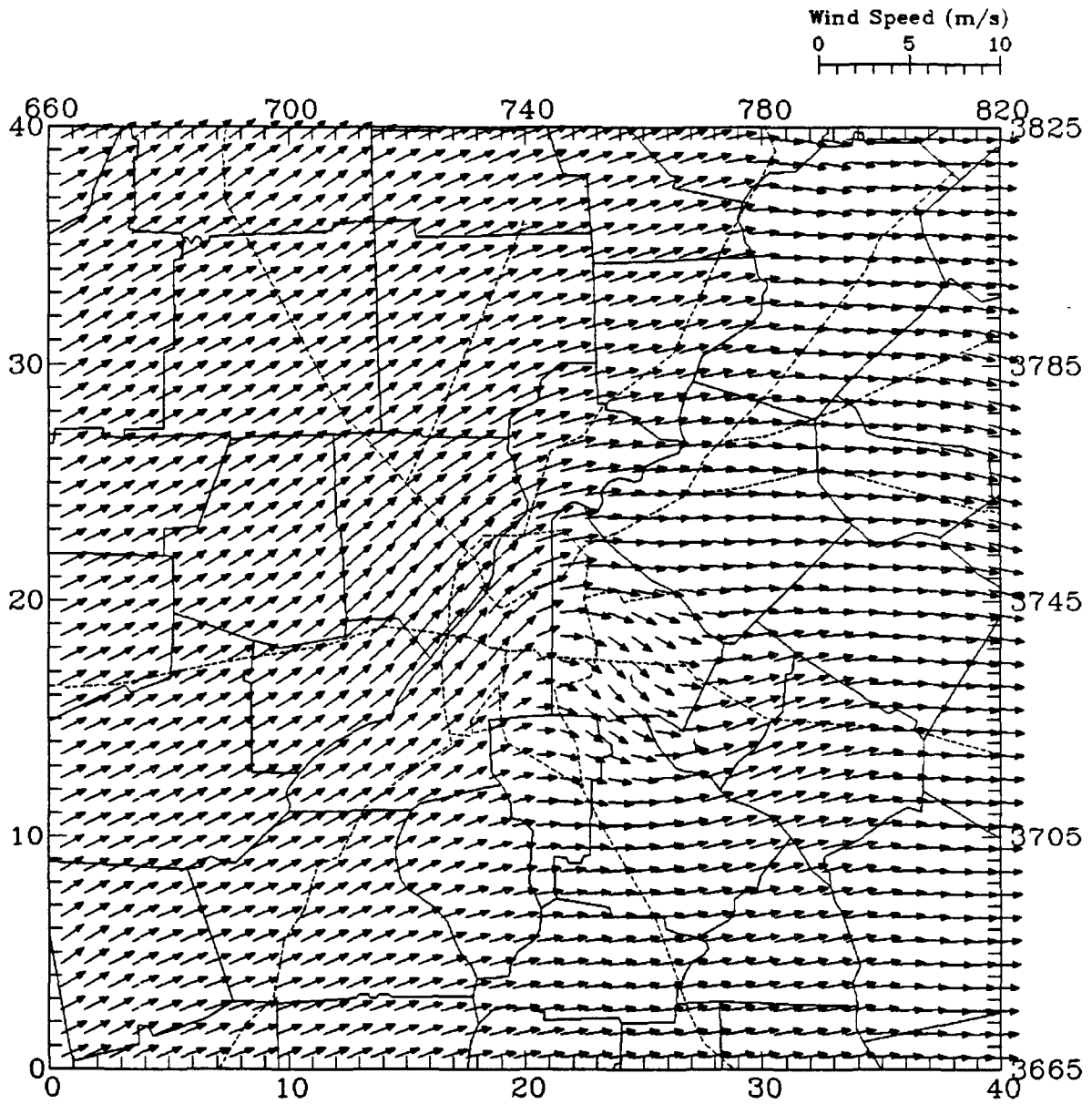

Atlanta PLANR Winds
Layer 1 at hour 13 on 84156

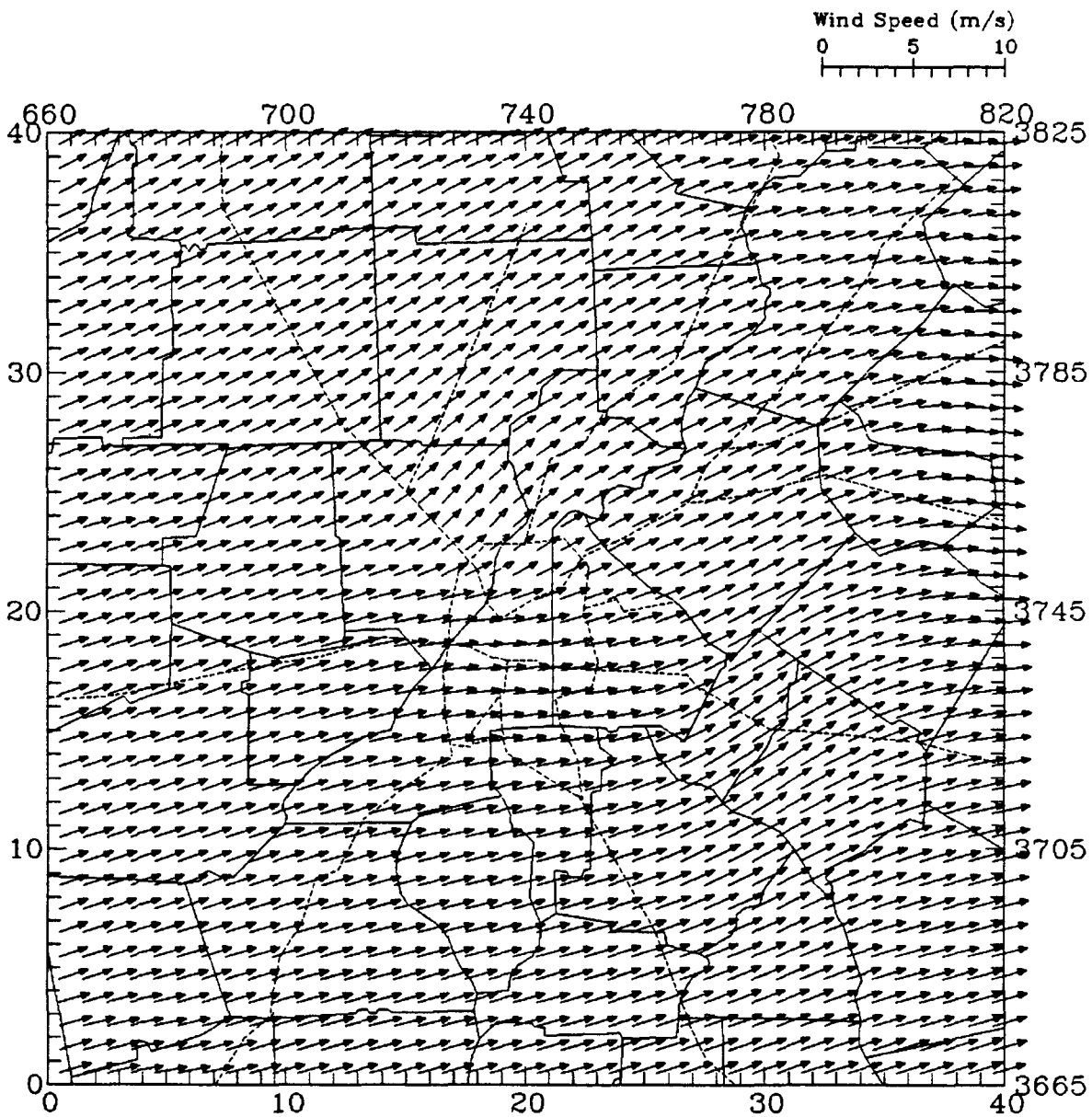

Atlanta PLANR Winds
Layer 1 at hour 14 on 84156

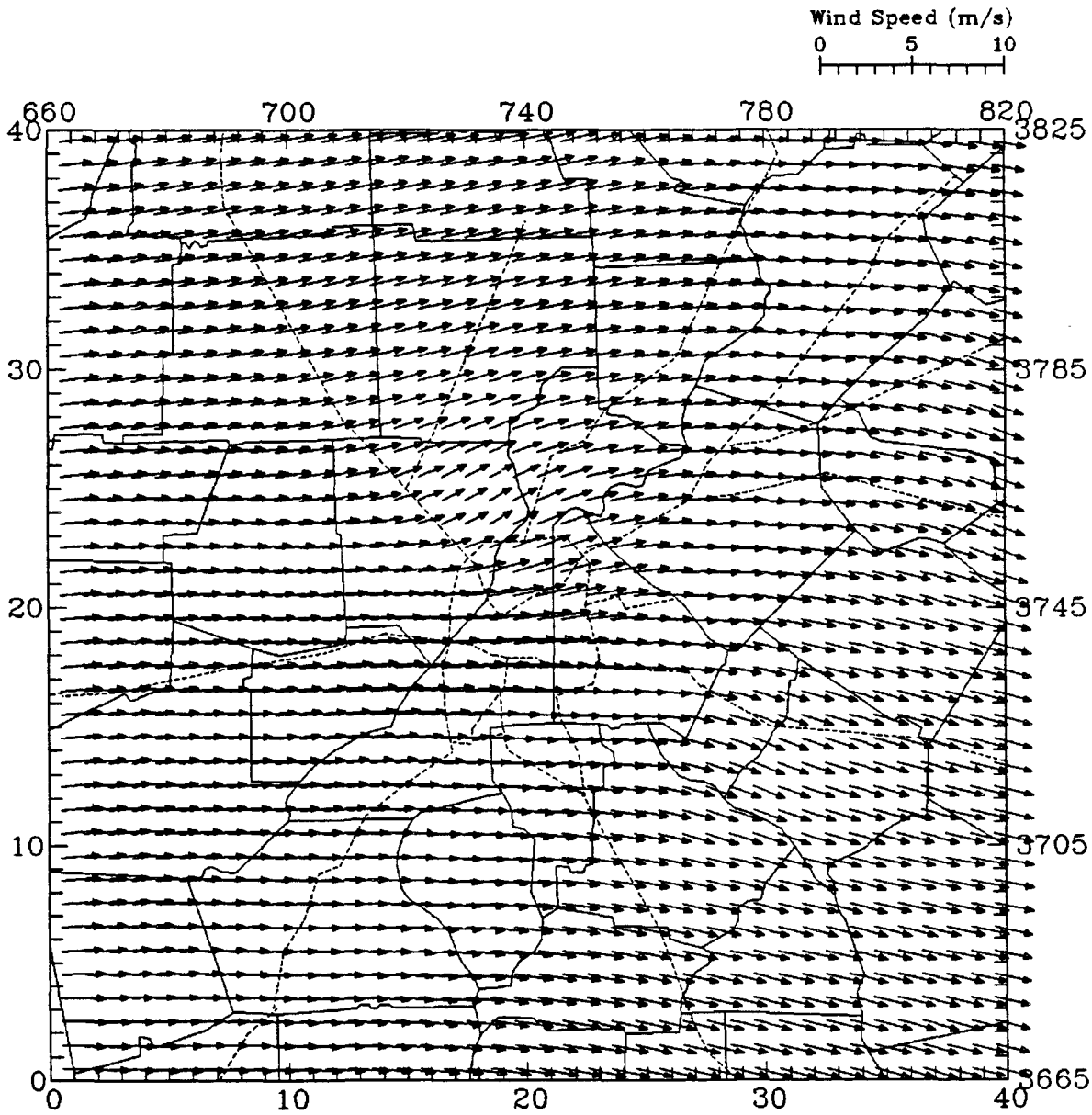

Atlanta PLANR Winds
Layer 1 at hour 15 on 84156

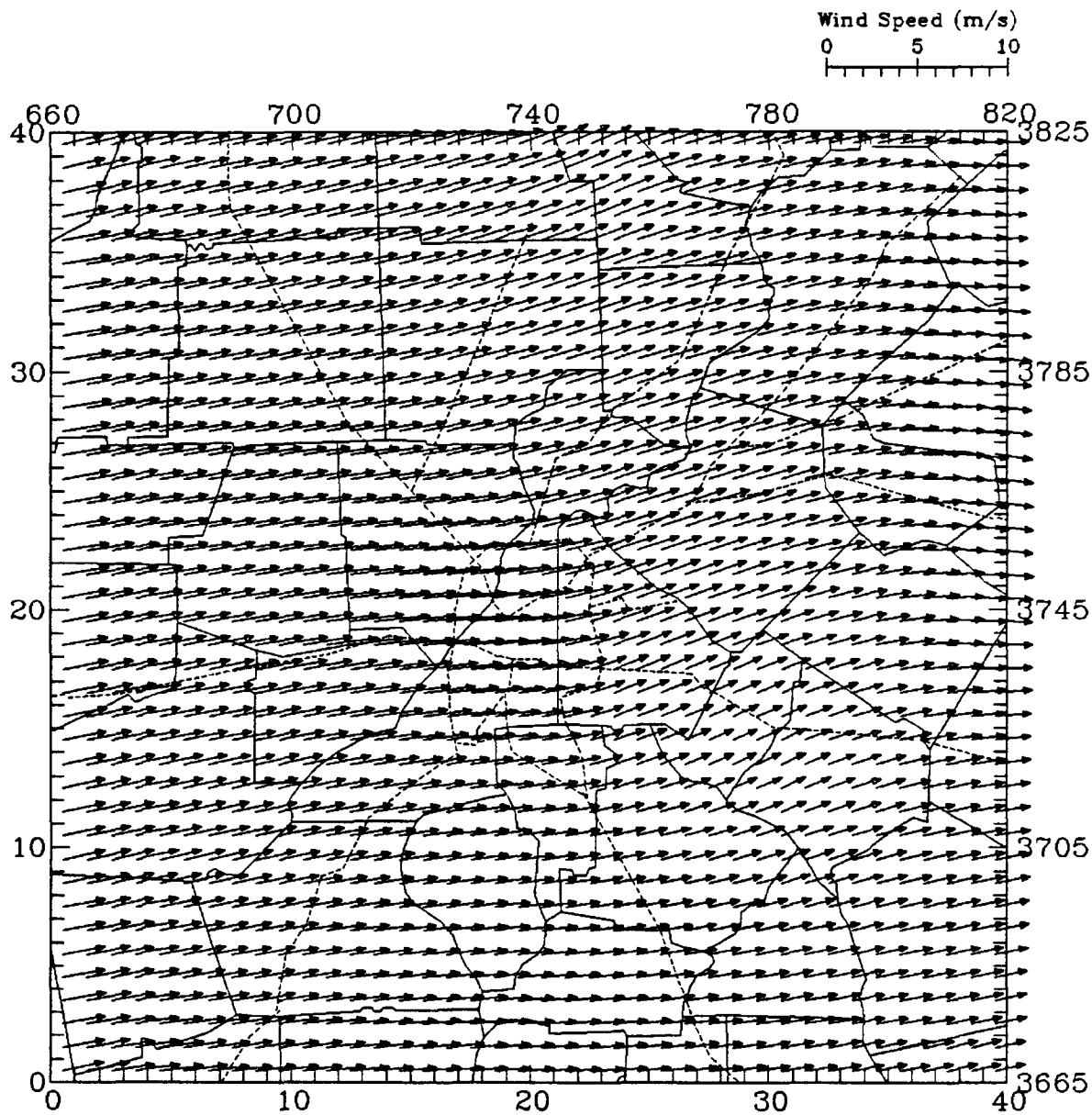

Atlanta PLANR Winds
Layer 1 at hour 16 on 84156

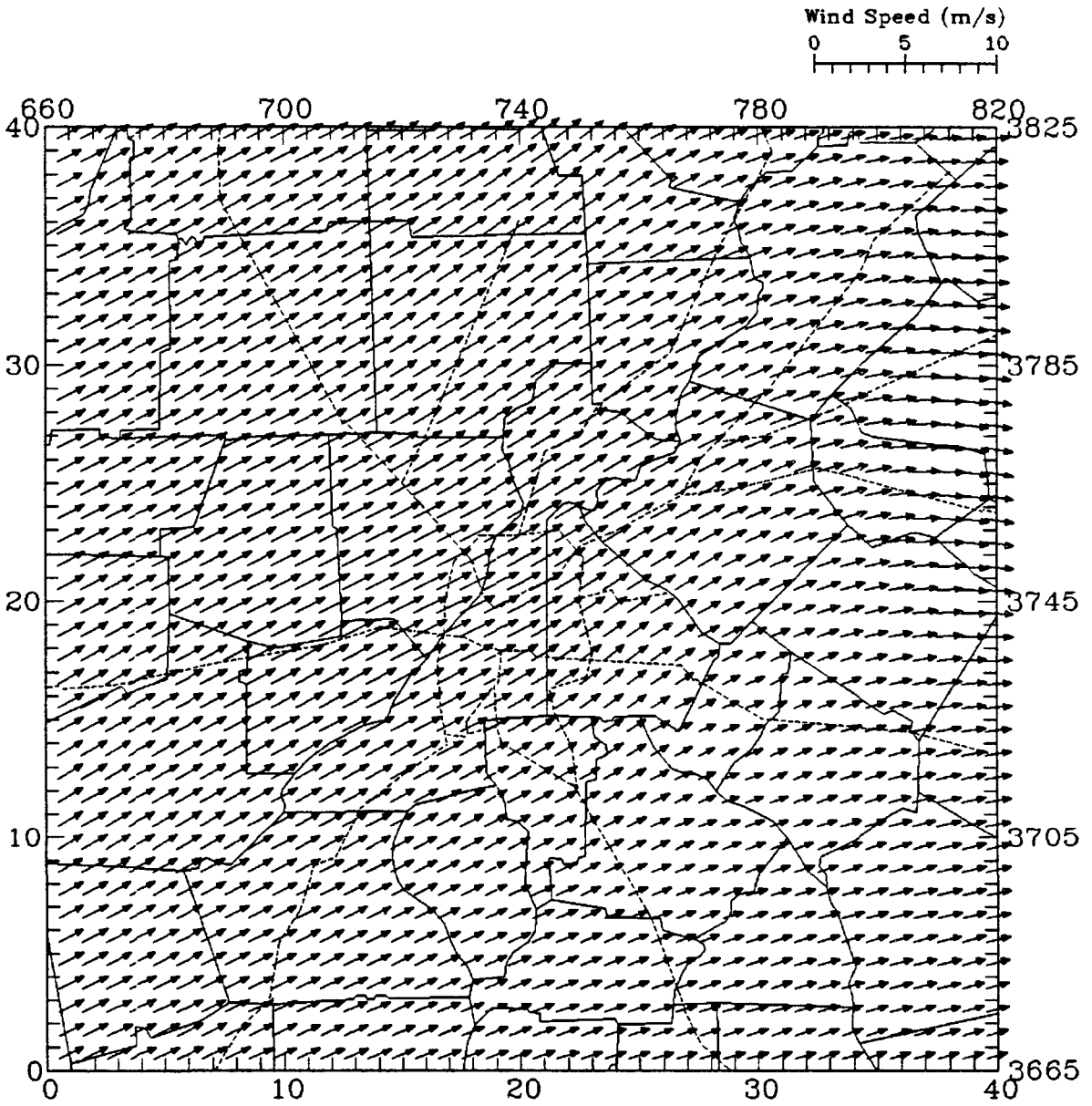

Atlanta PLANR Winds
Layer 1 at hour 17 on 84156

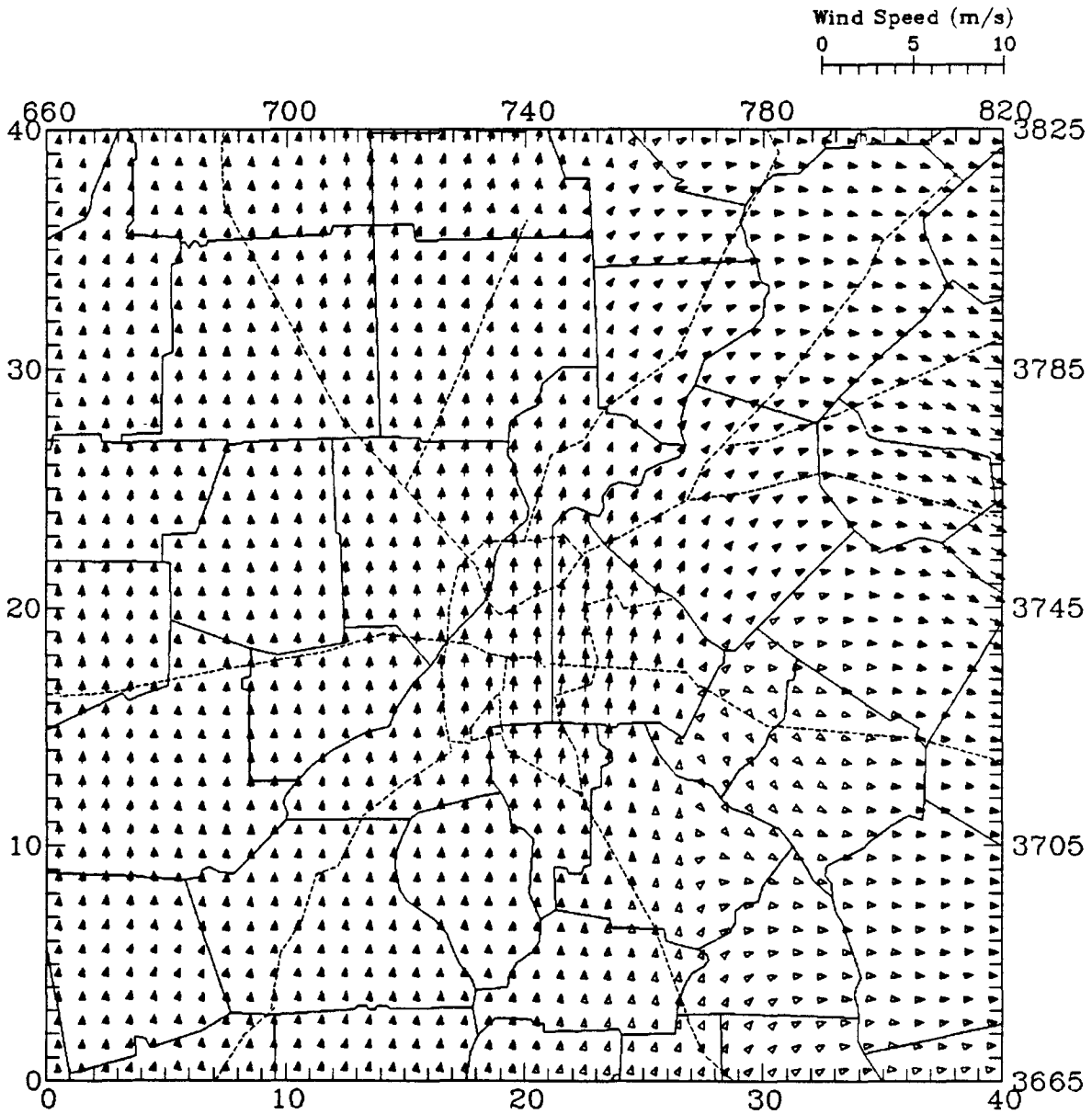

Atlanta PLANR Winds
Layer 1 at hour 18 on 84156

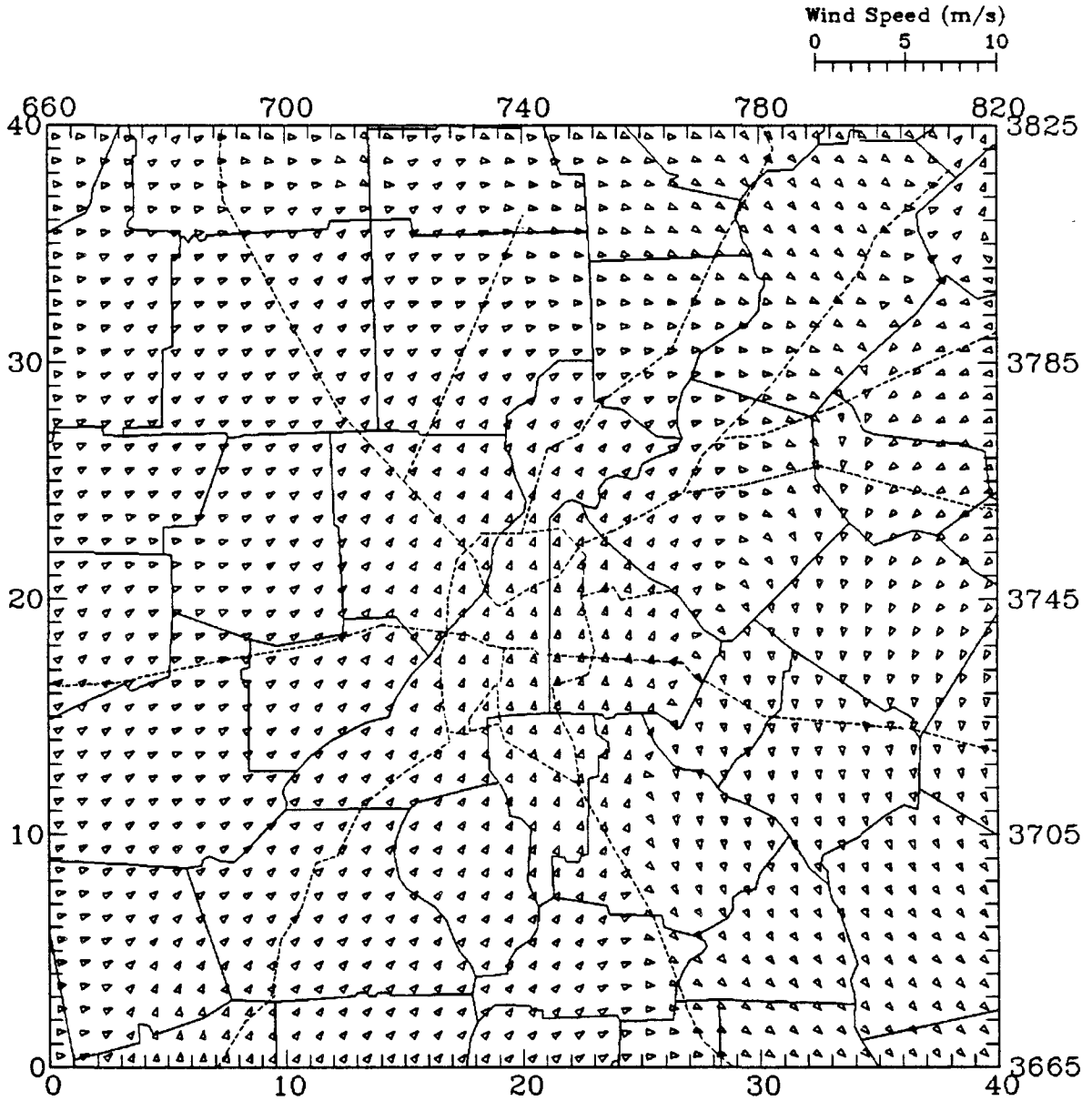

Atlanta PLANR Winds
Layer 1 at hour 19 on 84156

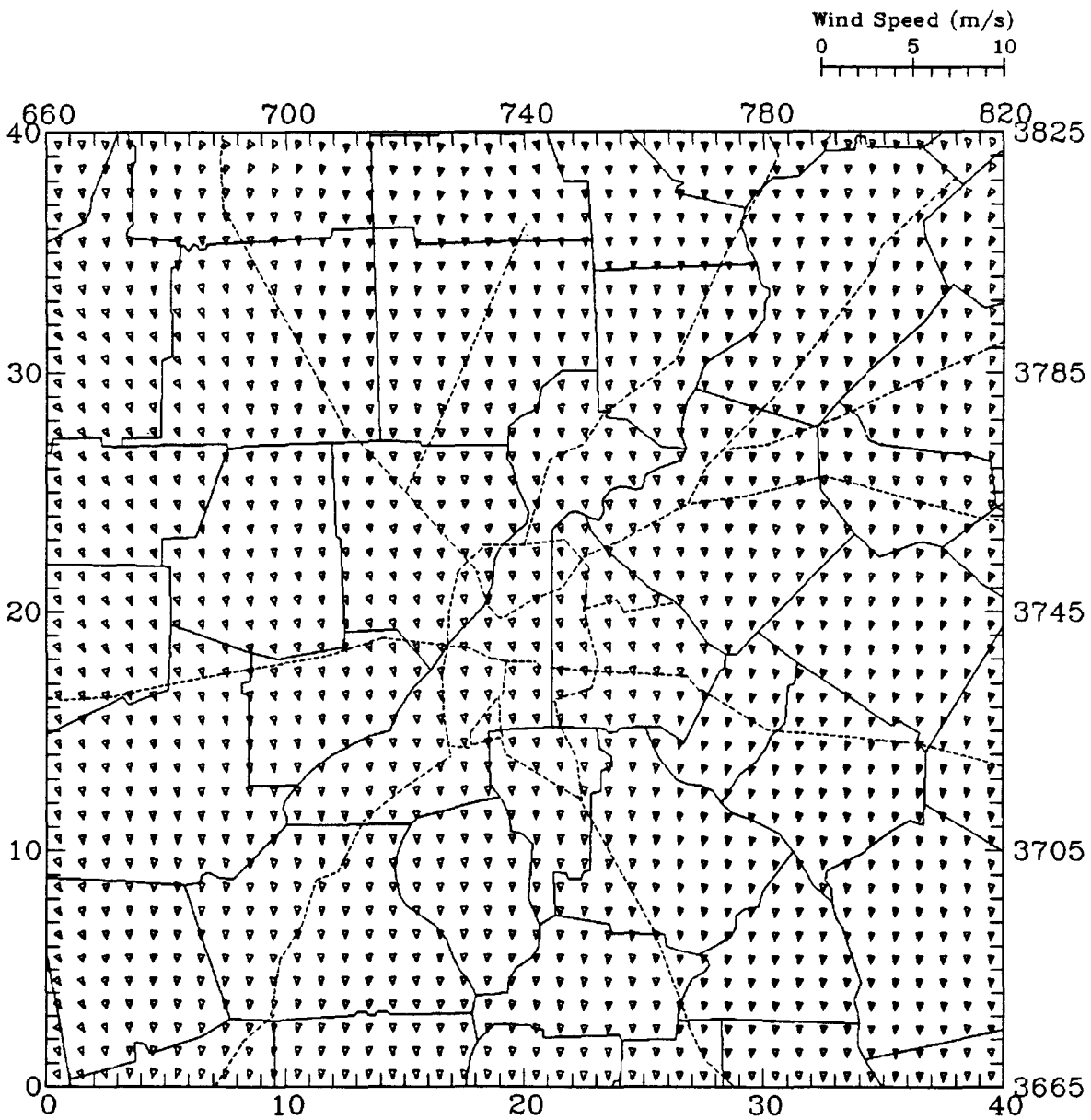

Atlanta PLANR Winds
Layer 1 at hour 20 on 84156

Appendix C

HOURLY PREDICTED OZONE CONCENTRATIONS (pphm) FOR DIAGNOSTIC RUN 1

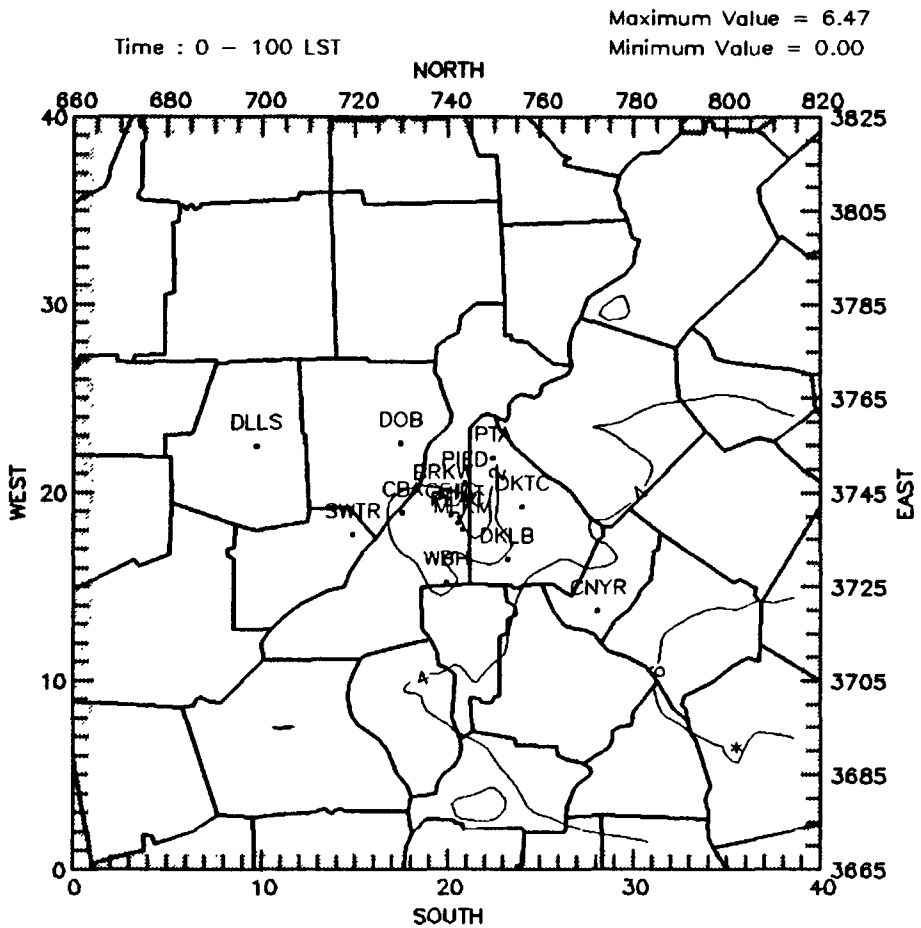

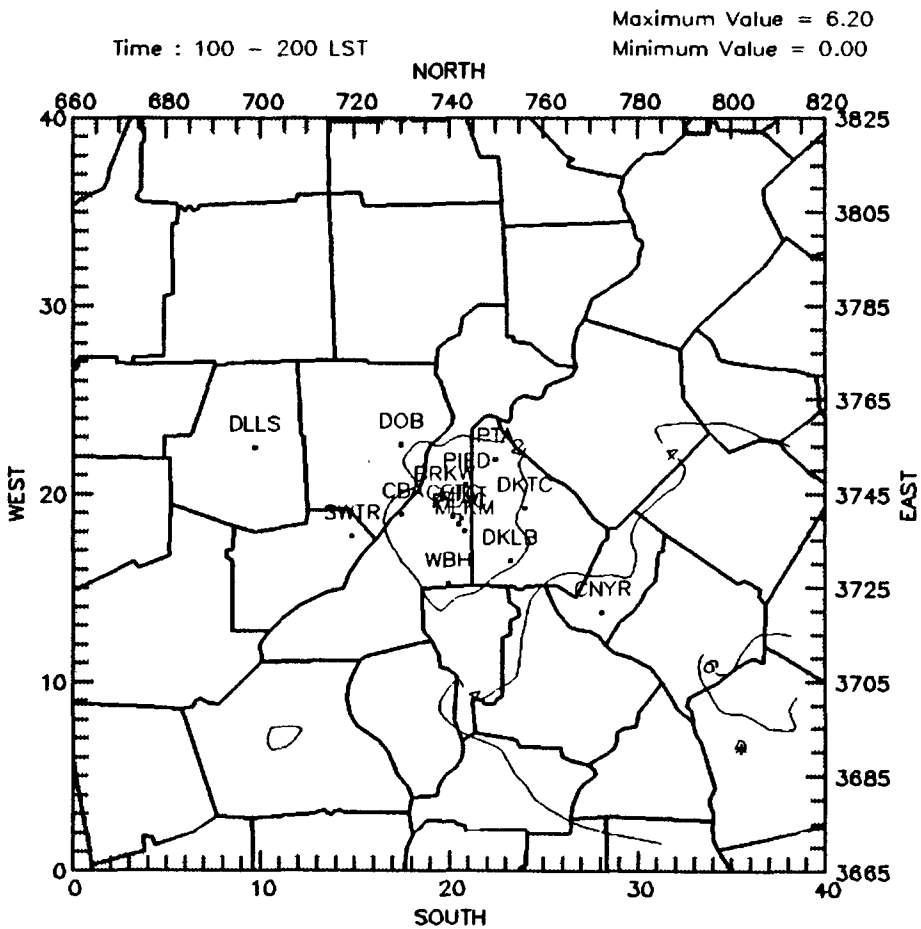

Ozone Concentration Evaluation run #1, June 4, 1984 (pphm)

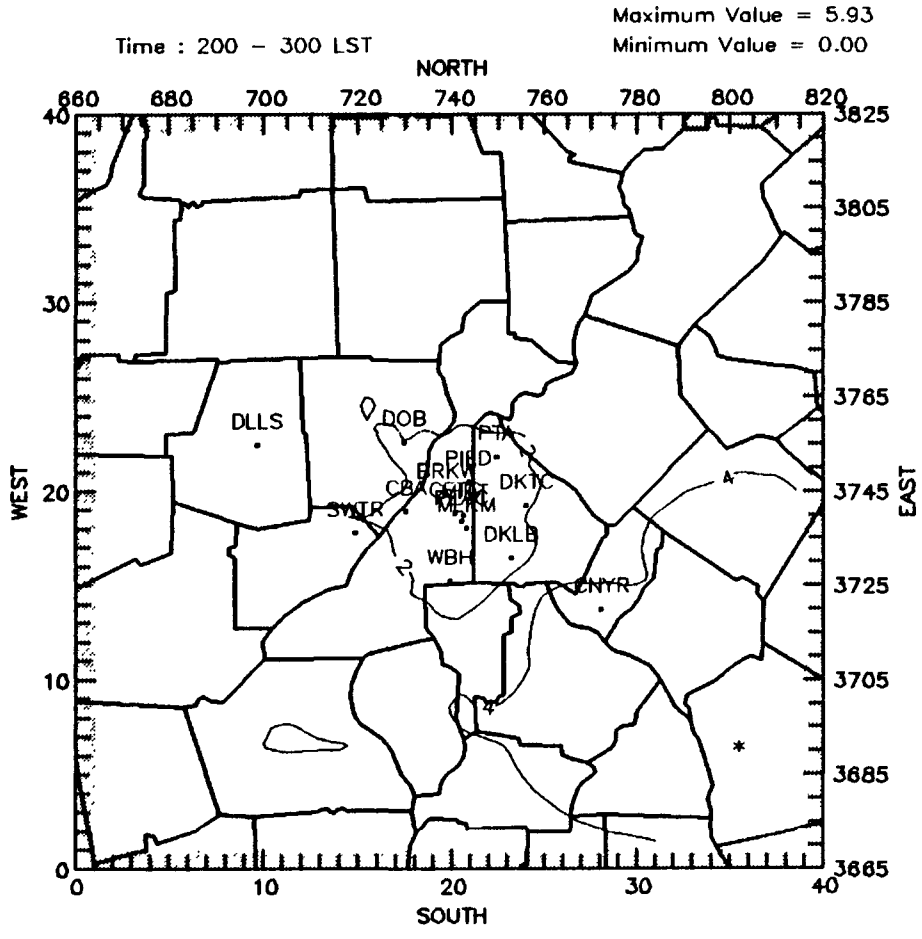

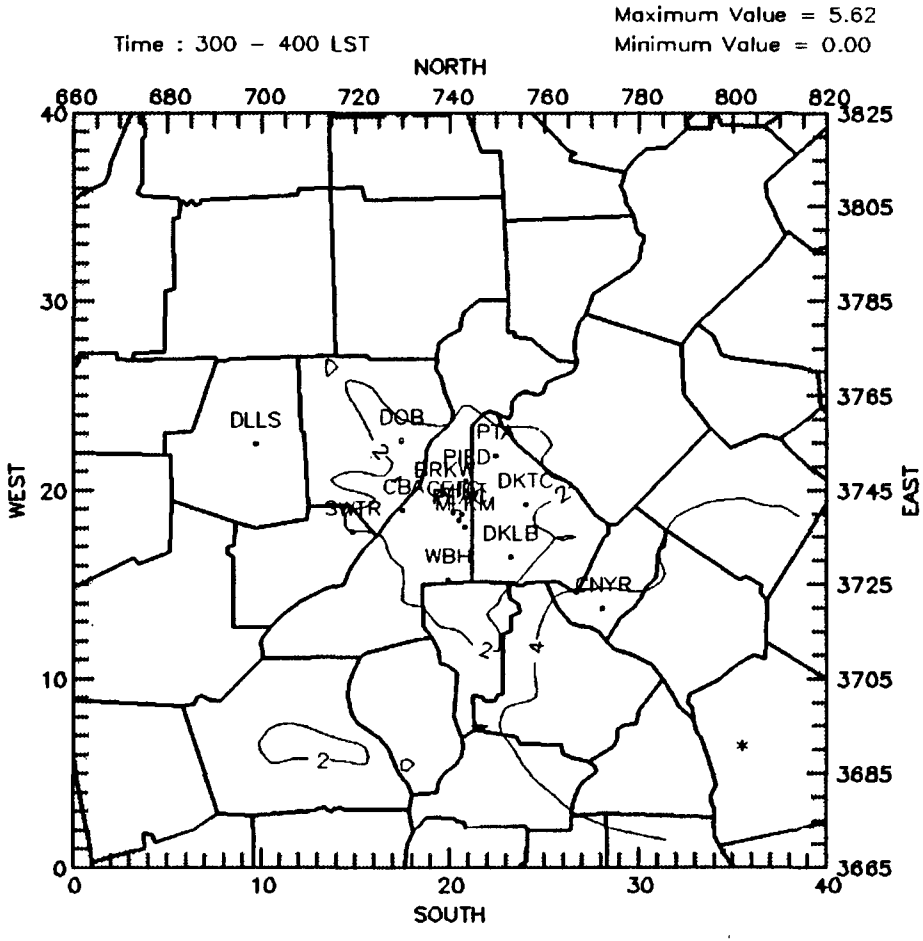

Ozone Concentration Evaluation run #1, June 4, 1984 (pphm)

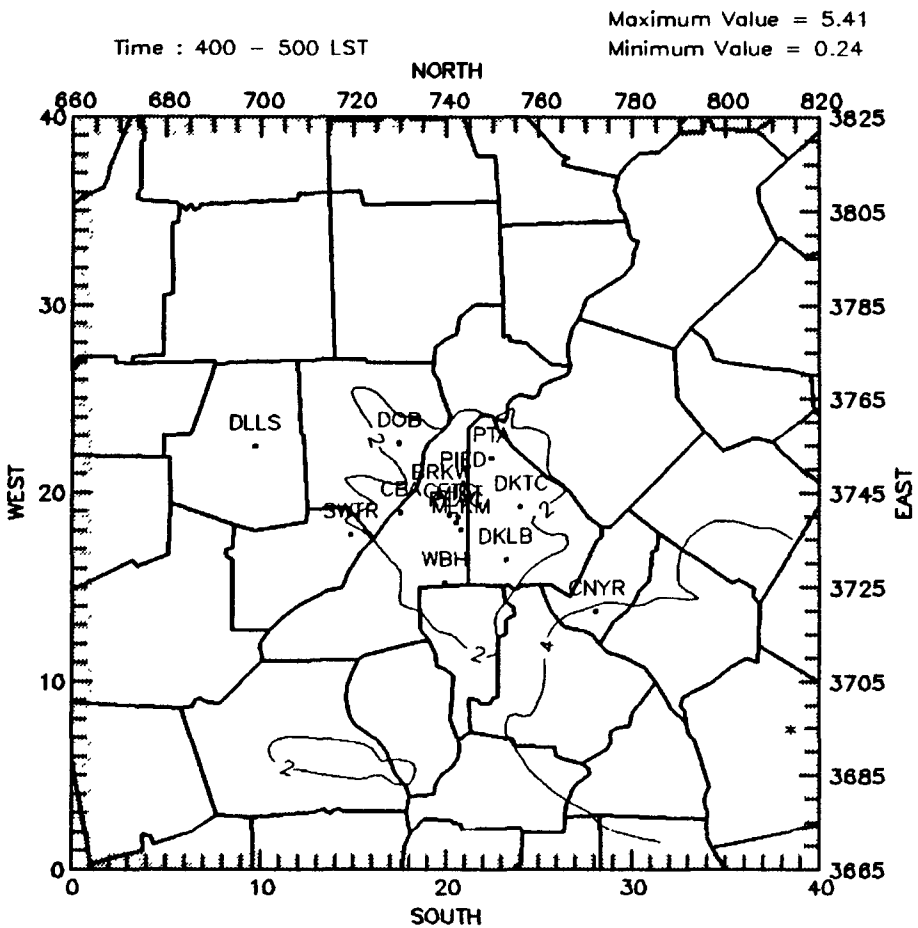

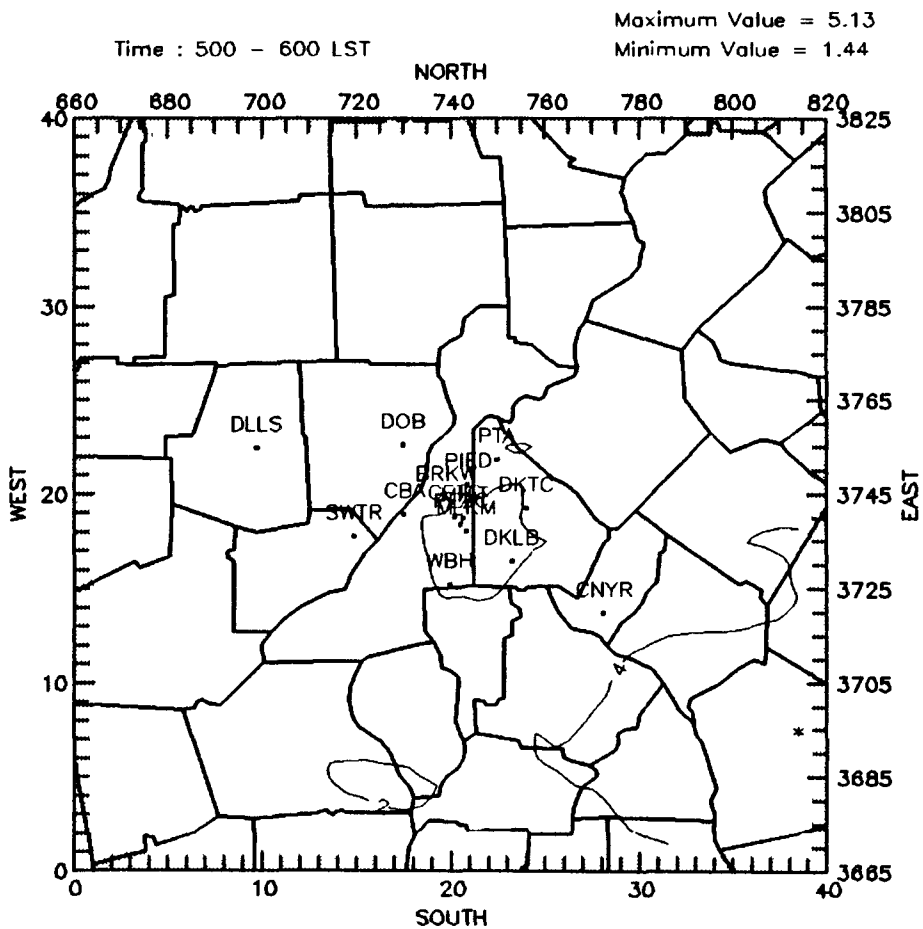

Ozone Concentration Evaluation run #1, June 4, 1984 (pphm)

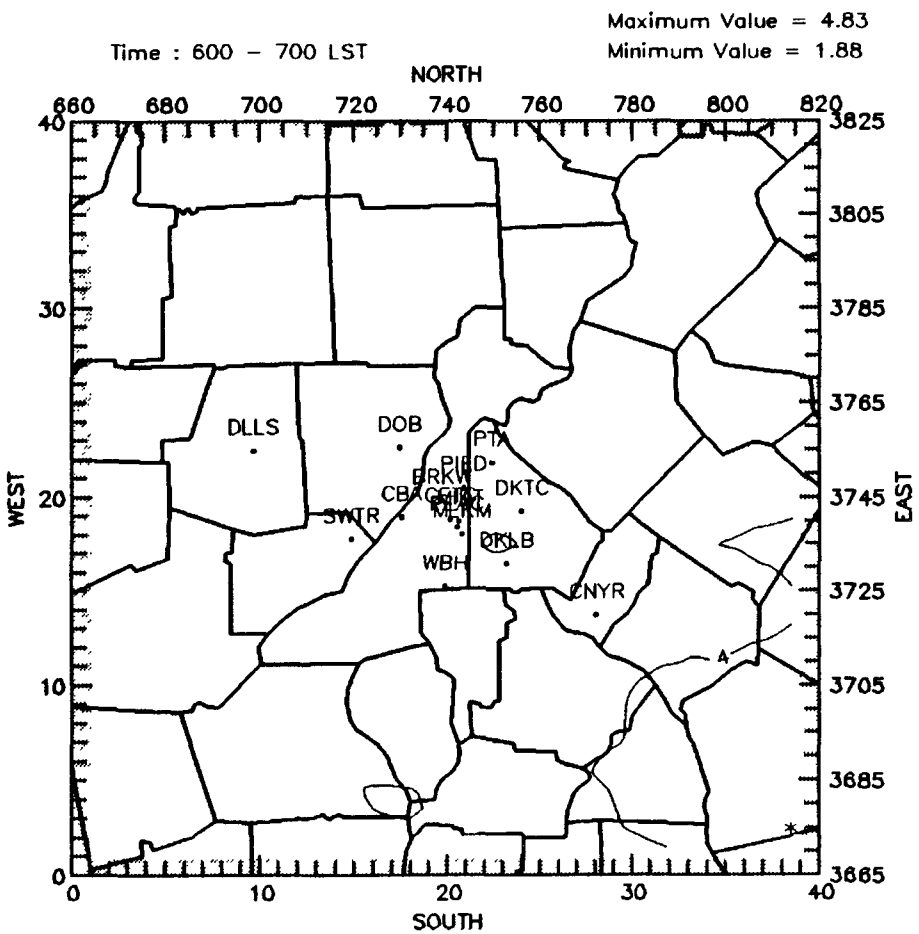

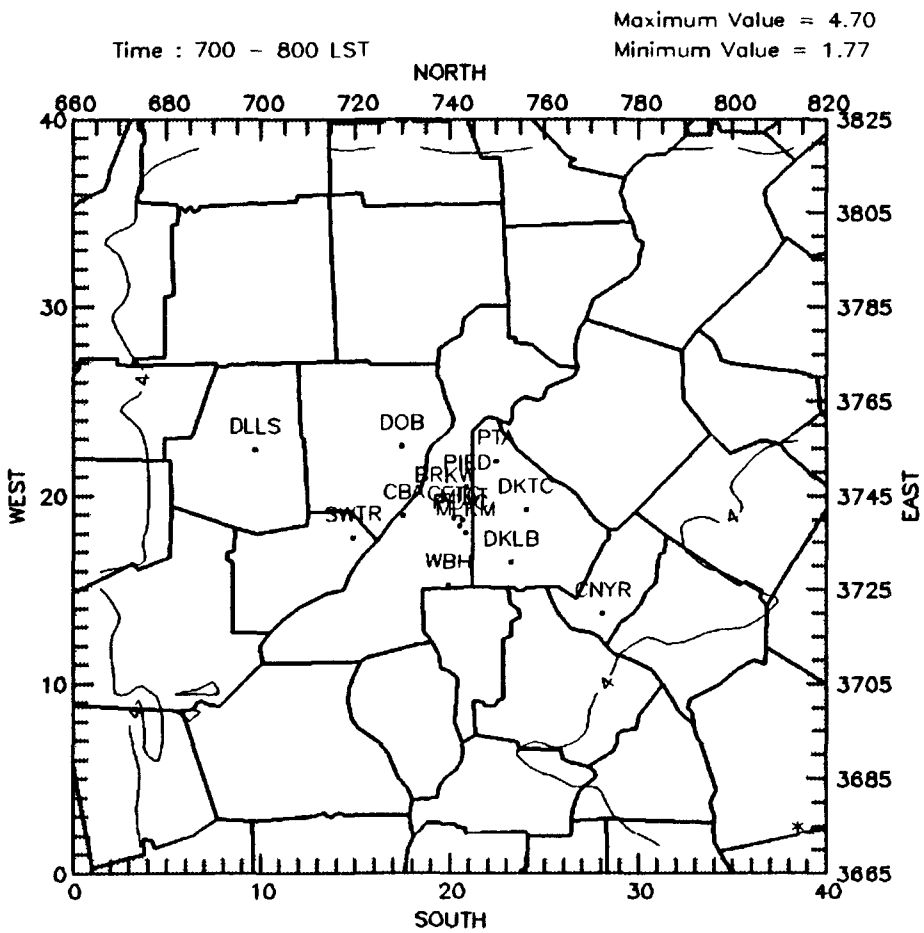

Ozone Concentration Evaluation run #1, June 4, 1984 (pphm)

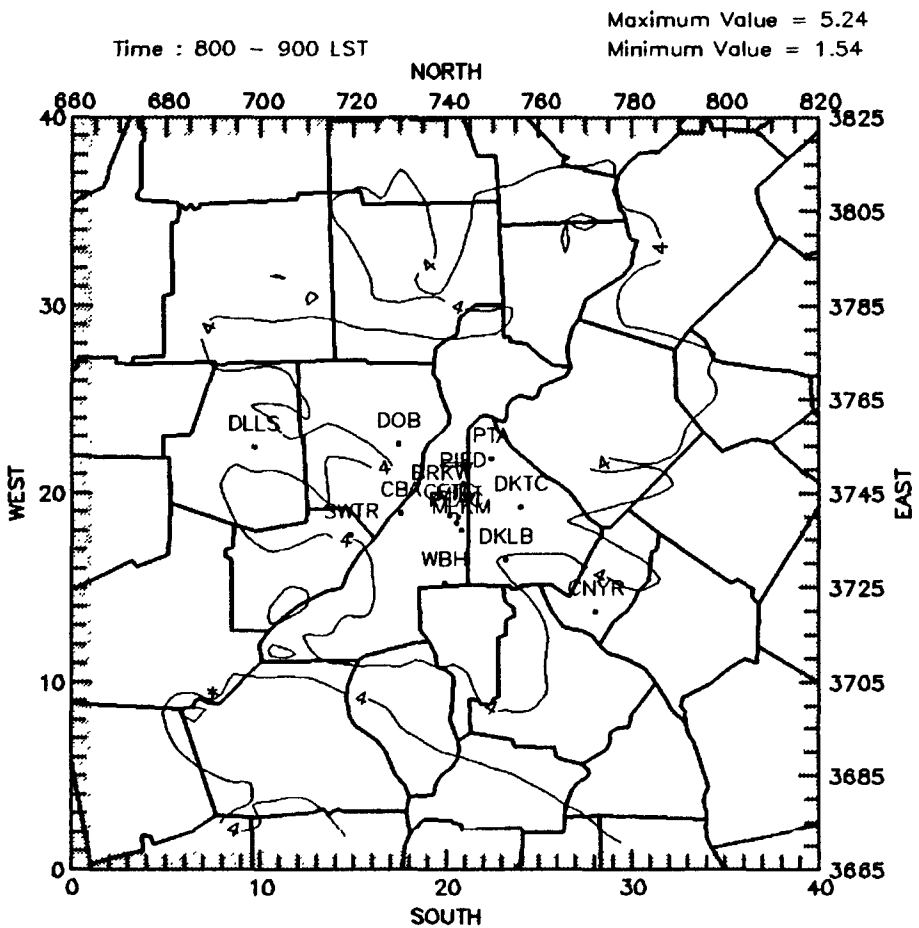

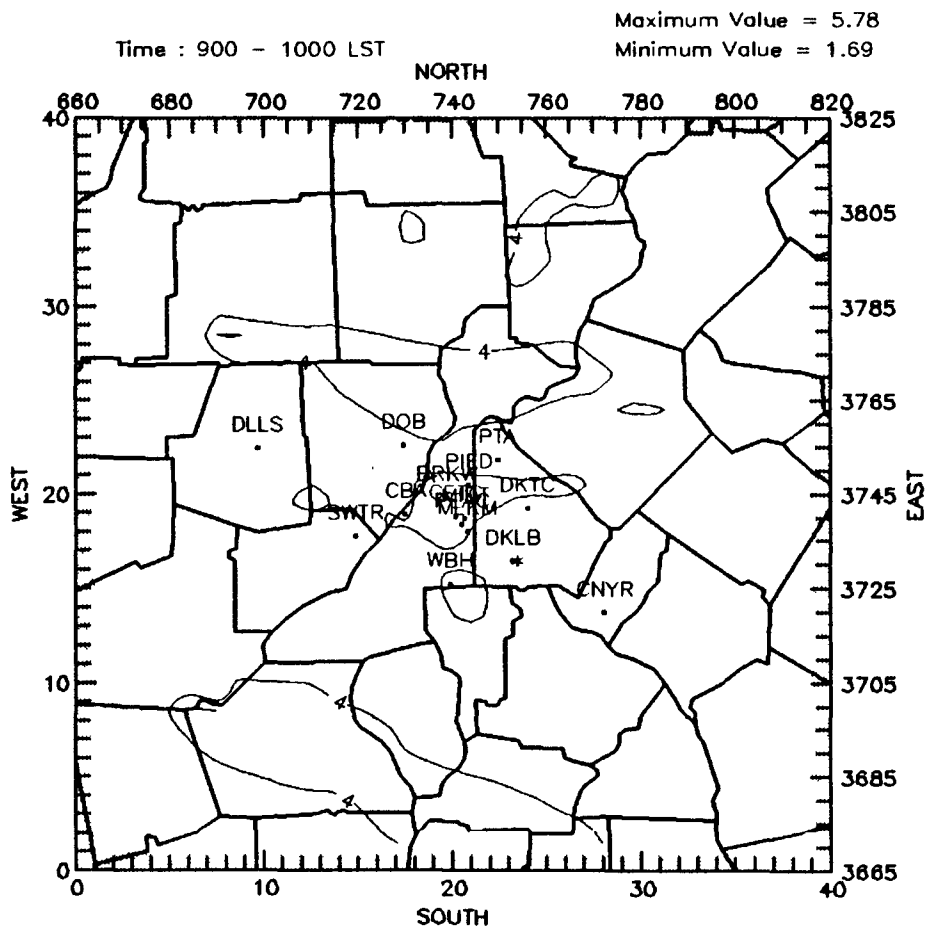

Ozone Concentration Evaluation run #1, June 4, 1984 (pphm)

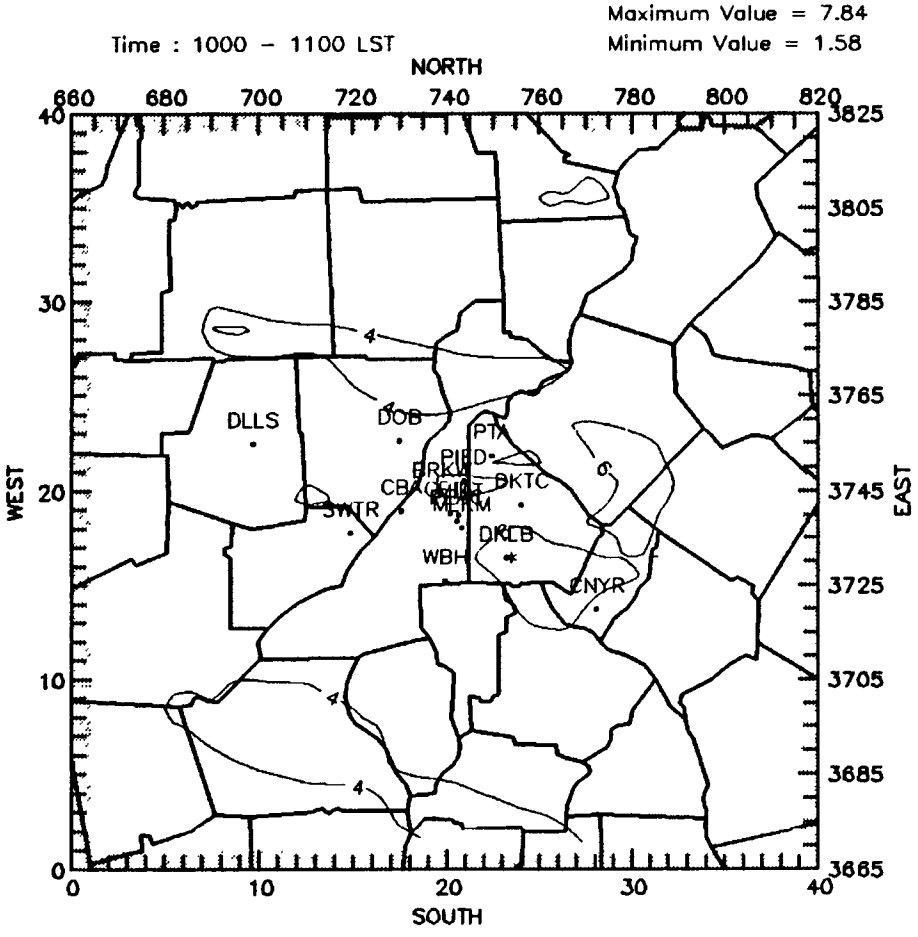

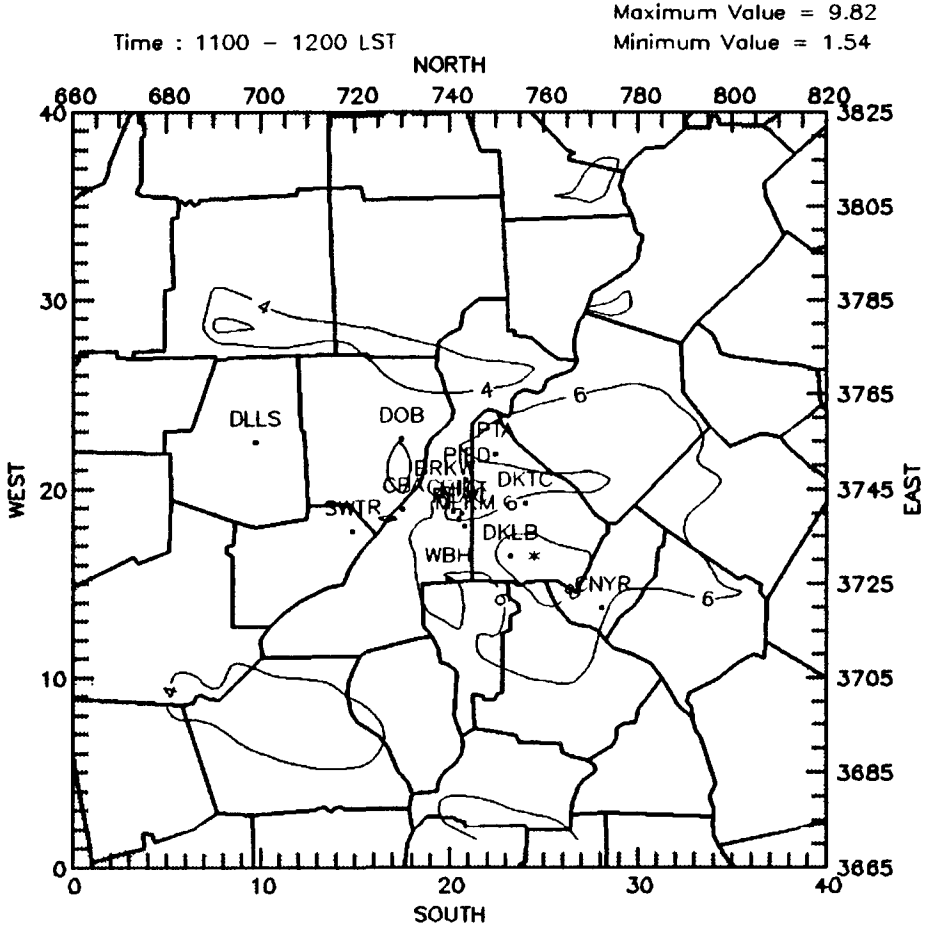

Ozone Concentration Evaluation run #1, June 4, 1984 (pphm)

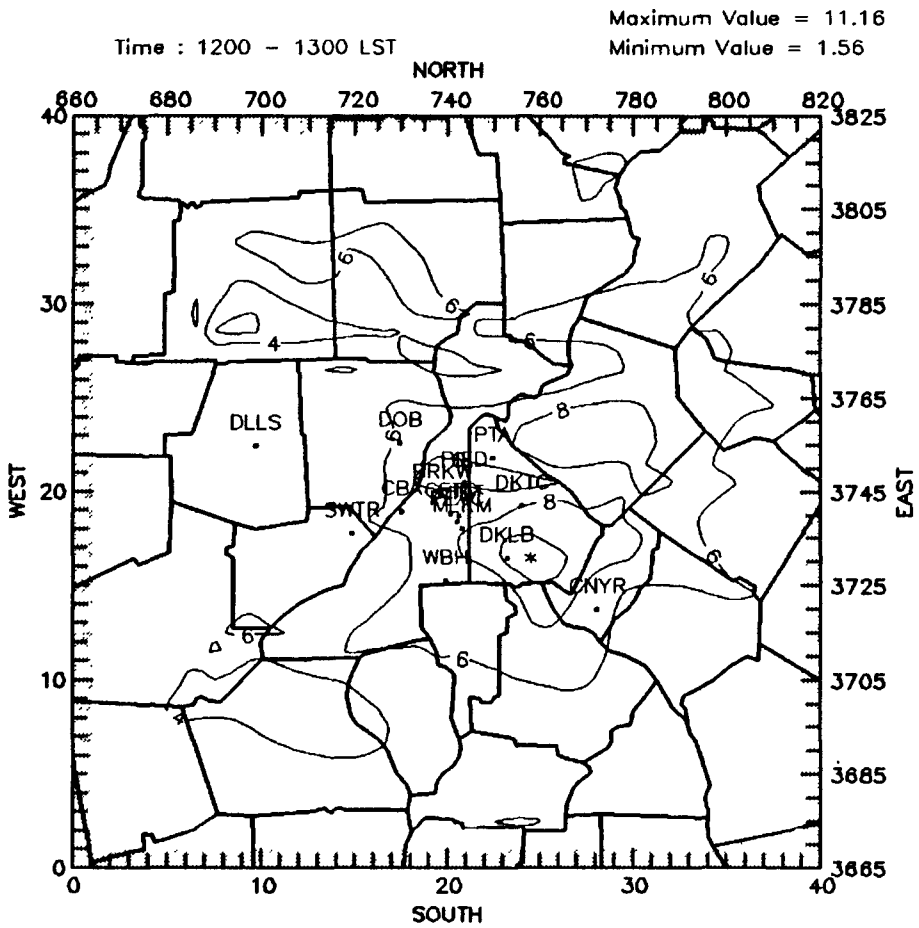

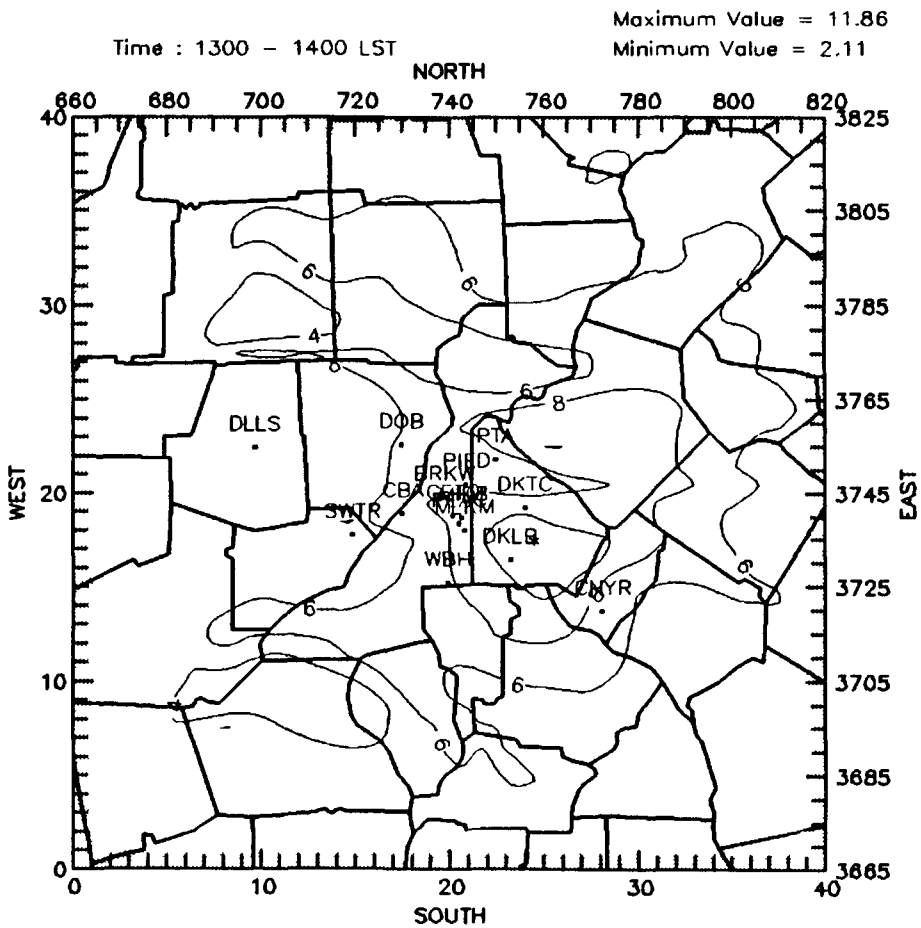

Ozone Concentration Evaluation run #1, June 4, 1984 (pphm)

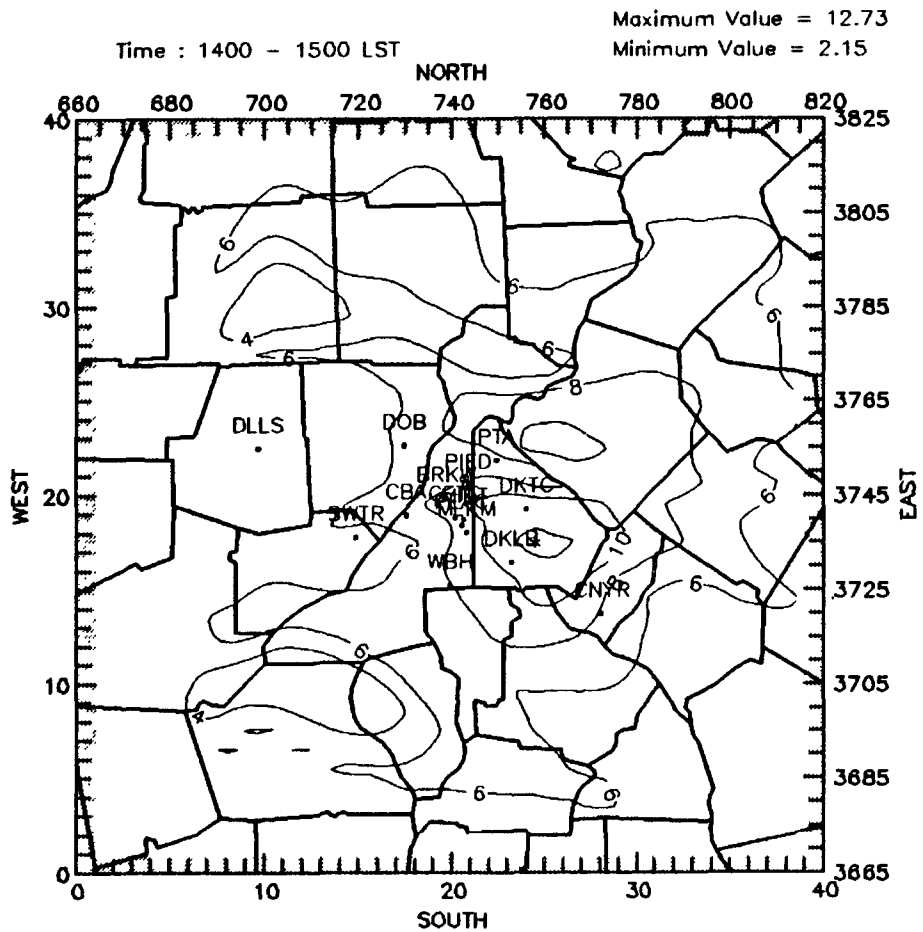

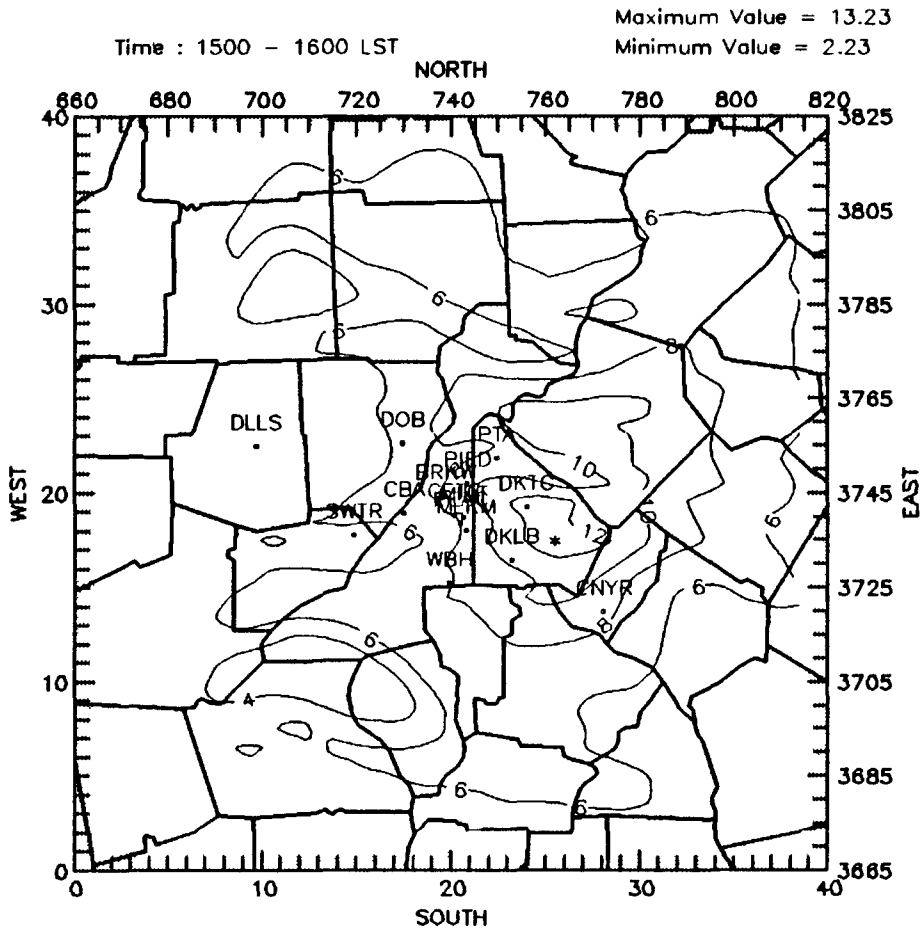

Ozone Concentration Evaluation run #1, June 4, 1984 (pphm)

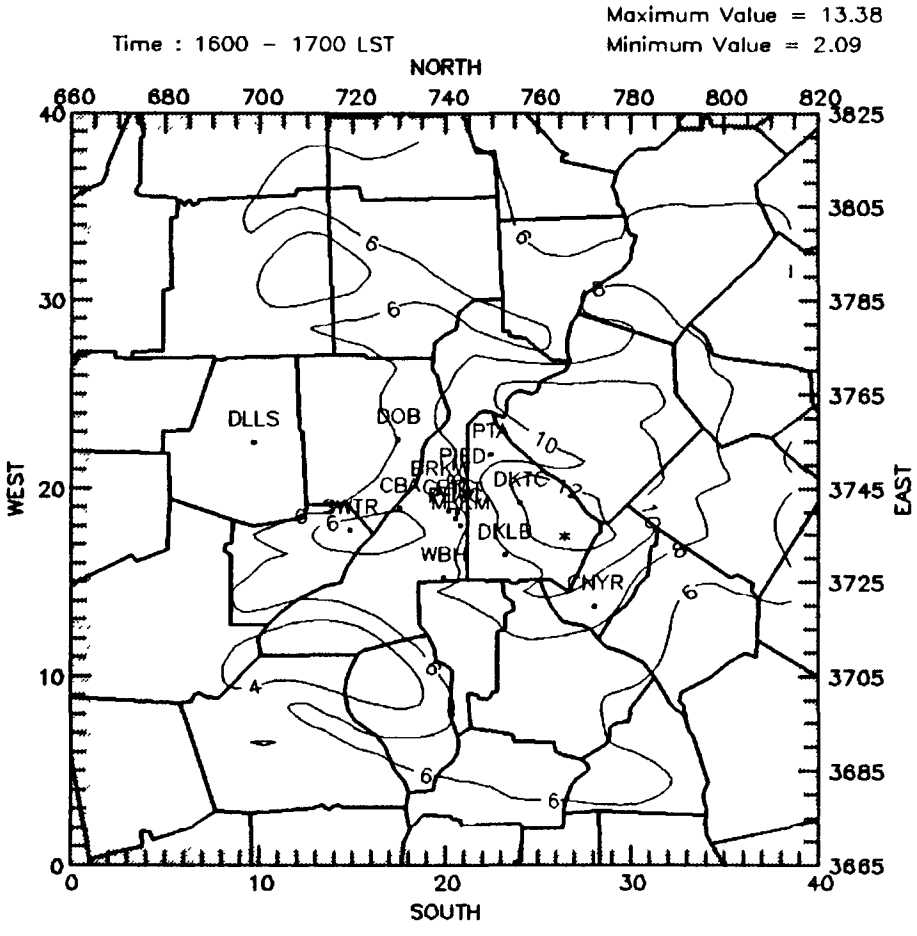

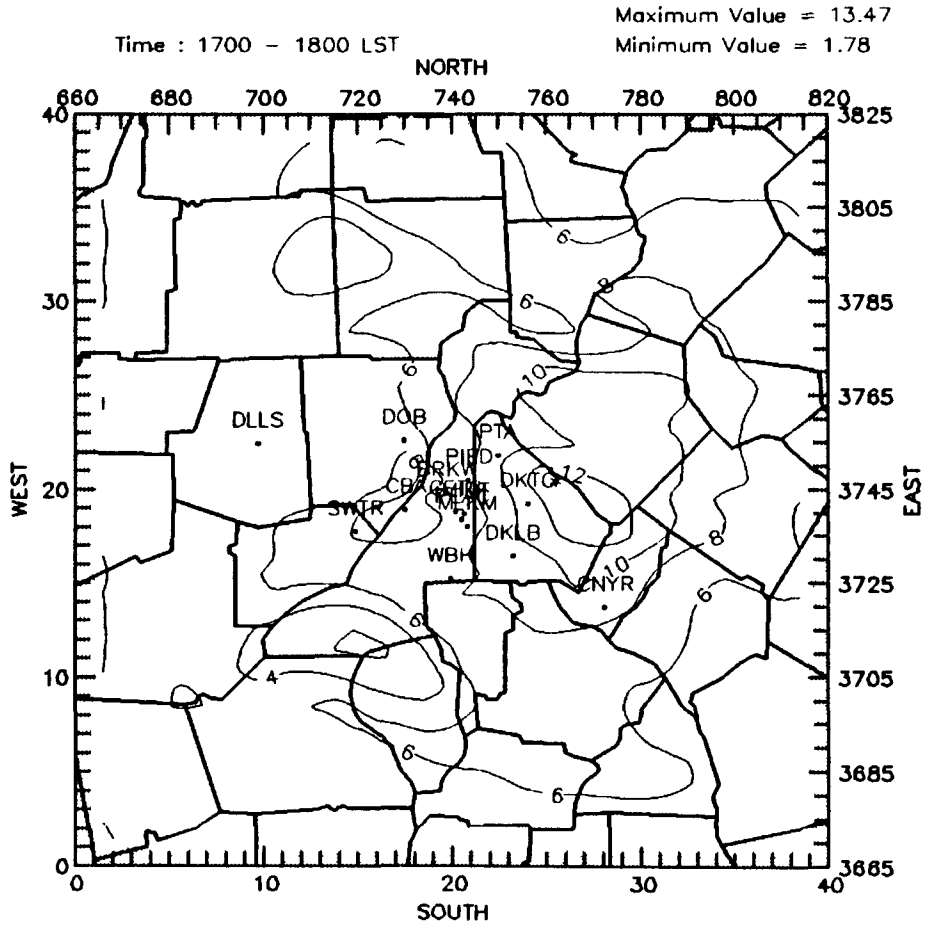

Ozone Concentration Evaluation run #1, June 4, 1984 (pphm)

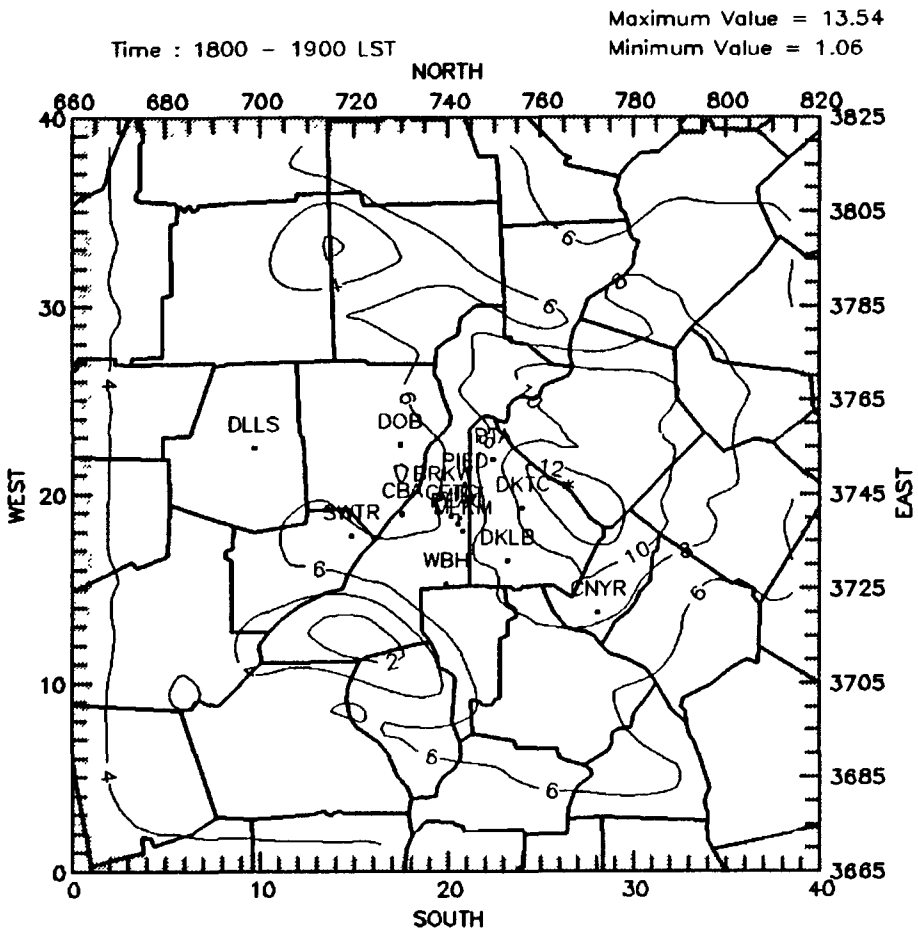

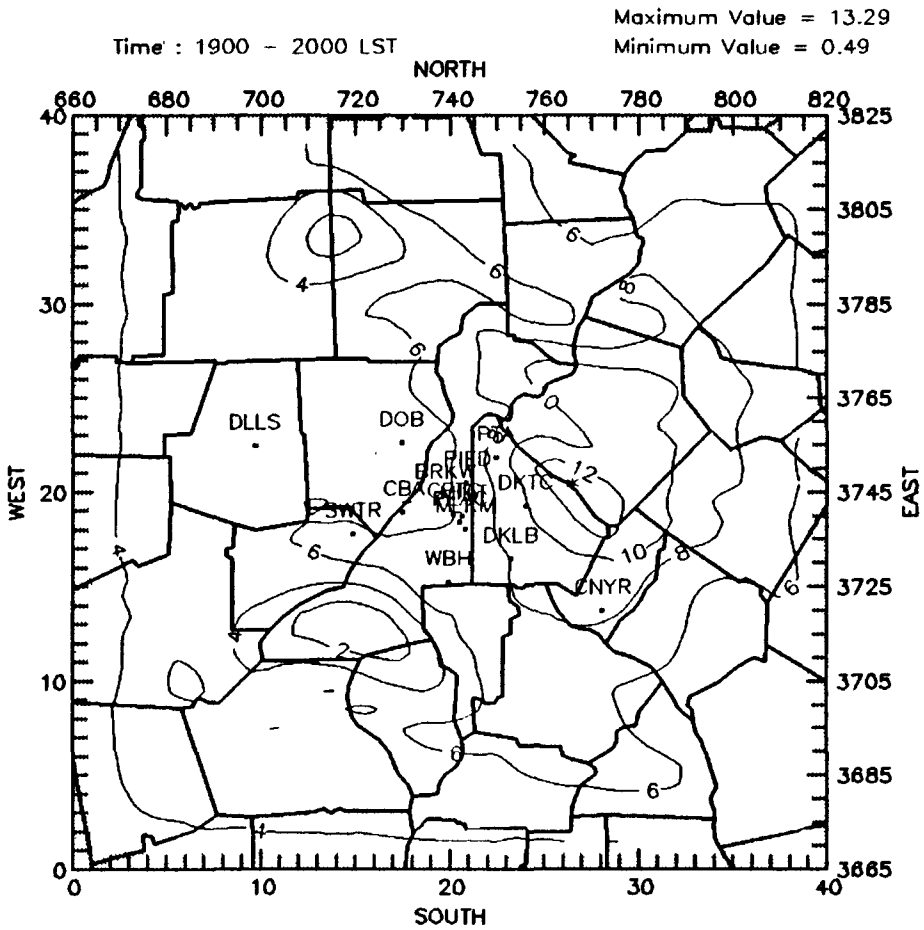

Ozone Concentration Evaluation run #1, June 4, 1984 (pphm)

Appendix D

HOURLY WIND FIELDS FOR UAM LAYER 1 USED IN DIAGNOSTIC RUN 2 (BASE CASE SIMULATION WITH BIOGENICS)

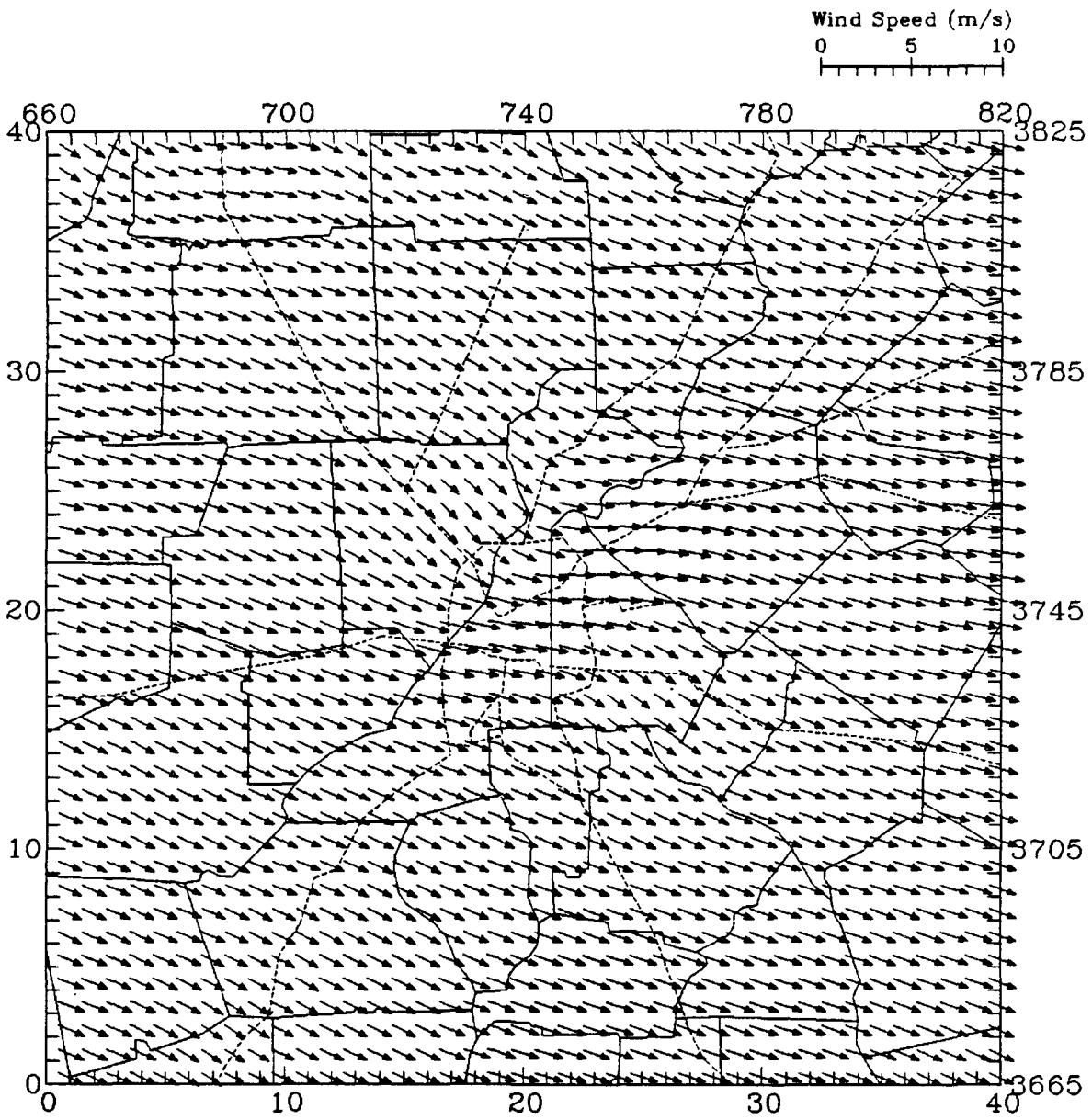

Atlanta PLANR Winds
Layer 1 at hour 10 on 84156

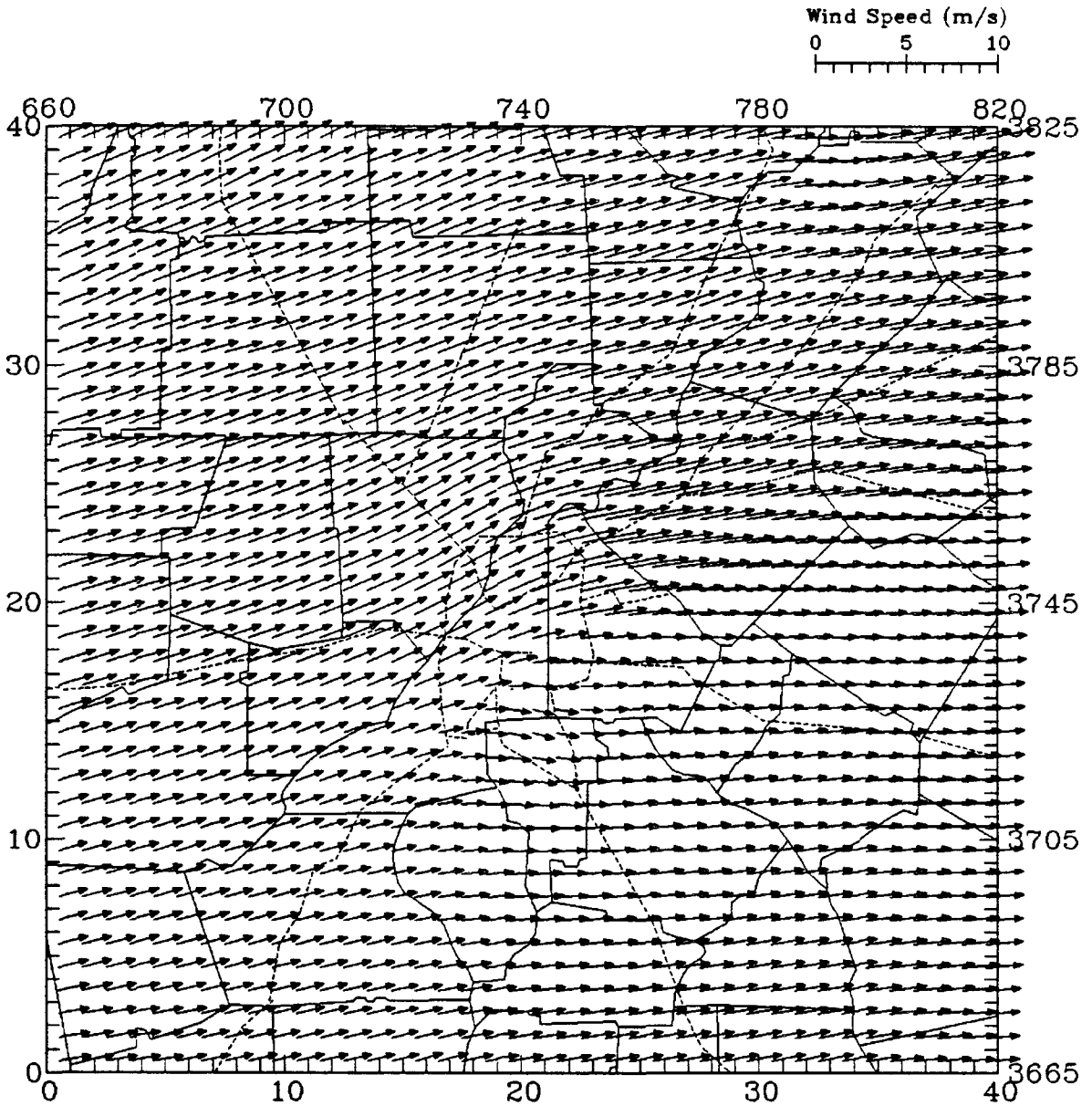

Atlanta PLANR Winds
Layer 1 at hour 11 on 84156

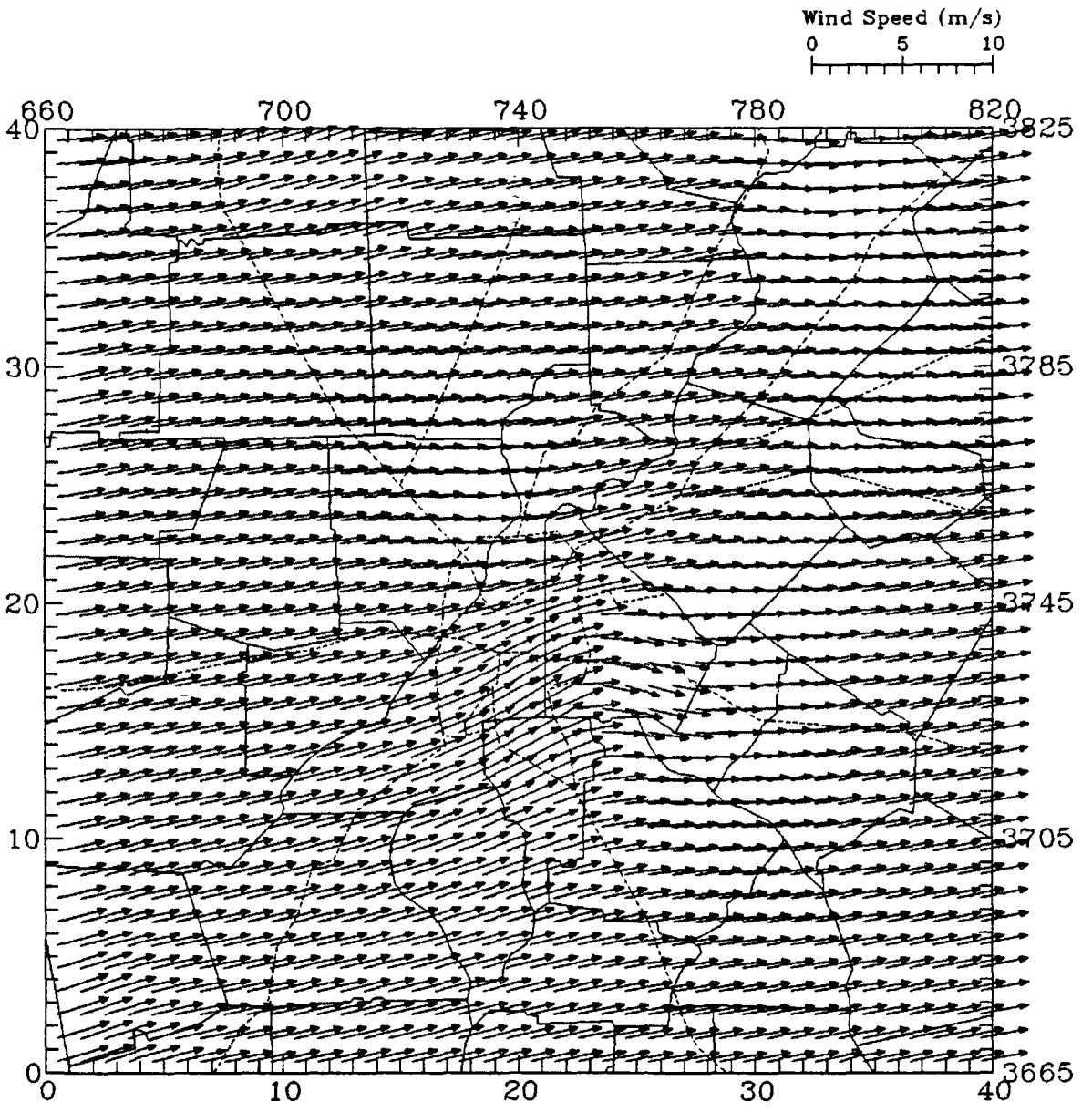

Atlanta PLANR Winds
Layer 1 at hour 12 on 84156

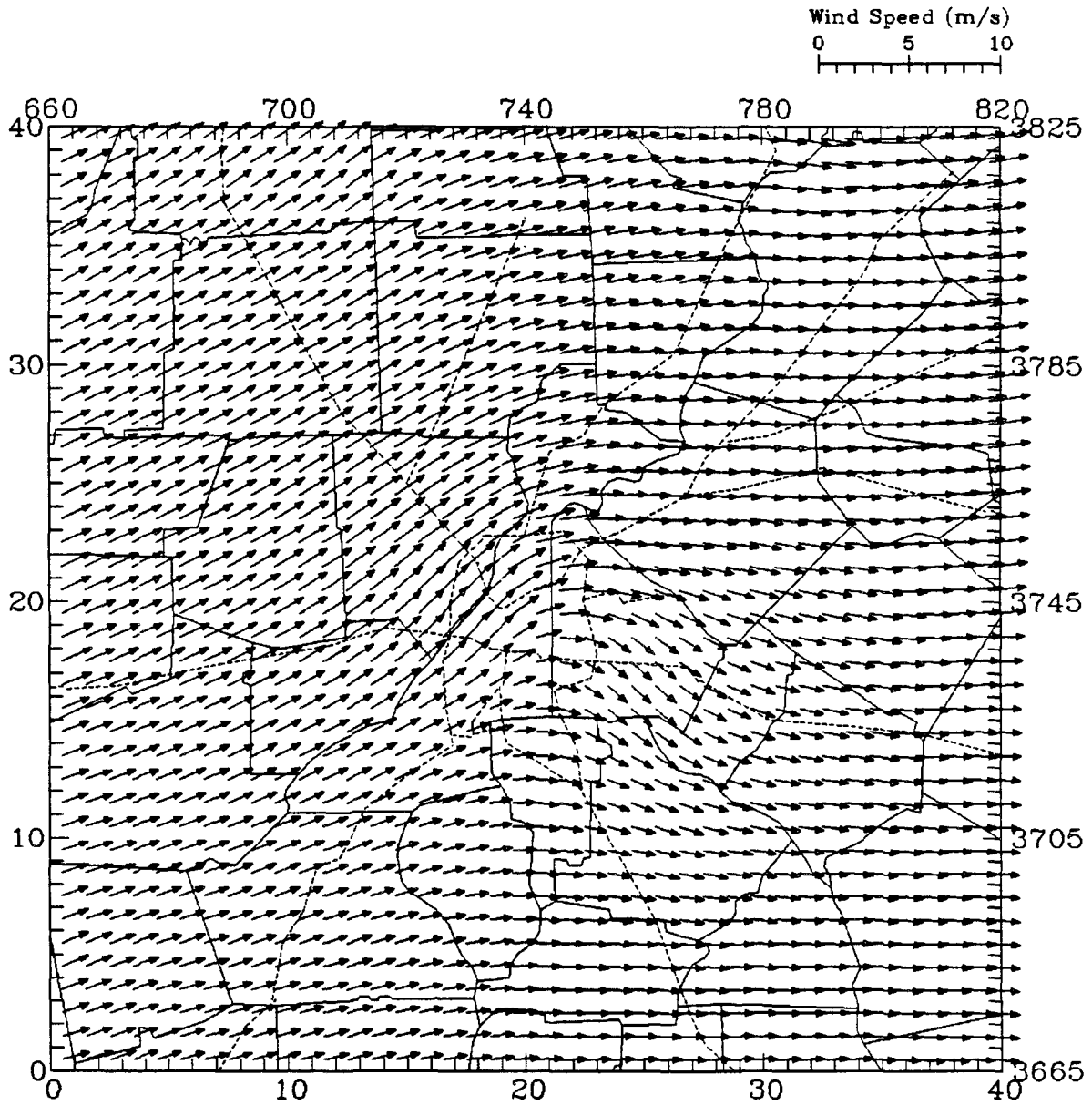

Atlanta PLANR Winds
Layer 1 at hour 13 on 84156

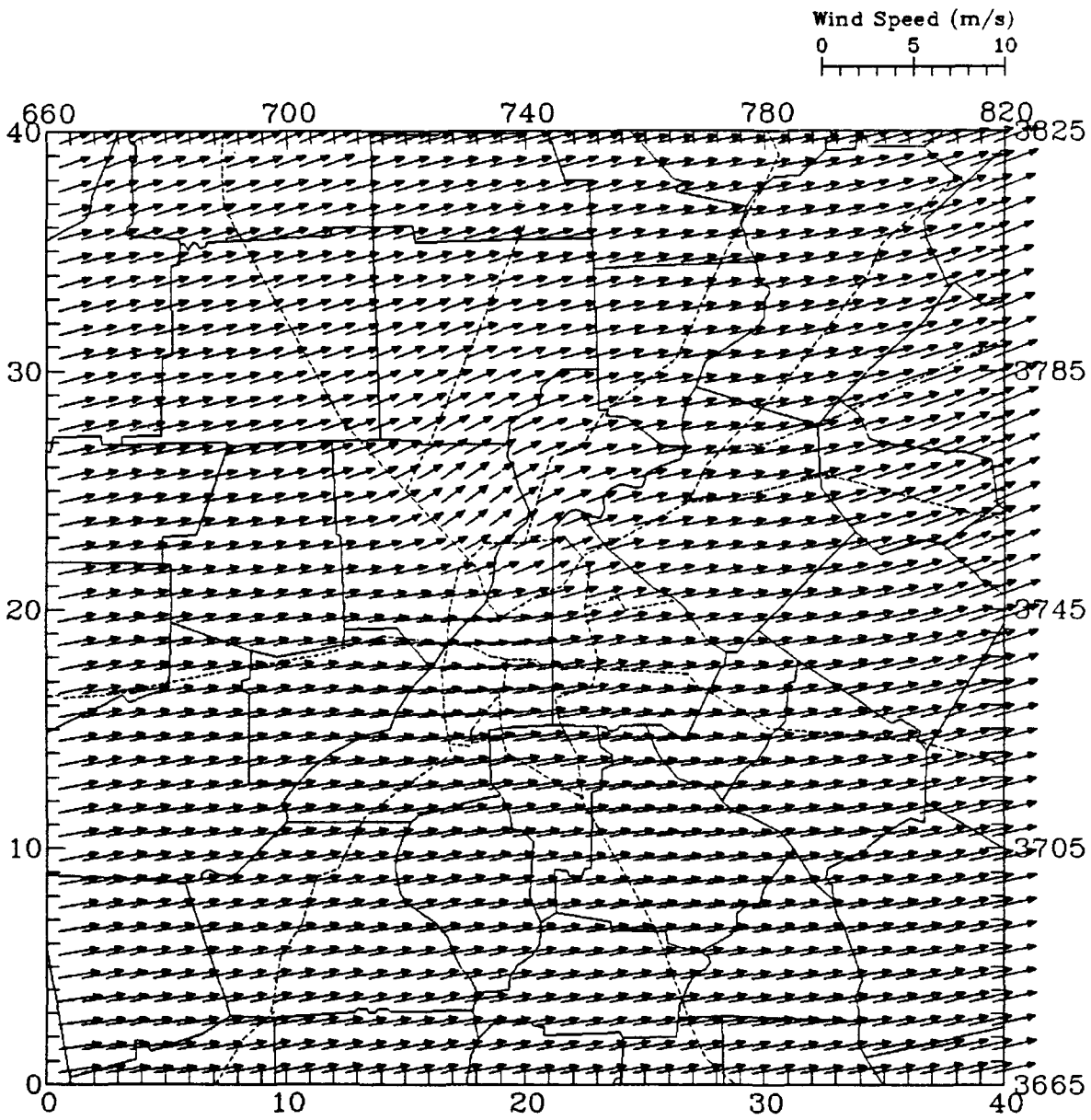

Atlanta PLANR Winds
Layer 1 at hour 14 on 84156

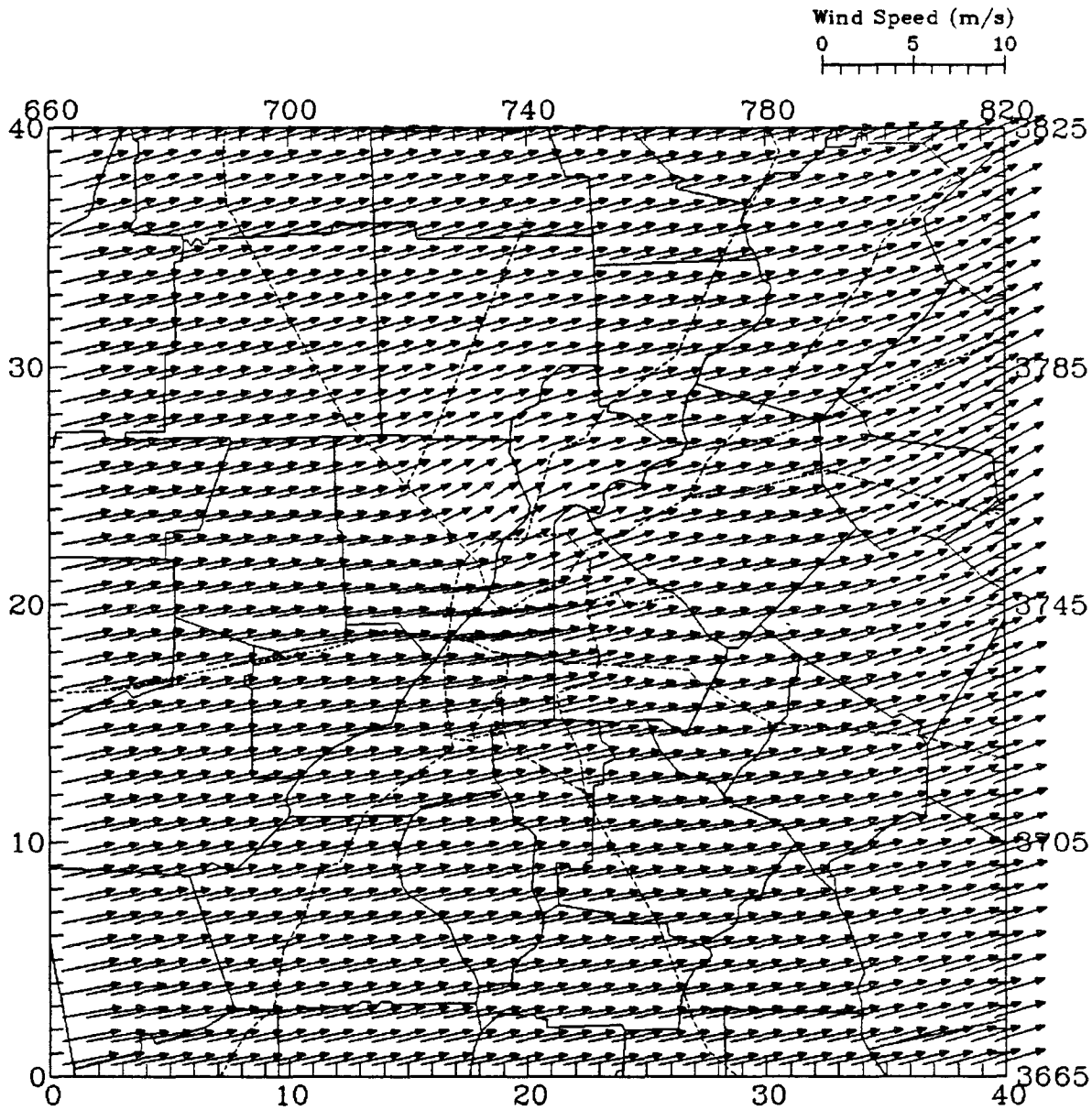

Atlanta PLANR Winds
Layer 1 at hour 15 on 84156

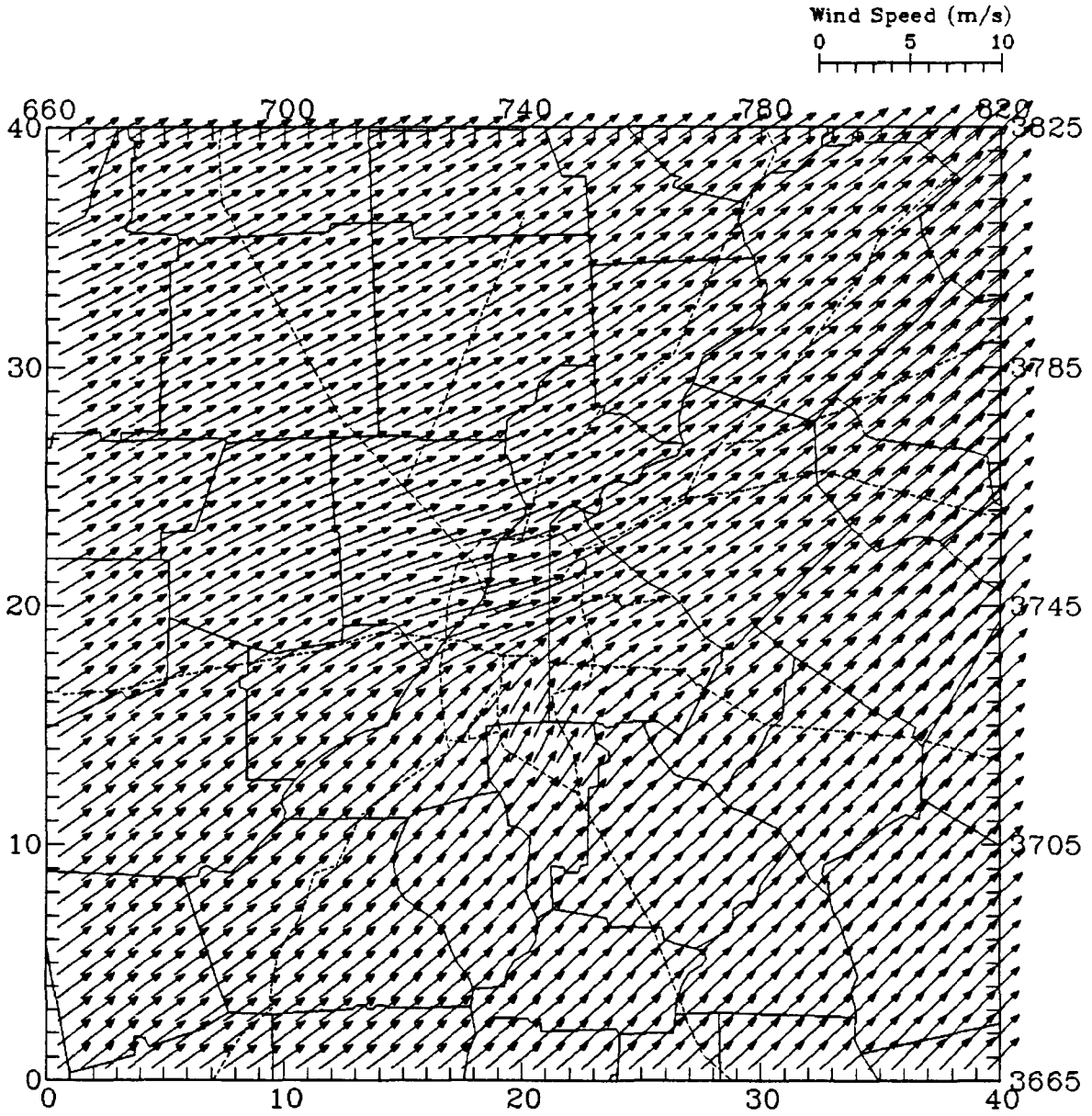

Atlanta PLANR Winds
Layer 1 at hour 16 on 84156

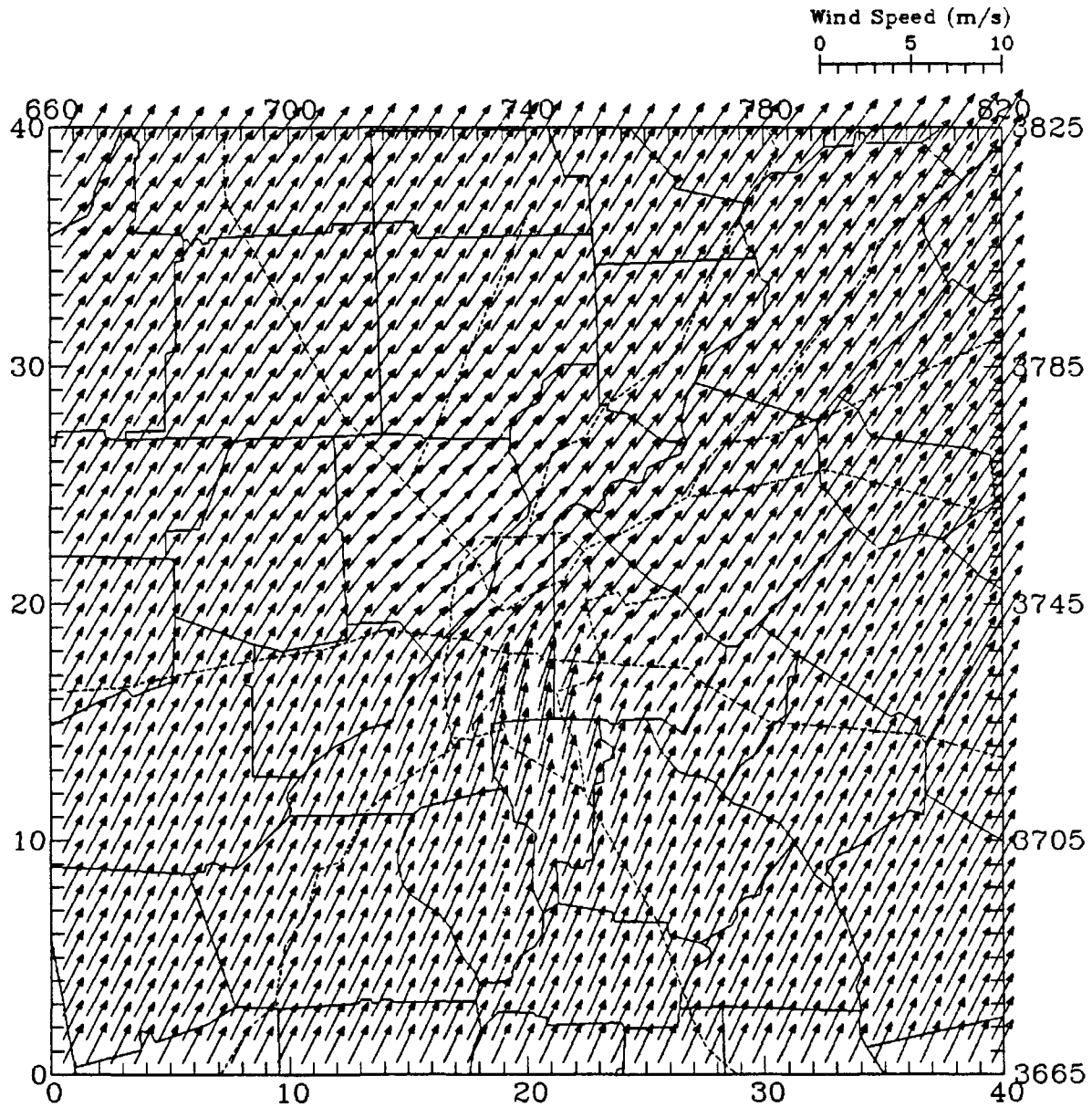

Atlanta PLANR Winds
Layer 1 at hour 17 on 84156

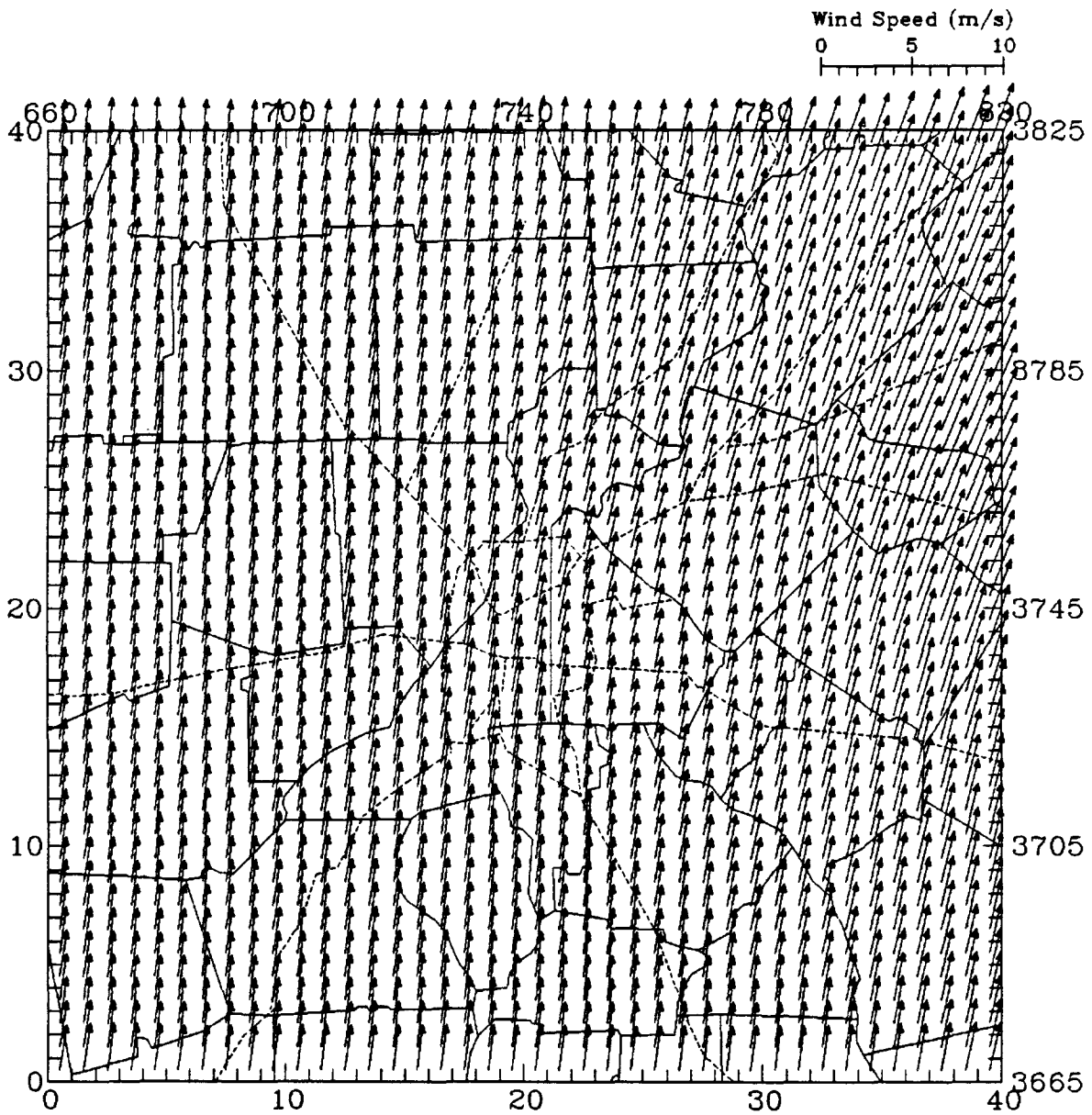

Atlanta PLANR Winds
Layer 1 at hour 18 on 84156

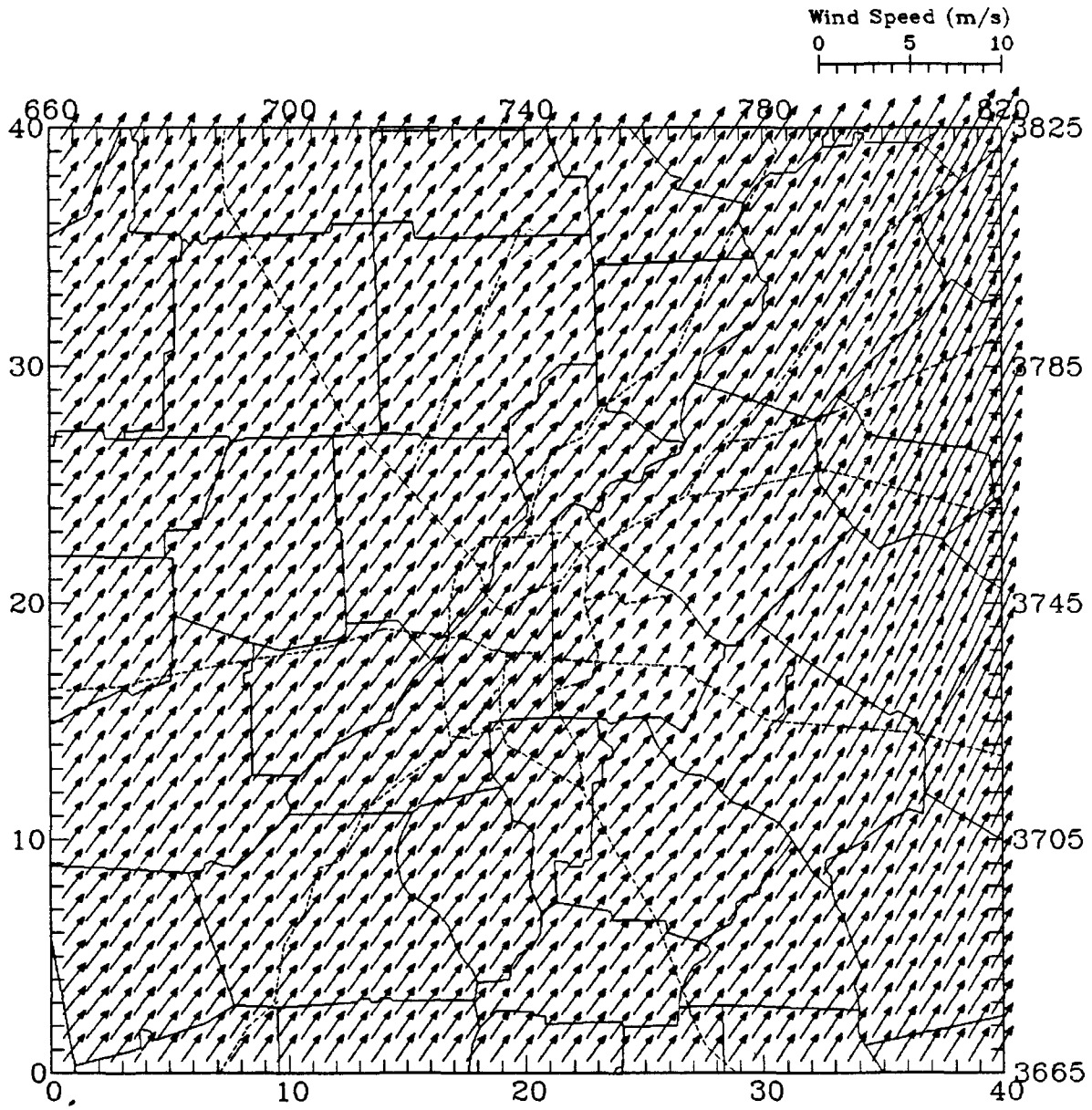

Atlanta PLANR Winds
Layer 1 at hour 19 on 84156

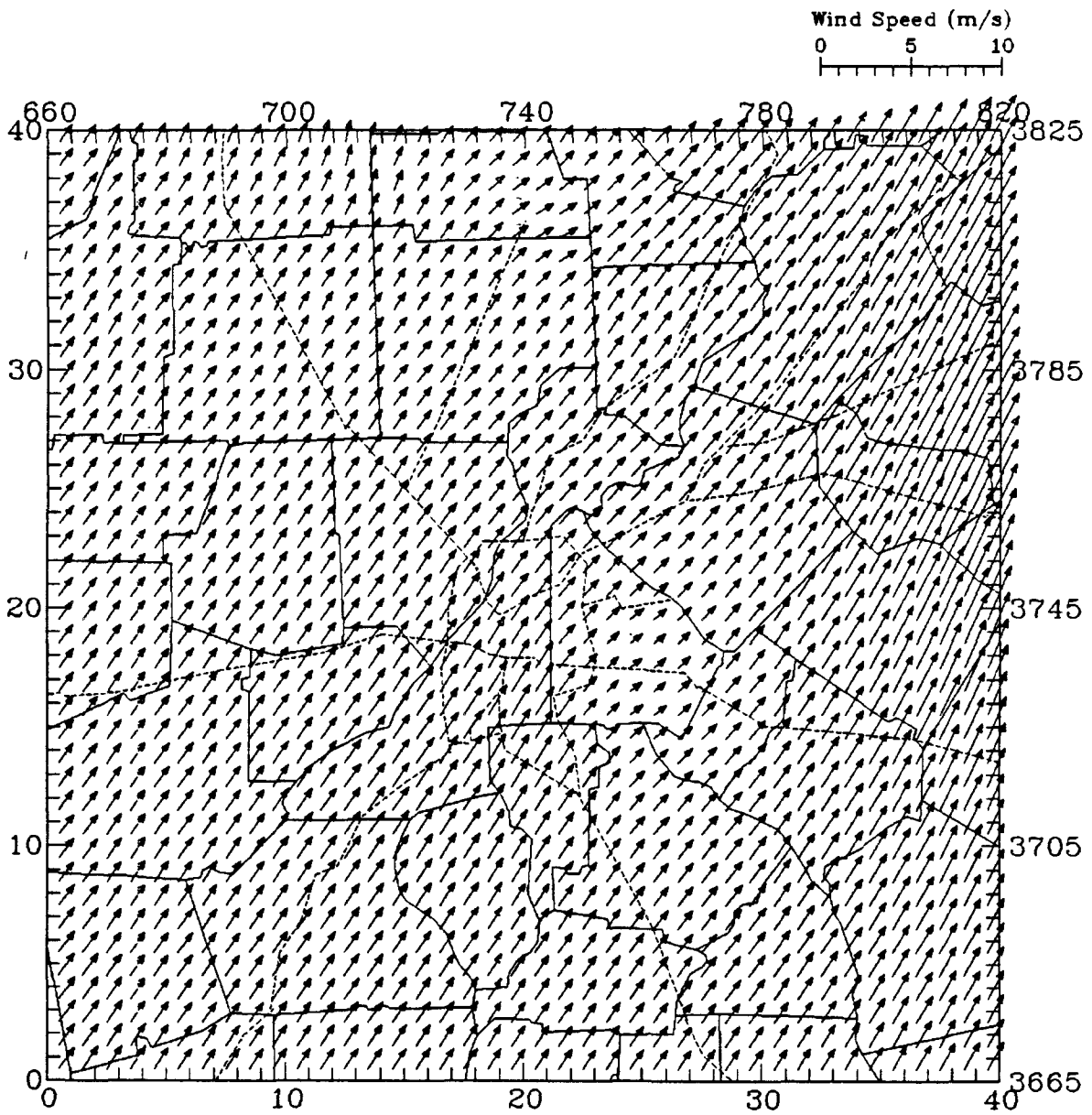

Atlanta PLANR Winds
Layer 1 at hour 20 on 84156

Appendix E

HOURLY PREDICTED OZONE CONCENTRATIONS (pphm) FOR DIAGNOSTIC RUN 2 (BASE CASE WITH BIOGENIC EMISSIONS)

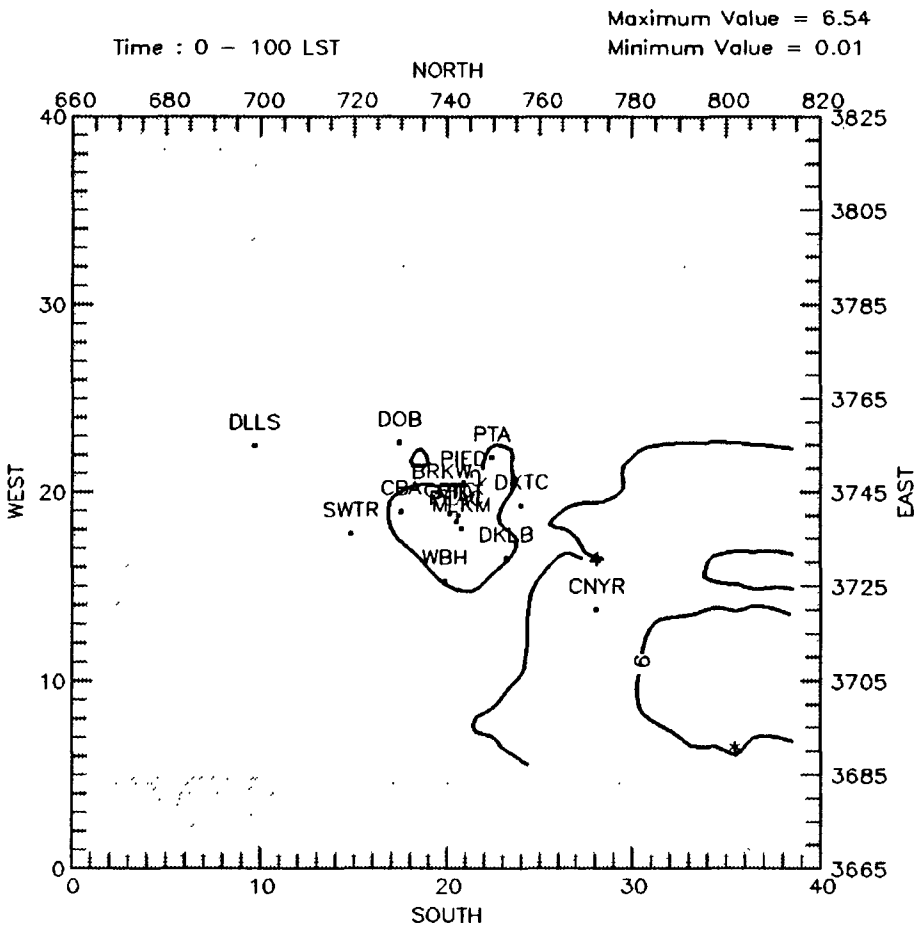

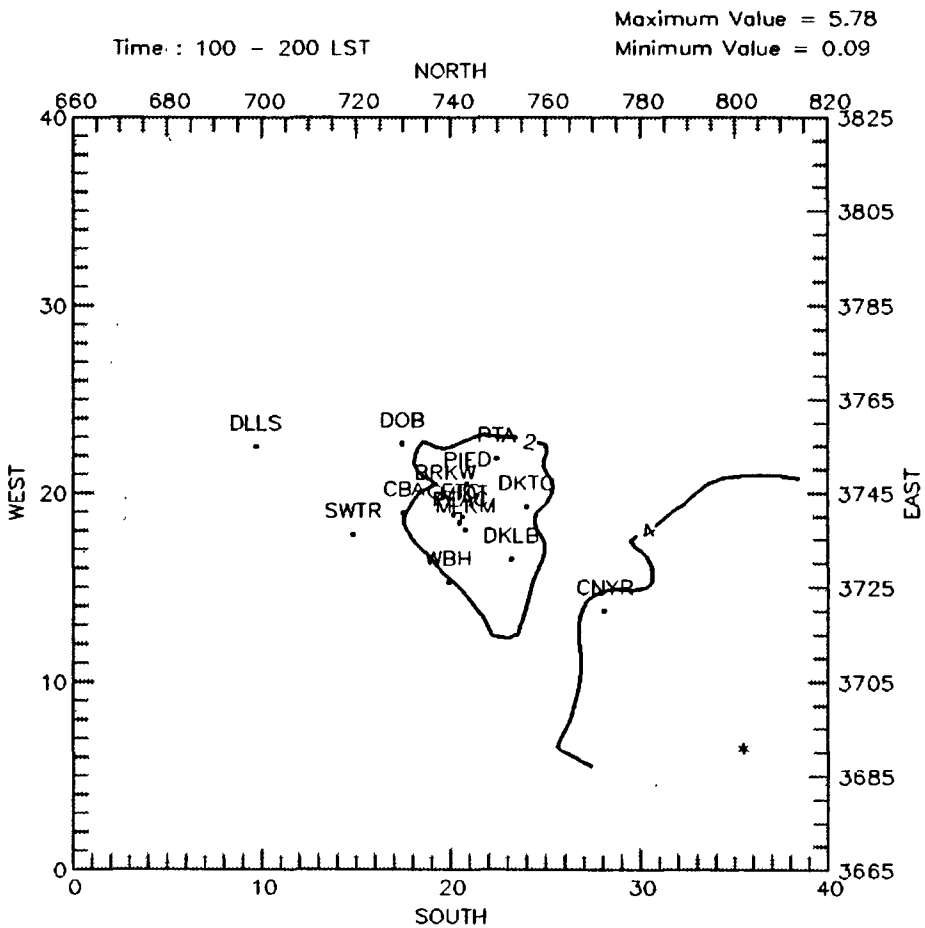

Ozone (pphm) 1985 base emissions, June 4, 1984 (pphm)

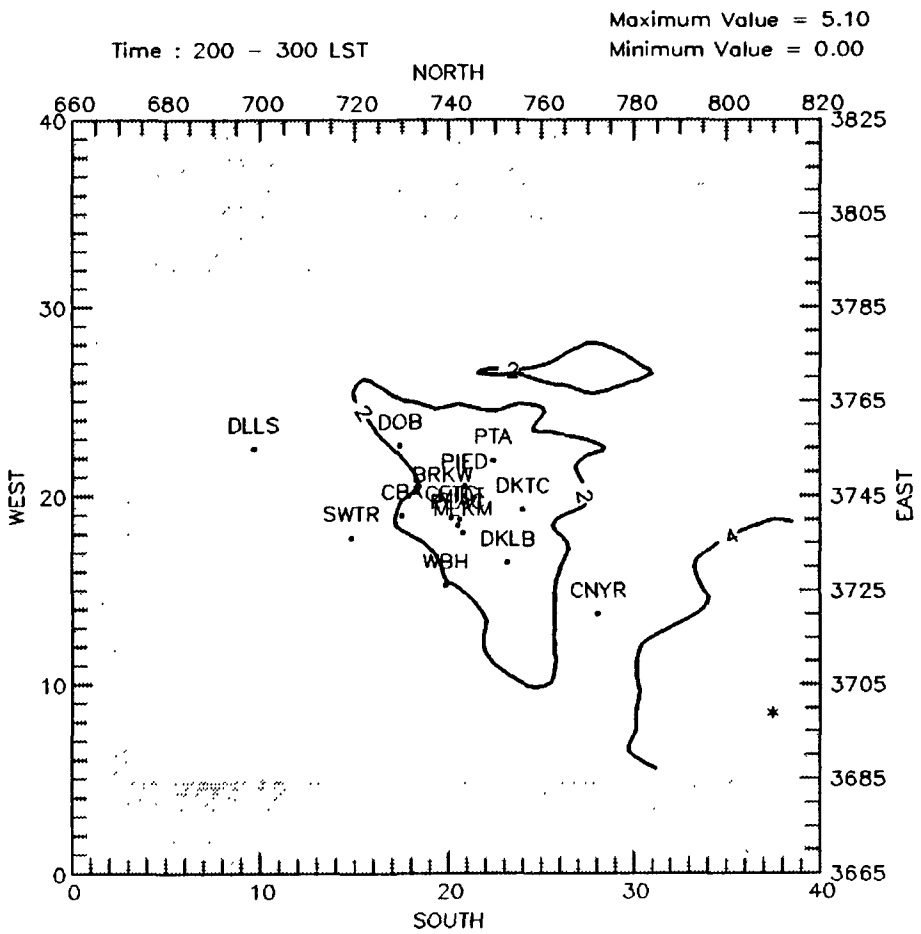

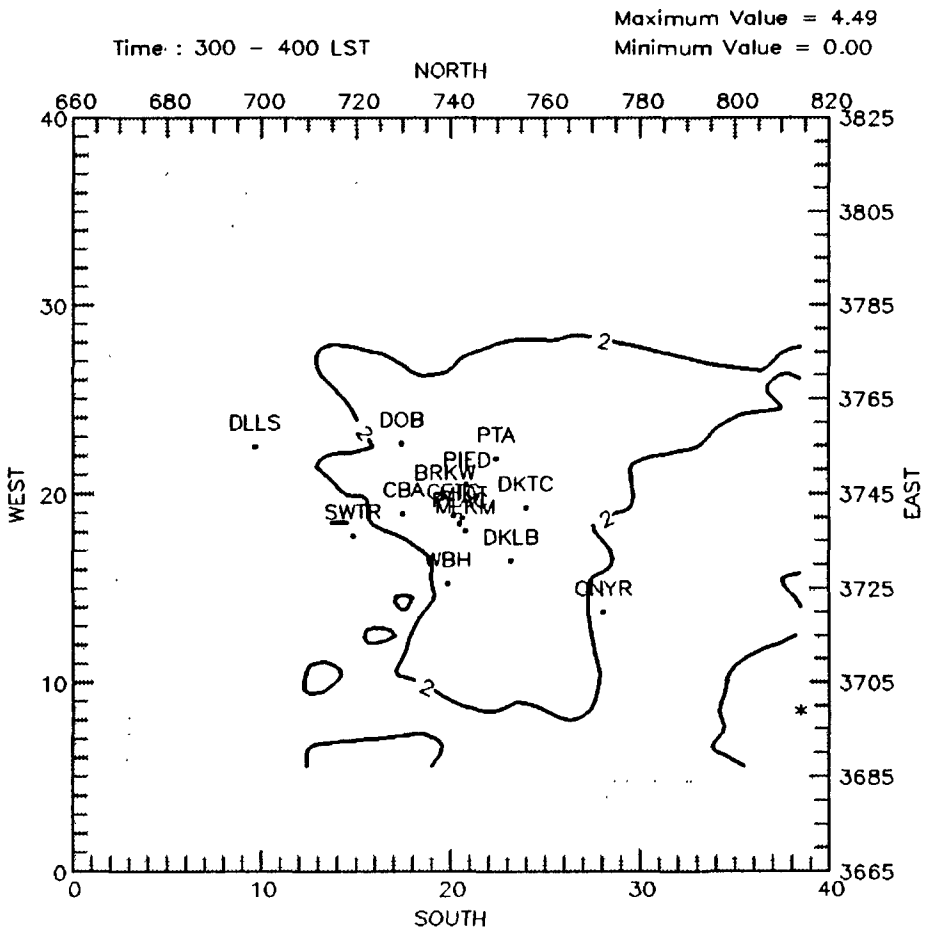

Ozone (pphm) 1985 base emissions, June 4, 1984 (pphm)

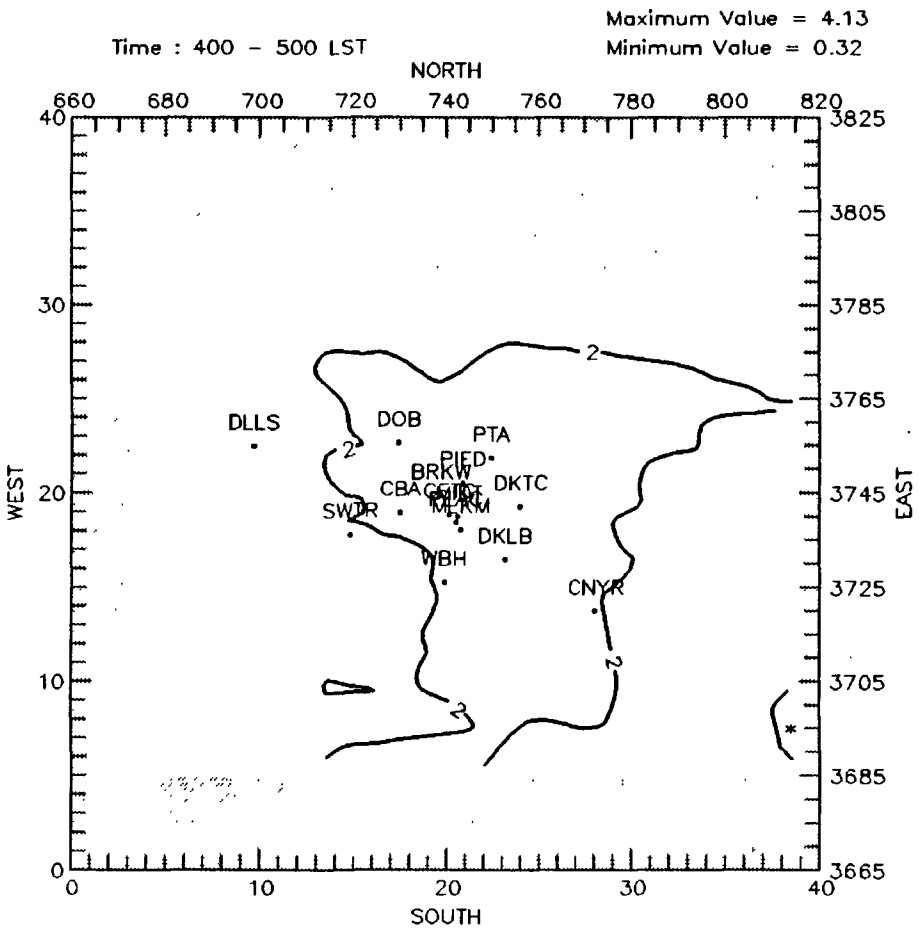

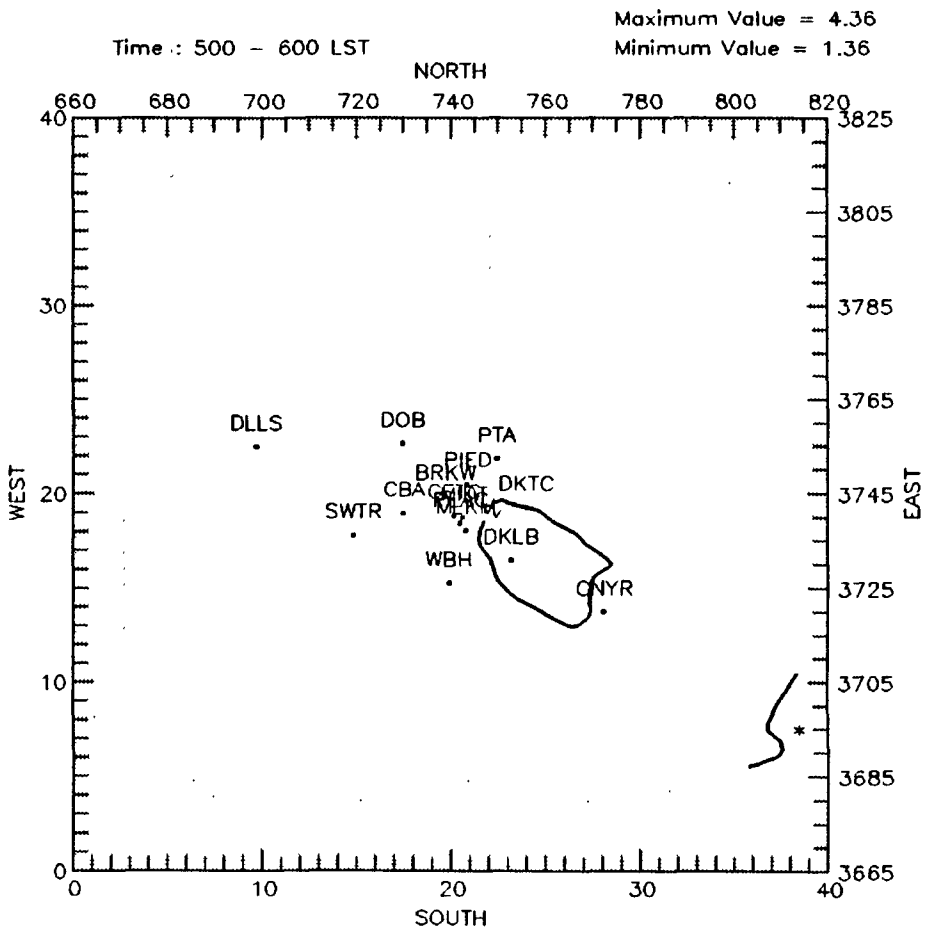

Ozone (pphm) 1985 base emissions, June 4, 1984 (pphm)

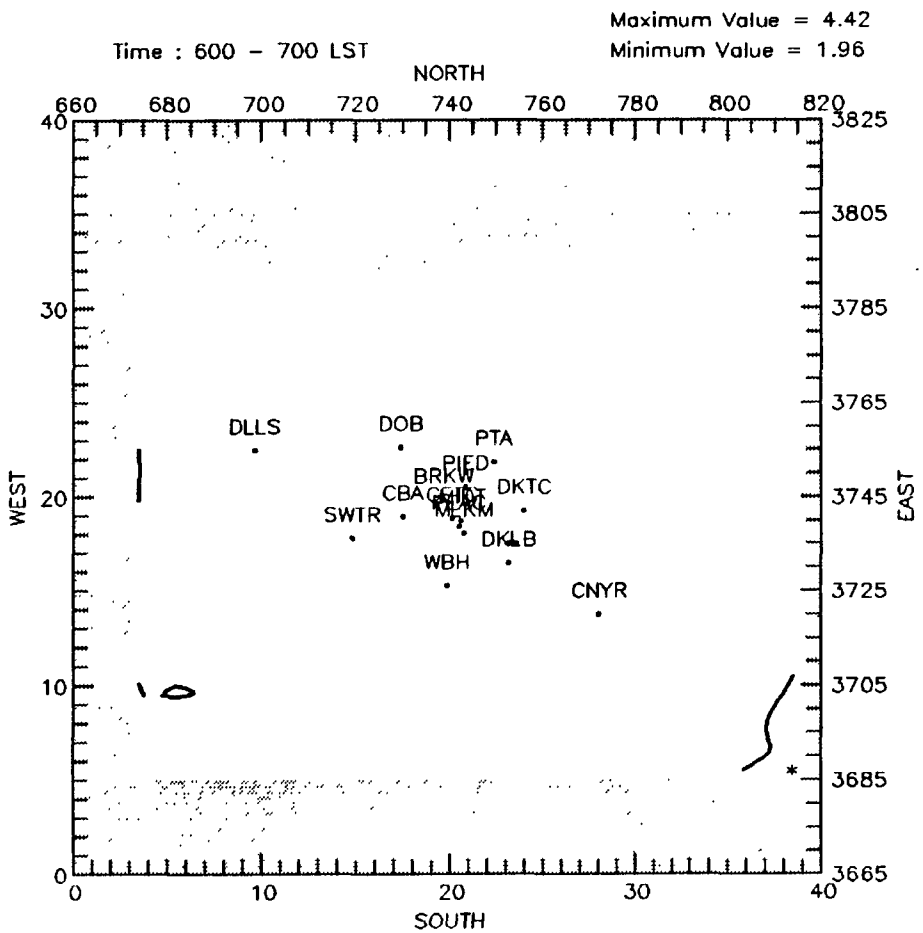

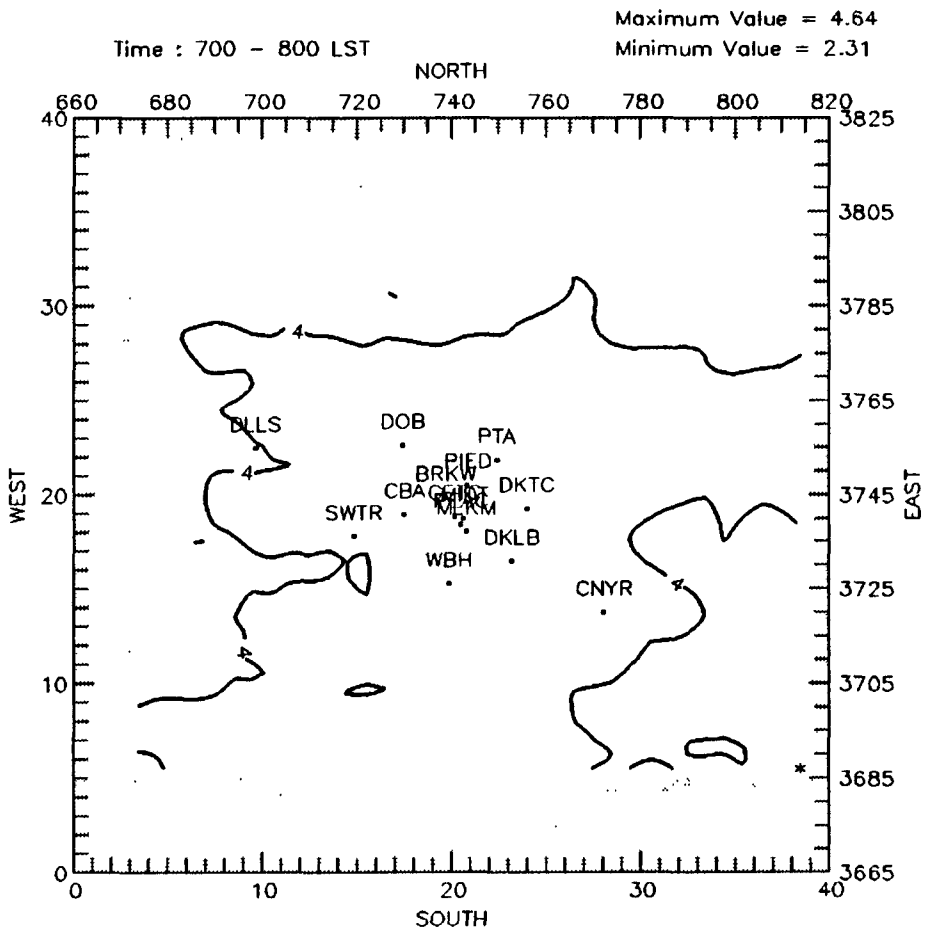

Ozone (pphm) 1985 base emissions, June 4, 1984 (pphm)

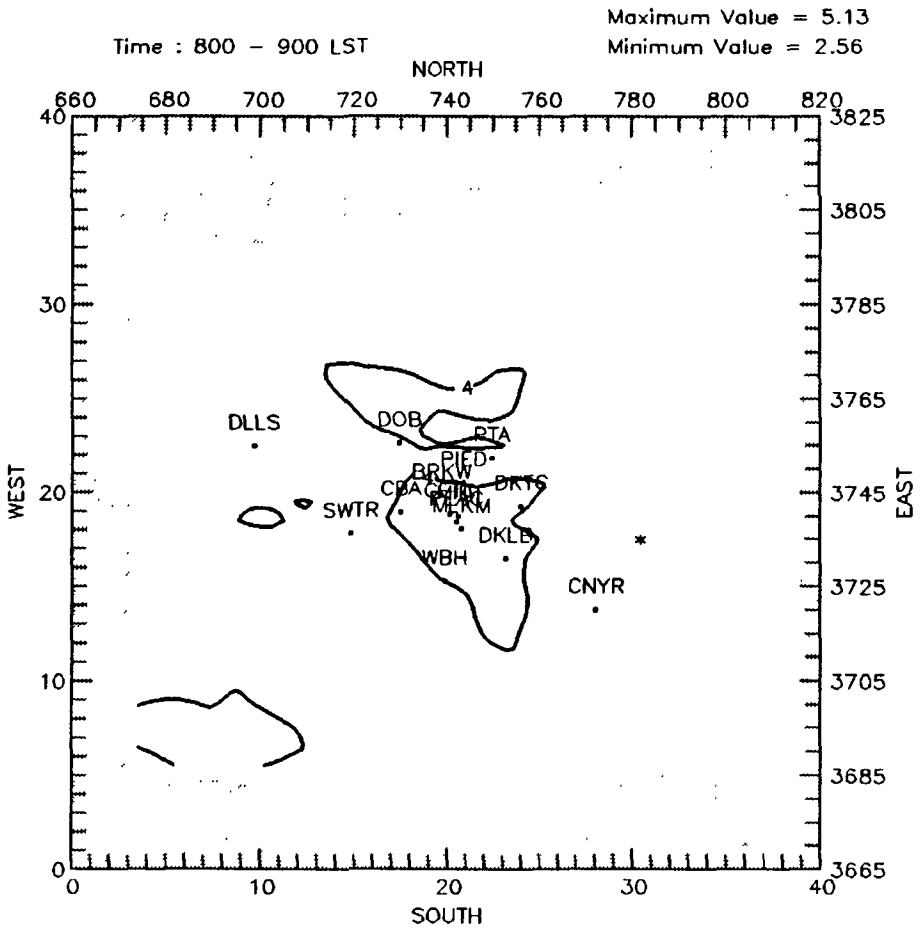

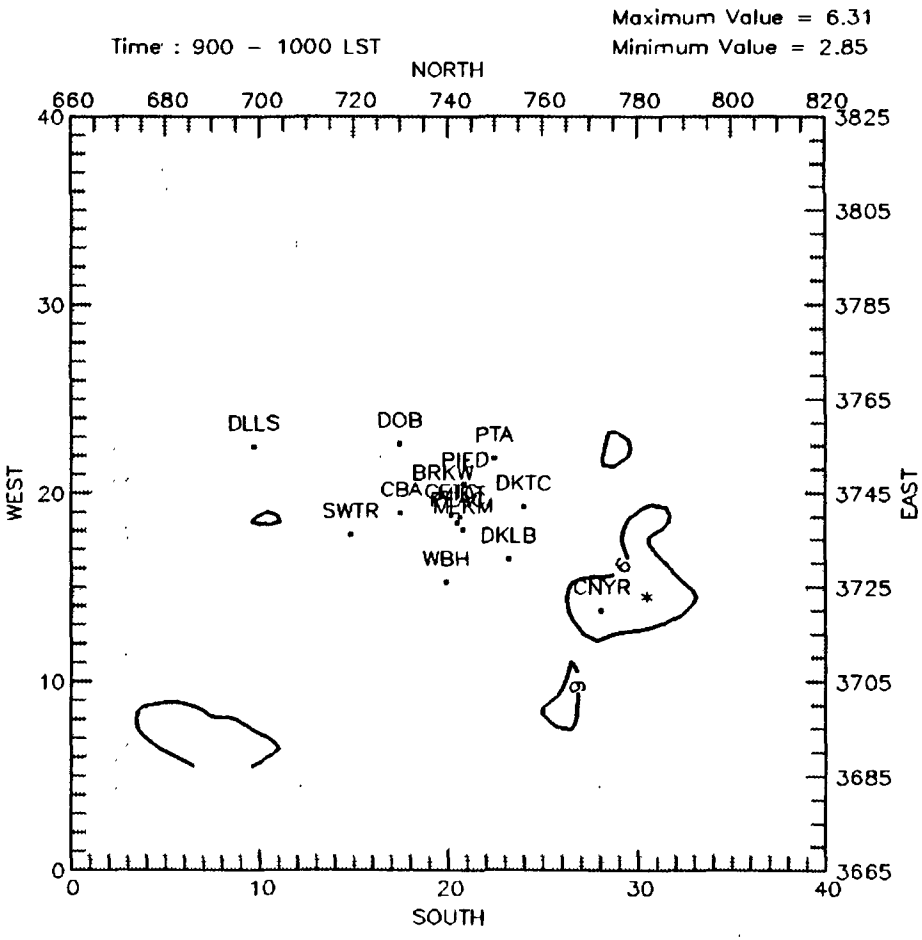

Ozone (pphm) 1985 base emissions, June 4, 1984 (pphm)

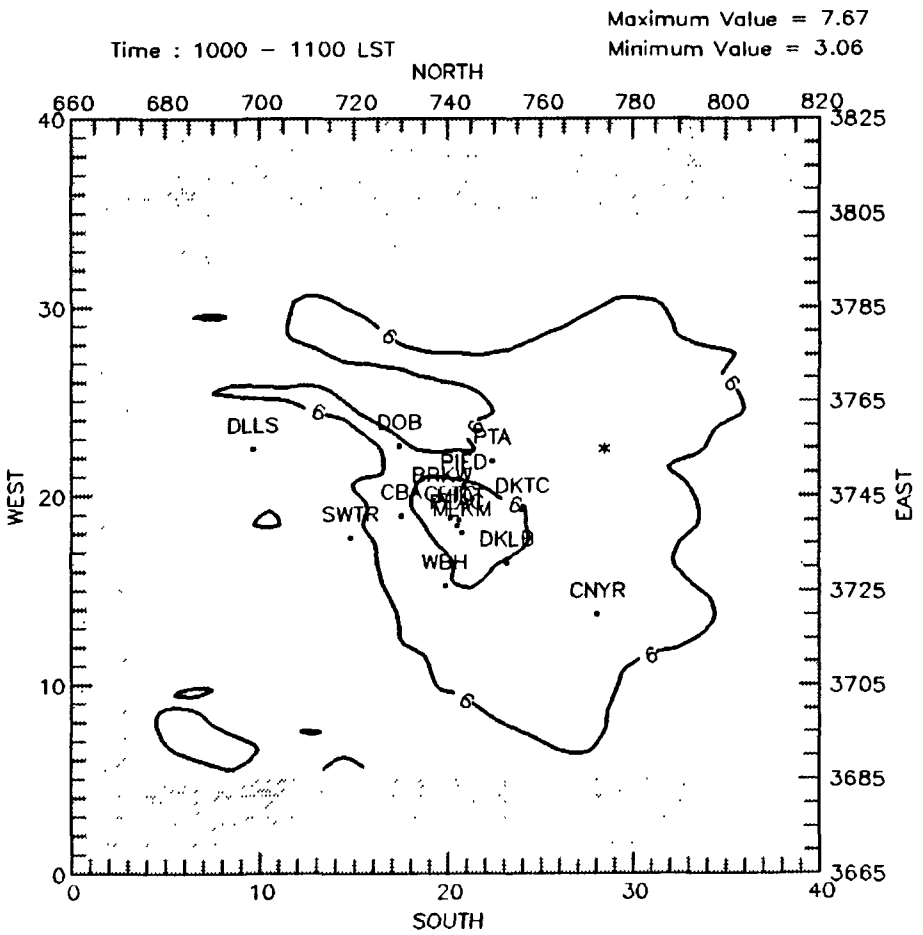

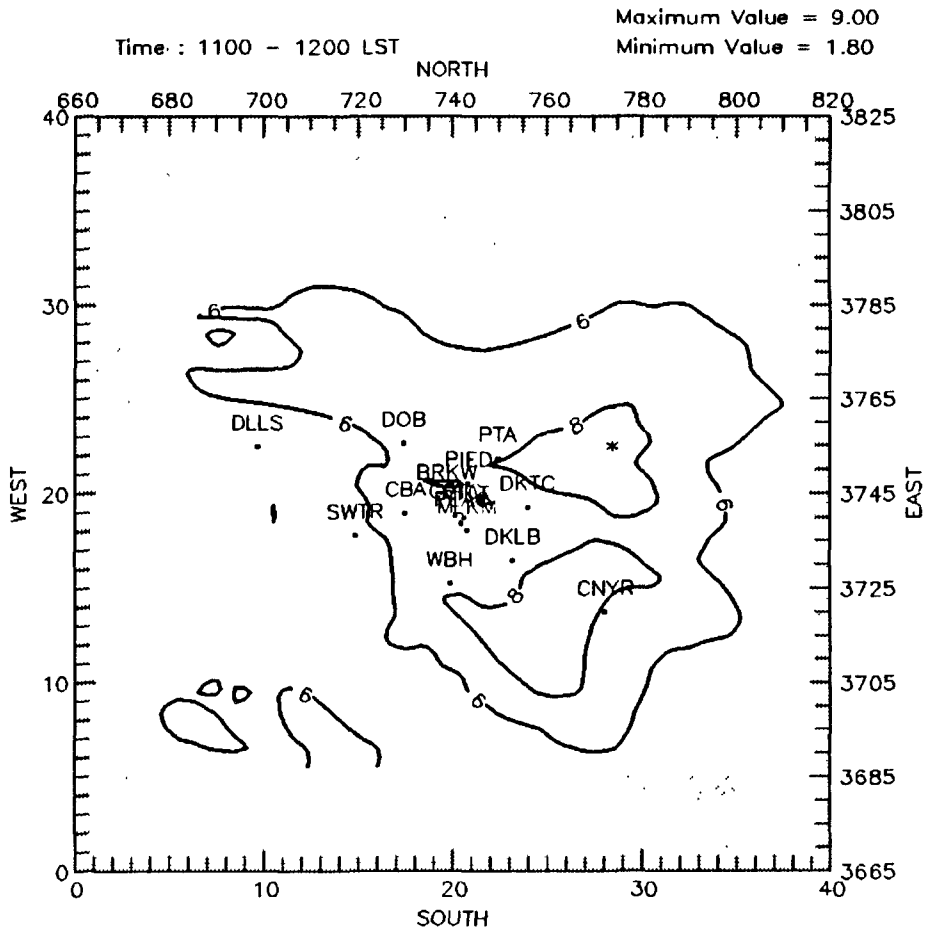

Ozone (pphm) 1985 base emissions, June 4, 1984 (pphm)

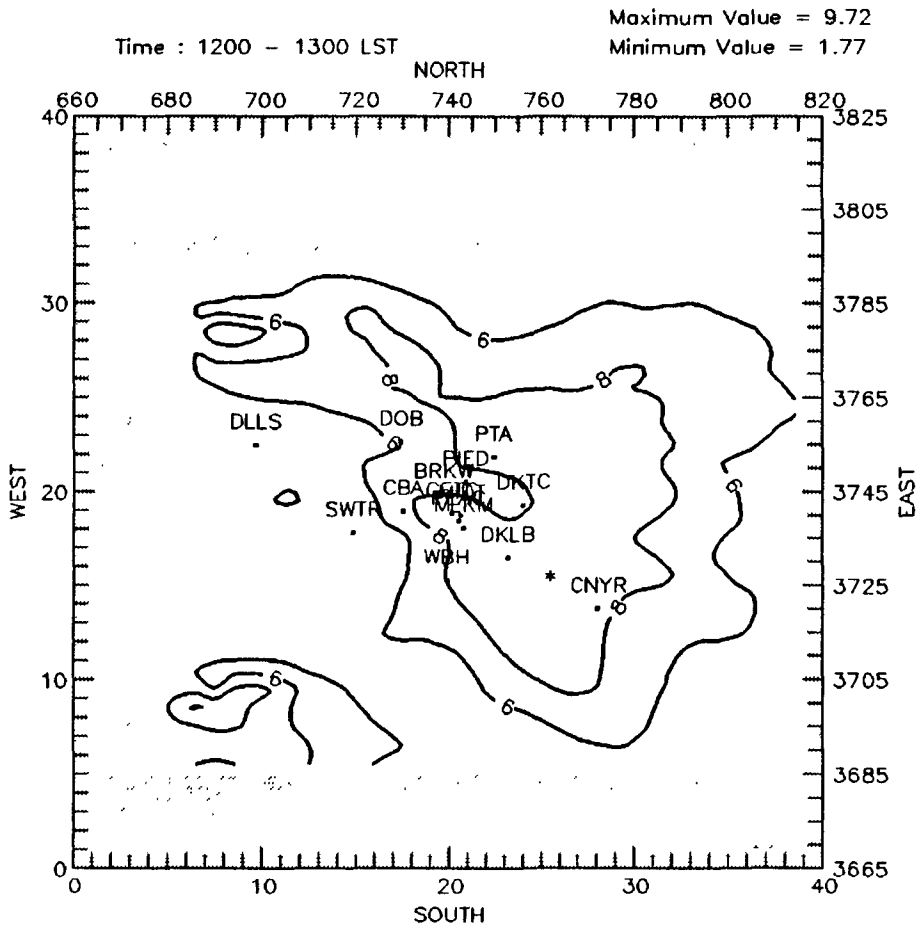

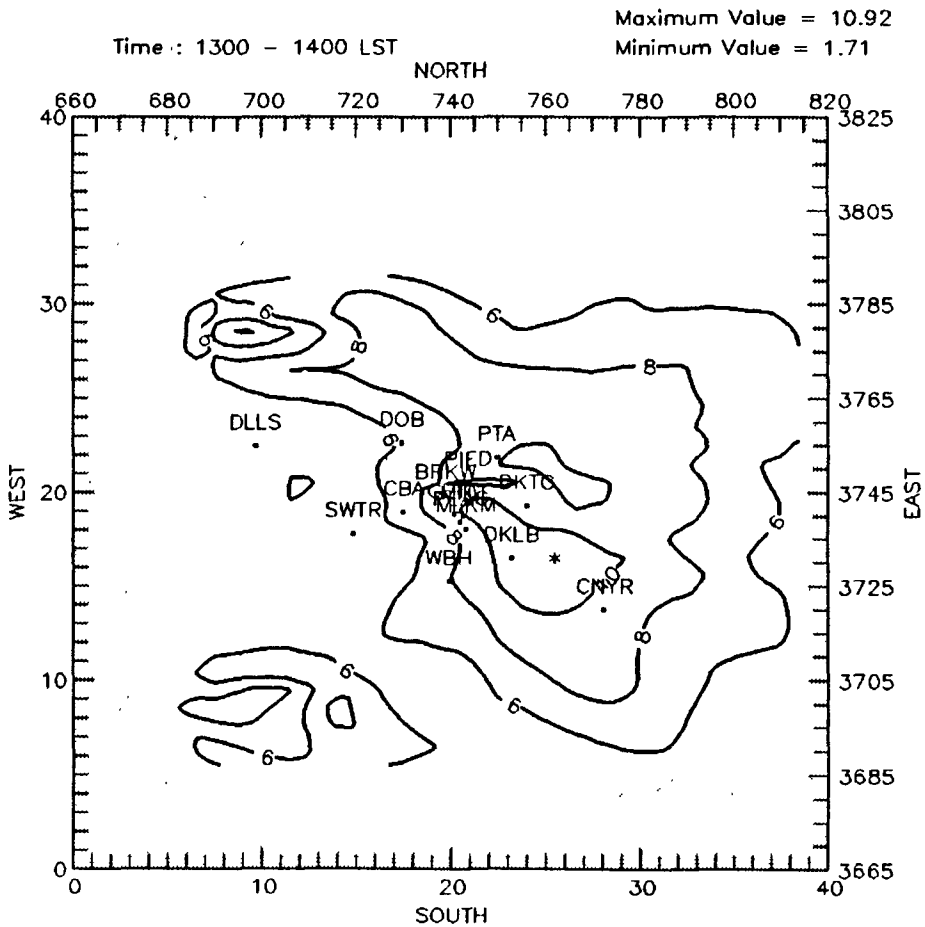

Ozone (pphm) 1985 base emissions, June 4, 1984 (pphm)

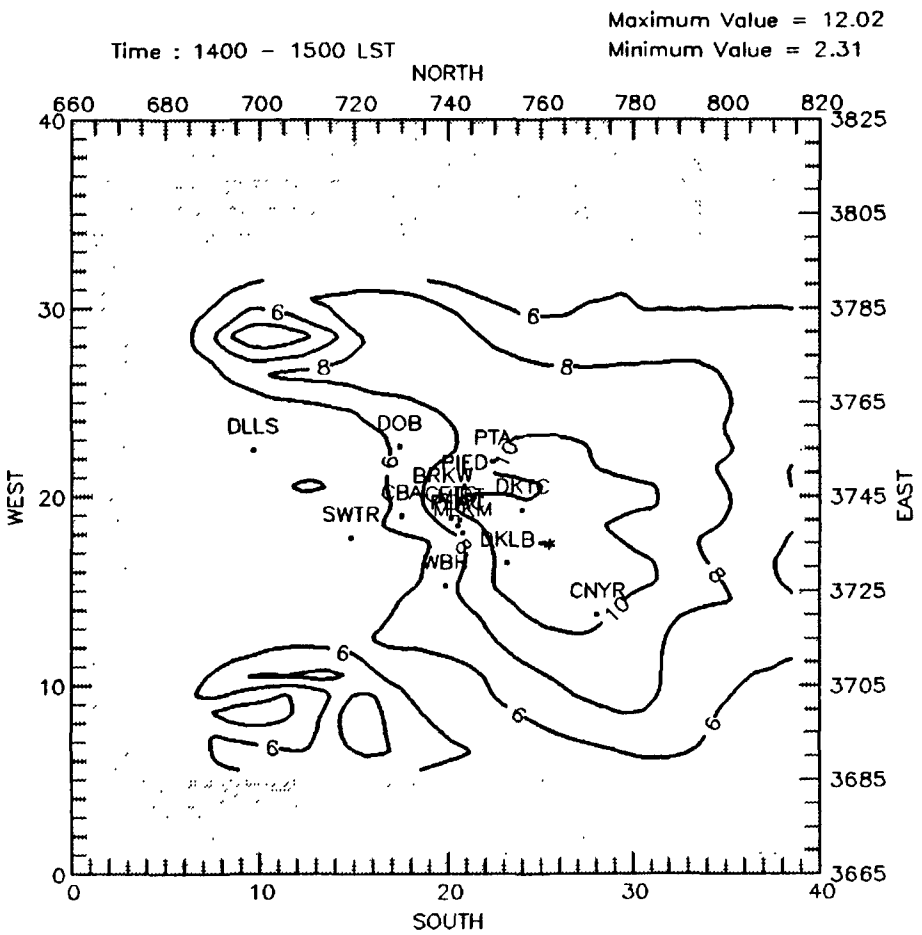

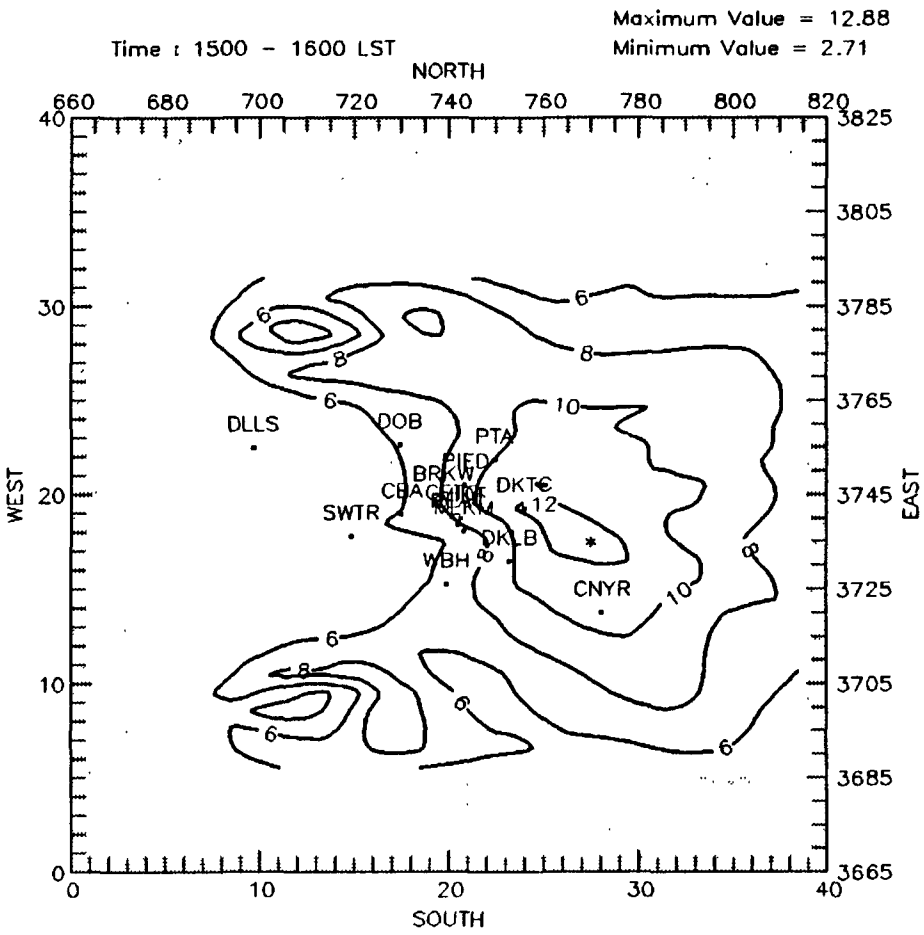

Ozone (pphm) 1985 base emissions, June 4, 1984 (pphm)

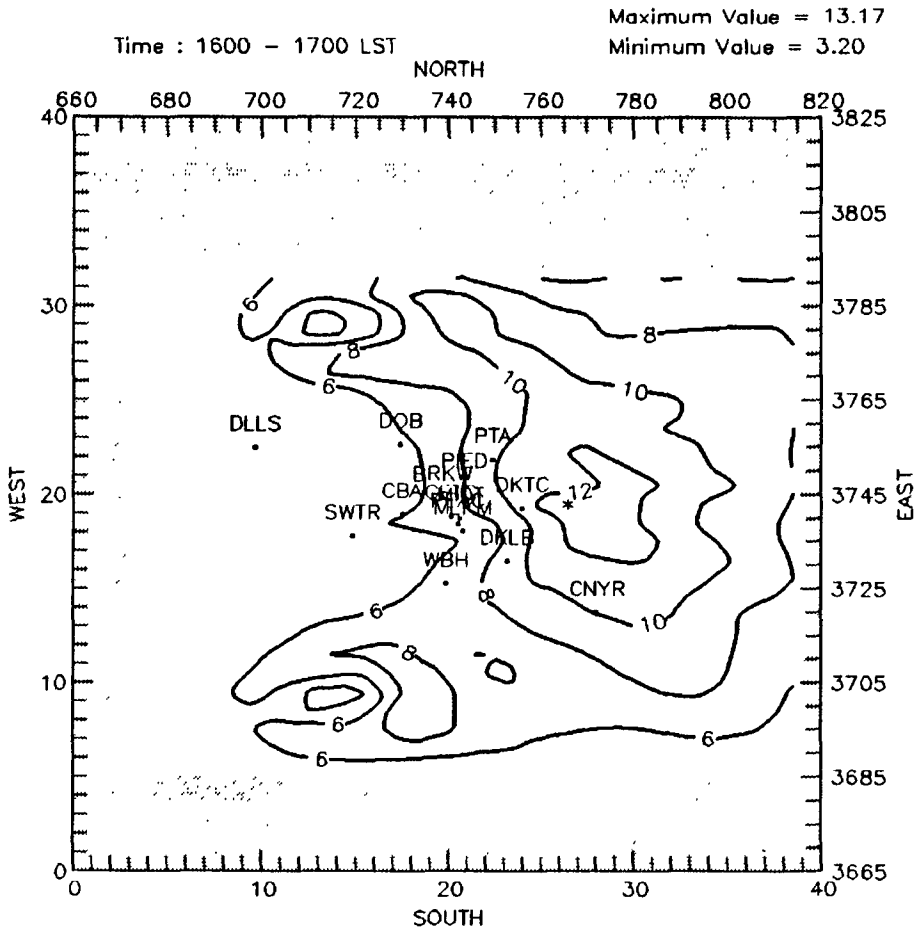

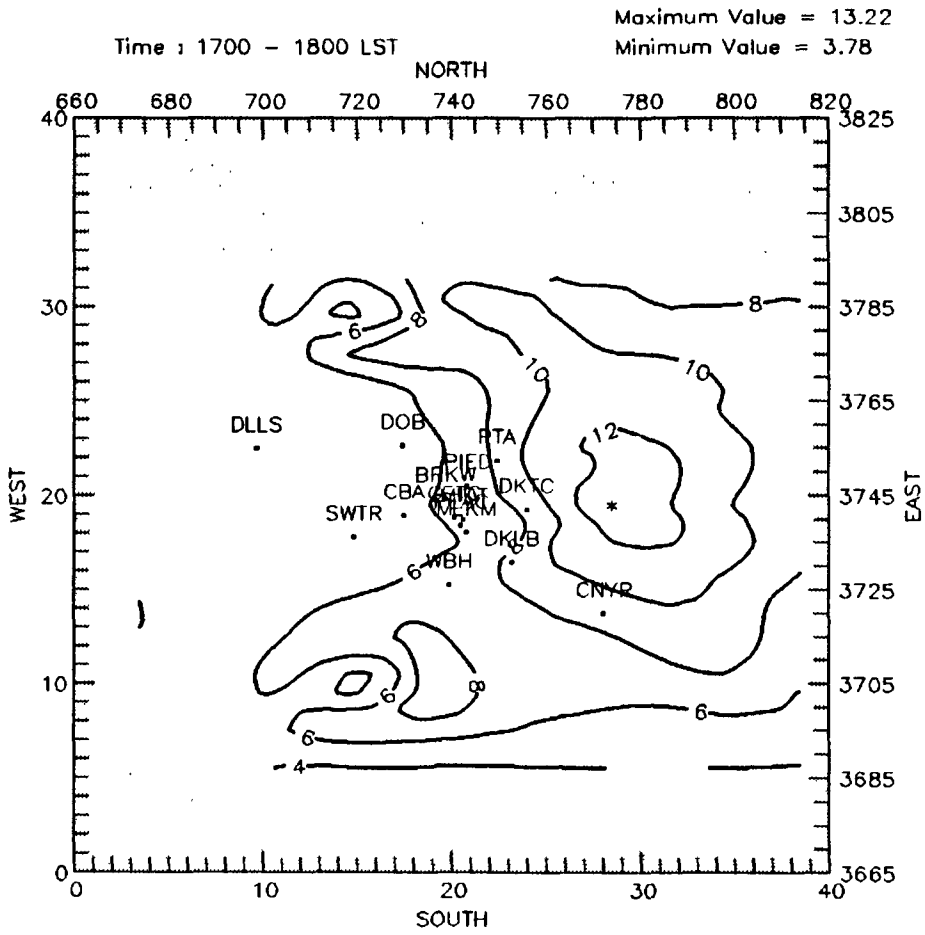

Ozone (pphm) 1985 base emissions, June 4, 1984 (pphm)

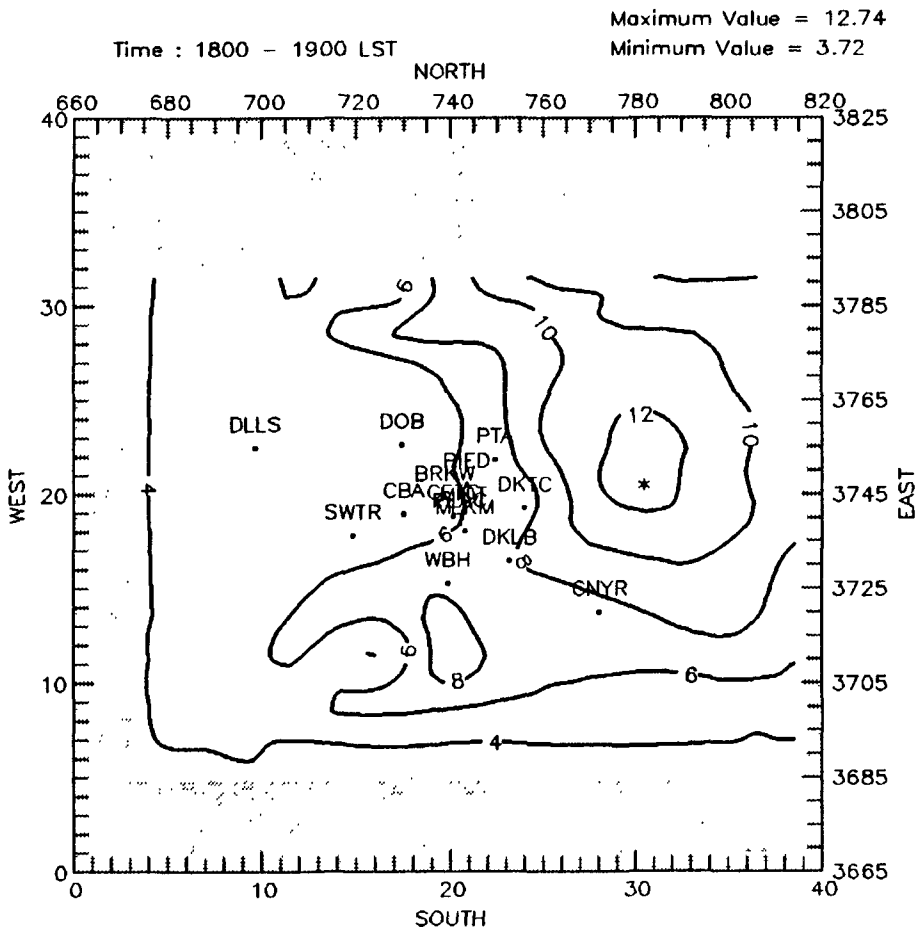

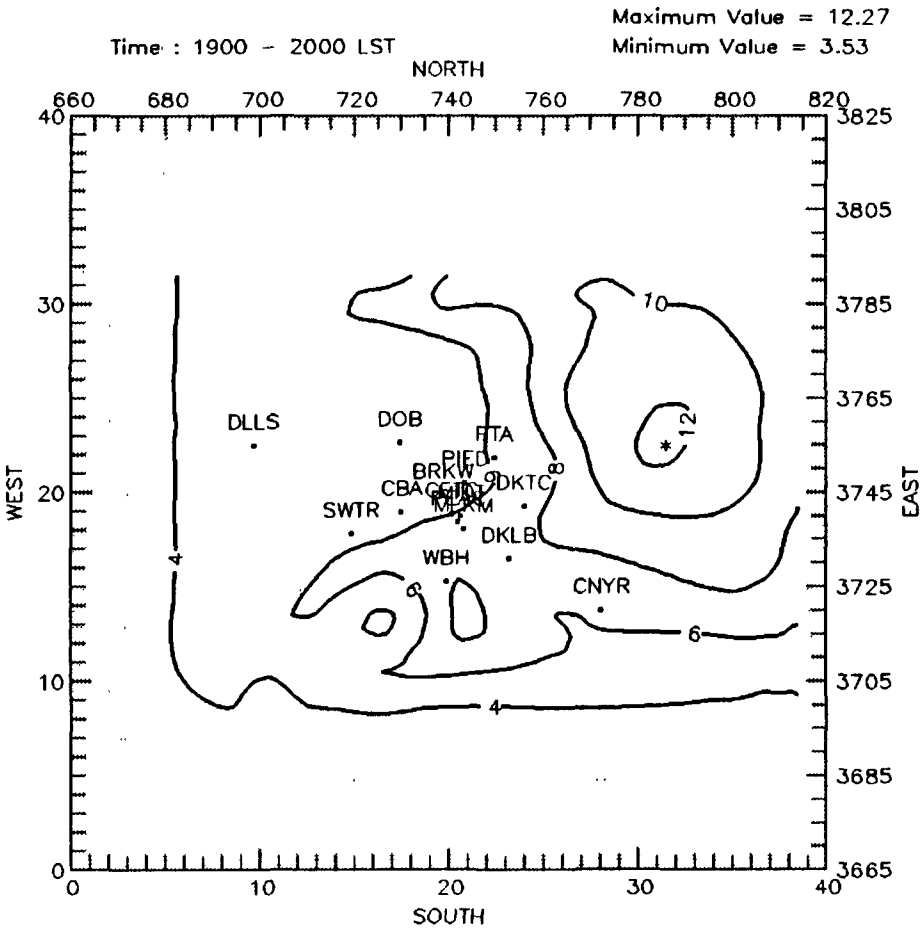

Ozone (pphm) 1985 base emissions, June 4, 1984 (pphm)

Appendix F

PERCENT CONTRIBUTION OF INITIAL CONCENTRATIONS, BOUNDARY CONDITIONS (FOUR LATERAL FACES PLUS TOP BOUNDARY) ANTHROPOGENIC AREA SOURCE EMISSIONS, POINT SOURCE EMISSIONS, AND BIOGENIC EMISSIONS TO HOURLY TRACER, NO_x, AND VOC CONCENTRATIONS ON 4 JUNE 1984

F-1a: 0800 Initial NO_x tracer contibution
F-1b: 0800 Boundary NO_x tracer contribution
F-1c: 0800 Area source NO_x tracer contribution
F-1d: 0800 Point source NO_x tracer contribution

F-2a: 0800 Initial VOC tracer contribution
F-2b: 0800 Boundary VOC tracer contribution
F-2c: 0800 Anthropogenic VOC tracer contribution
F-2d: 0800 Biogenic VOC tracer contribution

F-3a: 1200 Initial NO_x tracer contribution
F-3b: 1200 Boundary NO_x tracer contribution
F-3c: 1200 Area source NO_x tracer contribution
F-3d: 1200 Point source NO_x tracer contribution

F-4a: 1200 Initial VOC tracer contribution
F-4b: 1200 Boundary VOC tracer contribution
F-4c: 1200 Anthropogenic VOC tracer contribution
F-4d: 1200 Biogenic VOC tracer contribution

F-5a: 1600 Initial NO_x tracer contibution
F-5b: 1600 Boundary NO_x tracer contribution
F-5c: 1600 Area source NO_x tracer contribution
F-5d: 1600 Point source NO_x tracer contribution

F-6a: 1600 Initial VOC tracer contribution
F-6b: 1600 Boundary VOC tracer contribution
F-6c: 1600 Anthropogenic VOC tracer contribution
F-6d: 1600 Biogenic VOC tracer contribution

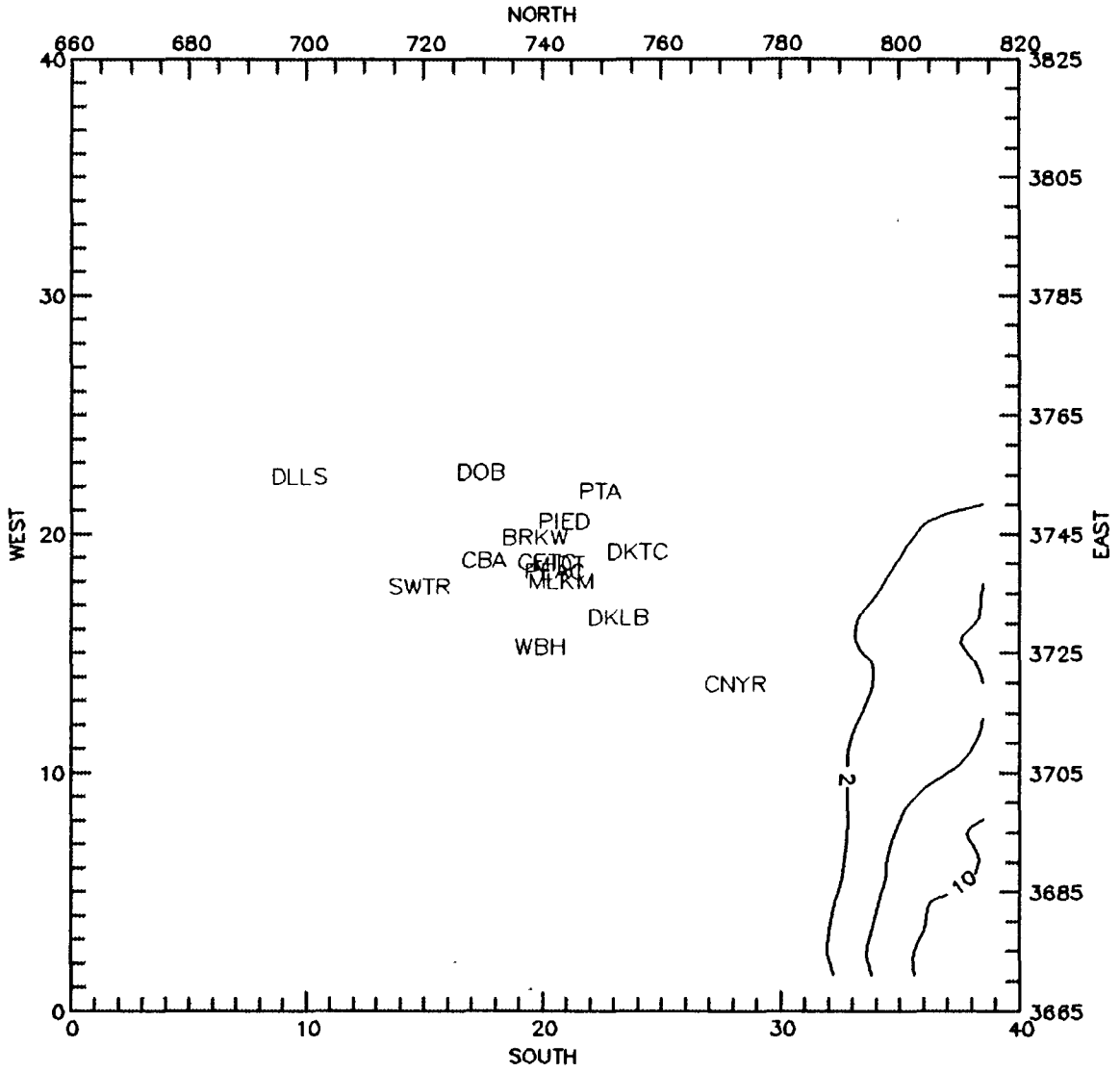

FIGURE F-1a. Percent contribution of initial NOx tracer at 800 EST, 4 June 1984.

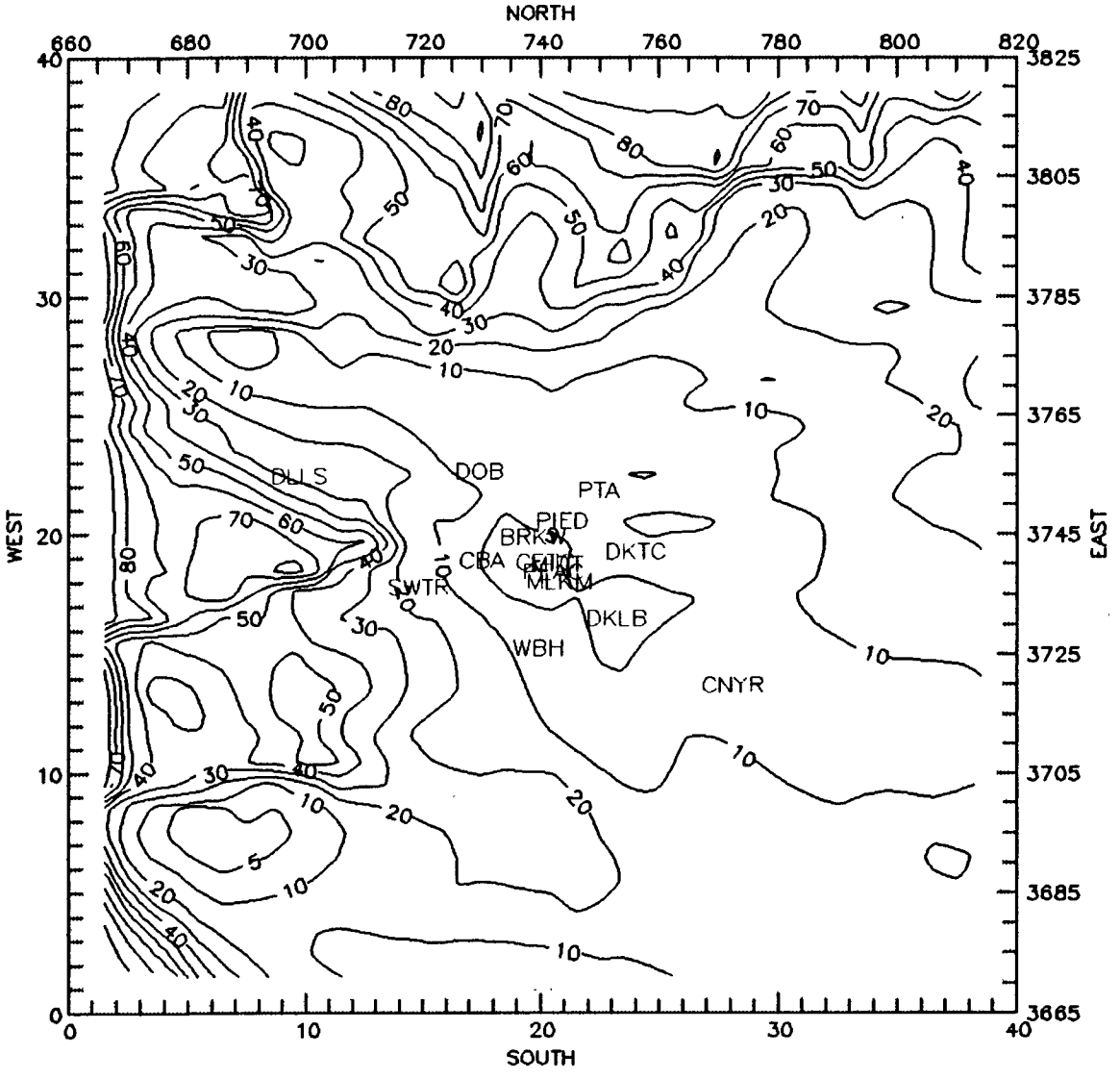

FIGURE F-1b. Percent contribution of boundary NOx tracer at 800 EST, 4 June 1984.

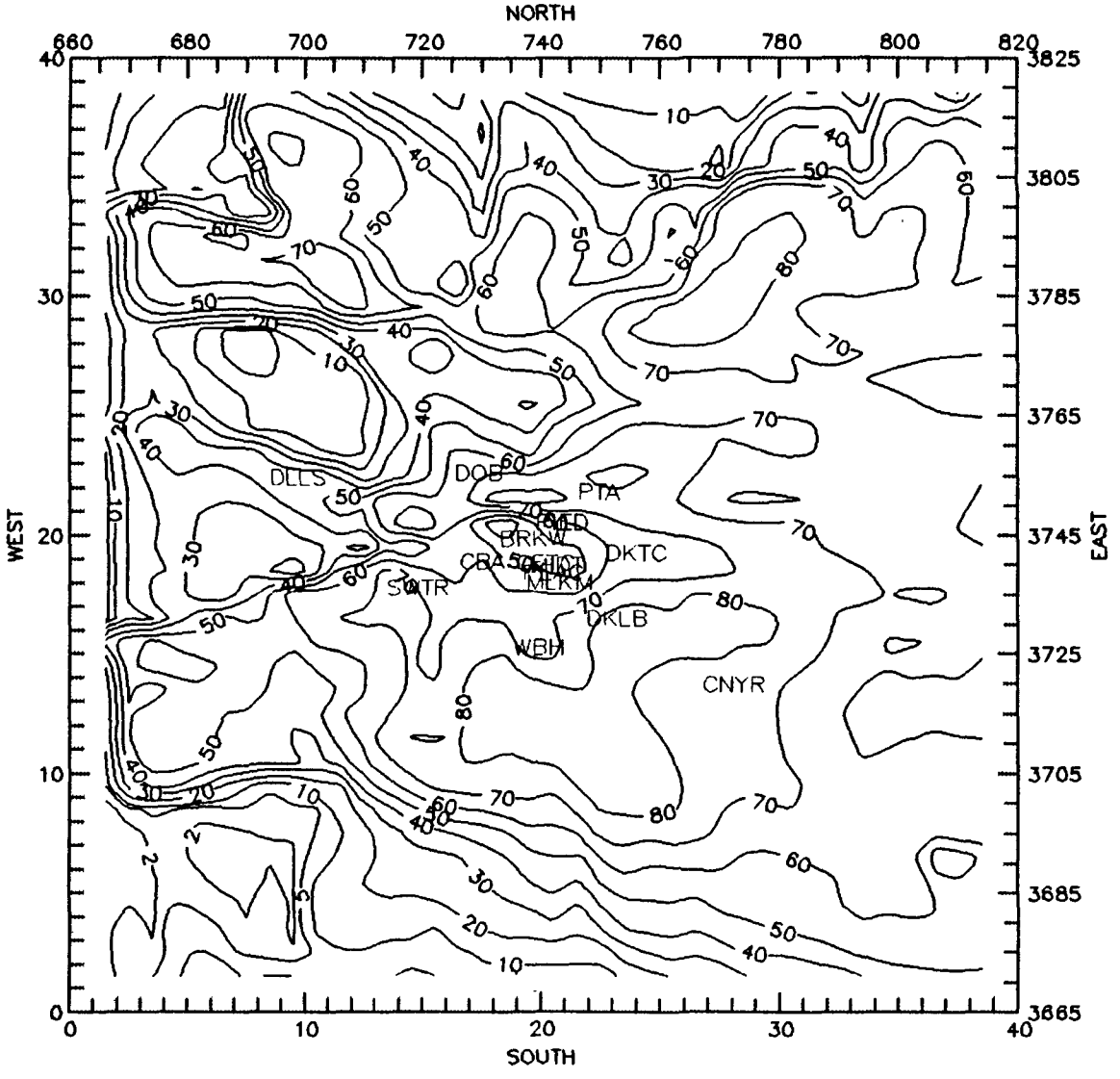

FIGURE F-1c . Percent contribution of area source NOx tracer at 800 EST, 4 June 1984.

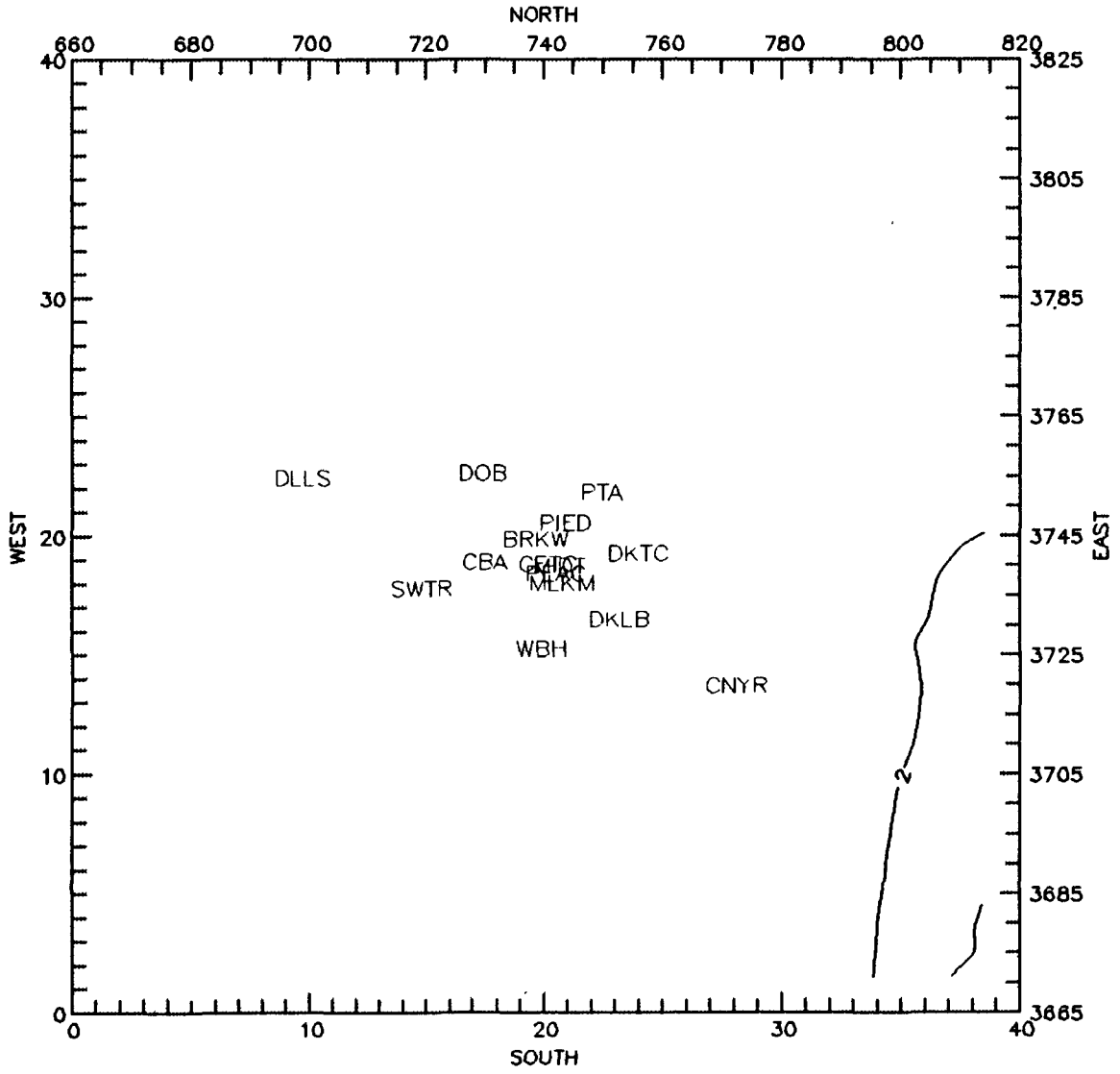

FIGURE F-2a . Percent contribution of initial VOC tracer at 800 EST, 4 June 1984.

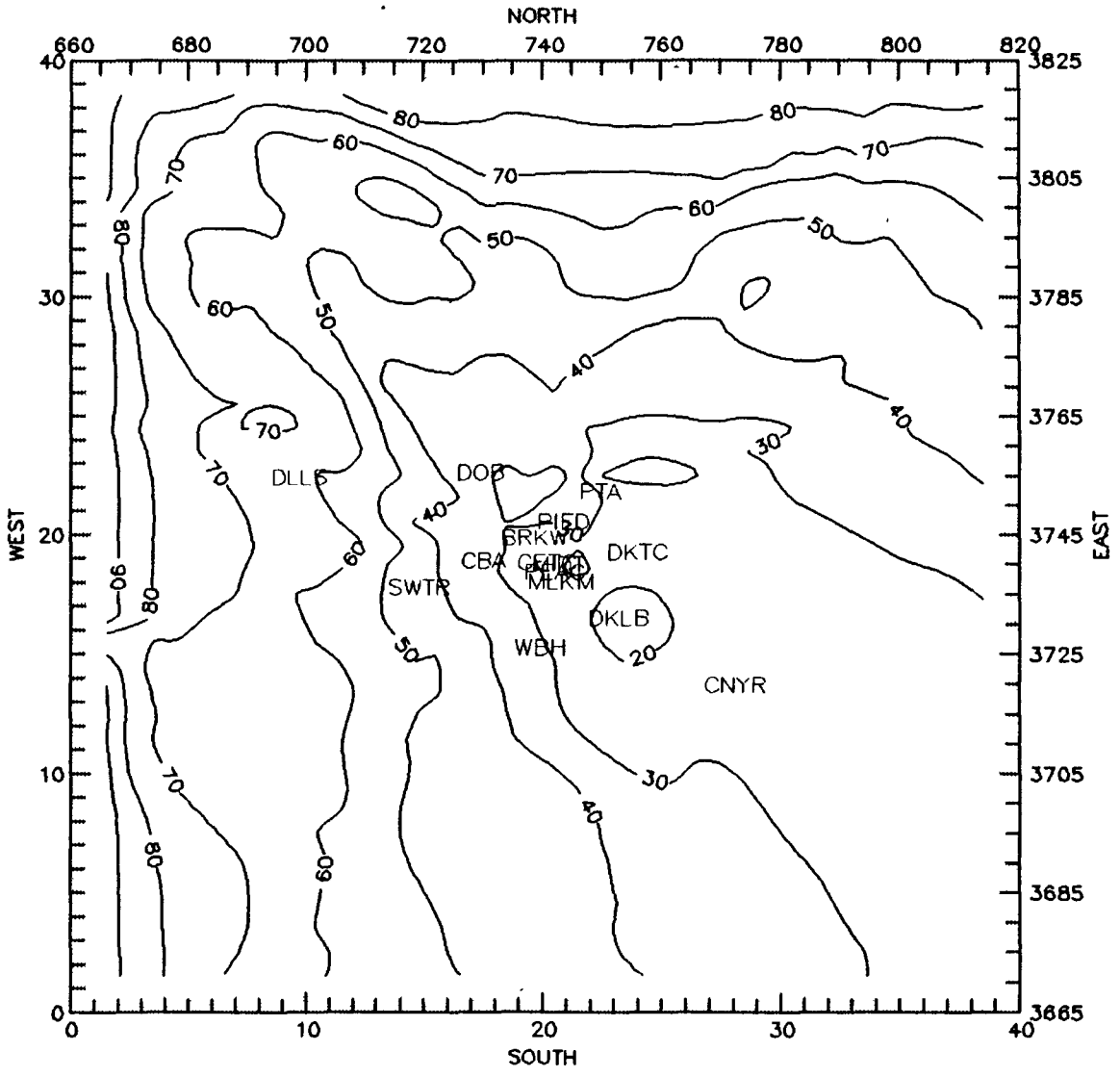

FIGURE F-2b . Percent contribution of boundary VOC tracer at 800 EST, 4 June 1984.

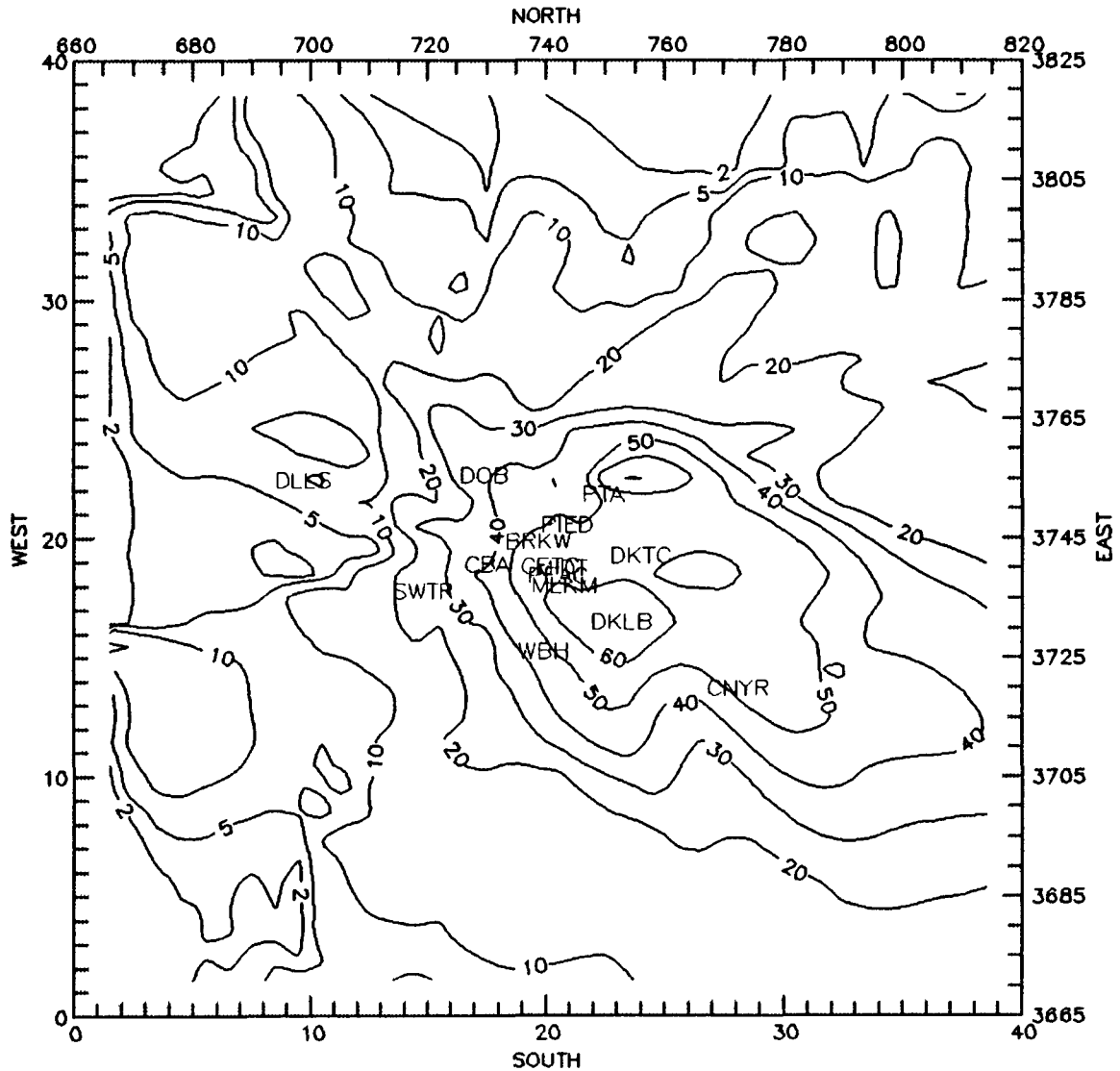

FIGURE F-2c. Percent contribution of anthropogenic VOC tracer at 800 EST, 4 June 1984.

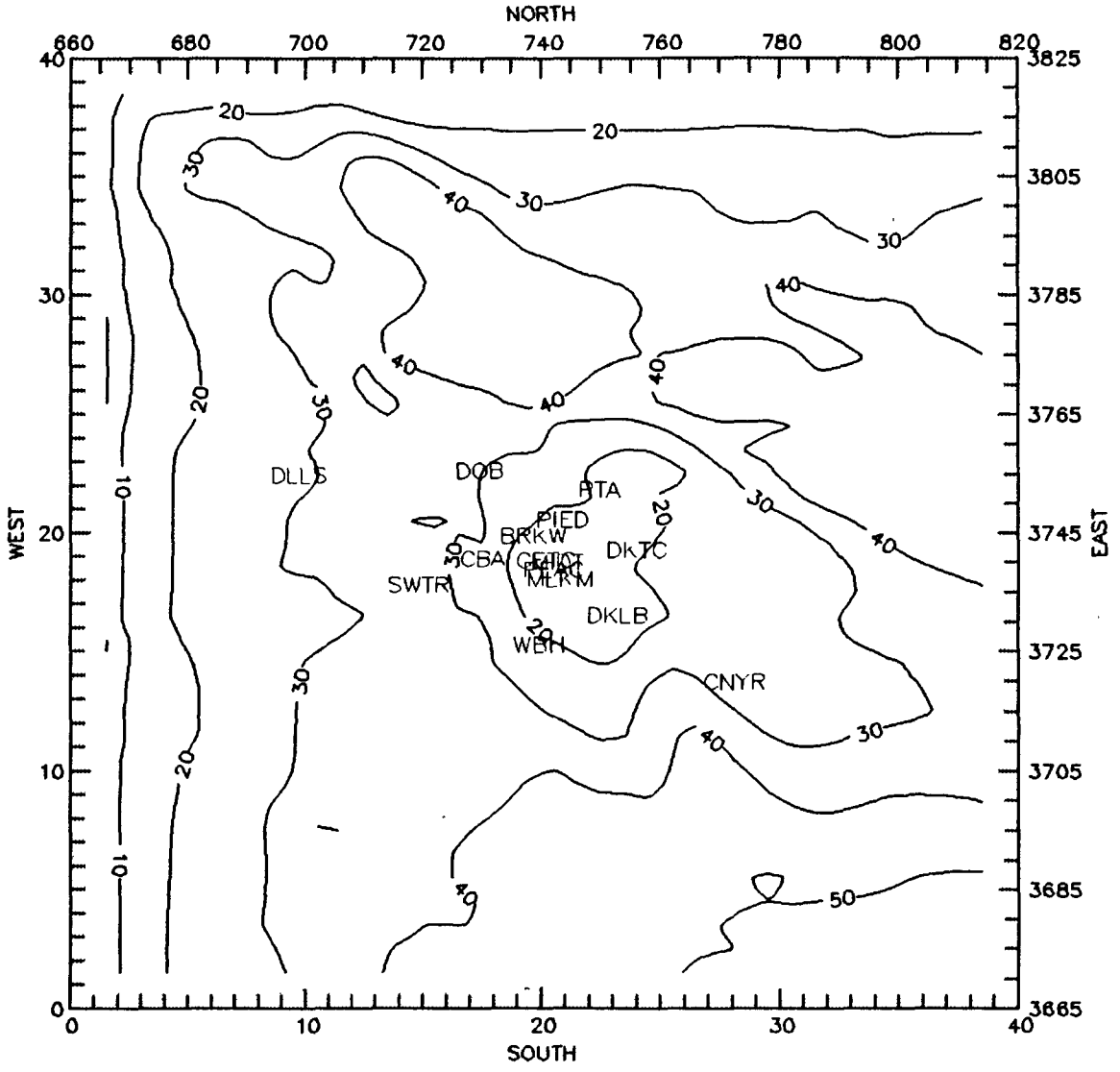

FIGURE F-2d . Percent contribution of biogenic VOC tracer at 800 EST, 4 June 1984.

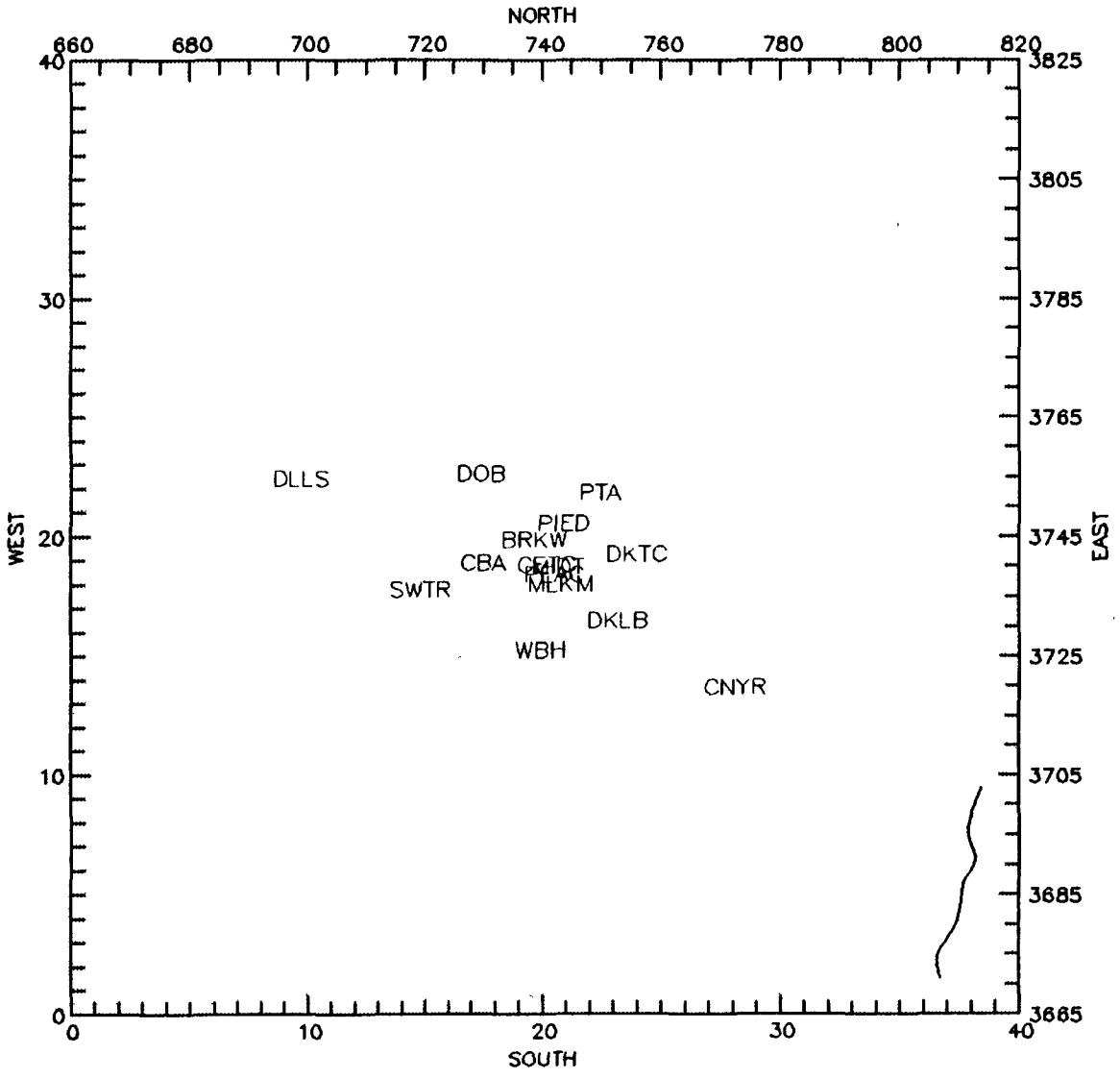

FIGURE F-3a. Percent contribution of initial NOx tracer at 1200 EST, 4 June 1984.

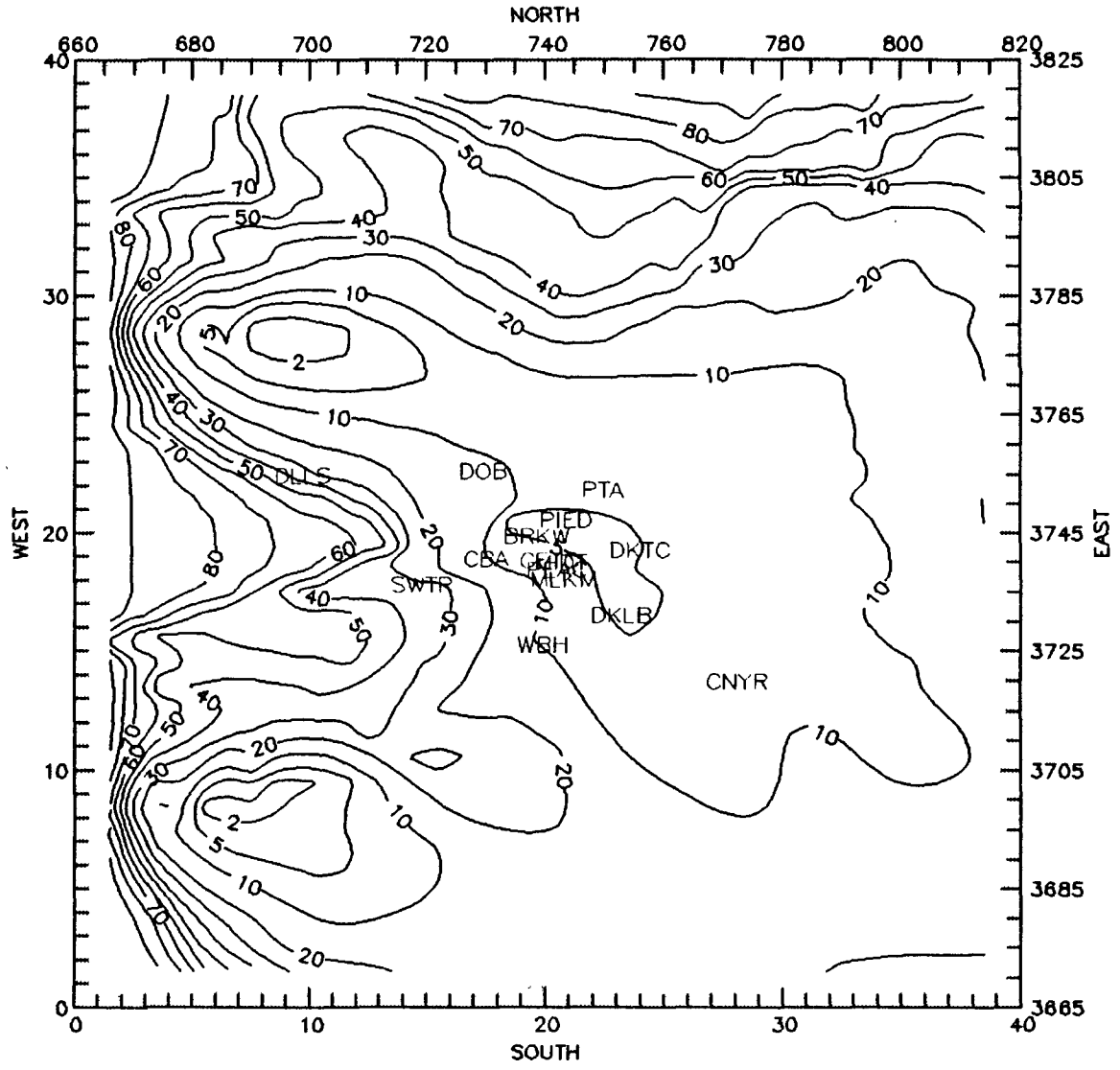

FIGURE F-3b. Percent contribution of boundary NOx tracer at 1200 EST, 4 June 1984.

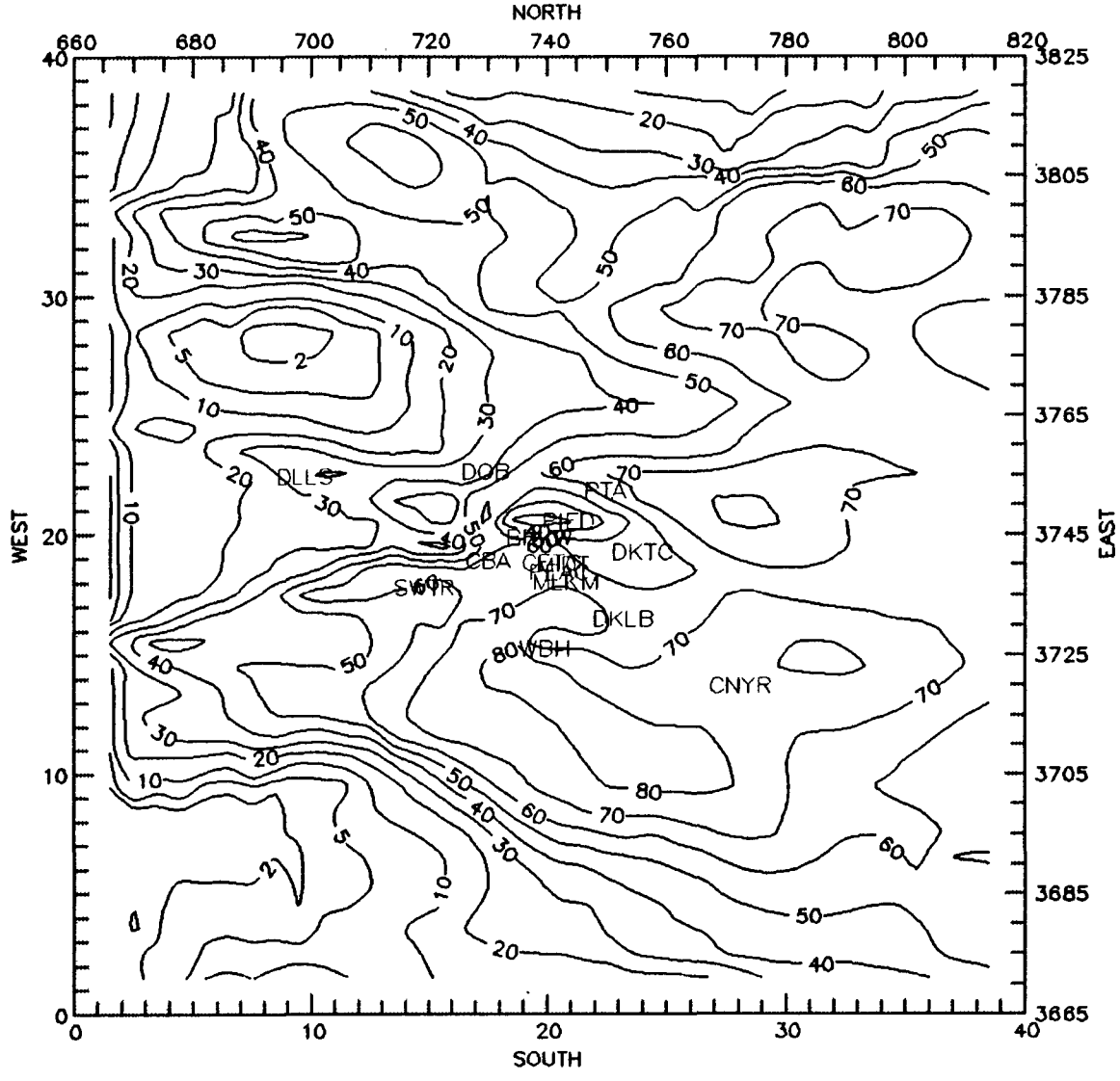

FIGURE F-3c . Percent contribution of area source NOx tracer at 1200 EST, 4 June 1984.

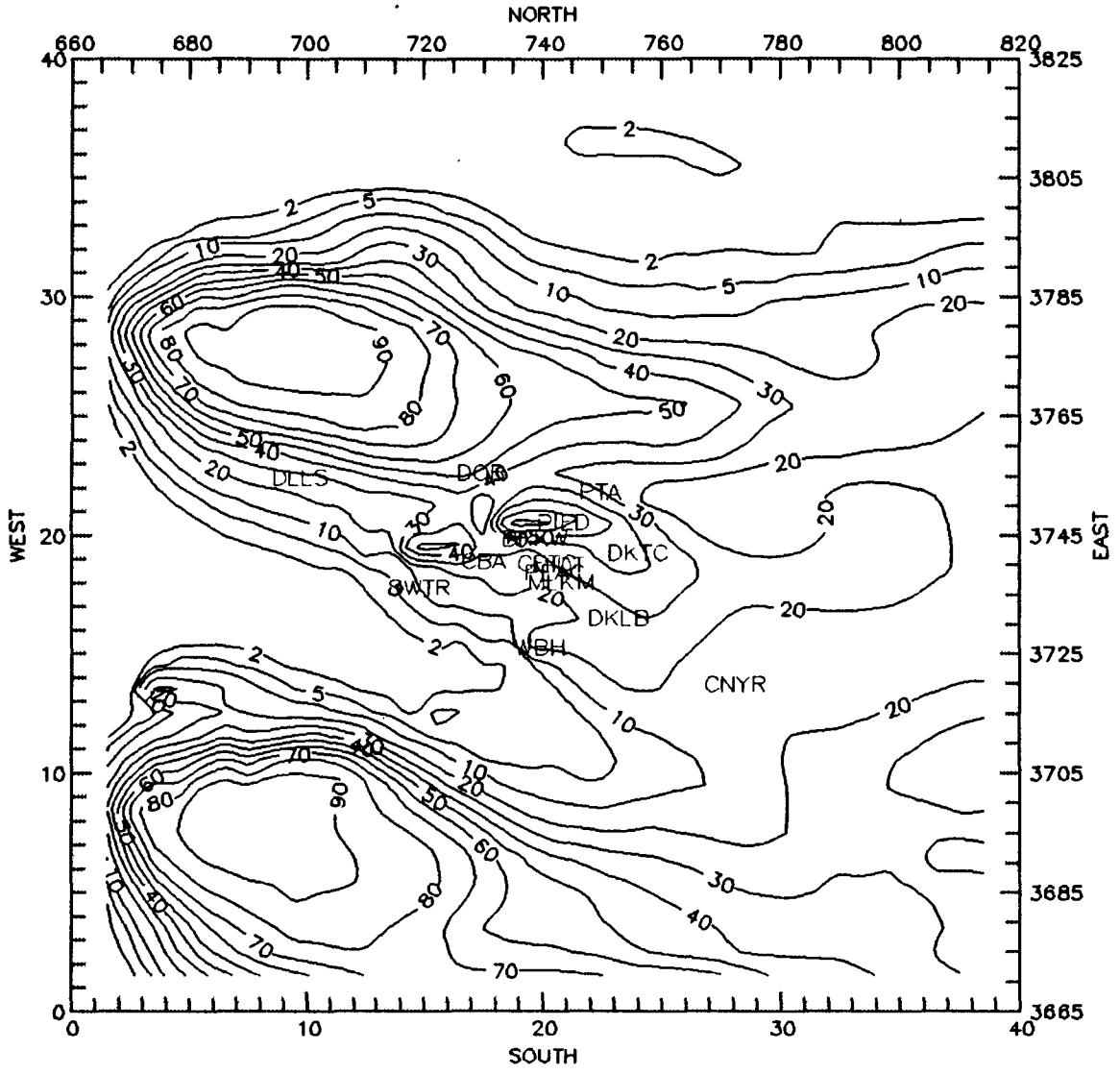

FIGURE F-3d. Percent contribution of point source NOx tracer at 1200 EST, 4 June 1984.

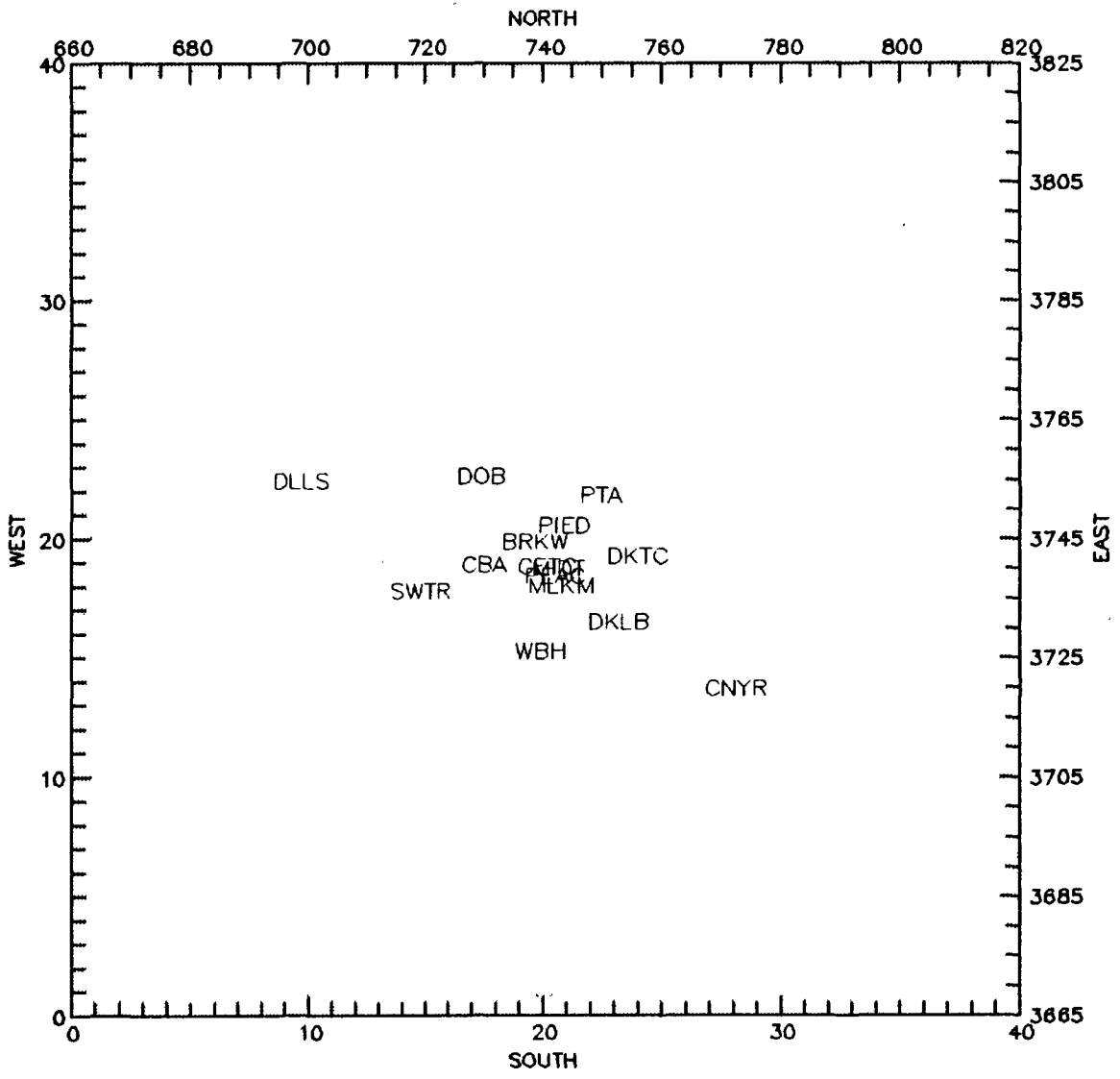

FIGURE F-4a. Percent contribution of initial VOC tracer at 1200 EST, 4 June 1984.

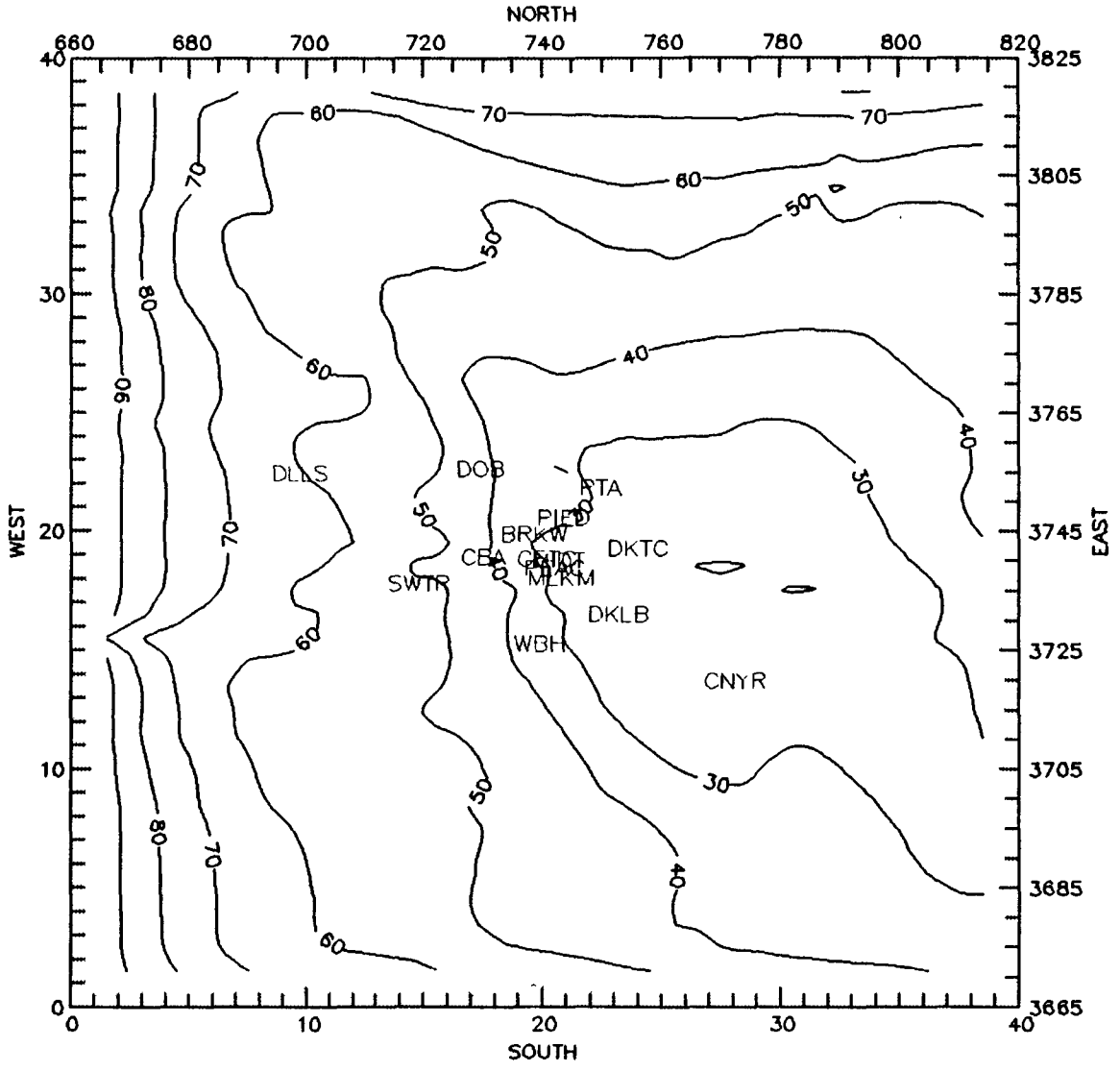

FIGURE F-4b . Percent contribution of boundary VOC tracer at 1200 EST, 4 June 1984.

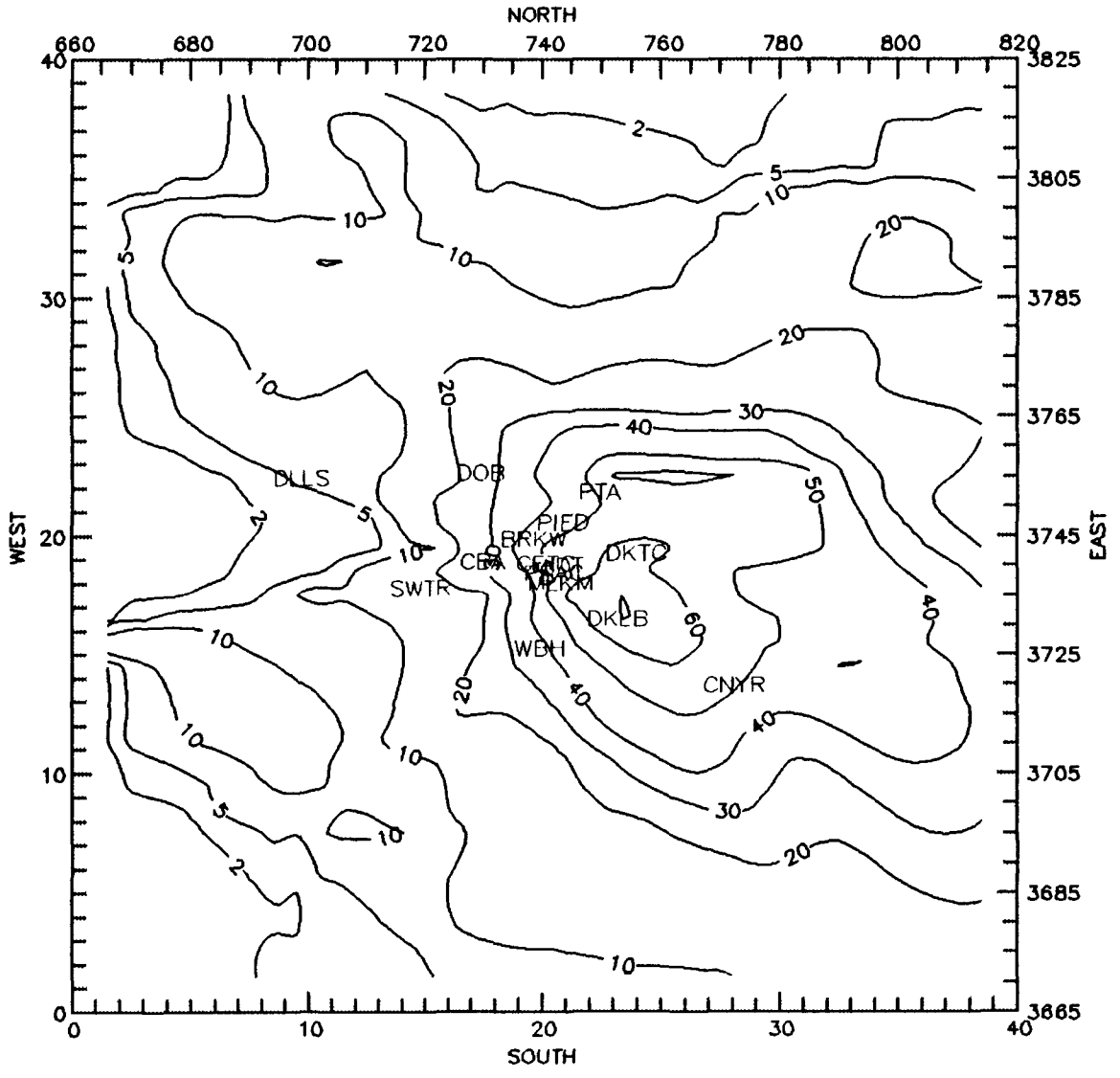

FIGURE F-4c. Percent contribution of anthropogenic VOC tracer at 1200 EST, 4 June 1984.

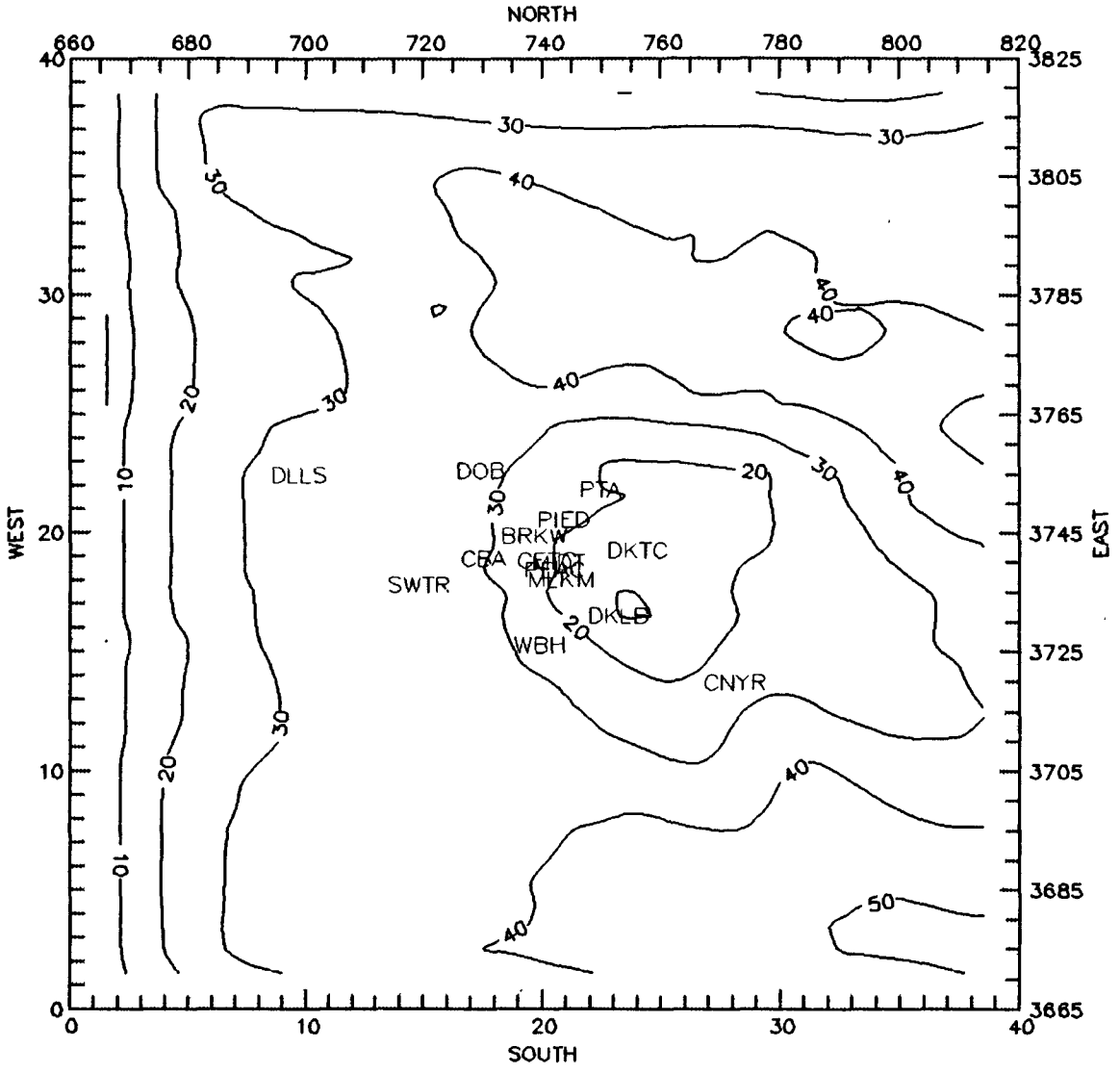

FIGURE F-4d. Percent contribution of biogenic VOC tracer at 1200 EST, 4 June 1984.

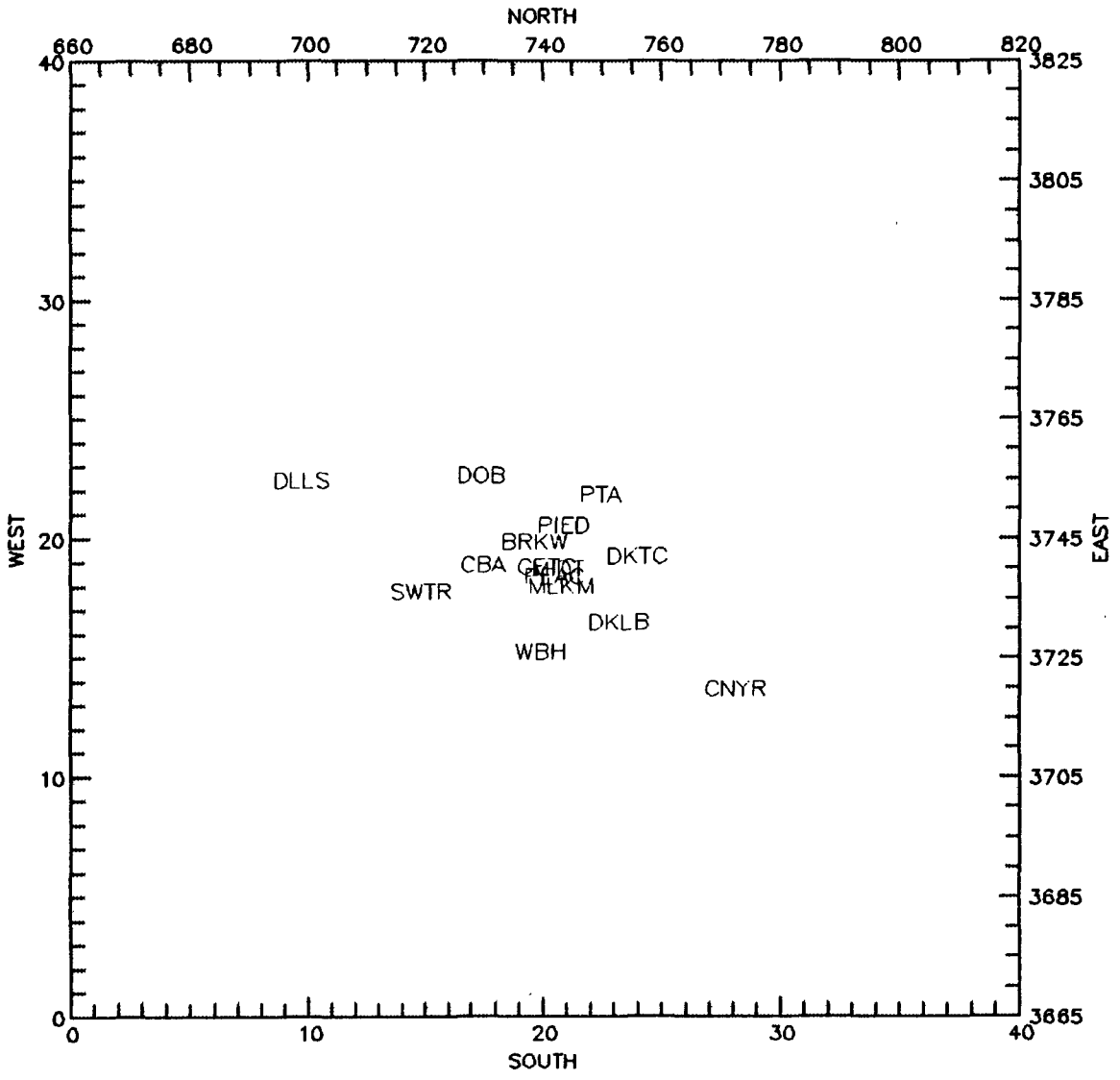

FIGURE F-5a. Percent contribution of initial NOx tracer at 1600 EST, 4 June 1984.

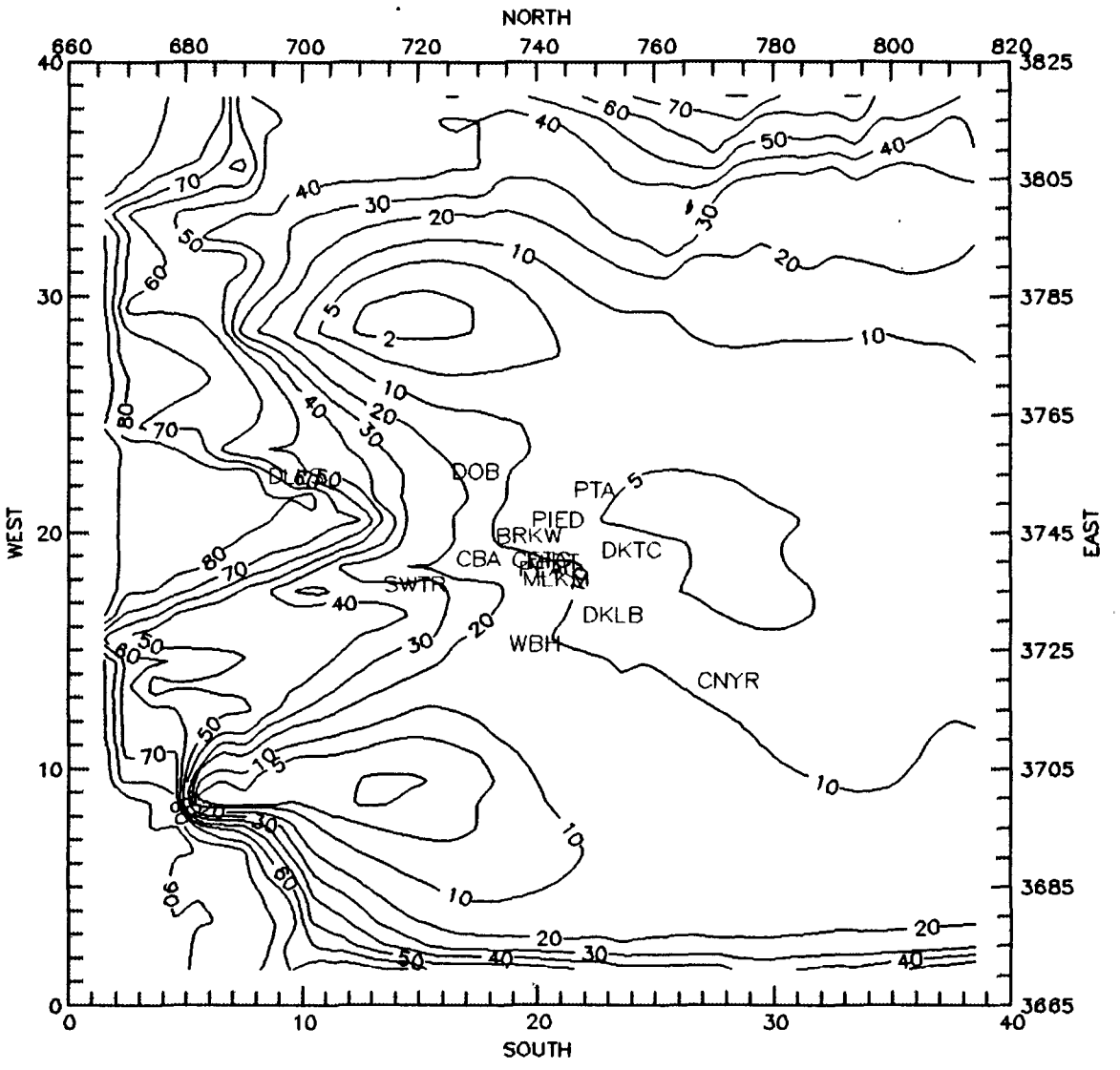

FIGURE F-5b . Percent contribution of boundary NOx tracer at 1600 EST, 4 June 1984.

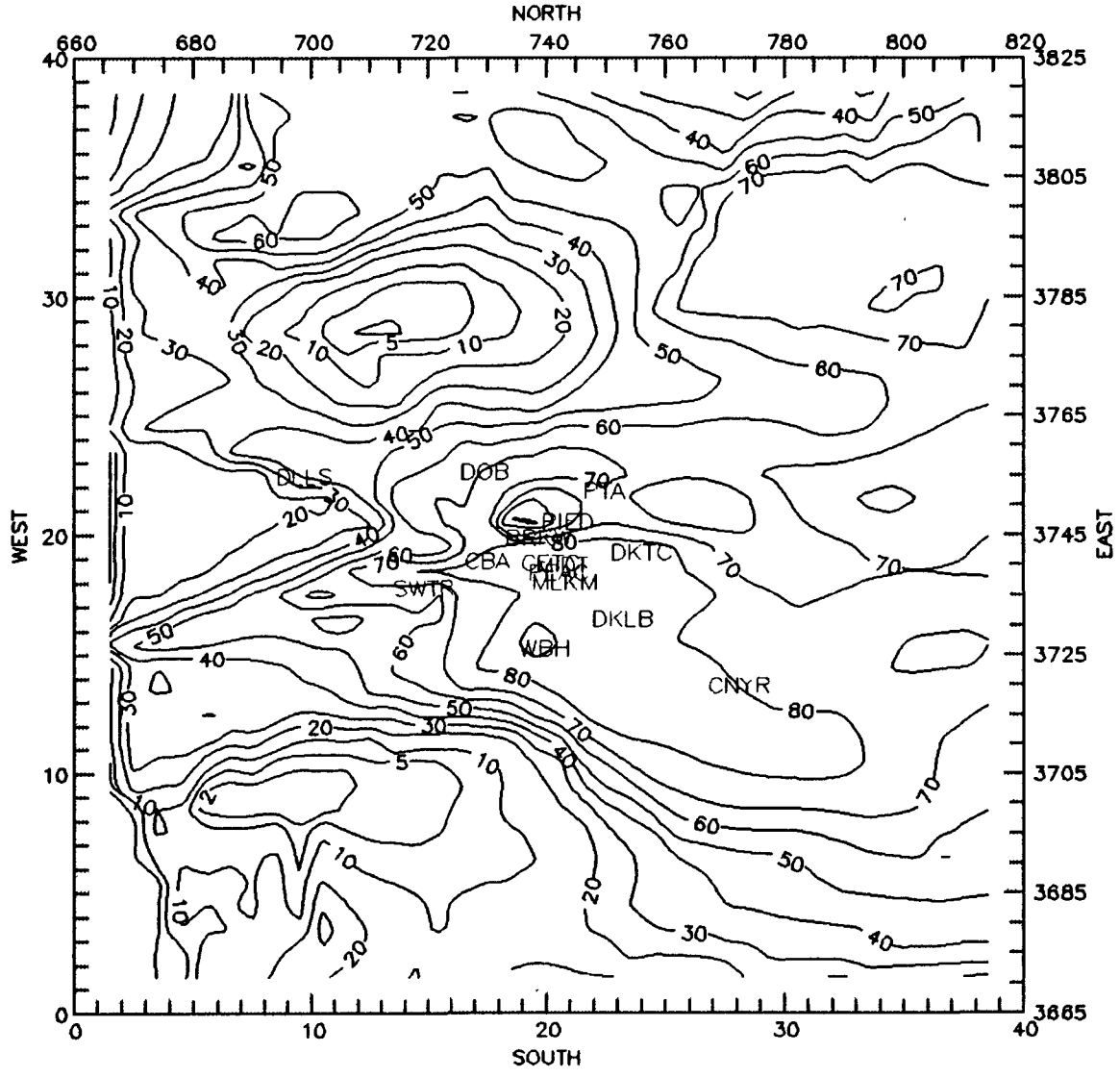

FIGURE F-5c . Percent contribution of area source NOx tracer at 1600 EST, 4 June 1984.

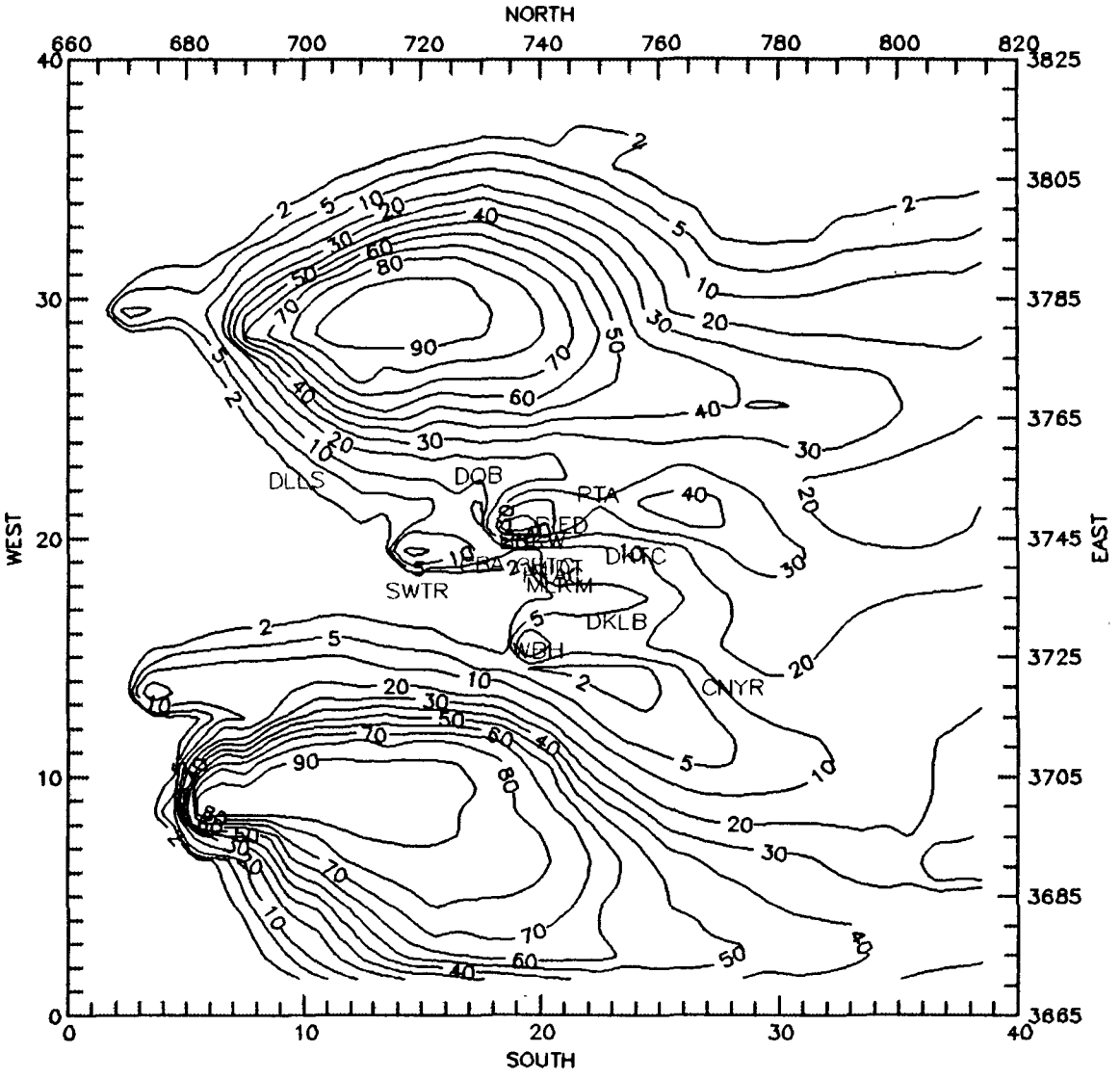

FIGURE F-5d . Percent contribution of point source NOx tracer at 1600 EST, 4 June 1984.

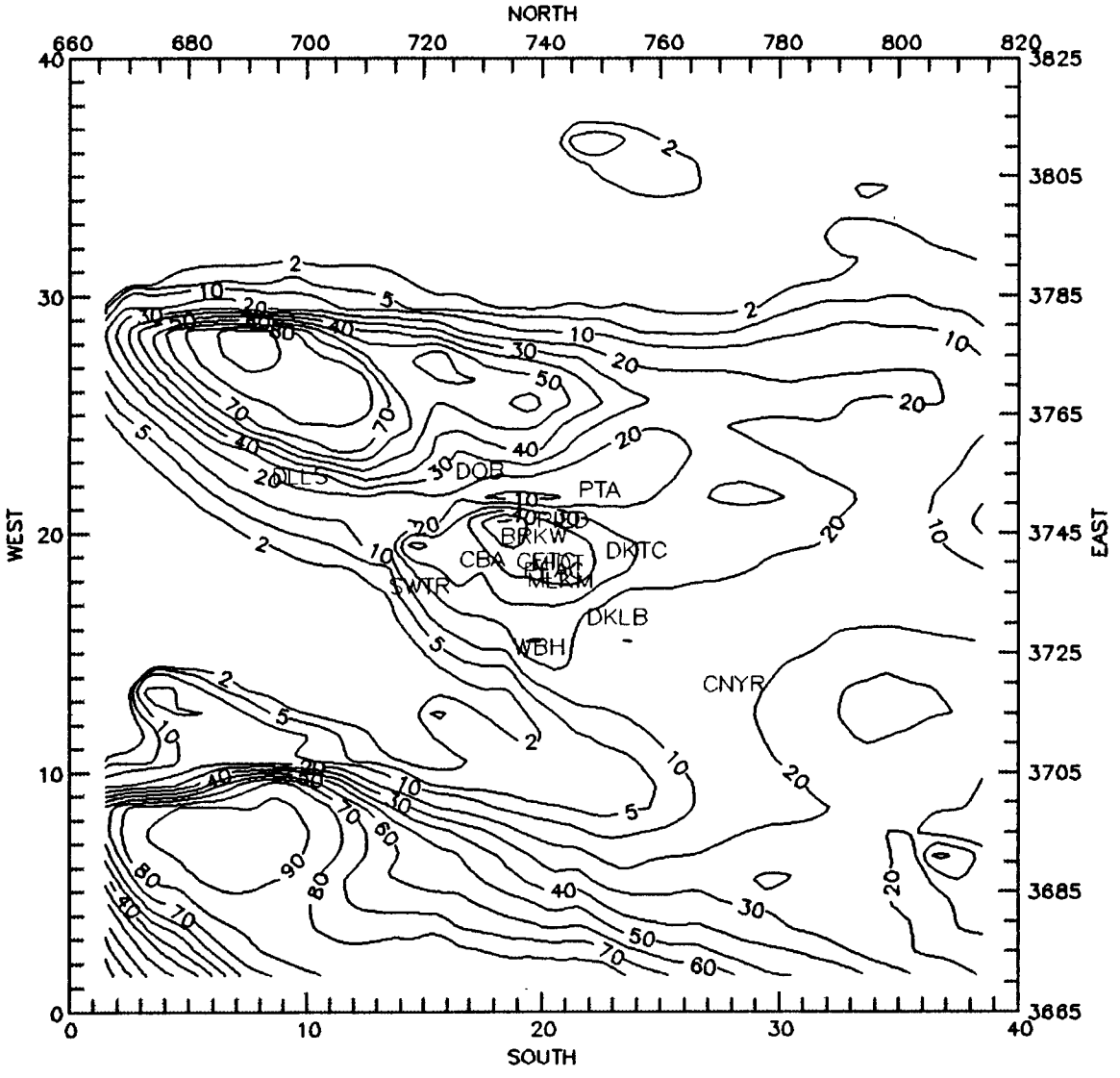

FIGURE F-1d . Percent contribution of point source NOx tracer at 800 EST, 4 June 1984.

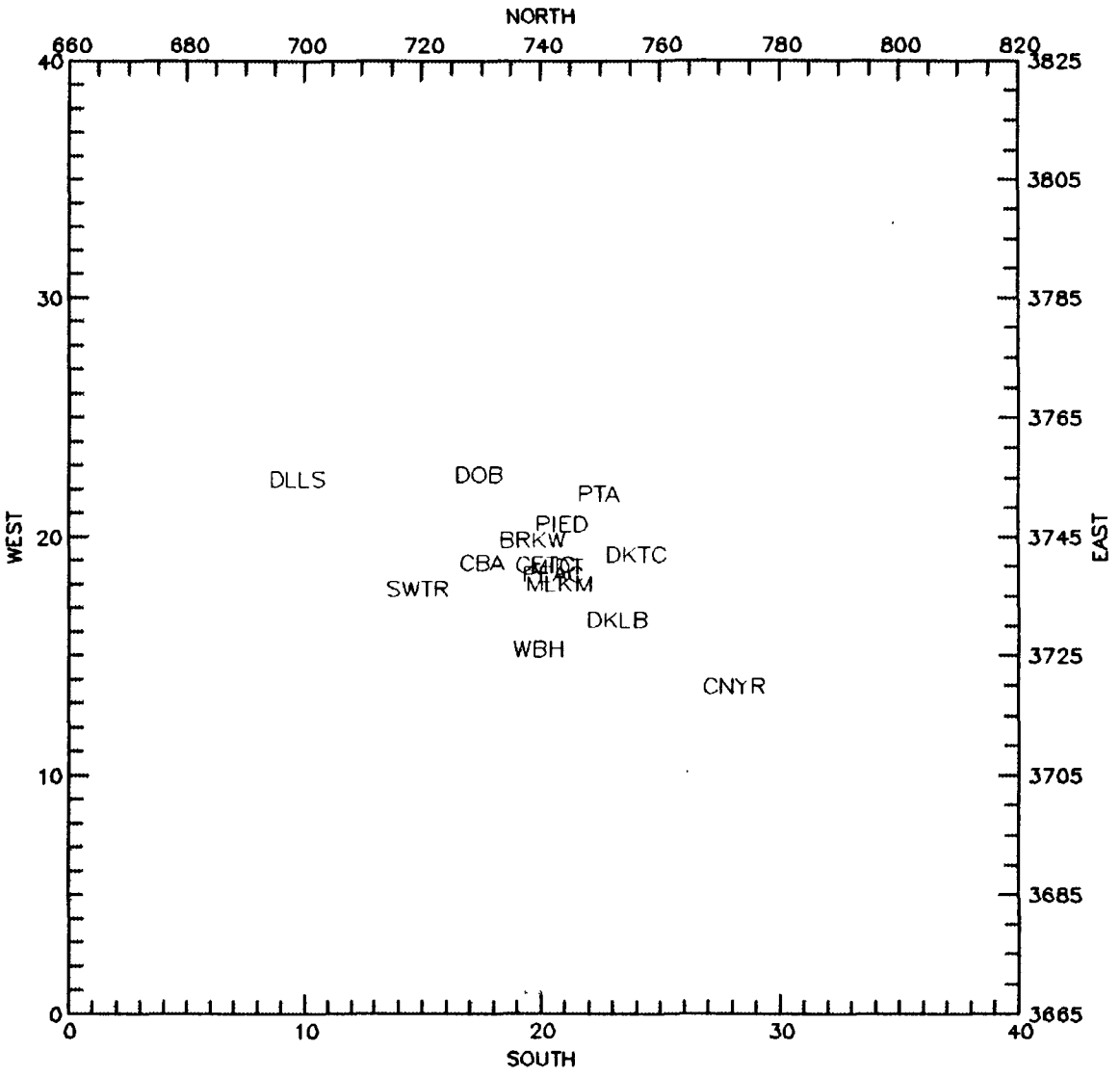

FIGURE F-6a . Percent contribution of initial VOC tracer at 1600 EST, 4 June 1984.

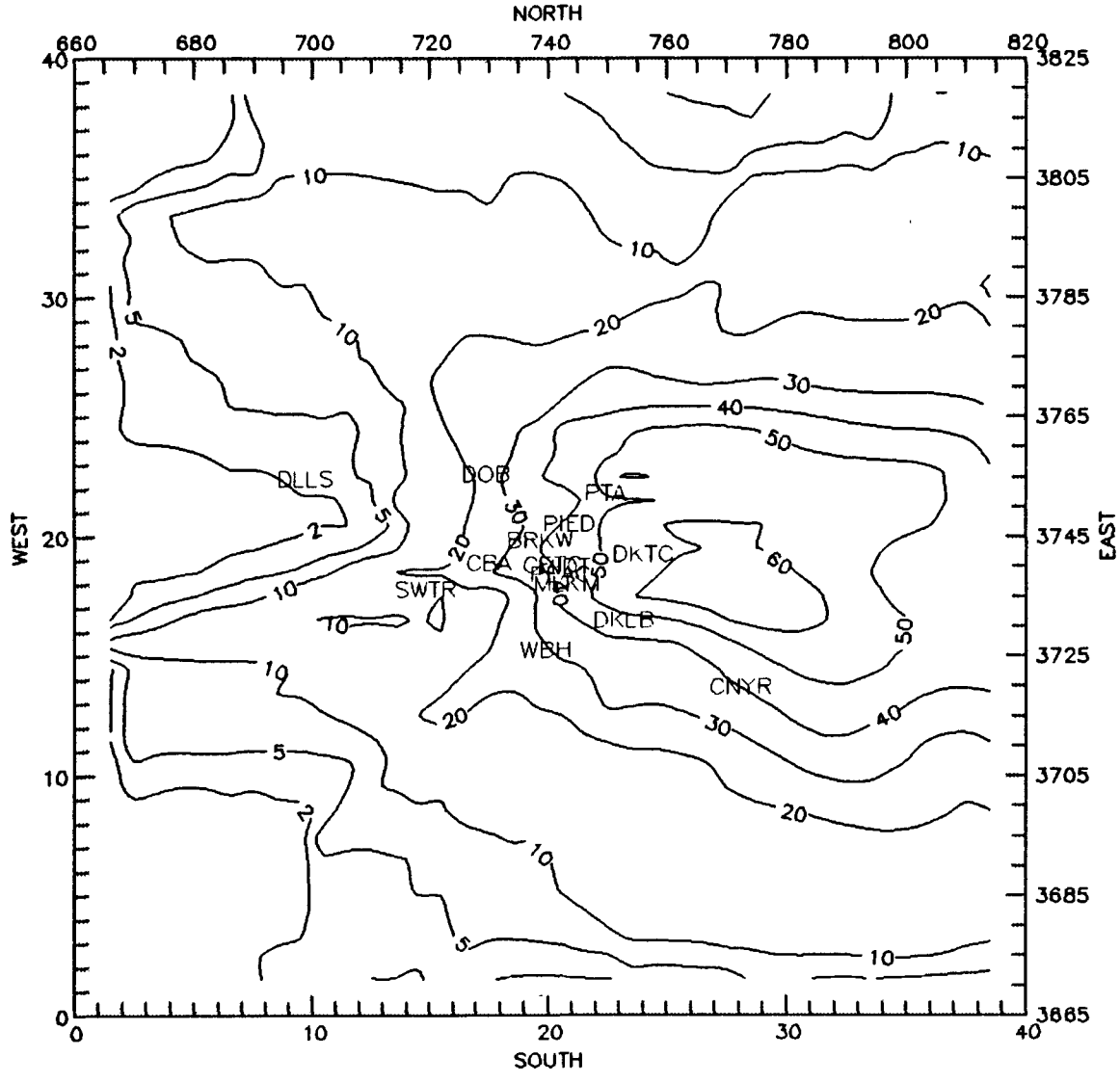

FIGURE F-6b. Percent contribution of anthropogenic VOC tracer at 1600 EST, 4 June 1984.

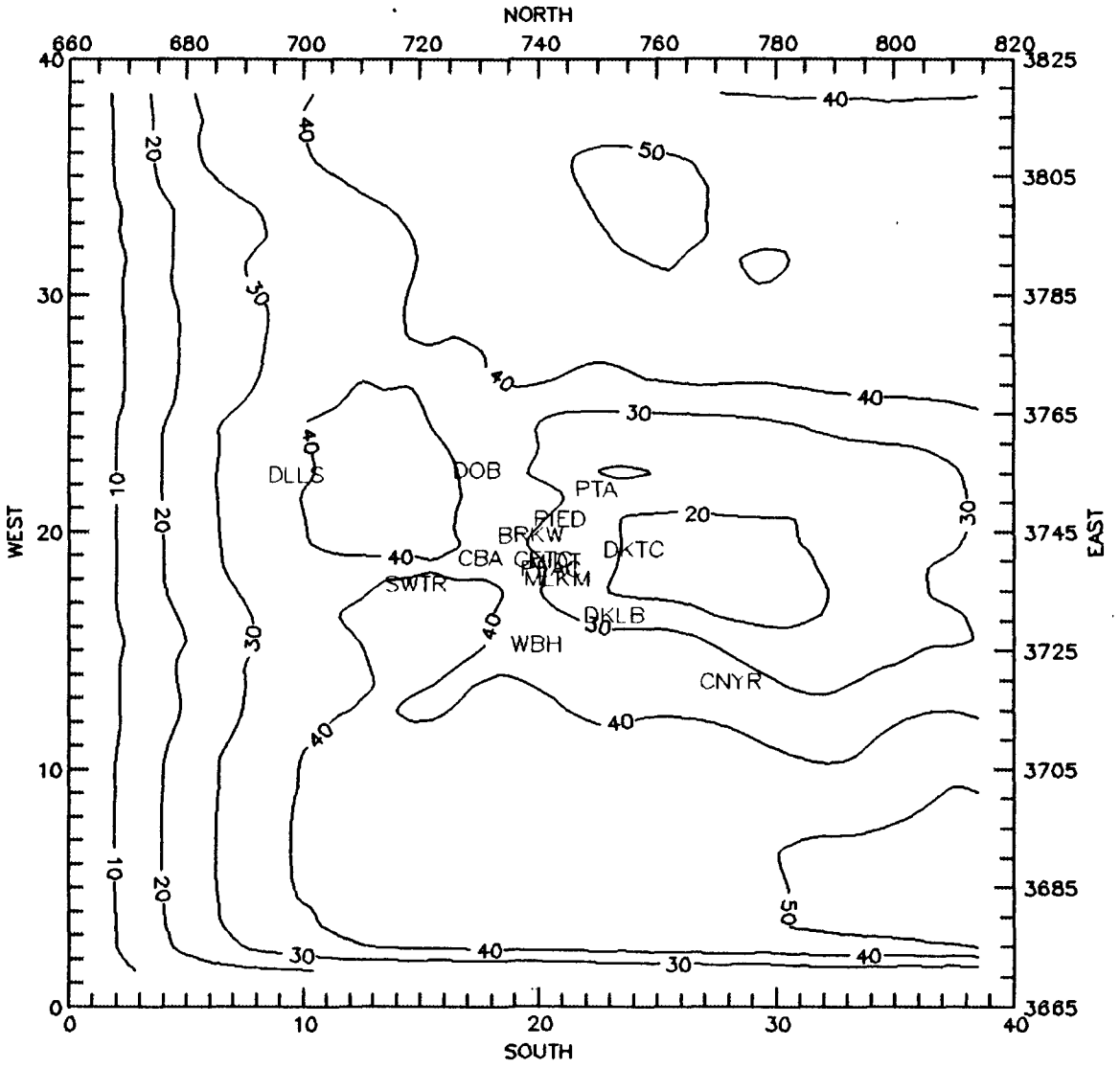

FIGURE F-6c. Percent contribution of biogenic VOC tracer at 1600 EST, 4 June 1984.

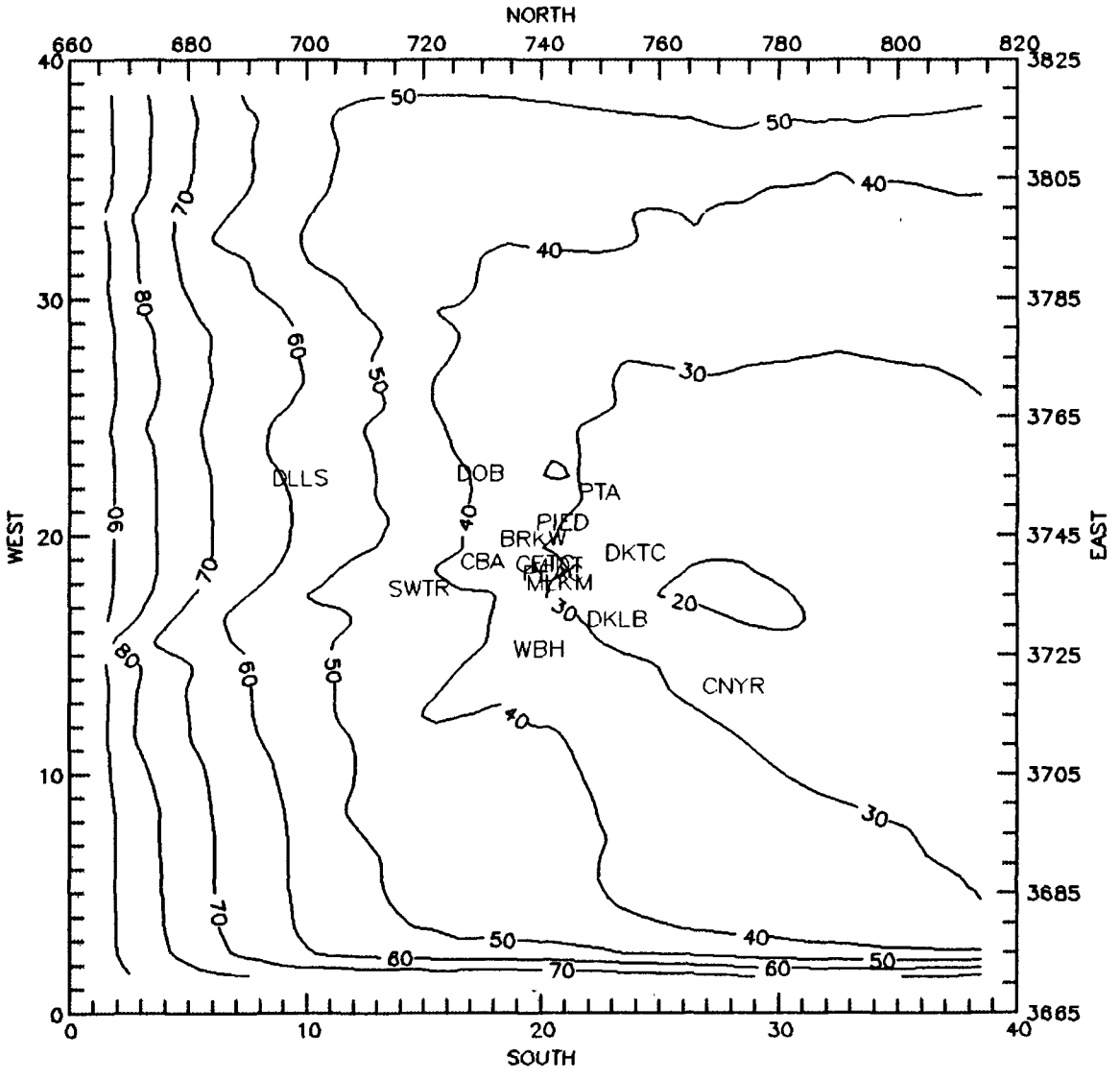

FIGURE F-6d. Percent contribution of boundary VOC tracer at 1600 EST, 4 June 1984.

Appendix G

SENSITIVITY ANALYSIS OF THE URBAN AIRSHED MODEL

Appendix G

SENSITIVITY ANALYSIS OF THE URBAN AIRSHED MODEL

Because of the limited air quality and meteorological monitoring data in the vicinity of Atlanta there is some question whether the base case simulated all of the pertinent physical, meteorological, and chemical processes that led to the high ozone episode of 4 June 1984. The only direct indication of whether the model correctly simulated the episode is its ability to predict the historical hourly ozone concentrations at the three ozone monitoring sites. Diagnostic run 2 barely passed the model performance goal used in this study (predicted region-wide maximum ozone must be within 20 percent and in the general location of the observed peak, and at the location of the observed peak the predicted daily maximum ozone concentration must be within 30 percent of the observed peak). The descrepancies between the predicted and observed ozone concentrations could be explained by any of several factors, including underestimation of the anthropogenic emissions inventory, use of too low boundary conditions, and excessive wind shear and wind speeds, both of which tended to dilute the urban plume. Thus it was decided to perform a sensitivity test that examined the sensitivity of the predicted ozone concentrations to less dilution of the urban plume to see if model performance could be improved. This was accomplished by reducing the wind speeds at all FAA wind observations sites by 50 percent.

This wind speed reduction is justified because the UAM requires hourly averaged wind speeds and wind directions, whereas the FAA meteorological sites report instantaneous wind observations. When the wind varies throughout the hour, the vector averaging of the hourly average wind speeds results in a lower value than the one reported at an FAA site. In addition, the FAA wind observations are used primarily to advise pilots of adverse wind conditions at the airport. Thus, during slow wind conditions, which are typical during an ozone episode, the FAA observer may report higher wind gusts that might affect flight operations. The hourly average wind speed is of no interest to the pilot if gusts exist that may affect flight operations. This bias of FAA wind speeds was first noticed while developing UAM inputs for the California South Coast Air Basin, where several hourly integrated and FAA wind observation sites are located near each other. A brief analysis of these sites is reported next.

COMPARISON OF HOURLY AVERAGED AND FAA WIND SPEED OBSERVATIONS

During the development of the California South Coast Air Basin (SOCAB) Air Quality Management Plan four three-day episodes of high ozone days were extensively studied. A systematic bias was seen between the one-hour vector-averaged observations at SCAQMD (South Coast Air Quality Management District) surface wind speed monitors and observations of one-minute averaged surface wind speed at nearby NWS/FAA (National Weather Service/ Federal Aviation Administration) sites. To estimate the extent of the bias, seven NWS/FAA stations were compared with SCAQMD wind monitors located nearby (i.e., within approximately one UAM grid cell). Table G-1 shows the station pairs and the distance between the NWS/FAA and SCAQMD sites.

The study periods were the high ozone episodes of 5-7 June, 12-14 August, 21-23 August, and 26-28 August 1985. A total of 1920 collocated data points were collected. This set was reduced by 801 data points because of either a missing station pair or a station pair that was below the speed of 1 knot, the lowest value that FAA/NWS wind monitoring stations can measure.

The mean value for the remaining 1119 data points for the FAA/NWS stations was 3.49 m/s, while the mean for the SCAQMD stations was 1.93 m/s, suggesting that the FAA/NWS stations were biased by approximately 45 percent (i.e., the hourly average wind speeds were a little over half of the FAA instantaneous observations). The differences in the median values were also very similar, with values of 3.10 m/s for FAA/NWS stations and 1.80 m/s for SCAQMD stations. Each day was examined to see if any particular day showed an extreme bias; the bias ranged from 36 percent on 13 August to 51 percent on 26 August.

Similarly, all seven stations were examined to see if any particular station may have been the cause of the bias. Five of the seven stations showed a similar bias, ranging from 45 to 56 percent. However, two pairs showed a significantly smaller bias; the Upland site and Ontario Airport pairs showed a bias of only 28.8 percent, and the San Bernadino site and Norton Air Force Base pair showed a bias of only 2.4 percent. In an attempt to see if the agreement was caused by low nighttime wind speeds at Norton Air Force Base, the wind observations during the daytime period were analyzed and almost no bias occurred for the San Bernadino-Norton Air Force pair. The possibility exists that the data may have been incorrectly processed or reported; for example, incorrect conversion from knots to m/s could account for the small bias.

We believe that the one-minute average wind speeds reported from FAA/NWS stations are correct. As a result of the SCAQMD study, which may be true for other locations also, it was concluded that FAA/NWS surface wind observations may have a positive bias of as much as a factor of 2.

This preliminary analysis is by no means complete or statistically roboust. However, it does have important implications for the development of wind fields for air quality simulations models, such as the UAM. It also helps explain some of the UAM's tendency to underpredict peak ozone concentrations at some locations in the past e.g., St. Louis and Philadelphia. Further analysis of the SCAQMD wind data base and data from other locations is necessary to determine the extent and frequency of this bias. For example, hourly average wind speeds are calculated by vector averaging of a series of lower frequency wind observations. A comparison of the one-minute wind speeds with the hourly average wind speed may give some indication of the extent of the bias.

MODEL PERFORMANCE EVALUATION

The UAM(CB-IV) was exercised with the exact same inputs as in diagnostic run 2 except that the observed wind speeds from FAA observations were reduced by 50 percent. The resultant predicted ozone concentrations at each of the ozone monitoring sites are shown in Figure G-1. Similar time series plots of predicted and observed ozone concentrations using a one-cell and two-cell search are shown in Figures G-2 and G-3. Scatterplots, residual analysis plots, and model performance statistics for predicted and observed hourly ozone concentrations and the reduced wind speed sensitivity test are shown in Figure G-4. The isopleths of hourly ozone concentrations for the reduced wind speed sensitivity test are given in Figure G-5. Note that these five figures can be compared to Figures 3 through 6 in the main body of the report and Appendix E to obtain a comparison of model performance.

The predicted region-wide maximum ozone concentration in the sensitivity test matches the observed peak ozone concentration exactly (14.7 pphm). At the location of the observed peak ozone the model prediction (11.4) is within 22 percent. At other ozone monitors, the model predicts the peak within 2 percent (DKLB) and 33 (DLLS) percent. The performance of the sensitivity test is superior to that of diagnostic run 2, as shown in the scatterplots of hourly predicted and observed ozone concentrations (Figures G-4, and Figure 6 in the main body of the report).

VOC EMISSION REDUCTION SCENARIOS

Three across-the-board anthropogenic VOC emission reduction scenarios (30, 60, and 90 percent) were simulated using the inputs from the reduced wind speed sensitivity test. Table G-2 shows the effects of these reduction scenarios, with and without biogenic emissions, on the predicted region-wide maximum ozone concentrations. The information in Table G-2 is graphically presented in Figure G-7. The reduced wind speed sensitivity test estimated that anthropogenic VOC emission reductions of 62 percent are required to meet attainment of the ozone NAAQS when biogenic emissions are included, and 53 percent when biogenic emissions are not included. Thus, compared to diagnostic run 2, the percent increase in anthropogenic VOC

emission reductions required to reach attainment of the ozone NAAQS when biogenic emissions are included is 9 percent higher, and 38 percent higher when biogenic emissions are not included.

These differences of 9 and 38 percent can be explained because the sensitivity test results in less dilution of the urban plume, so that the ozone peak is generated mainly by the urban anthropogenic emissions. These differences illustrate the uncertainty in the model calculations, be they due to uncertainties in emissions (anthropogenic and biogenic), boundary conditions, or meteorology. Thus the emphasis in the findings concerning biogenic emissions reported here and elsewhere (e.g., Chameides et al., 1988) should be on the directions rather than the absolute magnitudes of the calculations. However, the reduced wind speed sensitivity test does not change the basic result--biogenic emissions in Atlanta do increase the level of reduction in anthropogenic VOC emissions required to meet attainment of the ozone standard.

TABLE G-1. Surface meteorological observation sites and distance between collocated observations pairs.

NWS/FAA Site Name	Location UTM (Zone10) UTM_x	UTM_y	SCAQMD Site Name	Location UTM (Zone 10) UTM_x	UTM_y	Distance between Collocated Stations
Burbank Airport	356.48	3768.00	Burbank	359.60	3766.40	3.52 km
Los Angeles International Airport	352.48	3744.40	Lennox	354.40	3744.00	1.96 km
Long Beach Airport	370.88	3733.76	Long Beach	368.00	3734.40	2.95 km
El Toro Airport	401.60	3720.16	El Toro	404.8	3716.72	4.70 km
Ontario Airport	411.68	3754.16	Upland	408.00	3758.48	5.67 km
Norton Air Force Base	438.80	3756.96	San Bernardino	434.40	3759.20	4.94 km
Compton Airport	364.40	3740.24	Lynwood	366.40	3743.20	3.57 km

TABLE G-2. Regional maximum ozone concentrations (pphm) predicted by the UAM for the base cases (with and without biogenic emissions) and the different emission scenarios using the reduced wind speed sensitivity test modeling inputs.

	Maximum Ozone Concentration (pphm)	Percent Reductions from Base Case	Maximum Ozone Normalized to Peak Observation (pphm)
Peak Observed	14.7	0.0	14.7
Ozone NAAQS*	12.0	18.4	12.0
<u>With Biogenics</u>			
0% VOC Reduction	14.70	0.0	14.7
30% VOC Reduction	13.17	10.4	13.2
60% VOC Reduction	12.09	17.8	12.1
90% VOC Reduction	11.24	23.5	11.2
<u>Without Biogenics</u>			
0% VOC Reduction	12.93	0.0	14.7
30% VOC Reduction	11.83	8.5	13.5
60% VOC Reduction	10.09	22.0	11.5
90% VOC Reduction	8.82	31.8	10.0

* Technically, the ozone NAAQS is 0.12 ppm rounded. Thus, an ozone concentration of 12.4 pphm (15.6% reduction from observed peak) is considered attainment.

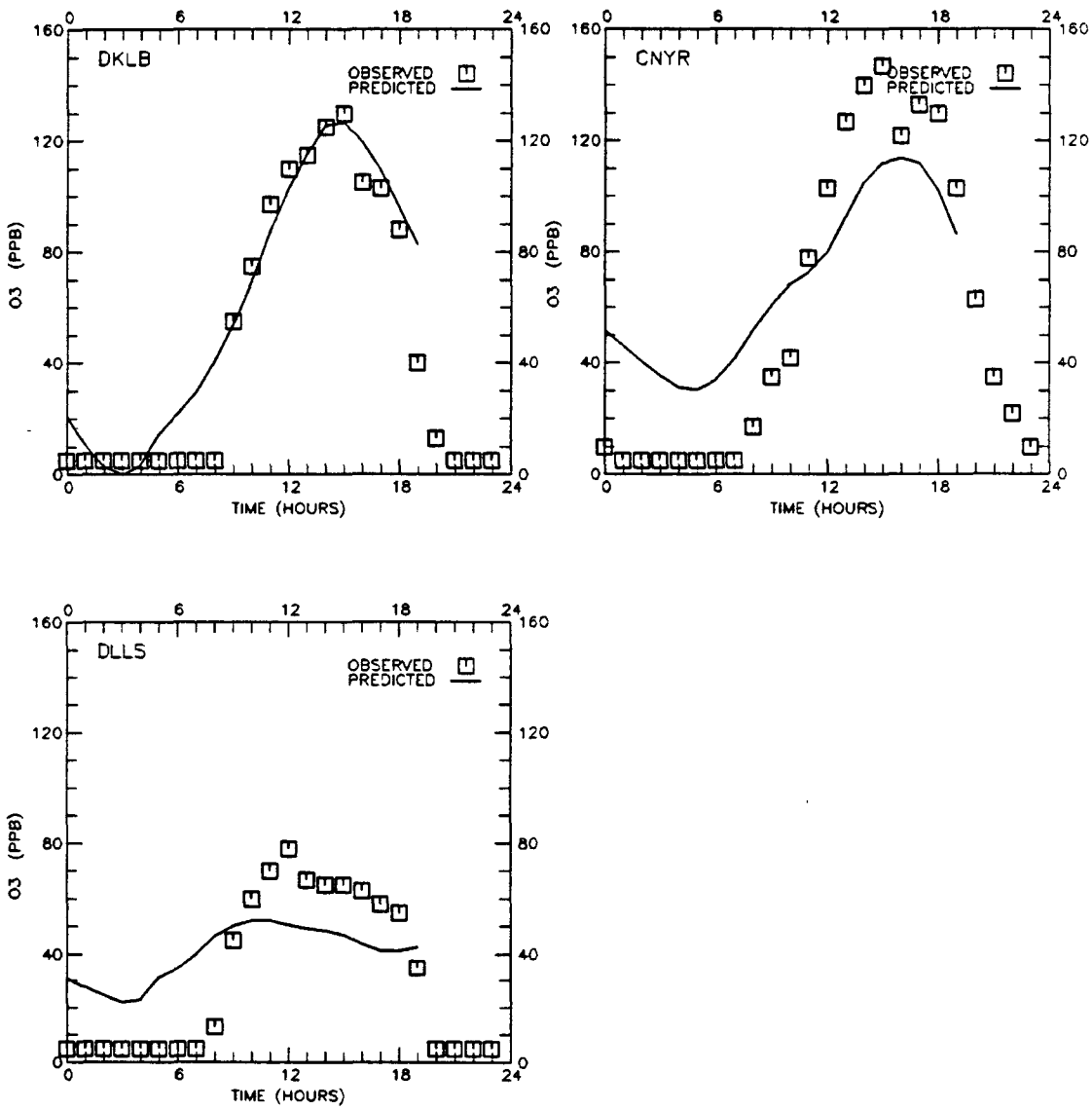

FIGURE G-1. Observed and predicted ozone concentrations (ppb) for Atlanta reduced wind speed sensitivity test.

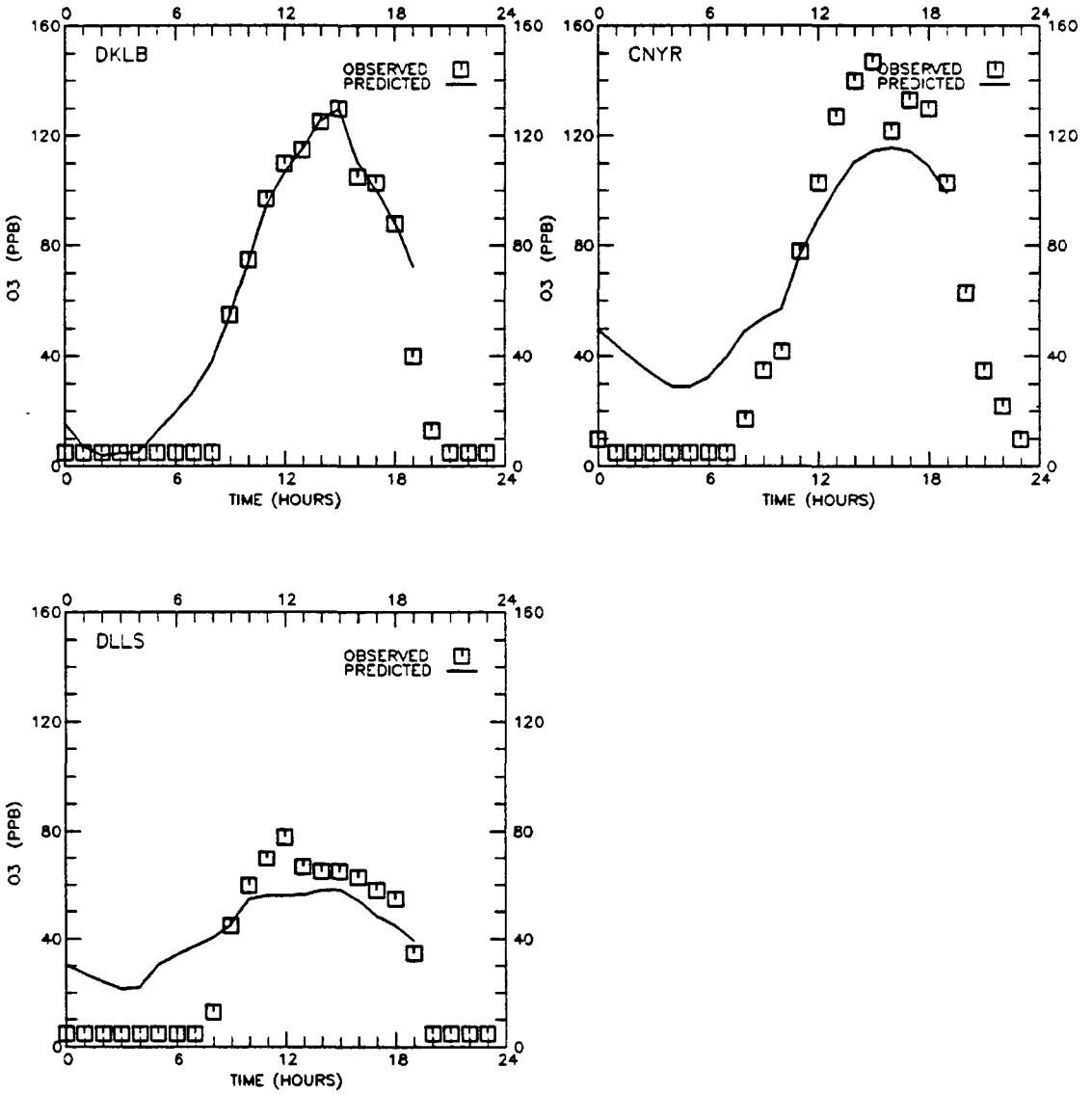

FIGURE G-2. Observed and nearest-neighbor predicted (one-cell search) ozone concentration (ppb) for the Atlanta reduced wind speed sensitivity test.

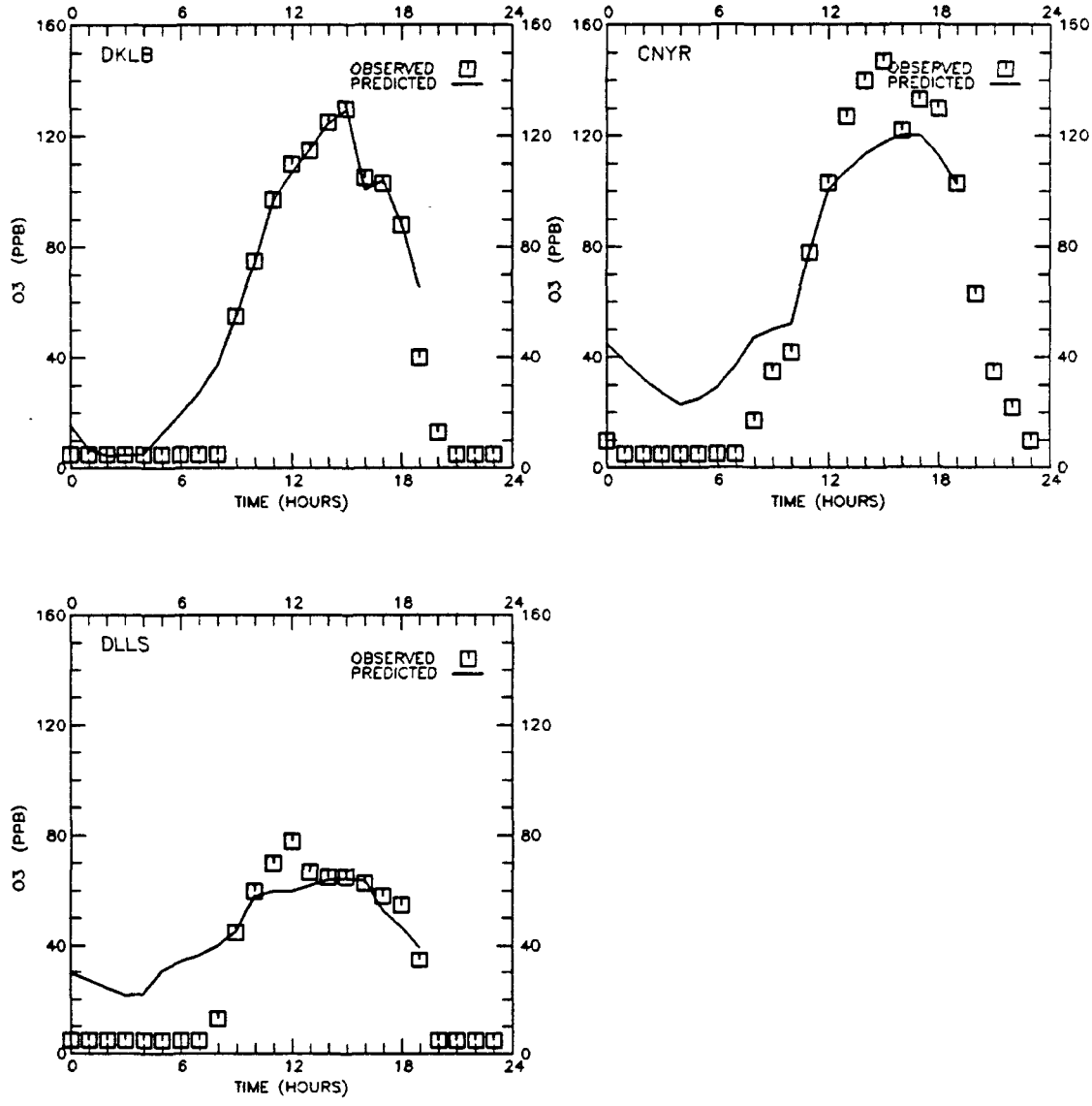

SYSTEMS APPLICATIONS, INC.

FIGURE G-3. Observed and nearest-neighbor predicted (two-cell search) ozone concentration (ppb) for the Atlanta reduced wind speed sensitivity test.

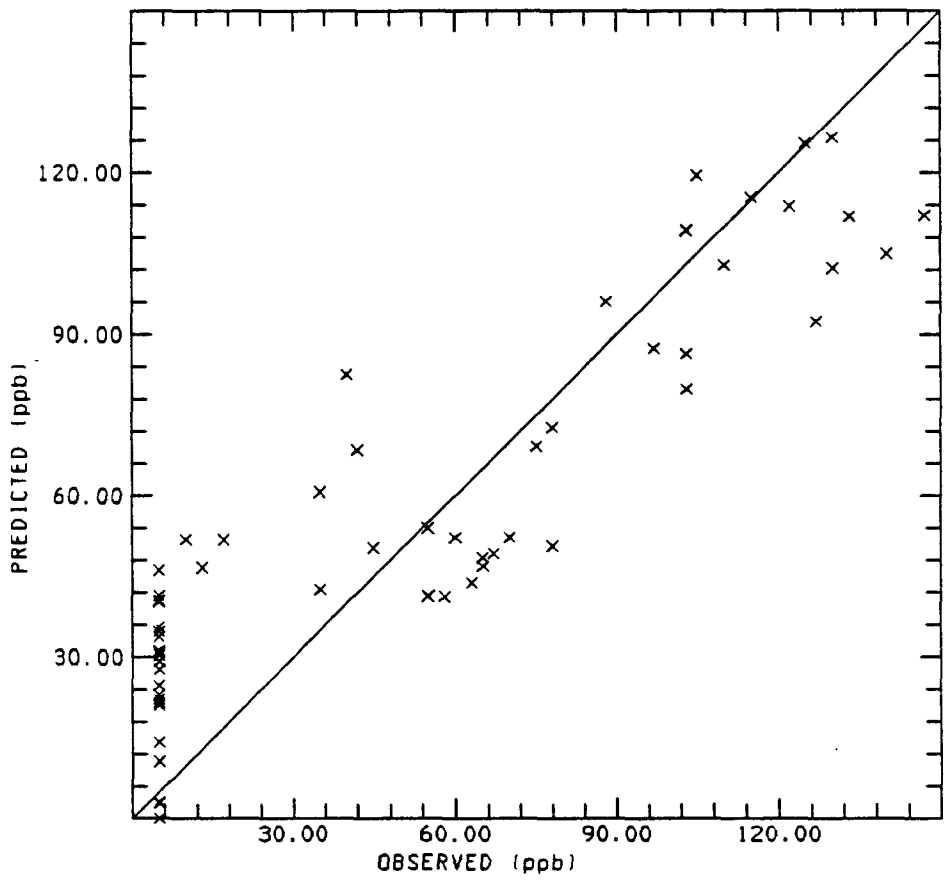

MOMENTS OF THE PROBABILITY DENSITY FUNCTION

	OBSERVED	PREDICTED
AVERAGE	50.39999	56.68703
STANDARD DEVIATION	47.63355	34.20863
SKEWNESS	0.51320	0.52057
KURTOSIS	-1.22432	-0.84048
OTHER MEASURES		
MEDIAN	40.00000	46.90000
UPPER QUARTILE	88.00000	82.56000
LOWER QUARTILE	5.00000	31.13000
MINIMUM VALUE	5.00000	0.02000
MAXIMUM VALUE	147.00000	126.60000

SKILL OF PREDICTION PARAMETERS

CORRELATION COEFFICIENT OF PREDICTED VERSUS OBSERVED 0.904
THE BOUNDS OF THE CORRELATION AT THE CONFIDENCE LEVEL OF 0.050 ARE
LOW BOUND 0.844 HIGH BOUND 0.942
RATIO OF OVER TO UNDER PREDICTIONS 1.308
PERCENT OF OVER PREDICTIONS GREATER THAN 200 PERCENT OF THE OBSERVED 41.667
PERCENT OF UNDER PREDICTIONS LESS THAN 50 PERCENT OF THE OBSERVED 1.667

FIGURE G-4a. Scatterplot and model performance statistics for hourly ozone concentrations and Atlanta reduced wind speeds sensitivity test (N = 60).

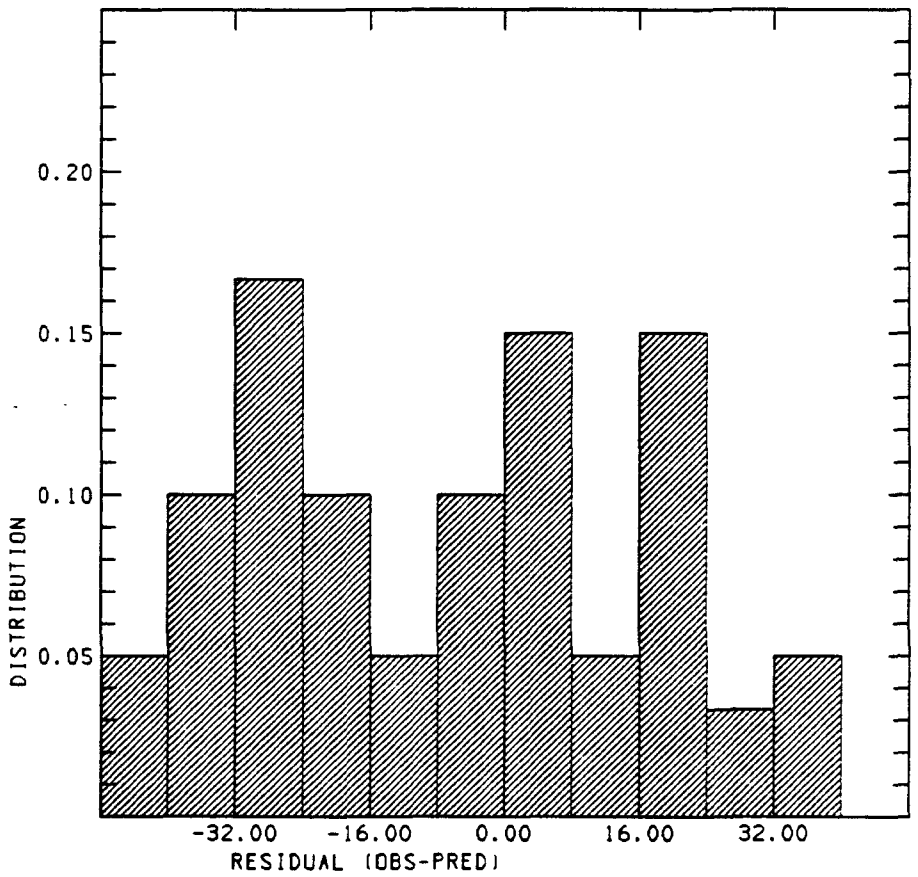

THE BINSIZE EQUALS 8.000

RESIDUAL ANALYSIS

AVERAGE	-6.28719
STANDARD DEVIATION	22.19390
SKEWNESS	0.10702
KURTOSIS	-1.19285
OTHER MEASURES	
MEDIAN	-6.30000
UPPER QUARTILE	9.57001
LOWER QUARTILE	-26.13000
MINIMUM VALUE	-42.56000
MAXIMUM VALUE	35.00000

BIAS CONFIDENCE INTERVAL
AT THE 0.0500 LEVEL
LOWER BOUND -18.9385
UPPER BOUND 6.3641

STD RESIDUAL CONFIDENCE INTERVAL
AT THE 0.0500 LEVEL
LOWER BOUND 373.7107
UPPER BOUND 684.3732

THE MEASURES OF GROSS ERROR
THE ROOT MEAN SQUARE ERROR IS 22.89
THE AVERAGE ABSOLUTE ERROR IS 19.52

VARIOUS MEASURES OF RELATIVE VARIABILITY
OBSERVATION COEFFICIENT OF VARIATION
0.9451
RESIDUAL COEFFICIENT OF VARIATION
0.4404
RATIO OF RESIDUAL TO OBSERVED ST. DEV.
0.4659

FIGURE G-4b. Residual analysis plot and model performance statistics for hourly ozone concentrations and Atlanta reduced wind speeds sensitivity test.

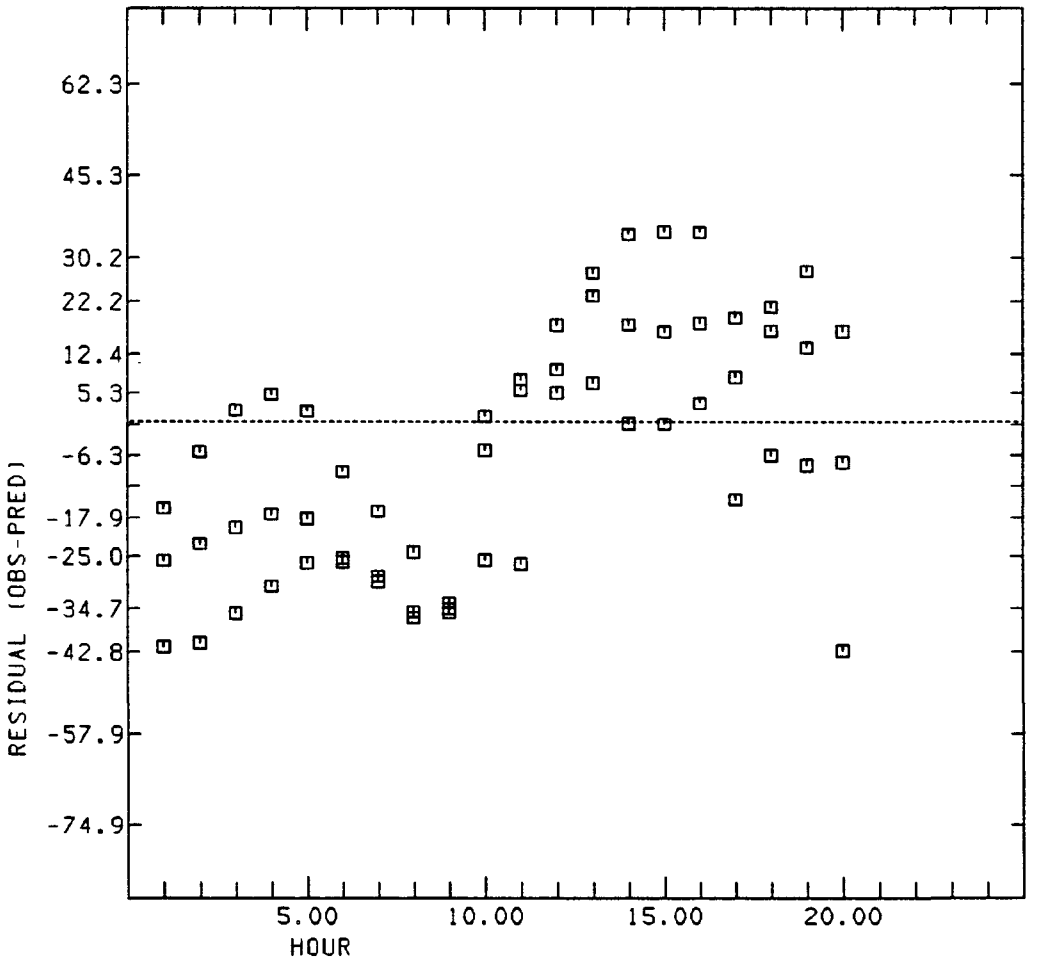

THE LINEAR MODEL PARAMETERS
THE CORRELATION IS 0.5829
THE LOWER BOUND IS 0.3861
THE UPPER BOUND IS 0.7290
AT THE 0.0500 PERCENT LEVEL
THE Y-X LINEAR MODEL INTERCEPT IS 11.460
THE Y-X LINEAR MODEL SLOPE IS 0.153
THE X-Y LINEAR MODEL INTERCEPT IS -29.647
THE X-Y LINEAR MODEL SLOPE IS 2.225

FIGURE G-4c. Plot of residuals versus time of day for hourly ozone concentrations and Atlanta reduced wind speeds sensitivity test.

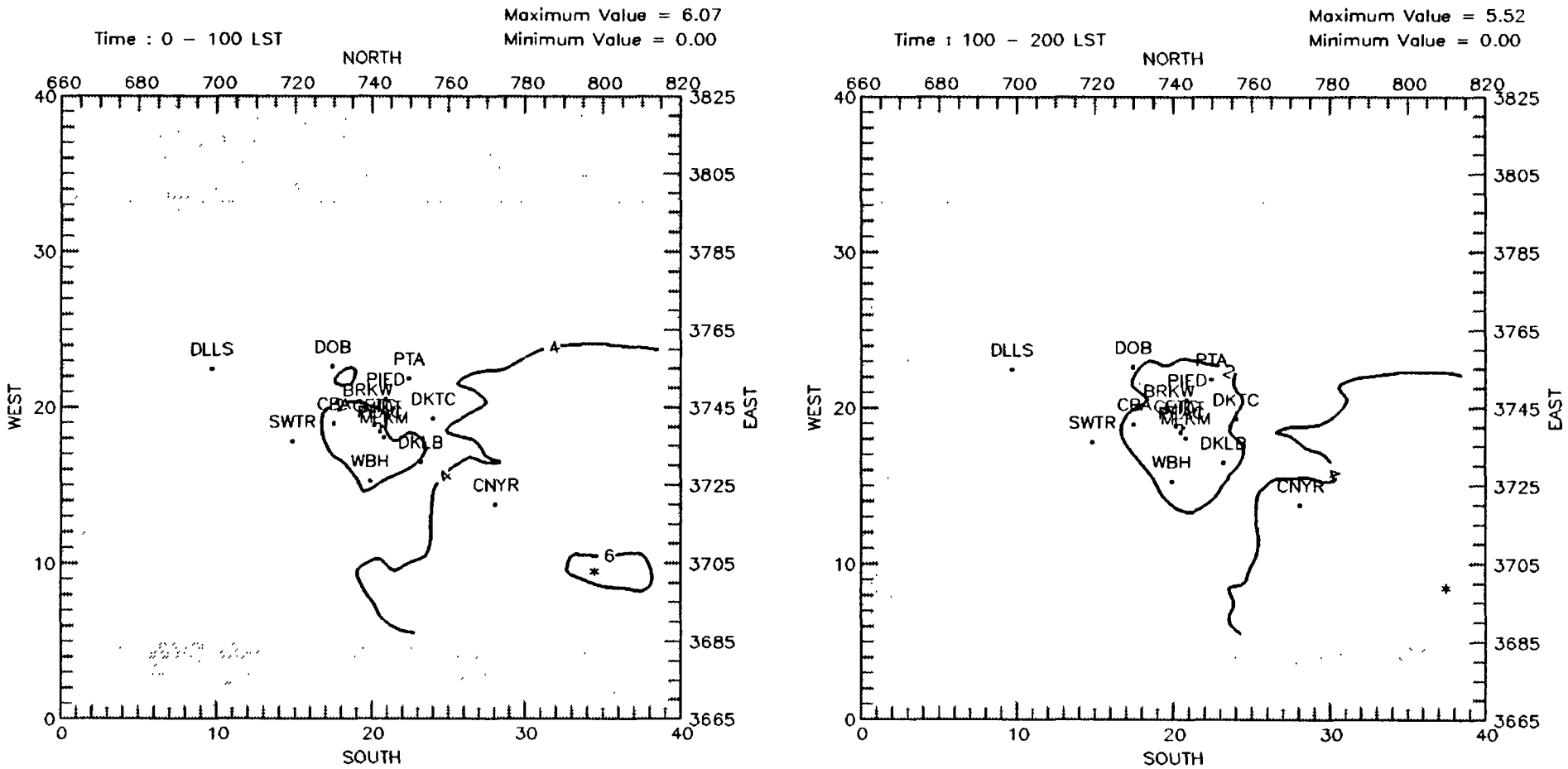

FIGURE G-5. Ozone (pphm) 1985 base emissions, June 4, 1984 (pphm).

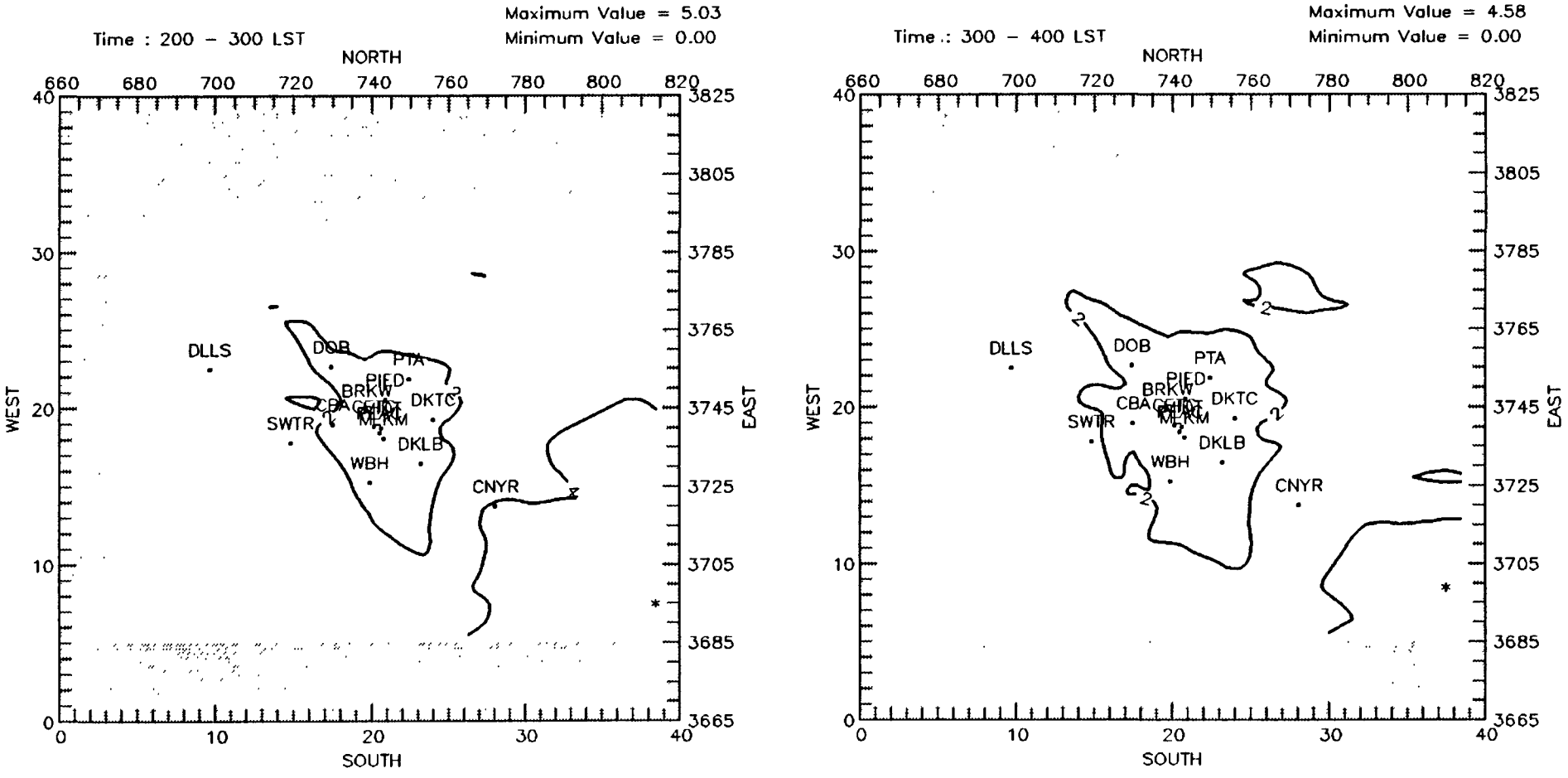

Ozone (pphm) 1985 base emissions, June 4, 1984 (pphm)

FIGURE G-5. Continued.

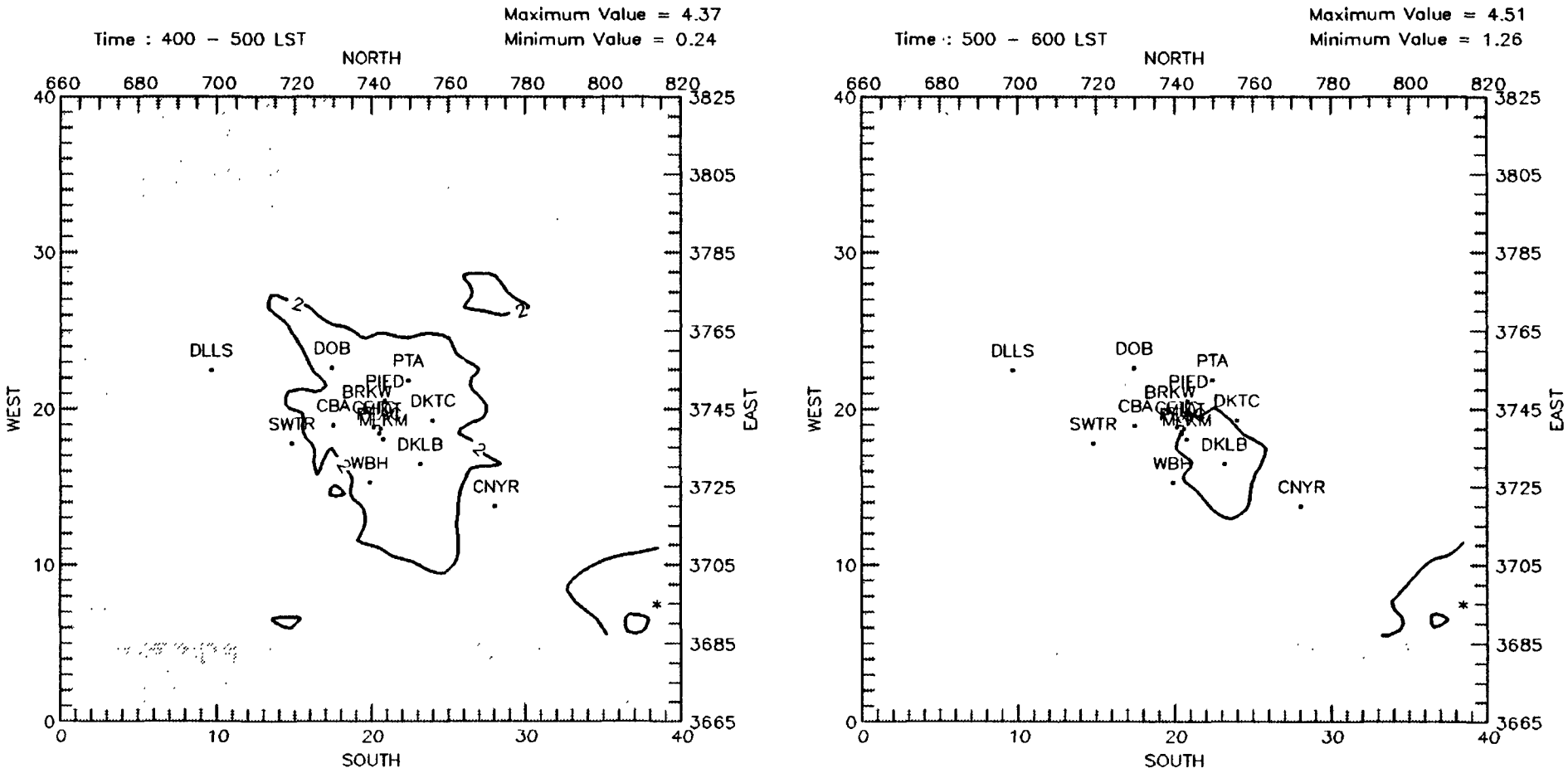

Ozone (pphm) 1985 base emissions, June 4, 1984 (pphm)

FIGURE G-5. Continued.

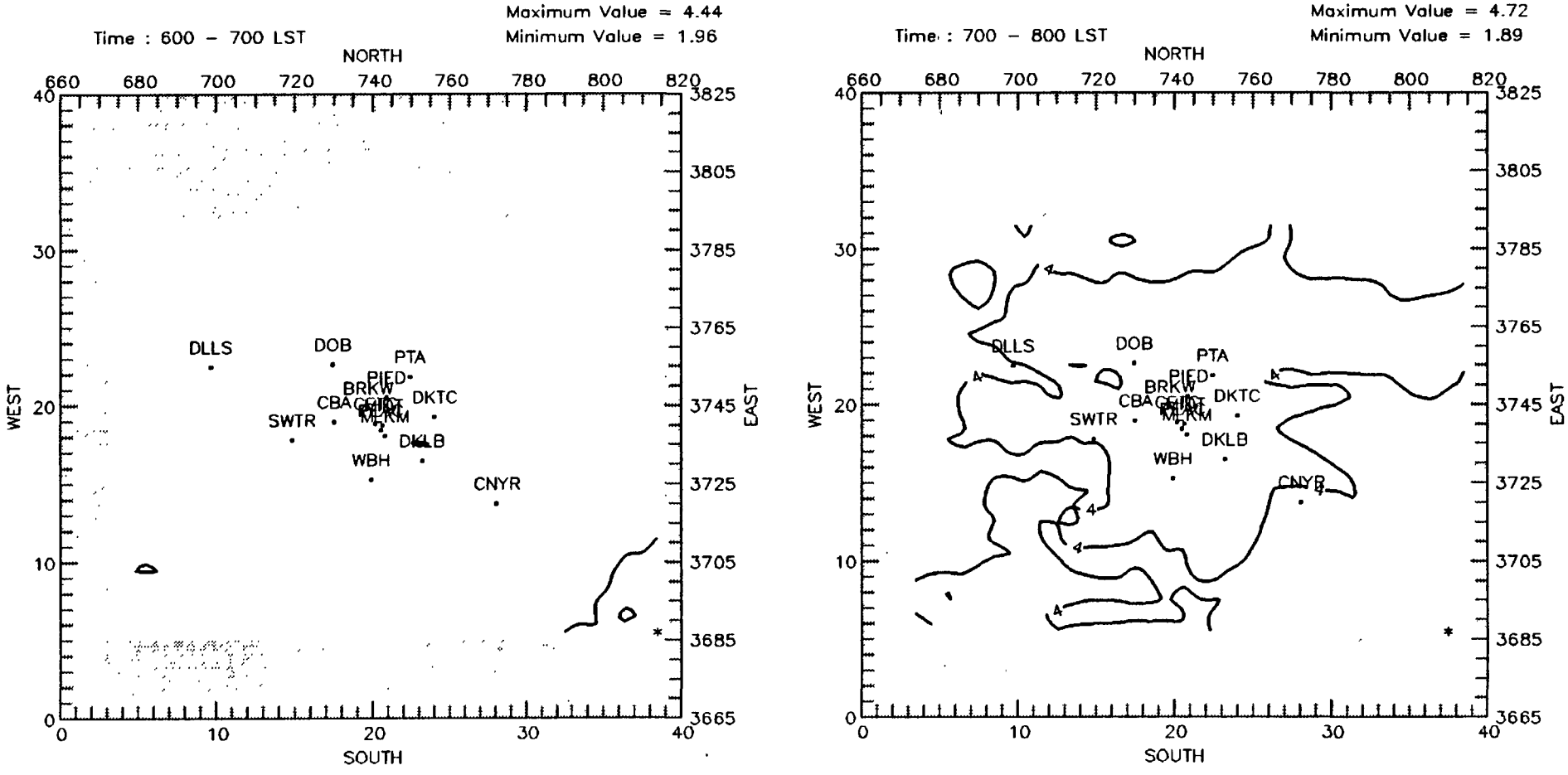

Ozone (pphm) 1985 base emissions, June 4, 1984 (pphm)

FIGURE G-5. Continued.

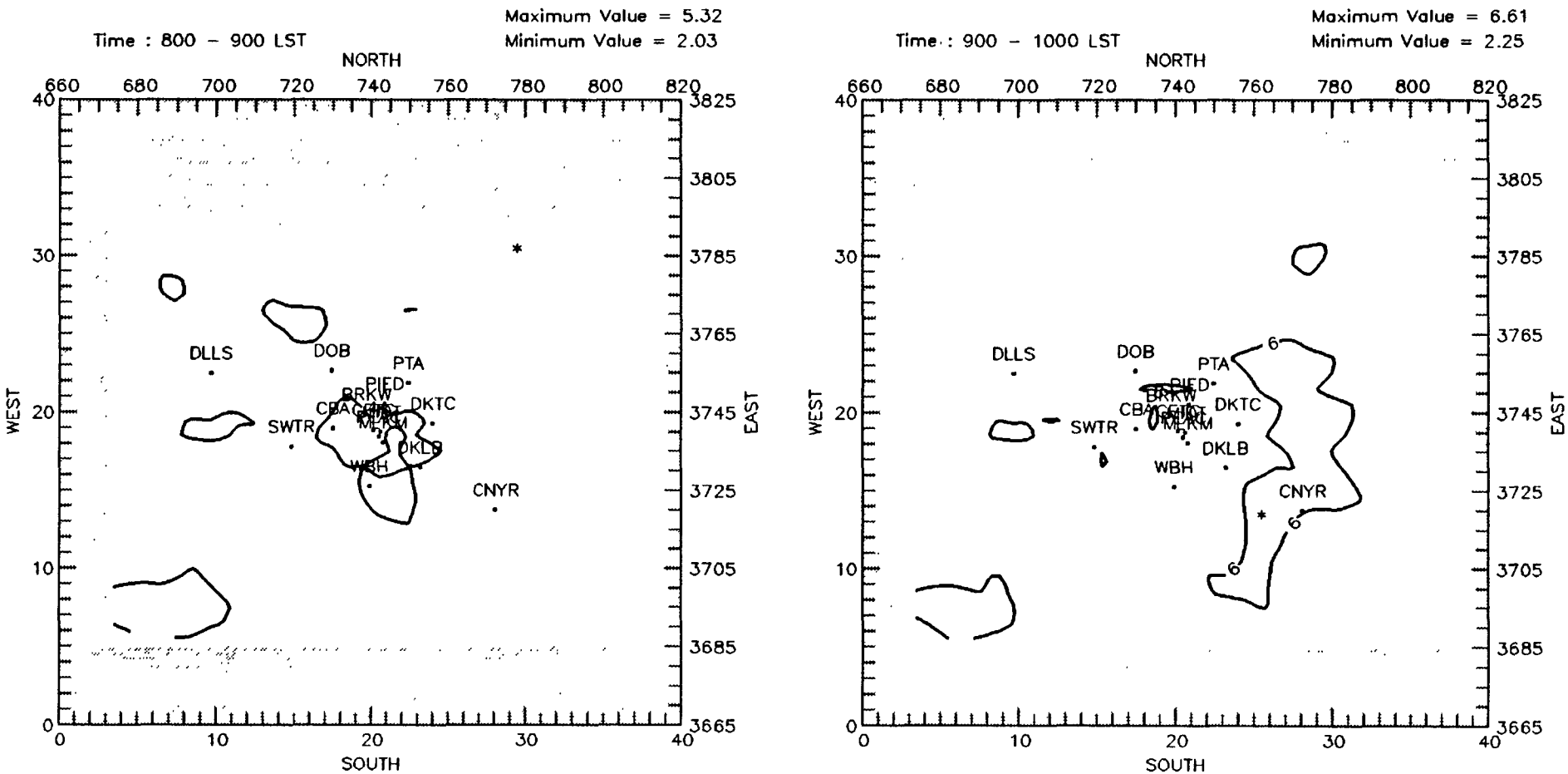

Ozone (pphm) 1985 base emissions, June 4, 1984 (pphm)

FIGURE G-5. Continued.

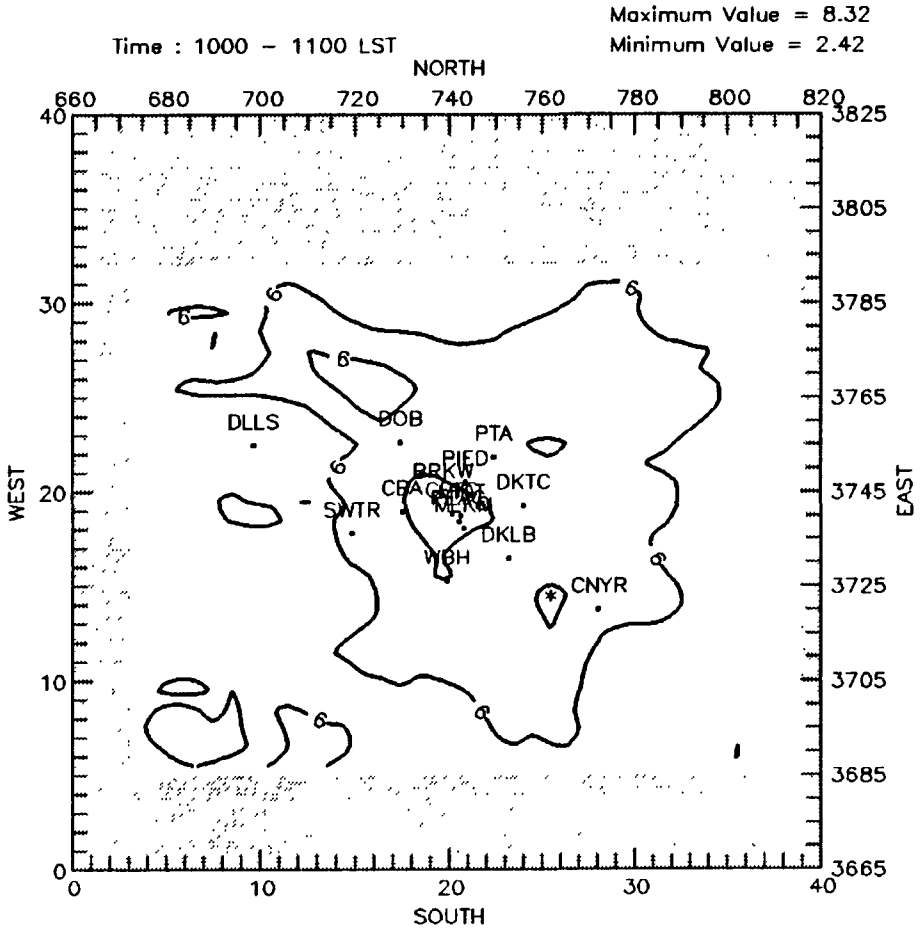

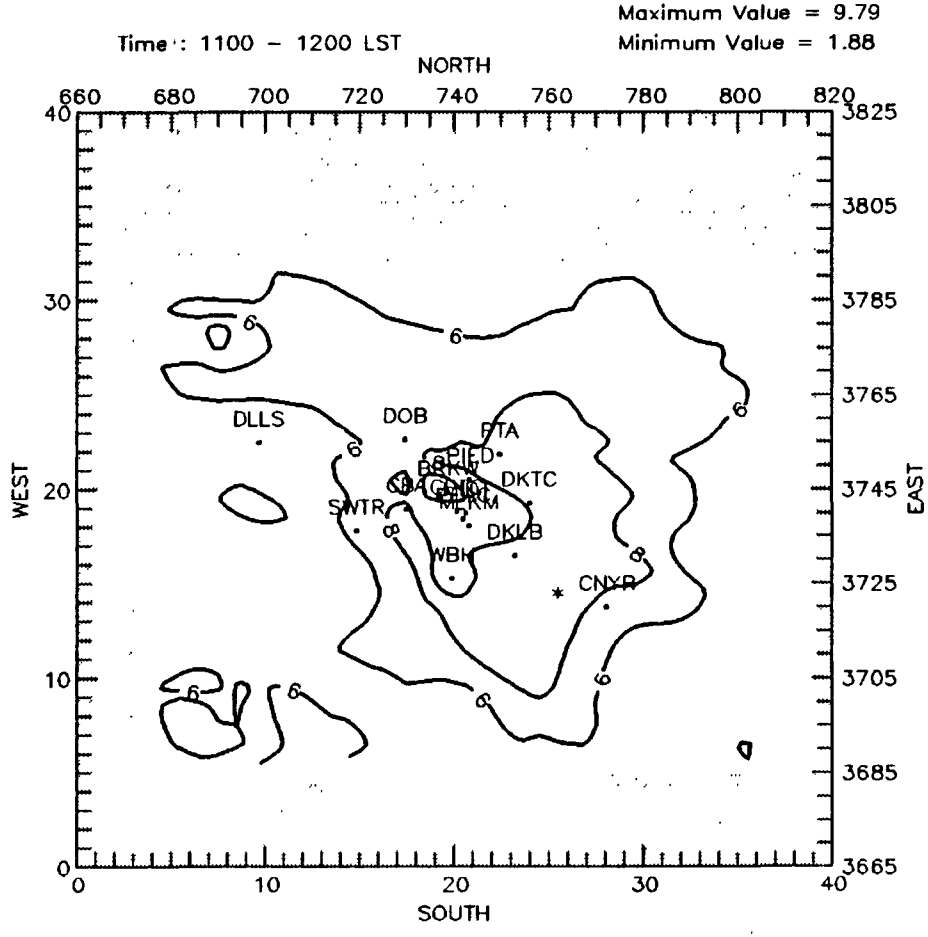

Ozone (pphm) 1985 base emissions, June 4, 1984 (pphm)

FIGURE G-5. Continued.

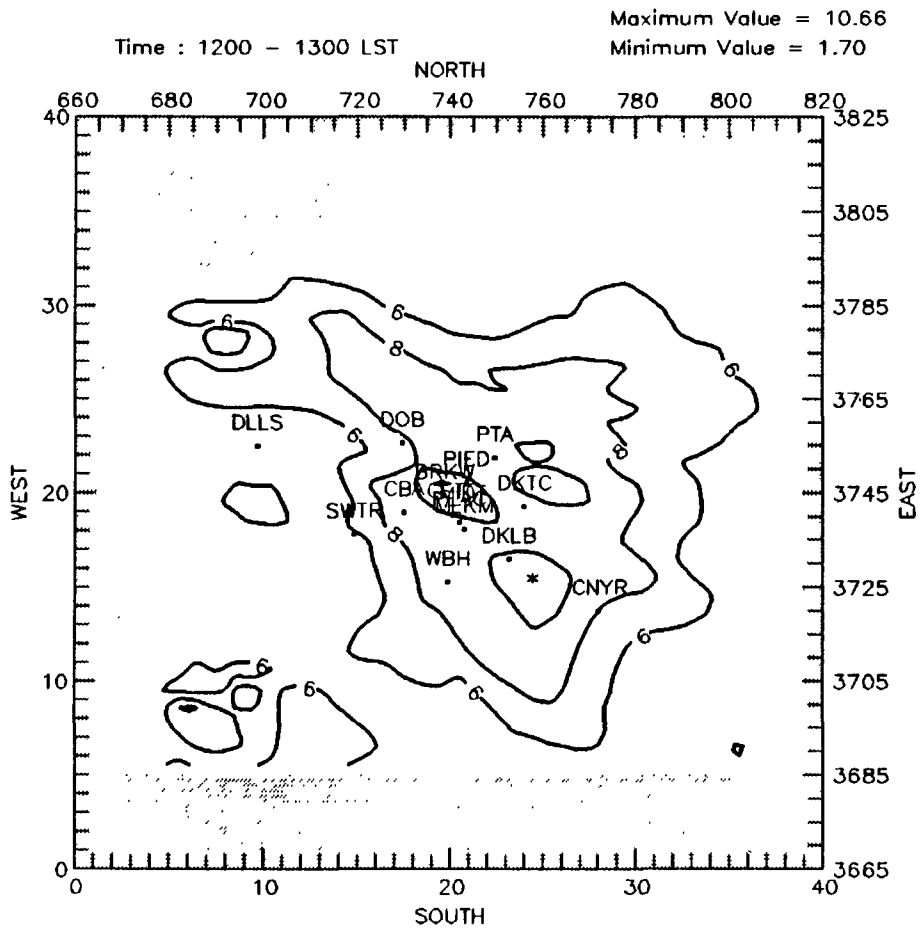

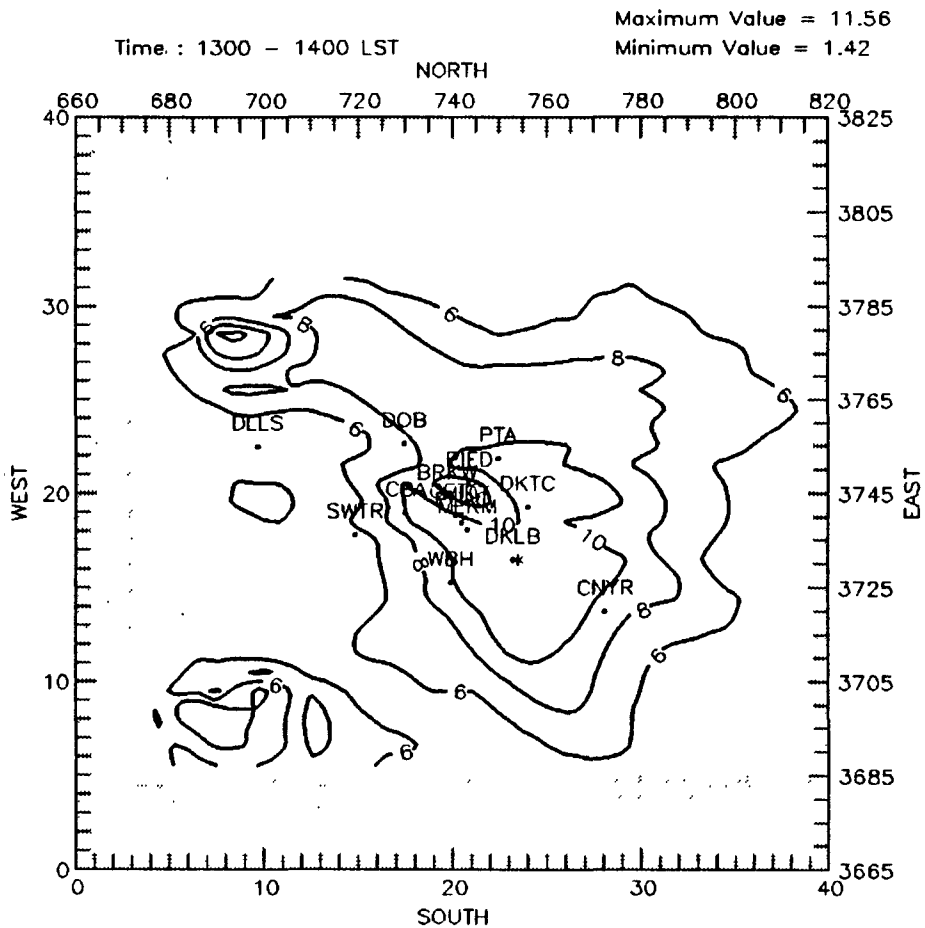

Ozone (pphm) 1985 base emissions, June 4, 1984 (pphm)

FIGURE G-5. Continued.

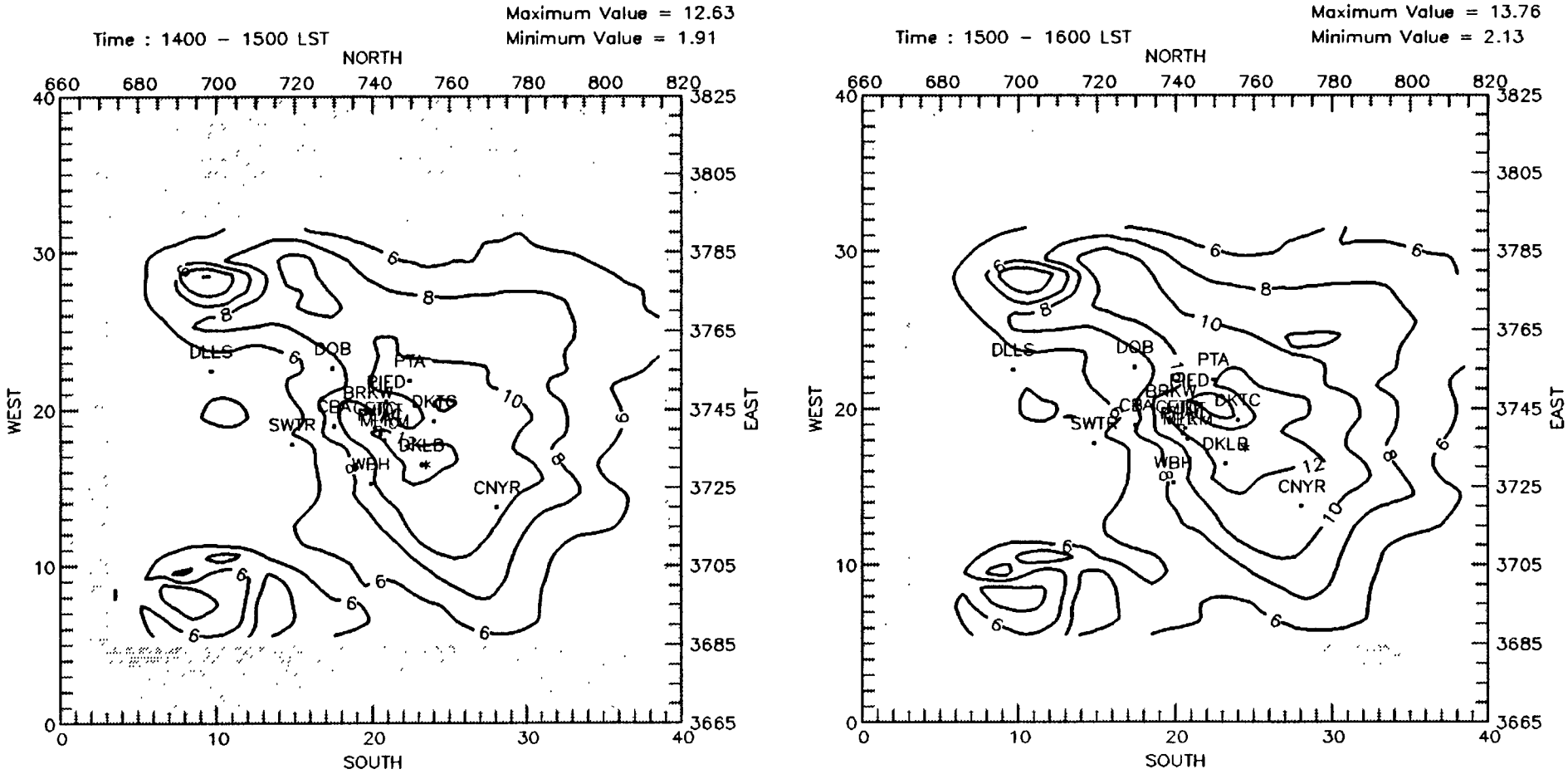

Ozone (pphm) 1985 base emissions, June 4, 1984 (pphm)

FIGURE G-5. Continued.

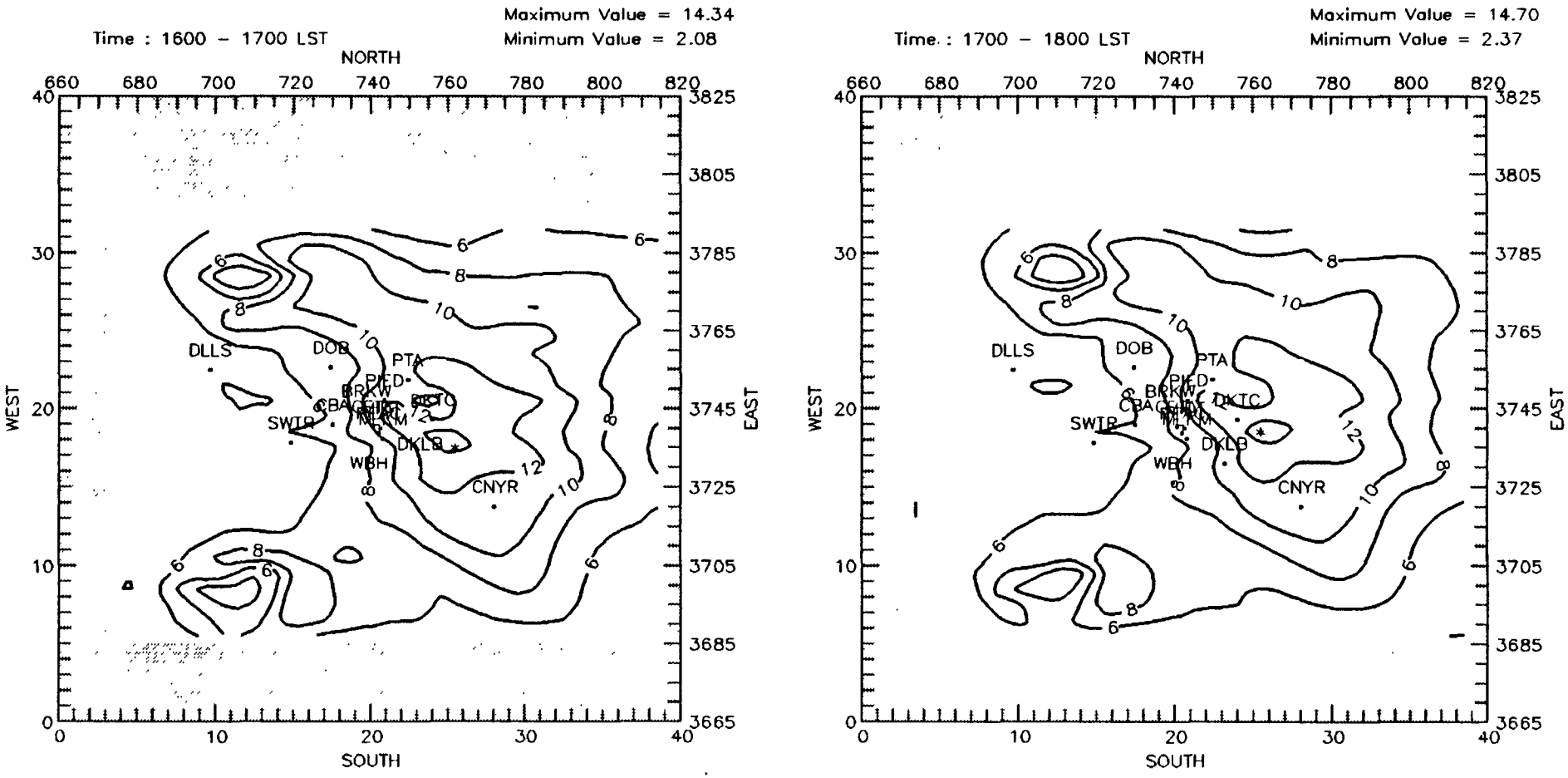

Ozone (pphm) 1985 base emissions, June 4, 1984 (pphm)

FIGURE G-5. Continued.

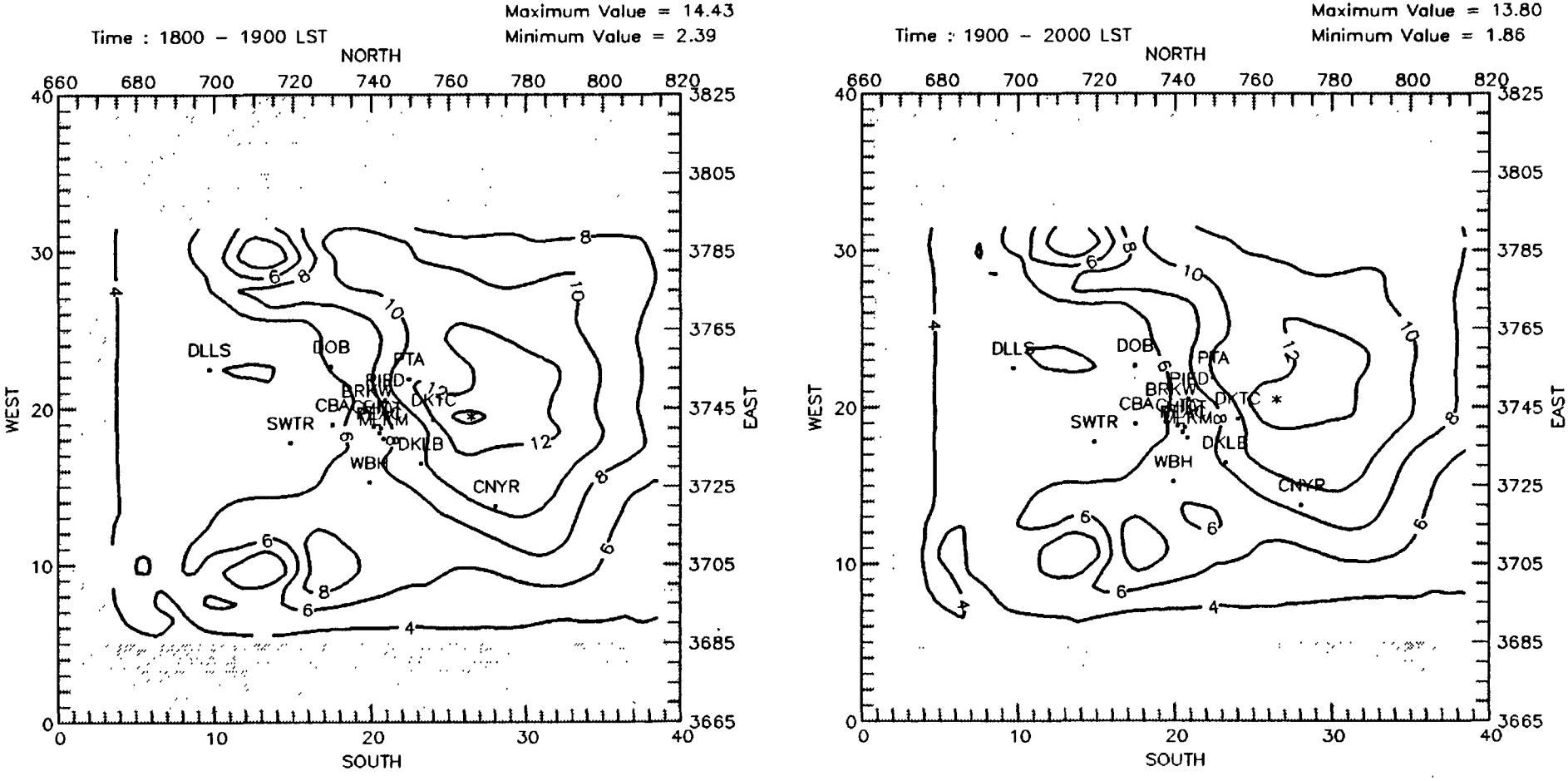

Ozone (pphm) 1985 base emissions, June 4, 1984 (pphm)

FIGURE G-5. Concluded.

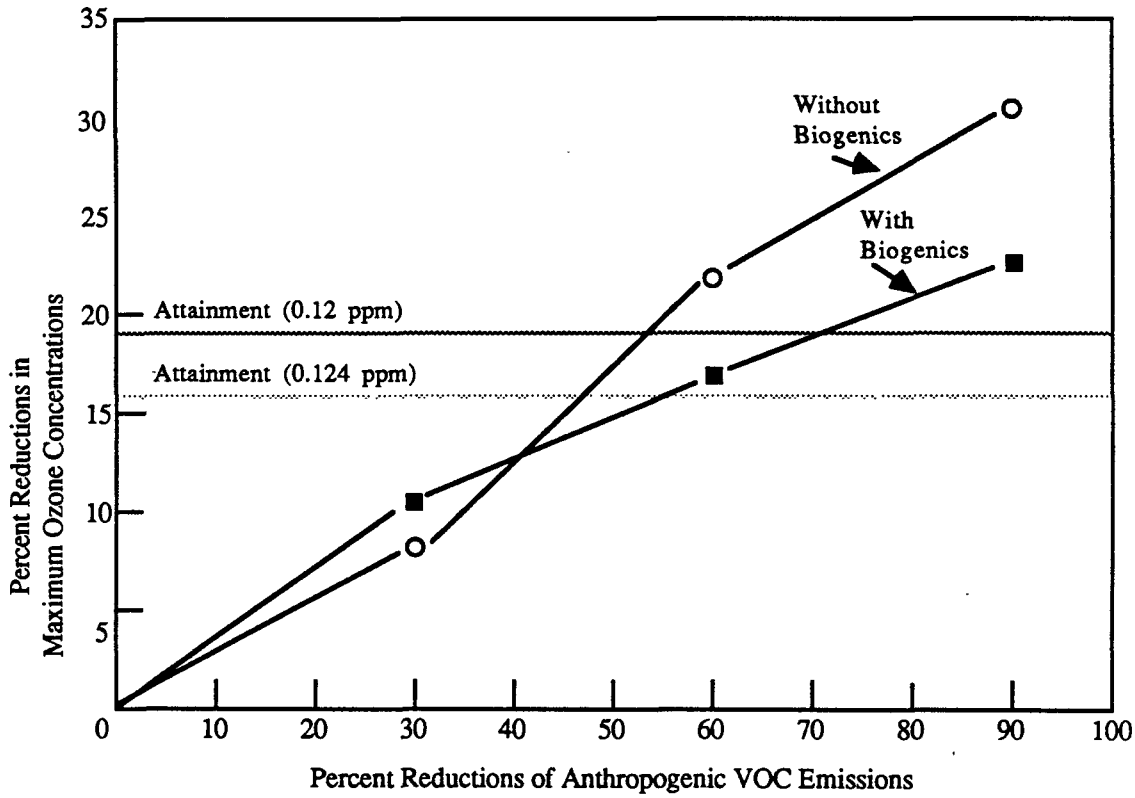

FIGURE G-6. Relationship between percent reduction of anthropogenic VOC emissions to percent reduction of the maximum ozone concentration at the location of regional maximum for the base case scenarios with and without biogenic emissions for Atlanta reduced wind speed sensitivity test UAM modeling inputs.

TECHNICAL REPORT DATA
(Please read Instructions on the reverse before completing)

1. REPORT NO.	2.	3. RECIPIENT'S ACCESSION NO.
EPA 450/4-90-006 D		

4. TITLE AND SUBTITLE
URBAN AIRSHED MODEL STUDY OF FIVE CITIES - Low-Cost Application of the Model to Atlanta and Evaluation of the Effects of Biogenic Emissions on Emission Control Strategies

5. REPORT DATE
April 1990

6. PERFORMING ORGANIZATION CODE

7. AUTHOR(S)
Ralph E. Morris, Thomas C. Myers, Marianne C. Causley, LuAnn Gardner, Edward L. Carr

8. PERFORMING ORGANIZATION REPORT NO.

9. PERFORMING ORGANIZATION NAME AND ADDRESS
Systems Applications, Inc.
101 Lucas Valley Road
San Rafael, CA 94903

10. PROGRAM ELEMENT NO.

11. CONTRACT/GRANT NO.

12. SPONSORING AGENCY NAME AND ADDRESS
U.S. Environmental Protection Agency
Office of Air Quality Planning and Standards
Research Triangle Park, NC 27711

13. TYPE OF REPORT AND PERIOD COVERED

14. SPONSORING AGENCY CODE

15. SUPPLEMENTARY NOTES

16. ABSTRACT

This document presents Urban Airshed Modeling results showing sensitivity of peak ozone to manmade hydrocarbon emissions reductions for two cases - inclusion and exclusion of biogenic emissions.

17. KEY WORDS AND DOCUMENT ANALYSIS

a. DESCRIPTORS	b. IDENTIFIERS/OPEN ENDED TERMS	c. COSATI Field/Group
Ozone Urban Airshed Model Photochemistry Biogenics		

18. DISTRIBUTION STATEMENT	19. SECURITY CLASS *(This Report)*	21. NO. OF PAGES
		152
	20. SECURITY CLASS *(This page)*	22. PRICE

EPA Form 2220-1 (Rev. 4-77) PREVIOUS EDITION IS OBSOLETE